A prefrontal–temporal network underlying state changes between Stimulus-Driven and Stimulus-Independent Cognition

Tomas Ossandon Valdes

A prefrontal – temporal network underlying state changes between Stimulus-Driven and Stimulus-Independent Cognition

THESE

préesenté et soutenue publiquement le 14 Decembre 2010
pour l'obtention du grade de

Docteur en Neurosciences Cognitives
de l'Université Claude Bernard – Lyon I
(arrété du 7 août 2006)

par

Tomas OSSANDON

Composition du jury

Directeurs de thèse : LACHAUX Jean-Philippe
BERTRAND Olivier

Rapporteurs : LUTZ Antoine
LE VAN QUYEN Michel

Jury : LACHAUX Jean-Philippe
BERTRAND Olivier
LUTZ Antoine
GERVAIS Rémi
LE VAN QUYEN Michel

Laboratoire Inserm *"Dynamique Cérébrale et Cognition"* — U821

ABSTRACT:

The brain displays moment-to-moment activity fluctuations that reflect various levels of engagement with the outside world. Processing external stimuli is not only associated with increased brain metabolism but also with prominent deactivation in specific structures, collectively known as the default-mode network (DMN). The role of the DMN remains enigmatic partly because its electrophysiological correlates and temporal dynamics are still poorly understood. Using unprecedented wide-spread depth recordings in epileptic patients, undergoing intracranial EEG during pre-surgical evaluation, we reveal that DMN neural populations display task-related suppressions of gamma (60-140 Hz) power and, critically, we show how millisecond temporal profile and amplitude of gamma deactivation tightly correlate with task demands and subject performance. The results show also that during an attentional task, sustained activations in the gamma band power are presented across large cortical networks, while transient activations are mostly specific to occipital and temporal regions. Our findings reveal a pivotal role for broadband gamma modulations in the interplay between activation and deactivation networks mediating efficient goal-directed behavior.

Key words: Default-mode network, intracranial EEG, gamma-band activity, gamma-band suppression, goal-directed behavior, attention, visual search, and epilepsy.

RÉSUME

Le cerveau présente des fluctuations de son activité qui reflètent différents niveaux d'engagement avec le monde extérieur. Le traitement des stimuli externes n'est pas seulement associé avec une augmentation du métabolisme cérébrale, mais également avec une désactivation importante dans un ensemble des structures spécifiques connus sous le nom de 'Default-Mode Network' (DMN, réseau par défaut). Le rôle du DMN reste énigmatique en partie parce que ses corrélats électrophysiologiques et sa dynamique temporelle sont encore mal compris. En utilisant des enregistrements éléctrophysiologiques intracrânien chez le patient épileptique, nous démontrons que la population neuronale de ce réseau montre des suppressions de l'activité gamma (60-140 Hz). Plus important, nous montrons de quelle manière le profil temporale (en millisecondes) et l'amplitude de cette désactivation sont étroitement corrélés avec la difficulté de la tâche et la performance individuelle. Les résultats mettent également en évidence que pendant une tâche attentionnelle, une activation soutenue dans le temps de la bande gamma est présente dans un large réseau, alors que des activations transitoires sont spécifiques aux régions temporale et occipitale. Nos résultats révèlent ainsi un rôle essentiel des mécanismes d'activation et de désactivation des oscillations large bande gamma dans l'exécution d'un comportement orienté vers un but.

Mots clés : Default Mode Network, électroencéphalographie intracrânien, oscillation gamma, désactivation gamma, épilepsie, attention, et recherche visuel.

Contents

Chapter 1

Electrophysiological correlates of the Default-Mode Network

1.1.1 Introduction ……..…….……..9

1.2 A brief history of the DMN…….…….…..13

1.2.1 Regional task non-specific deactivations during goal-directed activity ……...15

1.2.2 Coherence and functional connectivity within the DMN ……..17

1.2.3 DMN characterized by low frequency BOLD signal …….....18

1.2.4 Anti-correlated task-positive and task-negative resting network….……....20

1.3 A new view of the brain function……..21

1.3.1 Functional role of the Default-Mode Network……..……21

1.3.2 Anatomic considerations about the DMN……..……24

1.3.2.a Posterior Cingulate Cortex/ Precuneus……...…25

1.3.2.b Medial prefrontal cortex (MPFC)……...…...……..…25

a) Ventral MPFC……26

b) Dorsal MPFC…… 27

1.3.2.c Posterior lateral cortices……..27

1.3.2.d Rostral prefrontal cortex (BA 10, 47, 12)……..…..……29

Chapter 2

Neurophysiological basis of the fMRI signals

2.1 Introduction…….……31

a) General overview…….…….31

b) Functional MRI ……..……..……..…32

2.2 Electrophysiological correlates of BOLD, invasive studies…….……..…33

2.3 Electrophysiological correlates of BOLD, non-invasive methods ……..36

2.4 Electrophysiological correlate of BOLD deactivation …….……38

Chapter 3

Attention and electrophysiology: broadband gamma band activity as a neuronal marker

3 Introduction: Attention and electrophysiology……...41

3.1 Mechanisms of selective visual attention…….……41

3.2 On the functional importance of neural synchronization…….……44

3.3 Human studies on neuronal synchronization……..……..…...49

3.4 Gamma band responses in humans……..…..…..50

3.4.1 Eye-movements artifacts……..……..…..…..52

3.5 Intracerebral EEG studies in humans…….……...…..52

3.5.1 Invasive recordings in epileptic patients…….…..……..…...53

3.5.2 Dynamic spectral imaging……..…….…..……54

3.6 Gamma band synchrony and attention: insights from human ICE studies…….……..……57

3.6.1 Attention and visual perception……..…….57

3.6.2 Attention and reading……..…..…..58

3.6.3 Attention and memory……..……....59

3.7 Broadband activity reflects synchrony?.....61

3.7.1 Asynchronous neuronal populations can explain narrowband oscillations……...61

3.7.2 Broadband spectral gamma: synchrony or neural correlate of population firing

rate?.....62

3.8 Perspectives……..…….……...64

3.8.1 Long distance synchrony……..…….……64

3.8.2 Other frequency bands……..…….....65

3.8.3 Scalp recordings……..……...66

Chapter 4

Material and Methods

4.1 Subjects……..….....68

4.2 Stimuli and experimental design……..….69

4.3 Data Acquisition…….…….....70

4.3.1 Electrode implantation…….……..….…….70

4.3.2 SEEG recordings…….……...…..…..……..71

4.3.3 Specificity of SEEG compared to ECoG…….…….....…...……..71

4.4 Data analysis…….…….…….....72

4.4.1 Time-Frequency Maps (Wavelet analysis)…….…….....72

4.4.2 Estimation of gamma power profiles (Hilbert transform)…….……..…….…73

4.5 Mapping intracranial EEG data to standard MNI brain…..……..……...…74

4.6 Definition of anatomo-functional clusters……..……..…….…...75

4.7 Computing deactivation onset and duration…….……...…...75

4.8 Evaluating the relationship between GBD and performance……..……...76

a) Cluster-level approach……..…….....76

b) Single-trial analysis……..……..……...76

4.9 Gamma-band large-scale correlation and anti-correlation analysis……...77

Chapter 5, **Results**

First study: Electrophysiological correlates of the default mode network

5.1 **Hypothesis and Comments about the study**…….…….79

5.2 Article: **Transient suppressions of broadband gamma power in the default-mode network is correlated with task complexity and subject performance**…….……..…..……..83

5.3 Supplementary information……...……..……...93

Chapter 6, Results

Second study**: Efficient 'pop-out' visual search elicits sustained broadband gamma activity in the dorsal attention network**

6.1 **Hypothesis and Comments about the study**…….……..……..95

6.2 Article…….…….……97

Chapter 7 Discussion

7.1 **General Discussion**……...…….…….125

7.2 **Electrophysiological correlate of the Default Mode Network**……...126

7.3 **Clinical implications of our first study**…….....129

7.4 Transient and sustained gamma band responses…….....131

7.5 Conclusions…….……137

Bibliography……..……...…139
Annexes ……..153

Acknowledgment

I am sincerely grateful to my advisor, Jean-Philippe Lachaux, for the support and guidance he showed me throughout my PhD. I owe sincere and earnest thankfulness to Jean-Philippe Lachaux, Karim Jerbi, Juan Vidal and Olivier Bertrand by their helpful discussions. I would like to show my gratitude to all the members of the laboratory INSERM 1028.

Finally, I would like to thank Tamara Olivero for her contribution and patience, and MIDEPLAN, Chile, by the fellowship Presidente de la Republica.

1.1 Introduction

At the beginning of the last century took place a conspicuous debate around the brain function, in which two main views emerged (Raichle, 2009). Sir Charles Sherrington (Sherrington, 1906), postulated that the brain is primarily reflexive, driven by the momentary demands of the environment. Thomas Graham Brown put forth a competing hypothesis that the brain's operations are mainly intrinsic, involving the acquisition and maintenance of information for interpreting, responding to, and even predicting environmental demands (Brown, 1911).

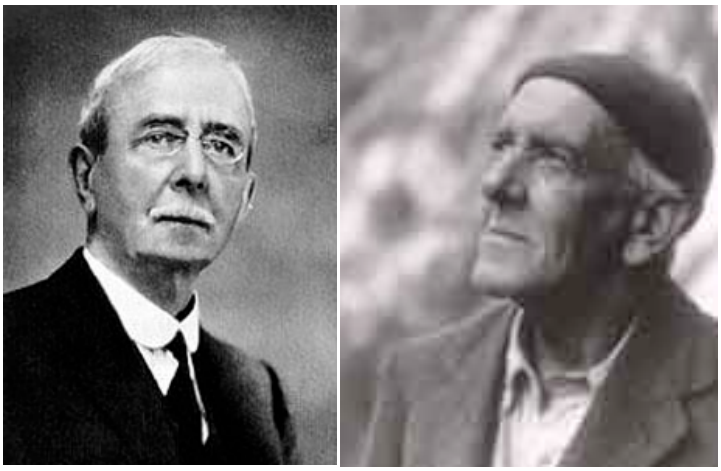

Figure 1: Portraits of Sir Charles Scott Sherrington (left) and Thomas Graham Brown.

In the seminal paper, '*On the nature of the fundamental activity of the nervous centres; together with an analysis on the conditioning rhythmic activity in progression, and a theory of the evolution of function in the nervous systems'*, Brown criticizes Sherrington's views of the reflex systems (T. G. Brown, 1911). According to Sherrington's interpretation, the reflex arc principally compensates the activity between an afferent and efferent limb. The arc that mediates this relation from periphery to periphery through is called the 'reflex arc'. That arc itself is usually regarded as built up of various subsidiary morphological units: the receptive organ, the afferent neuron, one or more interposed neurons, the efferent neuron, and the effectors organ (T. G. Brown, 1911; Sherrington, 1906). However, this vision is not valid for Brown for two principal reasons:

a) The first reason is that "*every afferent path tends, in its activity, to activate many efferent paths; and every path is activated by many afferent paths*", or in other words, the systems is more than a 'reflex arc' (T. G. Brown, 1911).

b) The phenomenon of 'narcosis progression'. In this phenomenon walking, running, or galloping movements may occur in all four limbs in cats under the influence of a general anesthetic. In other words, we can observe a rhythmical movement in the cat when the spinal reflexes are abolished (T. G. Brown, 1911).

In this sense, according to the Brown's view, the nervous system is composed by an intrinsic activity, with a rhythmicity that is disturbed by the reflex system.

A primarily reflexive brain has motivated most neuroscience research, principally because experiments designed to measure brain responses to controlled stimuli and carefully designed tasks can be rigorously controlled (D. Y. Zhang & Raichle, 2010). In fact, the tasks used in my thesis adopt this model. It does not surprise us the fact that several cognitive functions have been associated with specific patterns of activation in some brain regions.

Nevertheless, some works developed in the middle of the twentieth century propose a completely different point of view of the brain function. We will begin with the description of a classic article made by the Nobel Prize winner Roger W. Sperry, and developed and reinterpreted by Maturana et al. in the 1950s at the Massachusetts Institute of Technology (Lettvin, Maturana, McCulloch, & Pitts, 1959; Sperry, 1943). These experiments manipulated the optic nerve of tadpoles by rotating it with respect to the eye by 180 degrees. The tadpoles were then allowed to complete its larval development and metamorphosis into an adult frog. When a worm was presented with the rotated eye covered, the frog was able to perfectly strike it with its tongue. However, when the experiments was repeated with the normal eye covered instead, with the normal eye covered instead, the frog would miss every time, its tongue striking in the opposite direction of its intended target (Sperry, 1943; Maturana and Varela, 1980). A frog with such a rotated eye will always miss, with a deviation in aim equal to the rotation imposed by the experimenter.

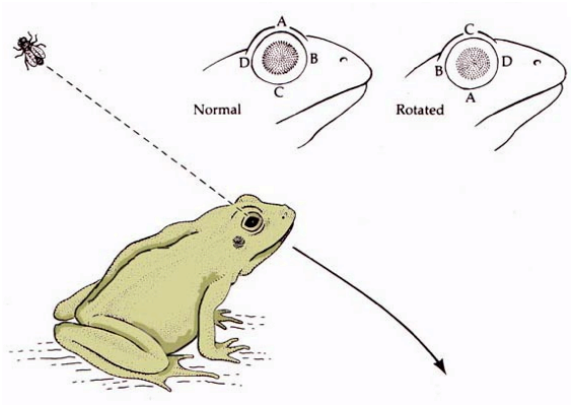

Figure 2. When the eye is rotated 180° the frog's prey catching behavior is inverted (From Sperry, 1943).

For Varela and Maturana this experiment "*reveals in a dramatic way that for the animal there is no such thing as up and down, front and back, in reference to an outside world, as it exists for the observer doing the experiment. There is only an internal correlation between the place where the retina receives a given perturbation and the muscular contractions that move the tongue, the mouth, the neck, and, in fact, the frog's entire body*" (Maturana and Varela, 1980).

According to these authors, as well as other experiments done since the 1950s, this finding can be direct evidence that the operation of the nervous systems is an expression of its connectivity and that behavior arises because of the nervous system's internal relations of activity (Maturana & Varela, 1970, 1980). Or, in other words, perception is not the precise reconstruction of an external world, because such properties depend on sensory motor coupling. Although the frog's action is indeed a reflex, its response is a reflex of its internal sensory-motor coupling.

Some years after the Sperry's experiment, Sokoloff and colleagues published an article that reinforces the notion that the nervous system is not only primarily reflexive (Sokoloff, Mangold, Wechsler, Kenney, & Kety, 1955). This group used the Kety-Schmidt nitrous oxide technique[1] to ask whether cerebral metabolism changes globally

[1] A method for measuring organ blood flow first applied to the brain in 1944 by C. F. Schmidt and S. S. Kety. A chemically inert indicator gas (in this case N2O) is equilibrated with the tissue of the organ of interest and the rate of disappearance from the organ is measured. Blood flow is calculated on the

when goes from a quiet rest state to performing a difficult arithmetic problem. To their surprise, metabolism remained constant in this task that demands focused cognitive effort. While their initial conclusion, the unchanged global rate of metabolism suggests that the rest state contains persistent brain activity that is as vigorous as that when individuals solve externally administrated math problems (Buckner & Carroll, 2007). This paper was the first to show that there are not large differences between the brain activity during undirected mentation and demanding cognitive task. We know today that, depending to the approach used, it is estimated that 60% to 80 % of the brain's enormous energy budget is used to support communication among neurons, functional activity by definition (Raichle & Snyder, 2007). The additional energy burden associated with momentary demands of the environment may be as little as 0.5% to 1% of the total energy budget (Raichle & Mintun, 2006; Raichle, 2010). This cost-based analysis alone implies that intrinsic activity may be at least as important as evoked activity in understanding overall brain function (Raichle & Snyder, 2007; Raichle, 2010). The experiments explained before really were exceptions in the exponential development of the neuroscience during the past century. In the third chapter of this thesis I develop the history of a sub-area, the visual attention.

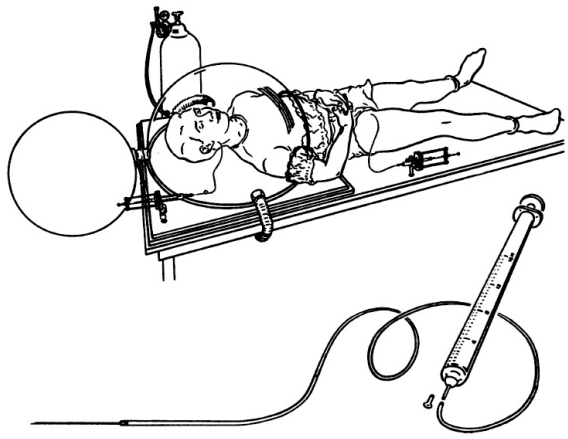

Figure 3: Scheme of the apparatus used by Sokoloff and colleagues (From (Sokoloff et al., 1955).

assumption that the tissue and venous blood concentrations of the indicator gas are in diffusion equilibrium at all blood flow rates and that the rate of disappearance of the indicator from the tissue is a function of how much is in the tissue at any time (it is assumed to be an exponential disappearance).

1.2. A brief history of the DMN

Two decades later to the Solokoff's results, the Swedish physiologist Davis Ingvar aggregate imaging findings from the rest task states and note the importance of consistent, regionally specific activity patterns, using the xenon 133 inhalation technique[2] to measure regional cerebral blood flown (rCBF). Ingvar and his colleagues observed a frontal activity that showed high levels during rest states. Ingvar proposed, to explain this unexpected phenomenon, that the hyperfrontal pattern of activity corresponded to undirected, spontaneous, conscious mentation, or in other words, "*the brain work which we carry out when left alone undisturbed*" (Buckner, Andrews-Hanna, & Schacter, 2008; Ingvar, 1979).

Despite the background information provided by Solokoff and Ingvar, the study related to the neural correlate of unconstrained states was neglected during several decades. However, this phenomenon drastically changed by an accidental discovery. The evidence began accumulating when researchers first measured brain activity during undirected mental states (Binder et al., 1999; Buckner et al., 2008; Raichle & Snyder, 2007; Shulman, Fiez et al., 1997). Even though no early studies were explicitly designed to explore unconstrained states, relevant data were nonetheless acquired because of the common practice of using rest or other types of passive conditions as an experimental control. These studies revealed that the activity in specific brain regions increased during passive control states as compared to most goal-directed tasks (Binder et al., 1999; Buckner & Carroll, 2007; Shulman, Fiez et al., 1997). In almost all cases, the exploration of activity during the control states occurred as an afterthought-as a part of reviews and meta-analyses performed subsequent to the original reports, which focused on the goal-directed tasks.

[2] Gamma emission from the radioisotope ^{133}Xe of xenon can be used to image the heart, lungs, and brain, for example, by means of single photon emission computed tomography (SPECT).

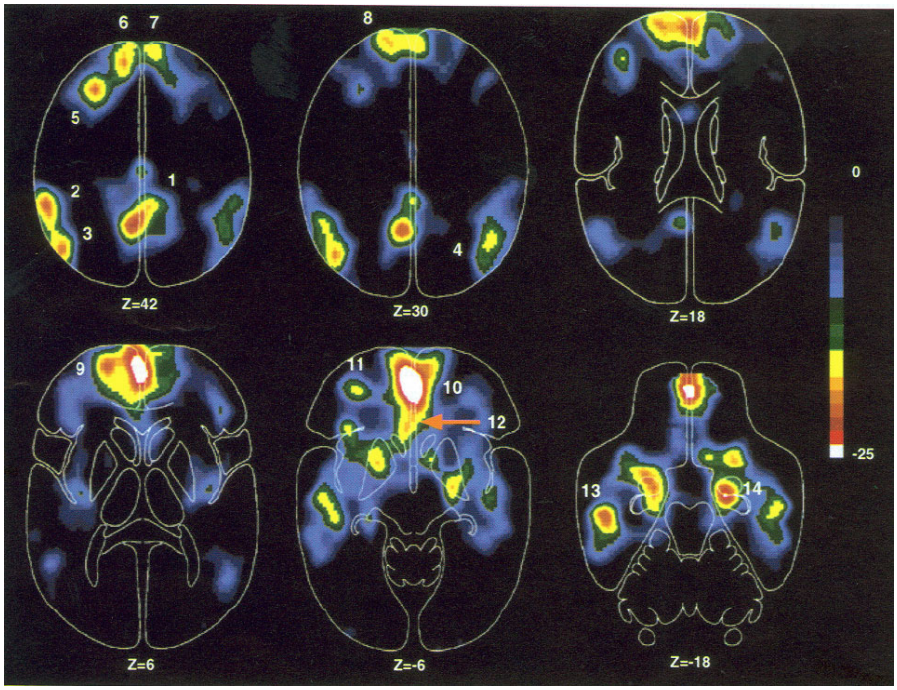

Area	Focus No.
Parietal Lobe	
31	
31/7	1
L 40	2
L 40	
L 39/19	3
R 40	4
Frontal Lobe	
L lateral 8	5
L 8/9	6
R 8/9	7
L 9	8
L 10	9
10 (superior)	
10	10
L 10/47	11
32	12
Temporal Lobe	
L 20	13
L amygdala	
R amygdala	14

Figure 4: Blood flow decrease in an overall megaimage that average the active minus passive scan pairs from many goal-directed tasks (From Shulman et al, 1997). Numbers indicate the 14 foci illustrated in the table.

Because of their intrinsically elevated baseline activity during rest, distinct brain regions that show systematic task-related deactivation collectively form a network known as the default-mode network (Gusnard & Raichle, 2001; Raichle et al., 2001). This concept, which was received with great skepticism by the community, breaks one of the cornerstones of neuroscience, an assumption that the period prior to a task, named baseline, is a neutral state, with low energy, that can be safely subtracted from a brain region to obtain the neural correlate of a specific behavior.

The first criticism that comes up with this result is related to the redistribution of cerebral blood supply (Shulman, Fiez et al., 1997). The apparent constancy of the blood supply to the brain had led to suggestions that large blood increases in some areas may require decreases in other areas (Haxby et al., 1994; Shulman, Fiez et al., 1997). Nevertheless, decreases were often not accompanied by increases in neighboring regions (Shulman, Fiez et al., 1997). The second main criticism is related to 'active decreases', because

active tasks may produce decreases in neural activity within an area that is tonically active. i.e. the tonic activity of neurons in the substantia nigra pars reticulata is decreased during a saccade (Hikosaka & Wurtz, 1983; Shulman, Fiez et al., 1997). Similarly, an active task may inhibit a primary area that would normally respond in the task environment. For instance, performance of a difficult visual discrimination in the presence of distracting auditory transient might produce inhibition of ongoing activity in auditory areas (Haxby et al., 1994; Shulman, Fiez et al., 1997).

In these examples, different tasks decreased neural activity in different areas. However, and how we will develop later, deactivations in the default mode network during a goal-directed behavior are largely tasks-independent.

The default mode network (DMN) concept although only first introduced into the published literature in 2001 (Raichle et al., 2001) has rapidly become a central theme in contemporary cognitive and clinical neurosciences (Andrews-Hanna, Reidler, Huang, & Buckner; Broyd et al., 2009; Castellanos et al., 2008; Gujar, Yoo, Hu, & Walker; Raichle, 2010; van Eimeren, Monchi, Ballanger, & Strafella, 2009). After a decade of studies, we can summarize **the principal characteristics of the DMN** as follows (adapted from Broyd et al., 2009):

1. During goal-directed activity some regions of the brain show task-non-specific deactivations (this is the origin of the concept "task-negative network").
2. The energy of this network varies in a coherent manner at rest (coherence and functional connectivity within the DMN).
3. This energy fluctuation is characterized by low frequency BOLD signal.
4. There is an anti-correlation between this task-negative and the task-positive networks at rest.

These four points are detailed below:

1.2.1 Regional task non-specific deactivations during goal-directed activity

Converging neuroimaging evidence supports the view that attention-demanding goal-directed behavior is mediated not only by distributed patterns of cerebral activation but,

remarkably, also by concurrent suppression of activity in specific brain regions (Shulman et al., 1997; Raichle et al., 2001), even when the control state consists of lying quietly with the eyes closed or passively viewing a stimulus (Raichle et al., 2001). As we have mentioned, whereas cortical increases in activity have been shown to be task specific and, therefore, vary in location depending of the task demands, many decreases appear to be largely task-independent (Raichle et al, 2001). This task-negative networks comprise the posterior cingulate cortex (PCC) / Precuneus (PrCC), medial prefrontal cortex (MPFC), lateral temporal cortex (LTC), and temporal parietal junction (TPJ)[3]. As we can see in the next figure, the brain regions that show a goal-directed deactivation are the regions that consume more oxygen during the rest. From these results (Raichle et al., 2001), the authors suggested the existence of an organized, baseline default mode of the brain function that is suspended during specific goal-directed behaviors.

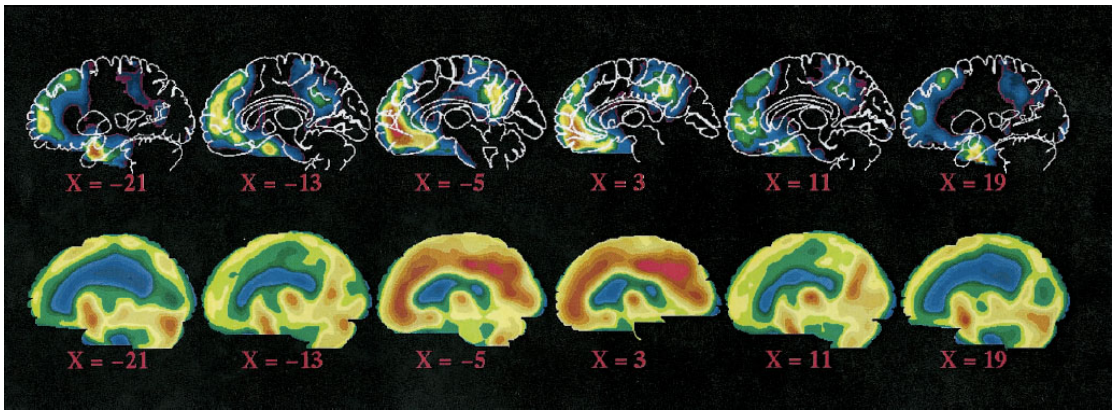

Figure 5: Regions of the brain regularly observed to decrease their activity during attention demanding cognitive tasks shows in sagittal projection (Upper) as compared with the blood flow of the brain while the subject rest quietly but awake with eyes closed (Lower). From Raichle et al., 2001.

1.2.2 Coherence and functional connectivity within the DMN

How are different brain regions functionally connected? This question has become one of the most widely explored topics in the last decade. To introduce this subject, we shall summarize some basic principles of functional connectivity. Principles of functional

[3] At the end of this chapter these regions are detailed.

magnetic resonance imaging (fMRI) and the blood oxygen level dependent (BOLD) signal will be presented in the second chapter.

Functional connectivity simply refers to the temporal correlation between fluctuations in the BOLD signal of discrete anatomical regions[4] (M. D. Fox et al., 2005). Or, more technically, the functional connectivity search patterns of statistical dependence between often-remote neural units or brain regions (Friston, Frith, Liddle, & Frackowiak, 1993; Sporns & Tononi, 2008). With the purpose of simplification of this concept we can think of the functional connectivity as a statistical concept that captures deviations from statistical independence (measuring correlation or covariance) between distributed brain regions across the time. In its most general form, statistical dependence is expressed as an estimate of mutual information (Sporns & Tononi, 2008). Unlike correlation, which is a linear measure of association, mutual information captures all linear or nonlinear relationships between variables.

One of the most robust characteristics of the DMN is the high level of functional connectivity during the rest (B. B. Biswal et al., 2010; Castellanos et al., 2008; Greicius, Krasnow, Reiss, & Menon, 2003). In the next figure we show one of the classical results in the DMN literature, that compares the connectivity across this network during a visual processing task and rest (Greicius et al., 2003).

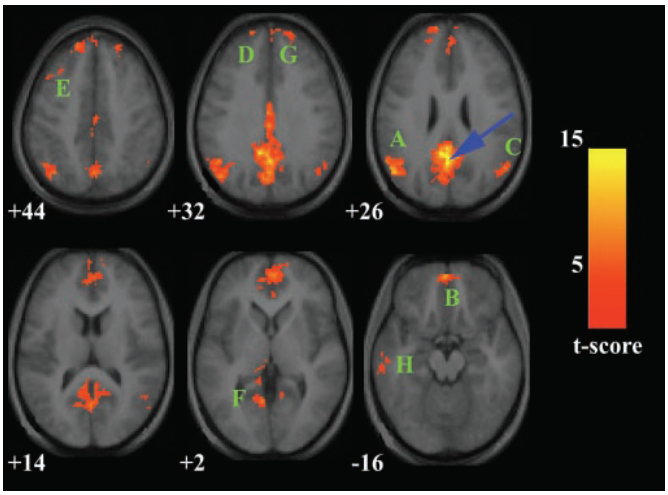

Figure 6: Comparison of the Posterior Cingulate Cortex (PCC) connectivity patterns during the visual processing task (Upper) and the resting-state (Lower). (From Greicius et al., 2003). We can see in this figure that resting PCC connectivity patterns remain constant during the visual processing.

[4] We can also study functional connectivity with PET, MEG, EEG and intracranial EEG.

1.2.3 DMN characterized by low frequency BOLD signal

Spontaneous activity, as measured with blood oxygen level-dependent (BOLD) functional MRI (fMRI) in the resting awake[5] or anesthetized brain, **is organized in multiple highly specific functional anatomical networks, called resting state networks**, RSNs (B. B. Biswal et al., 2010; Mantini, Perrucci, Del Gratta, Romani, & Corbetta, 2007). These RSNs fluctuate at frequencies between 0.01 and 0.1 Hz, and exhibits striking patterns of coherence within known brain systems (Raichle & Snyder, 2007). One point that we can emphasize is the following: although RSNs patterns of coherence do respect patterns of anatomical connectivity in both the monkey (Vincent et al., 2007) and human brain (D. Zhang et al., 2008), it is clear that they are not constrained by these anatomical connections (Raichle, 2010). Thus, the absence of monosynaptic connections between brain areas, e.g., right and left primary visual cortex (Vincent et al., 2007), does not preclude the existence of functional connectivity as expressed in the maps of resting state coherence (Raichle, 2010).

Here we describe the principals resting state networks (RSNs):

RSN 1: a network corresponding to **DMN**. Putatively associated with internal processing (Buckner & Carroll, 2007; Greicius et al., 2003; Raichle et al., 2001). This networks involves the posterior cinculate/precuneus, medial frontal gyrus, and bilateral inferior parietal lobule.

RSN 2: corresponding the **dorsal attention network** mediating goal stimulus-response selection (Corbetta, Patel, & Shulman, 2008; Mantini et al., 2007). The brain regions include in this network are the intraparietal sulcus (bilateral), the intersection of the

[5] We can define the resting state as a behavioral state characterized by relaxed wakefulness usually with eyes closed but occasionally, in the experimental setting, with eyes open with or without visual fixation (Gusnard & Raichle, 2001; Laufs et al., 2003; Raichle, 2010) We presume that during the resting state subjects experience an ongoing state of conscious awareness largely filled with stimulus-independent thoughts (or, more popularly, day dreaming or mind wandering). It is important to distinguish between the resting state, defined behaviorally, and the state of the brain that accompanies the resting state. The brain is never physiologically at rest as evidenced by ongoing intrinsic activity and a very high-energy consumption that varies little between the resting state and engagement in attention-demanding tasks (Raichle, 2010).

precentral and superior frontal sulcus (near the human frontal eye field), and the middle frontal gyrus (dorsolateral prefrontal cortex, DLPFC).

RSN 3: a **visual posterior network**, involving the retinotopic occipital cortex and the temporal-parietal regions including human MT (Lowe, Mock, & Sorenson, 1998; Mantini et al., 2007).

RSN 4: corresponding to **the auditory-phonological** system, and including the bilateral superior temporal cortex (Biswal et al., 1997).

RSN 5: a **motor network**, including the precentral, postcentral, and medial frontal gyri, the primary sensory-motor cortex and the supplementary motor area (B. Biswal, Yetkin, Haughton, & Hyde, 1995; Mantini et al., 2007).

RSN 6: network related to **self-referential mental activity** (D'Argembeau et al., 2005), including the medial-ventral prefrontal cortex, the pregenual anterior cingulate, the hypothalamus, and the cerebellum.

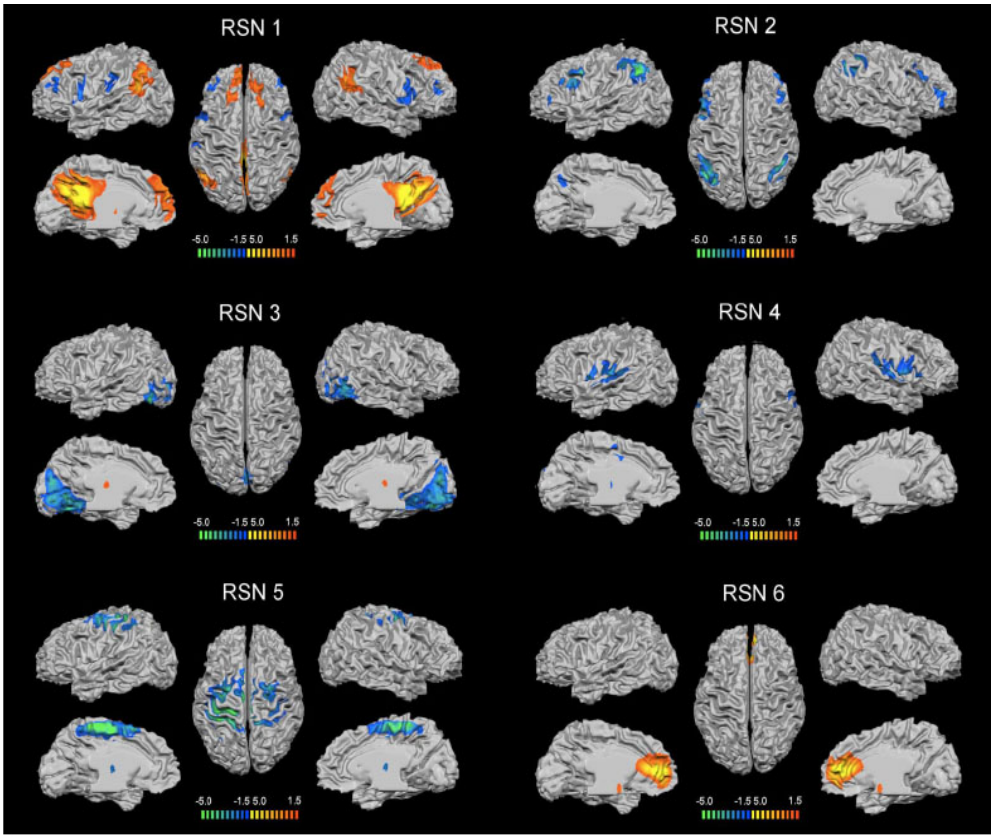

Figure 7: Cortical representation of the six RSNs. From Mantini et al., 2001

1.2.4 Anti-correlated task-positive and task-negative resting networks

In the resting state the brain activity incorporate both task-negative and task-positive components (Broyd et al., 2009). The **DMN (RSN 1) has been described as a task-negative network** given antagonism between its activation and task performance. On the other hand, **the dorsal attention network (RSN 2) has been described as task-positive network**, because appears to be associated with task-related patterns of increased alertness, and has also been related to response preparation and selection (Broyd et al., 2009; M. D. Fox et al., 2005; M. D. Fox, Corbetta, Snyder, Vincent, & Raichle, 2006; Fransson, 2005, 2006; Sonuga-Barke & Castellanos, 2007). Remarkably, the task-positive network and the DMN are temporally anti-correlated during the resting, and the high degree of temporal anti-correlation emphasizes the potential degree of antagonism between these two networks and the psychological functions that reflect (Sonuga-Barke & Castellanos, 2007).

In the next figure, we show a figure of a classic work (M. D. Fox et al., 2005), where we can summarize the concept of functional connectivity and anti-correlation.

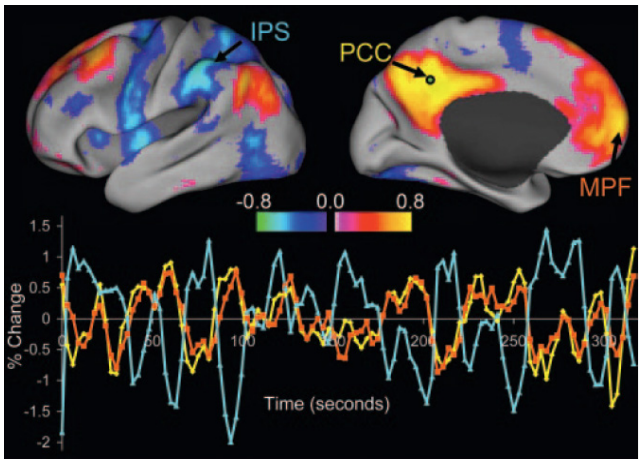

Figure 8: Intrinsic correlation between a seed region in the PCC and the other voxels in the brain for a single subject during resting fixation. The spatial distribution of correlation coefficients shows both correlations (positives values, in red) and anticorrelations (negatives values, blue). The time course for a single run is shown for the seed region (PCC, yellow), a region positively correlated with this seed in the MPFC (orange), and a region negatively correlated with the seed region in the IPS (blue). From Fox et al, 2005.

1.3 A new view of the brain function

As we mentioned in the first paragraph of this thesis, we can return to the old discussion of the brain function. Nevertheless, thanks to the advance of the imaging techniques, and especial to the discovery and robustness of the resting state networks, we can reformulate almost all the questions that have been developed in the field, from *what are the neural correlates of a particular behavior,* to, *how is intrinsic activity modulated by particular behavior?*

1.3.1 Functional role of the Default Mode Network

We have seen throughout this chapter that spontaneous activity (measured with BOLD) in the resting brain is organized in multiple functional networks (RSNs). In order to develop this thesis, we need to emphasize the role and characteristics of one of these, the DMN, or task-negative network, that is deactivated during task performances, and shows a high oxygen consumption during the rest with a high degree of functional connectivity (Raichle et al., 2001; Broyd et al., 2009). To understand the functional role of the DMN, we can develop two ideas:

a) First, the relation between the pattern of deactivation in the DMN and the degree of attention demanding. Recent articles deepen this issue. McKiernan and colleagues manipulated cognitive load using an auditory working-memory task and detected an increasing magnitude of deactivation in the DMN with increasing task difficulty. In other words, **the more demanding the task the stronger, the deactivation appears to be in the DMN** (McKiernan, Kaufman, Kucera-Thompson, & Binder, 2003; McKiernan, D'Angelo, Kaufman, & Binder, 2006; Singh & Fawcett, 2008). In the next figure we illustrate this important point:

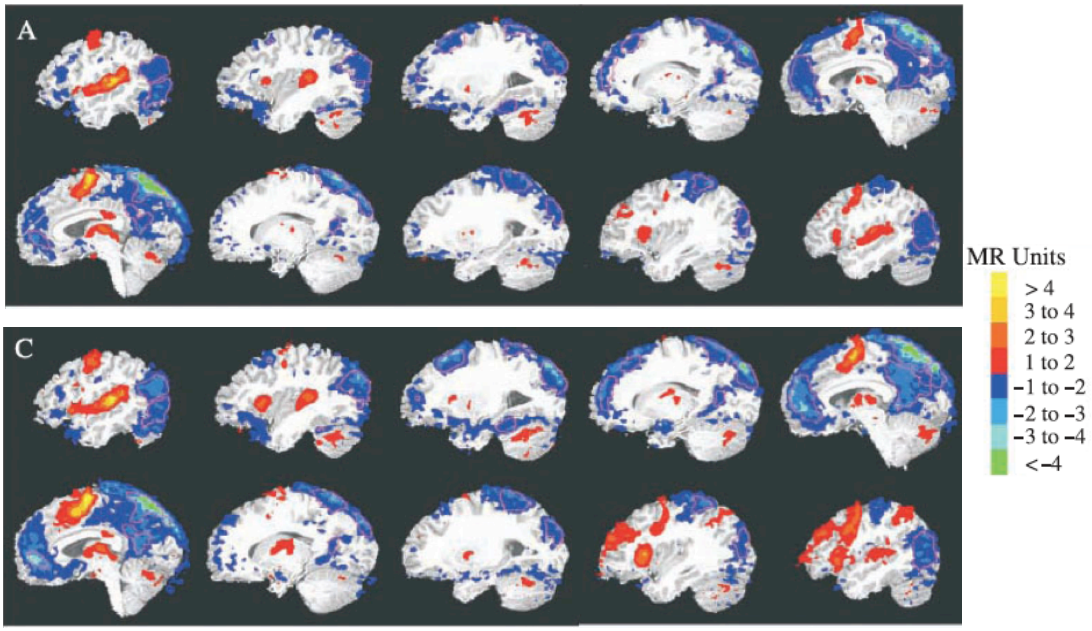

Figure 9: Magnitude of deactivation (and activation) as measured by fit coefficients averaged across 30 subjects within each ROI by condition. Each panel represents the magnitude of deactivation during: (A) easy task of stimulus discriminability, with moderate level for presentation rate; and (C) difficult level of stimulus discriminability with fastest stimulus presentation rate. From McKiernan et al., 2003.

The second point that we can explore for understanding the functional role of the DMN arise in a subgroup of tasks that are not associated to a deactivation in the DMN, but rather, with activation. A notable exception to this pattern of deactivation during goal-directed activity occurs in relation to tasks requiring self-referential thought where only specific DMN regions are specifically activated, i.e.: tasks involving judgments that were self-referential (Broyd et al., 2009; Gusnard, Akbudak, Shulman, & Raichle, 2001) resulted in increased activity in the dorsal MPFC, while the activity in the ventral MPFC is attenuated (Gusnard et al., 2001). In the same way, an increase in the PCC activity has been associated with increasing working memory load (Esposito et al., 2006). These results suggest that some brain regions of the DMN are associated with introspective thought (Buckner & Carroll, 2007).

In the same sense, some authors observed the behavioral competition between task-focused attention and processes subserving stimulus-independent thought. During

performance of cognitive tasks, thoughts occasionally emerge unrelated to the task or goal (M. D. Fox et al., 2005; Simpson, Snyder, Gusnard, & Raichle, 2001). The more stimulus-independent thoughts that occur during a task session, the worse the subject's performance (M. D. Fox et al., 2005). Conversely, increasing the difficulty and attentional demand of the task results in fewer stimulus-independent thoughts (M. D. Fox et al., 2005). Given this and other evidence, the principal functional interpretation that we done to DMN denote in the control of a state in which an individual is awake and alert, but not actively involved in an attention demanding or goal-directed task.

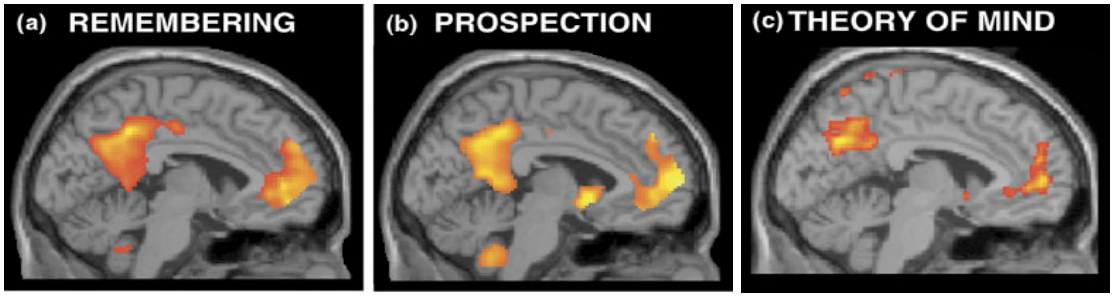

Figure 10: Brain activation during three forms of self-projection. Each image displays the midline of the left hemisphere with brighter colors, indicating regions of increased activation. Note the remarkable similarity between the default regions and those engaged during self-projection. From Buckner and Carroll, 2007.

In conclusion, the broad range of exogenous stimuli that cause deactivation in DMN related areas lead to the view that endogenous processes need to be inhibited for the successful execution of a task (Buckner and Carroll, 2007; Broyd et al., 2009; Raichle, 2010). This suppression of internal mental activity is thought to enable the reallocation of attentional resources from internal processes to goal-directed behavior (Gilbert, Dumontheil, Simons, Frith, & Burgess, 2007; Mason et al., 2007). As discussed earlier, these results opened the door to the study of unconstrained states, present during rest and modulated in a goal-directed behavior, e.g., monitoring of the body image, unconstrained verbal thought or monitoring the external environment. As we will discuss below, some researchers consider the DMN, as a system in the same way we might think of the motor or visual system (Raichle, 2010).

1.3.2 Anatomic considerations about the DMN

We had mentioned that the regions that make up the DMN comprise principally the posterior cingulated cortex (and the adjacent precuneus), the medial prefrontal cortex, and the posterior lateral cortex. Then, we summarize in anatomical and physiological terms the main characteristics of these regions. In order to facilitate the description, we illustrate the Brodmann Areas in the Human Brain.

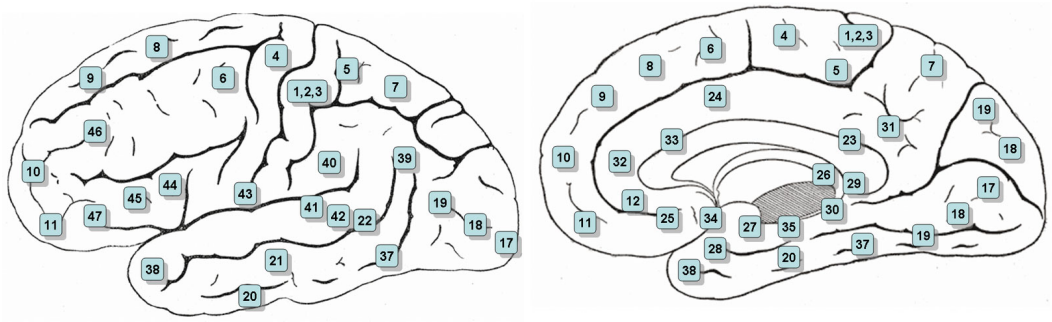

Figure 11: Lateral and Medial surface of the brain with Brodmann's areas (BA) numbered. Kornibian Brodmann (1868-1918) was an anatomist who divided the cerebral cortex into numbered subdivisions based on cell arrangements, types, and staining propierties.

1.3.2.a Posterior Cingulate Cortex/ Precuneus

Cytoarchitectonically the posterior cingulate cortex (PCC) is associated with Brodmann areas 23 and 31, while the precuneus (PrCC) is associated with area 7. These regions remain some of the less precisely mapped areas of the whole cortical surface (Vogt & Laureys, 2005).

We highlight three main features about the PCC/PrCC: The first characteristic is anatomical; PrCC has reciprocal corticocortical connections with the PCC and retrosplenial cortices. This intimate interconnection is also bilateral, bridging homologous components of the two hemispheres, and to some extent providing an anatomical basis for their functional coupling (Cavanna & Trimble, 2006). PrCC is also selectively connected with other parietal areas, namely the caudal parietal operculum, the inferior and superior parietal lobules (SPLs), and the IPS, known to be involved in visuo-spatial information

processing (Cavada & Goldman-Rakic, 1989; Cavanna & Trimble, 2006; Leichnetz, 2001; Selemon & Goldman-Rakic, 1988). As we illustrated in Figure 12, the PrCC has cortical and subcortical connections, most of which are bidirectional.

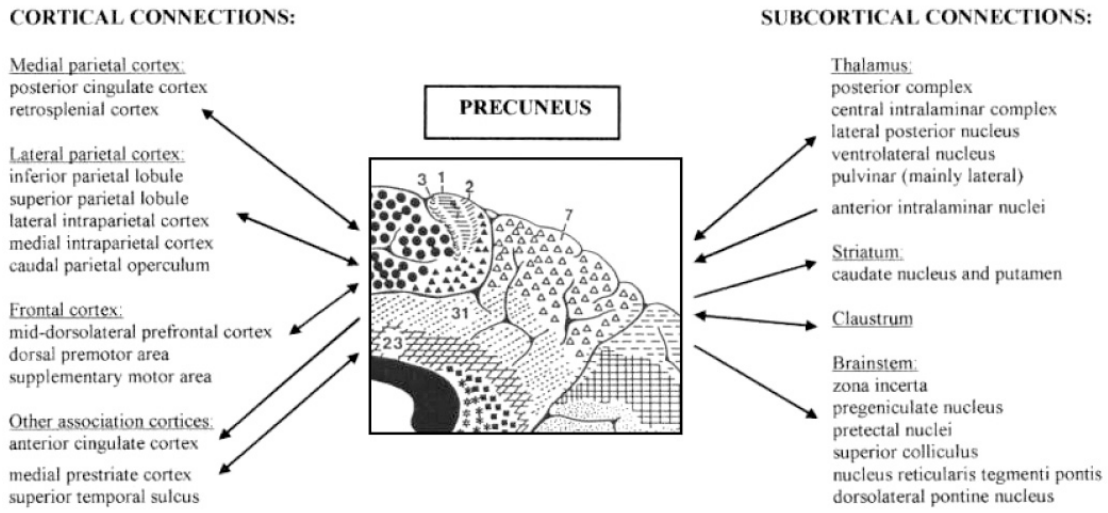

Figure 12: Summary of the cortical (left) and subcortical (right) connections of the precuneus. Bidirectional arrows indicate reciprocal projections; unidirectional arrows indicate afferent/efferent projections. From Cavanna and Trimble, 2006.

The second main characteristic of these regions is their particular metabolism. The PCC/PrCC has the highest level of metabolism in human brain (Andreasen et al., 1995; Maquet, 1997; Minoshima et al., 1997; Vogt & Laureys, 2005). Finally, the third main feature is behavioral. PrCC and PCC are involved in episodic memory retrieval (D'Argembeau et al., 2010; Greicius, Supekar, Menon, & Dougherty, 2009; Ries et al., 2006; Shannon & Buckner, 2004; Szpunar, Chan, & McDermott, 2009), self-processing (D'Argembeau et al., 2010; J. M. Moran, Lee, & Gabrieli, 2010; Ries et al., 2006), consciousness (Cavanna & Trimble, 2006; Vogt & Laureys, 2005), and visuo-spatial imagery[6]. These studies suggest that the precuneneus and the posterior cingulated cortex play an important role in a diverse array of highly integrated functions that can no longer

[6] Some experiments have shown that the PrCC is more responsive during motor imagery than during real execution of joystick and finger movements (Stephan et al., 2005; Cavanna, 2006).

be regarded as a simple extension of the visual-spatial processes subserved by the lateral parietal cortices (Cavanna & Trimble, 2006).

1.3.2.b Medial prefrontal cortex (MPFC):

a) Ventral MPFC

Among the areas most prominently exhibiting a deactivation during a goal-directed behavior is medial prefrontal cortex (MPFC) (Gusnard et al., 2001). The MPFC areas involved often include elements of both its dorsal and ventral aspect. Dorsally, when decreases are observed, they tend to spare the cingulated cortex, which usually exhibits an increase activity during attention-demanding tasks (Gusnard & Raichle, 2001).

The ventromedial prefrontal cortex has been described as equivalent to Brodmann area 10. Sometimes, the term is saved for the area above the medial orbitofrontal cortex, while at other times, 'ventromedial prefrontal cortex' is used to describe a broad area in the lower (ventral) central (medial) region of the prefrontal cortex, of which the medial orbitofrontal cortex constitutes the lowermost part. The orbitofrontal cortex (OFC) is composed of cytoarchitectonically discrete areas that receive a range of sensory information from the body and external environment (Gusnard & Raichle, 2001). This information is relayed to the ventral MPFC through a complex set of interconnections. Ventral MPFC also heavily connect to limbic structures, such the amygdala, ventral striatum, hypothalamus, and brainstem autonomic nuclei (Doron & Moulding, 2009; Sheline, Price, Yan, & Mintun, 2010; Shu, Wu, Bao, & Leonard, 2003). Because these anatomical data implicate ventral MPFC in aspects of emotional processing, it has been suggested that decreases in this area during focused attention might reflect a dynamic interplay between continuous cognitive and emotional processes, as shown in many functional imaging studies (Gusnard & Raichle, 2001; Shulman, Fiez et al., 1997).

b) Dorsal MPFC

The dorsal MPFC often decreases its activity together with the ventral MPFC during goal-directed activities (Gusnard & Raichle, 2001); however, both activities can sometimes be dissociated. In some occasions, dorsal MPFC (BA 8, 9 and 10) present an increase above baseline in its activity. The cognitive processes that are covered fall into two general categories. The first involves monitoring or reporting one's own mental states, such as self-generated thoughts (Gusnard & Raichle, 2001; McGuire, Paulesu, Frackowiak, & Frith, 1996; Pardo, Pardo, & Raichle, 1993), intended speech and emotions (Frith & Frith, 1999; Gusnard & Raichle, 2001; Pardo et al., 1993). A second category of experiments that engage this region involves attributing mental states to others, or explicit representations of states of self (Frith & Frith, 1999).

Similar mental activity arises spontaneously when subjects are not actively engaged in goal-directed behaviors, i.e., stimulus-independent thoughts (or daydreams) (Burgess, Dumontheil, & Gilbert, 2007) and task-unrelated imagery and thought (Giambra, 1995).

1.3.2.c Posterior lateral cortices

Task-independent decreases in the posterior lateral cortex occur bilaterally in BA 40 and 39 (parietal lobe), and in BA 22 (temporal lobe) and 19 (occipital lobe) (Gusnard & Raichle, 2001; Raichle et al., 2001; Shulman, Fiez et al., 1997). In order to describe these regions, we need necessarily to make a differentiation between the DMN and the ventral attention network (VAN). Corbetta and collaborators have developed a detailed work about this network, that comprise the supramarginal gyrus, the superior temporal gyrus (or temporal parietal junction, TPJ), and middle and inferior prefrontal cortex (Corbetta & Shulman, 2002a; Corbetta et al., 2008). As with the DMN, we can observe a sustained deactivation in VAN when we focus the attention in an object. In contrast to the DMN, when an unexpected but important event evokes a reorienting of attention these region are transiently activated (Corbetta et al., 2008). In the next figure we illustrate this point.

Figure 13: Focusing attention on an object (Left panel) produces sustained deactivations in ventral regions as supramarginal gyrus, superior temporal gyrus (TPJ), and middle and inferior prefrontal cortex (blue colors), but sustained activations in dorsal fronto-parietal regions in the intraparietal sulcus, superior parietal lobe, frontal eye fields, as well as visual regions in the occipital cortex (yellow and orange colors). When an unexpected but important event evokes a reorienting of attention, both the dorsal regions and the formerly deactivated ventral regions are now transiently activated (Right panel). From Corbetta et al. (2008).

Following the argument of these authors, this ventral frontoparietal network detects salient and behaviorally relevant stimuli in the environment, especially when unattended (Corbetta et al., 2008). This system, VAN, dynamically interacts during normal perception to determine where and what we attend to. See Figure 14 for an illustration.

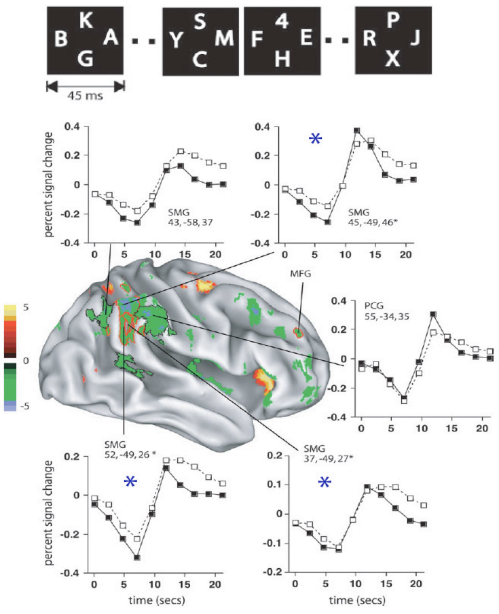

Figure 14: (A) Stimulus display of a task in which the subjects must detect a digit among letters during a rapid serial visual presentation sequence. (B) Voxels that showed significant search-related deactivation (green colors) and search-related activations (warm colors). Temporo-parietal junction (TPJ) ROIs that showed a significant mean BOLD-detection (after 7 seconds) relationship are indicated by an asterisk. In this figure we can see the fine dissociation between VAN and DMN areas along the posterior lateral cortices. While the supramarginal gyrus (VAN) is transiently activated during target detection, the angular and postcentarl gyrus (DMN) is not. From (Shulman, Astafiev, McAvoy, d'Avossa, & Corbetta, 2007).

1.3.2.d Rostral prefrontal cortex (BA 10, 47, 12)

The study of the functions of rostral prefrontal cortex presents one of the greatest scientific puzzles to cognitive neuroscience (Burgess et al., 2007). An interesting hypothesis, '*the gateway hypothesis*', has been developed by Sam Gilbert and Paul Burgess. According these authors, the rostral prefrontal (lateral and medial) cortex plays a crucial role in the switch between stimulus-oriented and stimulus-independent thought. Nevertheless, a key to this puzzle is the role of the ventral lateral prefrontal cortex (VLPFC), which is unfortunately difficult to record with imaging techniques due to slow signal-to-noise ratio (G. G. Brown & Eyler, 2006; Burdette, Durden, Elster, & Yen, 2001; Robinson & Milanfar, 2004)[7].

Finally, it would be good to emphasize that methodologically; most of the results described above rely on human imaging and more specifically on fMRI. However, because the BOLD response in fMRI is rather sluggish, clear-cut experimental separation between RSNs and stimulus-induced activity changes can be difficult (Northoff, Qin, & Nakao, 2010). Hence, techniques other than fMRI could be more suitable or RSNs studies: for instance, the background noise in EEG or MEG recordings is not as extensive as in fMRI. Finally, one can discuss the functional correlates of RSNs. Do high RSNs merely reflect suspension of functional activity, or do they instead represent some specific functions that are continuously operating in the background? This shall be the main question developed in this dissertation.

[7] The different physiological compartments of the head—brain, cerebrospinal fluid, bone, and air—are characterized by different magnetizabilities, i.e., by different magnetic susceptibilities (Elster & Burdette 2001). Boundaries involving the air and brain compartments, in particular, will be sites of broad magnetic field gradients that will offset the precessing frequency from the target frequency and dephase spins, reducing the MR signal. This dephasing causes signal dropout, **especially in the orbitofrontal and anterior medial temporal regions**, adjacent to nasal sinuses, or lateral temporal regions adjacent to the auditory canal. In all of these regions, the air-brain boundaries cause relatively strong magnetic gradients across large portions of the head. These strong magnetic gradients diminish in areas of signal dropout and greatly reduce the signal-to-noise ratio (Robinson et al., 2004; Brown & Eyler, 2006).

2. Neurophysiological basis of the fMRI signals

As we have seen in the first chapter, spontaneous slow fluctuations in the blood-oxygen-level-dependence (BOLD) signals of fMRI appear to reflect a fundamental aspect of brain organization (B. Biswal et al., 1995; He, Snyder, Zempel, Smyth, & Raichle, 2008; Vincent et al., 2007). These fluctuations temporally covary within large-scale functional brain networks, i.e. attention (M. D. Fox et al., 2006), sensorimotor (B. Biswal et al., 1995) and DMN (B. B. Biswal et al., 2010; Castellanos et al., 2008; Greicius et al., 2003). But, unlike the BOLD response, the electrophysiological correlate of these spontaneous covariant BOLD fluctuations (or resting state networks, RSNs) is relatively unknown (He et al., 2008; Laufs et al., 2003). Then, throughout this chapter we will try to answer the following question: How might the integrative and signaling aspects of neuronal activity individually contribute to the BOLD signal? Let us begin with a general overview of brain imaging techniques.

2.1.a General overview

Brain imaging includes the use of various techniques to either directly or indirectly image the brain and falls into two broad categories: structural imaging and functional imaging. Structural imaging is used to measure brain volume or the volume of sub regions, or to look at diffuse changes in grey or white matter or to assess localized lesions. Functional imaging detects changes in regional cerebral blood flow or metabolism as an indirect measure of neural activity. This can be used to map patterns of brain activity that corresponds to various mental operations (Huettel, Song, & McCarthy, 2008).

Common techniques used for structural imaging are computed tomography (CT) or magnetic resonance imaging (MRI). For functional brain imaging there are several techniques; usually, the choice is based on weather high temporal versus high spatial resolution is of main interest.

In contrast, the hemodynamic techniques, positron emission tomography (PET) and functional magnetic resonance imaging (fMRI), measure neuronal activity indirectly through the associated changes in metabolism or blood flow. They provide a relatively high spatial resolution (1-10 mm) but rather low temporal resolution (hundreds of milliseconds for fMRI, several seconds for PET), being limited by the rate of the much slower homodynamic changes that accompany neuronal activation.

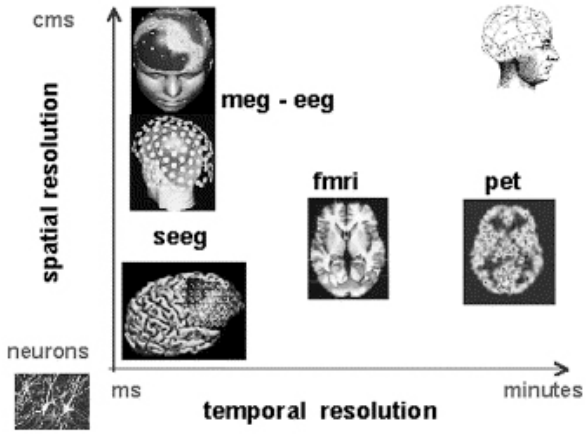

Figure 15: Spatio-temporal resolution of the major brain imaging techniques. IEEG combines the temporal resolution of MEG and EEG with a spatial resolution close to that of fMRI and PET (from (Lachaux, Rudrauf, & Kahane, 2003a).

2.1.b Functional MRI:

fMRI detects changes in regional cerebral blood flow (rCBF) as an indirect measure of neuronal activity. The basis for this inference is an assumption of a roughly linear coupling between neural activity, metabolic activity, and rCBF (Logothetis, Pauls, Augath, Trinath, & Oeltermann, 2001; Scannell & Young, 1999). In other words, increases in neural activity in a given brain region will increase the energy consumption, which in turns implies increased blood flow in order to supply the neurons with glucose and oxygen. However, for unknown reasons, the increased supply of oxygenated blood exceeds oxygen utilization (P. T. Fox & Raichle, 1986). As a consequence, the ratio of oxygenated to deoxygenated blood will be higher than normal in areas of increased metabolism. Oxygenated hemoglobin is diamagnetic (essentially nonmagnetic) whereas deoxygenated hemoglobin is paramagnetic, meaning that deoxyhemoglobin disturbs the

applied magnetic field more than oxyhaemoglobin does. Thus, as a relative amount of deoxyhemoglobin decreases in activated brain areas – due to disproportionate increases in blood flow – the MR signal increases. This effect is termed the BOLD (blood-oxygen-level-dependent) effect (Ogawa et al., 1992) and is the major source of contrast in most fMRI experiments (Huettel et al., 2008).

The basis for the BOLD measures is an assumption of a roughly linear coupling between neural activity and metabolic activity increases. However, one of the most controversial details regarding this assumption is the temporal resolution; while the basic unit of neural activity, action potential firing, occurs on the millisecond scale, the changes detected in BOLD take place over seconds. But, as mentioned in Figure 15, electrophysiological methods can provide near real-time temporal accuracy (on the millisecond scale) for the recorded neuronal activity by measuring either the electric field change (electroencephalography, EEG) or magnetic field change (magnetoencephalography, MEG).

2.2 Electrophysiological correlates of BOLD, invasive studies

Few studies have directly compared electrophysiological and BOLD fMRI measurement (Huettel et al., 2008). A seminal article that partially resolves this dilemma was published a decade ago by Logotethis and colleagues (Logothetis et al., 2001). To study the neural origin of the BOLD signal, the authors examined the degree of correlation of the hemodynamic response to three types of electrophysiological activity: single units (firing of an individual neuron close to the electrode), multi-unit (the collective firing rate of neurons, in a few hundred microns), and local field potentials (LFP, synchronous charges in integrative activity from cells within a few millimeters). The authors recorded simultaneously the BOLD and the intracranial responses elicited by a visual stimulus in the primary visual cortex in 10 anesthetized monkeys. As we can see in the next figure, single-units and multi-units activity occurred transiently at the onset of the stimulus and did not persist over time, while the LFP activity showed both transient and persistent activity. The authors show that the LFP activity— a stimulus-induced fast oscillation in the range 30-150 Hz which includes both post-synaptic potentials and integrative activity

occurring at the soma— better predicted the BOLD signal change than the multi-unit (see Figure 16).

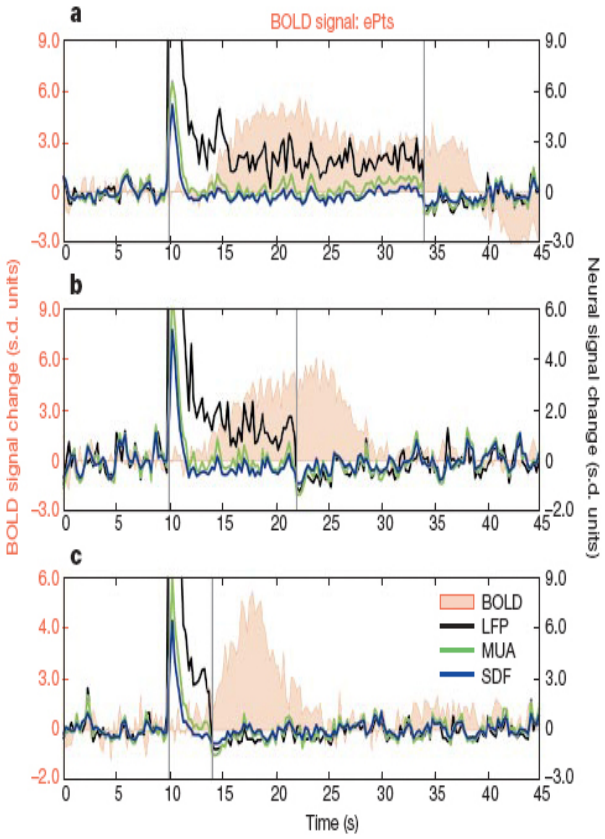

Figure 16: The relationship between BOLD activation and neural activity. Simultaneous electrophysiological and fMRI data were recorded in monkeys during the presentation of visual stimuli. The time course of BOLD activation evoked by the visual stimulation is shown as a solid red histogram, while the time course of multi-units activity (MUA) is shown in green, the time course of single-unit is shown in blue, and the time course of local field potentials (LFP) is shown in black. The duration of visual stimulation, indicated by vertical black bars, varied from 24 to 12 to 4 s, shown in the top, middle and bottom panels, respectively. Note that the BOLD activation and the LFP activity are extended in time throughout stimulus presentation, while the single-and multi-units activities rapidly return to baseline. From Logothetis et al. (2001).

In summary, Logothetis et al. (2001) presents three principal findings: first, the BOLD contrast mechanism directly reflects the neural response elicited by stimulus; second, neural signals are characterized by considerably higher signal-to-noise ration than the hemodynamic response; and finally, as the hemodynamic response seems to be better correlated with the LFPs; then they would reflect the incoming input and the local processing in a given area rather than the spiking activity (or output activity) (Logothetis et al., 2001)(Logothetis et al, 2001). This result was reinforced by an article published in 2005 (Niessing et al., 2005), that shows a strong correlation between the BOLD and the LFP in the gamma range (30_70 Hz) in cat visual cortex. This article adds the notion of correlation between hemodynamic responses and neuronal synchronization.

In the same year, the group of Rafael Malach published for the first time the correlation between the hemodynamic response and neural activity in the human cortex, thanks to a

very simple protocol: record single unit activity and LFP in auditory cortex of two neurosurgical patients and compared them with the fMRI signals of 11 healthy subjects during presentation of an identical movie segment (Mukamel et al., 2005). The spiking activity of these neurons in each patient was summed and converted into a predicted fMRI BOLD response (spike predictor) by convolution with a standard hemodynamic response function. This measure was extremely correlated with the fMRI activity (r = 0.75). Thus, this work strengthens the idea that fMRI signals can provide a reliable measure of the firing rate of human cortical neurons. In the next figure, we represent the principal results of this work.

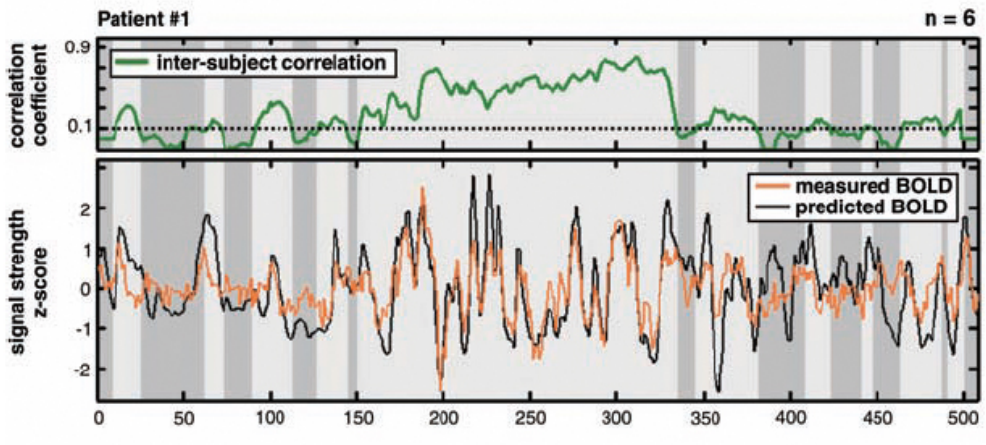

Figure 17: Correlation between the spike predictor with measured fMRI activation. fMRI BOLD activations in Helschl's gyrus of each subjects were sampled by using the spike predictor of each patient (for this figure the patient 1). Bottom graph depicts the average measured BOLD activation of all subjects (orange traces).

Following with the same view, but using a method developed by Leopold (Leopold, Murayama, & Logothetis, 2003), that consists principally in smooth the filtered LFP (a new time in the gamma range) after a Hilbert transformation (see materials and methods for a exhaustive explanation of this method), Nir and colleagues found that the coupling between the gamma LFP and the BOLD fMRI is related to interneuronal correlations (Nir et al., 2007). To end the idea of the close correlation between the BOLD fMRI and the gamma-LFP we must mention a paper that has gone of our laboratory, that reveal a close spatial correspondence between regions of fMRI activations and recording sites showing EEG energy modulations in the gamma range (Lachaux, Fonlupt et al., 2007). In this study were combined fMRI and intra-cranial EEG recordings of the same epileptic patients during a semantic decision task. These and others results have led to a simple conclusion: **The BOLD contrast mechanism reflects primarily the input and**

intracortical processing in a given area, that which we have characterized as the integrative aspect of neuronal processing, rather than the output reflected in action potential firing (Huettel et al., 2008).

2.3 Electrophysiological correlates of BOLD, non-invasive methods

Despite the great signal to noise ratio of the intra-cerebral electroencephalography (ICE), this technique must be complemented in the study of the spontaneous slow fluctuations of the resting state networks with non-invasive methods. As the principal objective of ICE is to find the epileptic foci (the location in the brain where the seizures originate), the electrodes normally are concentrated in a specific region, i.e. the temporal lobe. And as we have said repeatedly, these networks are scattered in remote areas, i.e. the posterior cingulated and the medial prefrontal cortex in the RSN 1, or DMN. For the same reason, several groups have tried to find the electroencephalographic signatures of these brain networks (Laufs et al., 2003; Mantini et al., 2007).

Before the description of the more relevant results found in this domain with scalp-EEG, we need to emphasized two technical difficulties. First, as we have recently read, the best candidate for neural correlate of BOLD-fMRI is the gamma-LFP, and several recent articles have shown the difficulty of capturing high frequencies with this technique, principally due to motors artifacts (Yuval-Greenberg, Tomer, Keren, Nelken, & Deouell, 2008). The second reason is topographic, in the DMN, for example, two of the core regions, PCC and MPFC, are located in the central x-axe (in Tailarach coordinates). Because voltage fields fall off with the square of the distance, activity from deep sources is more difficult to detect than currents near the skull (Dandekar, Ales, Carney, & Klein, 2007).

An interesting work published in 2003 (Laufs et al., 2003) explores the neuroanatomical patterns of resting state fluctuations of human brain activity by simultaneously applying two neurophysiological techniques, the fMRI and the EEG (Laufs et al., 2003). The principal findings of this work was found positive correlation between the BOLD signal and a sub-group of the beta band (17-23 Hz) in several areas, namely the posterior cingulated and the adjacent precuneus as well the temporo-parietal junction (TPJ) and

dorsal medial prefrontal cortex, the major brain regions of the DMN (Castellanos et al., 2008; Greicius et al., 2003; Raichle et al., 2001). Unfortunately, the authors only analyzed low frequencies (<30 Hz).

Using independent component analysis (ICA, see methods for an explanation) on the fMRI data, Mantini and colleagues identified the electrophysiological signatures of the six RSNs in the human brain mentioned in the firs chapter (Mantini et al., 2007), from the simultaneous acquisition in fMRI and EEG across fifteen healthy subjects. In the next figure we represent the cortical representation of the association between EEG rhythms and fMRI RSNs.

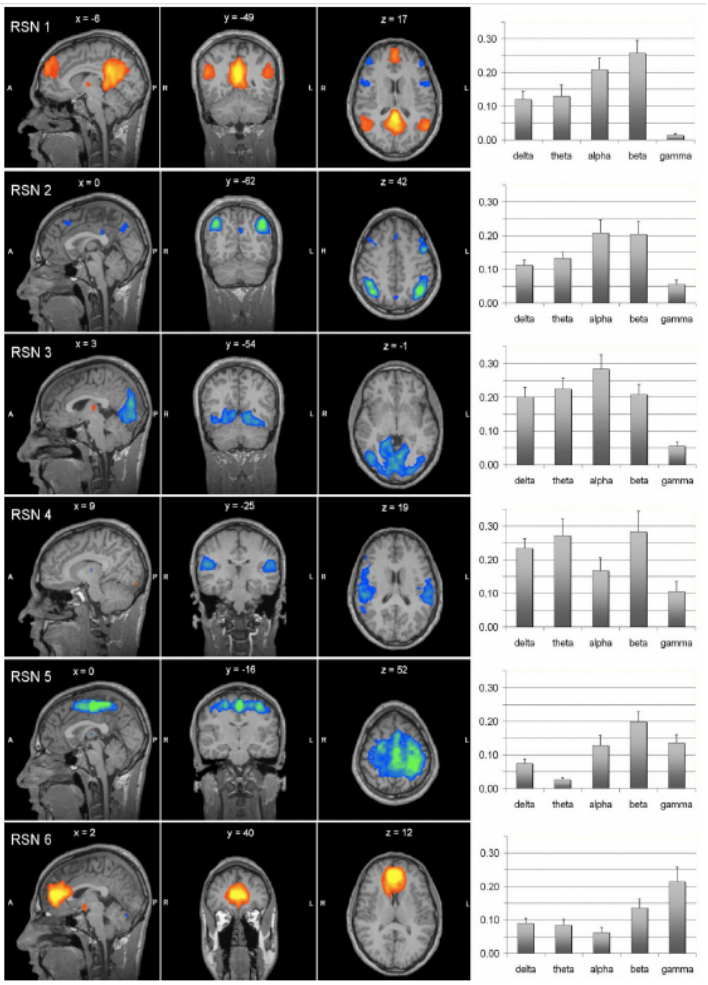

Figure18: Association between EEG rhythms and and fMRI RSNs. Sagital, coronal, and axial spatial maps of the six RSNs. In the right column are represented the bar plots of the average correlation between the brain oscillatory activity in the delta, theta, alpha, beta and gamma bands (<50Hz), and the RSN time courses. From Mantini et al. (2007).

We must not forget that the main objective in this thesis was to find the neural correlate of the default mode network, and as mentioned in the first chapter, one of the principal characteristics of this network is that it shows task non-specific deactivations during goal-directed activity. In the same way, the logical question that follows is: such us the neuronal correlate of a BOLD fMRI activation is the gamma-LFP activity, will be the gamma-LFP deactivation the neuronal correlate of the BOLD deactivation?

2.4 Electrophysiological correlate of BOLD deactivation

To date, the origin of the BOLD deactivation (or negative BOLD response, NBR) remains controversial. The first article that focuses this issue was publish by Amir Shmuel and collaborators in 2006 (Shmuel, Augath, Oeltermann, & Logothetis, 2006). To address this question, the authors applied electrical recordings simultaneously with fMRI in anesthetized macaque monkeys. As we can see in the next figure, the negative BOLD response beyond the stimulated regions of visual cerebral area V1 was found to be associated with-and couple to-decreases in neuronal activity below spontaneous baseline activity (Shmuel et al., 2006).

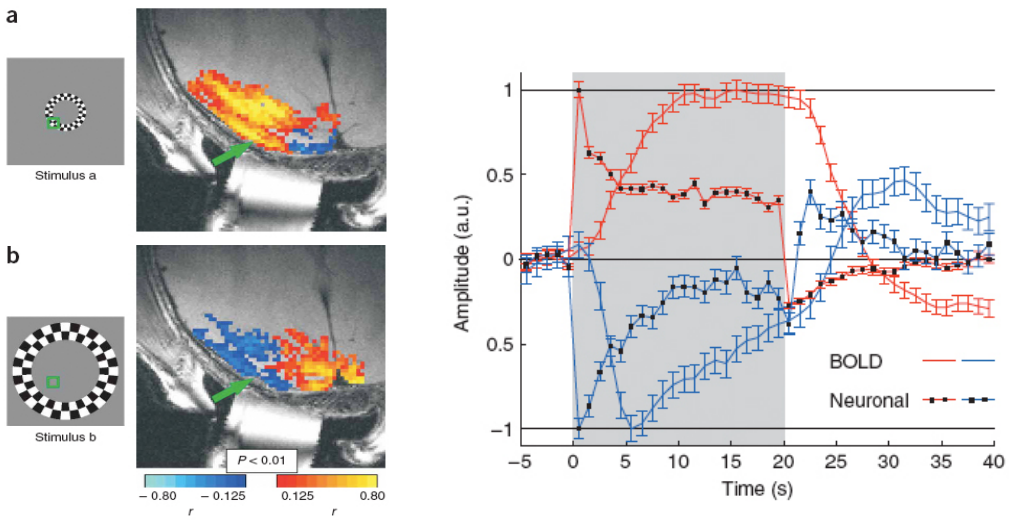

Figure 19: BOLD response to stimulation of part of the visual field. (a,b) Patterns of response to central (3.5°-6.1°) and peripheral (8.5°-14.7°) visual field stimulus. One oblique anatomical slice is shown, whit the fMRI response superimposed on it. Green arrows represent the location of the recording electrode within visual area V1. We can observe activation in both measures, LFP and BOLD, when the visual field stimulus is central (c). In contrast, when the stimulus is peripheral, both measures show a deactivation (we can observe a BOLD activation in central V1 in this condition). From Shmuel et al, 2006.

As we can see in this figure, he authors found the concurrent BOLD and gamma deactivation in the center of V1 (activated by peripheral stimuli), when the stimuli are in the center of the visual field, and lateral V1 during peripherals stimuli. If we return to the first chapter, this result can respond the deactivations grouped with the term 'active-decreases'[8]. Nevertheless, the electrophysiological correlates of the deactivation across the DMN remained unknown.

Two years later, Lachaux and colleagues showed that visual presentation of words induced a strong (and transient) deactivation in a broad (30-150) frequency range in the human left ventral prefrontal cortex[9] (Lachaux et al., 2008), in parallel with a gamma band activation within the reading network (in special the Broca's area), only when the words were read with attention and semantically interpreted (Stories experiment). This surprising result, obtained from intracerebral EEG in epileptic patients, opened the door to the study of the neural correlate of the goal-directed deactivations.

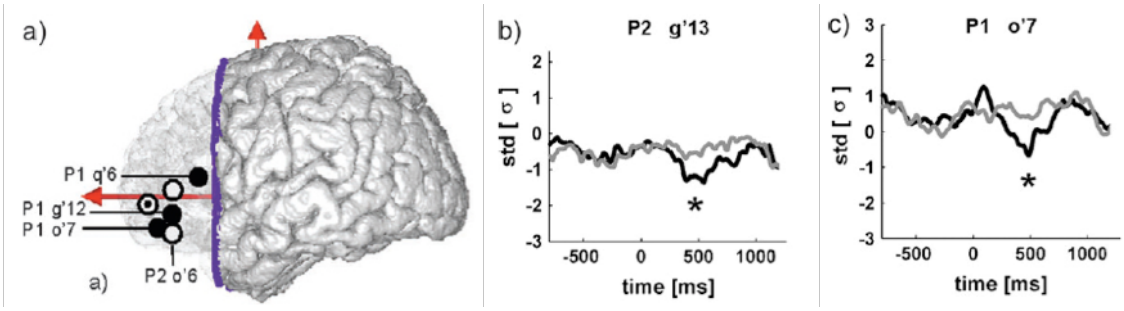

Figure 20: Effect of attention on the VLPFC responses in the Stories experiment. (b,c) Gamma-band deactivation profiles for two VLPFC electrodes during semantic reading. Energy was significantly lower for attended versus unattended words (Kruskal-Wallis comparison). We can see that unattended words (gray lines) induced no significant deactivation.

Finally, we can conclude this chapter with two recent findings. Hayden and colleagues have shown the electrophysiological correlate of the default mode processing in macaque posterior cingulated. To address this question, the authors measure the LFP and the multi-unit activities in two monkeys during two attention-demanding tasks, as well at as rest. The principal result was the following, the firing rates of the posterior cingulate neurons

[8] An active task may inhibit a primary area that would normally respond in the task environment.
[9] These deactivations were related to the attentional charge of the stimuli.

(CGp) were elevated at rest and suppressed during task performance (also the LFP in the gamma range, see figure 21), and the spontaneous firing rates predicted behavioral indices of task engagement on a trial-by-trial basis- whit higher rates associated with poorer performance (Hayden, Smith, & Platt, 2009).

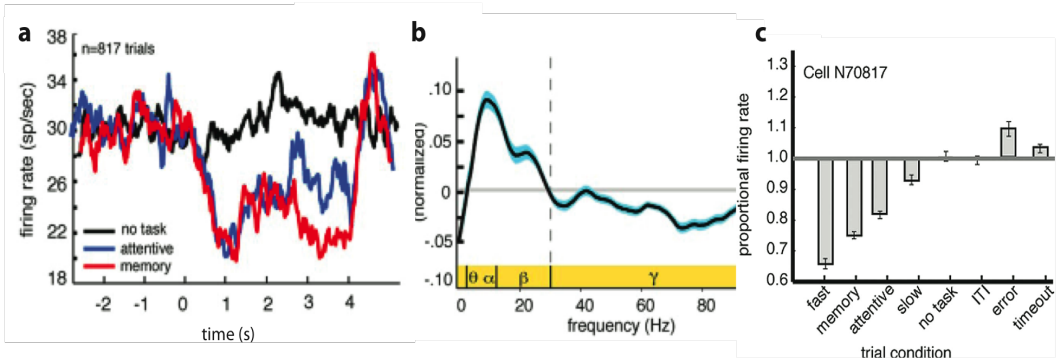

Figure 21: Attentive vigilance suppresses activity of CGp neurons. (a) Peristimulus histograms show average firing rates of single cGp neurons during attentive task (blue line), working memory task (red line) and no task condition (black line). Responses are aligned to cue fixation. (b) Differential power spectra of LFPs for attentive task minus control condition. Power in the gamma band was suppressed relative to ITI, whereas power in lower frequency bands was enhanced. (c) Neuronal activity in CGp covaries with exteroceptive vigilance. Bar graph showing average normalized firing rate of a single example of CGp neurons. From Hayden et al, 2009.

In the same year Miller and colleagues address the same question, to find the neural correlate of the DMN (Miller, Weaver, & Ojemann, 2009). In difference to Hayden, these authors performed a set of task in three epileptic patients, implanted with intracerebral EEG by medical reasons. Miller shows that amplitude in the very high gamma band frequency (70-200 Hz) drops, respect to the rest, in some electrodes placed in the DMN (in PCC and MPFC) in a visual target detection task.

Summarizing, we have today a set of different studies that point to the same address. **The best neural candidate that correlates with BOLD deactivation is a broadband suppression in the gamma-band power** (Karim Jerbi et al., 2010).

3. Attention and electrophysiology[10]

Attention has been arguably one of the main topics of interest of cognitive neuroscience for the last thirty years, especially since the recent boom of functional neuroimaging. The progress of Positron Emission Tomography (PET) and, in special, the functional Magnetic Resonance Imaging (fMRI), has led to a precise delineation of the major neural networks underlying the various types of attention in the human brain (Corbetta & Shulman, 2002a; Corbetta et al., 2008; Kanwisher & Wojciulik, 2000b). Yet, our understanding of the precise neural mechanisms underlying attention within those networks is still fragmentary, mainly because the same imaging techniques used to describe the functional organization of the human brain, fMRI and PET, measure only metabolic changes induced by neural activity, with low temporal resolution, and not the actual, fast-changing, behavior of the neural networks themselves. Electro and Magneto-encephalography (EEG and MEG) have been used to record this behavior in humans, however, those techniques measure the average activity of hundreds of millions of neurons and do not possess the spatial precision to required to access the fine neural mechanisms of attention. To date, the only data sufficiently precise to reveal those mechanisms have been obtained in animals, with invasive intracranial micro-electrodes recording from groups of individual neurons.

Recent animal studies have revealed a mechanism for attention based on neural synchronization (Fries, Reynolds, Rorie, & Desimone, 2001; Steinmetz et al., 2000). The purpose of this chapter is to introduce this mechanism and discuss its validity in humans, based on results obtained in patients with intracerebral EEG electrodes, at a level of precision intermediate between animal micro-electrodes studies and traditional human non invasive recordings. We will support the view that this neural mechanism of synchronization and desynchronization may indeed be widely at play during attentional processes in the human brain (K. Jerbi et al., 2009; Lachaux & Ossandon, 2008). **Finally, we explain why we chose a visual search task for to investigate the role of broadband gamma modulations in the interplay between activation and deactivation networks mediating efficient goal-directed behavior.**

[10] It is needless to say that this chapter is an adaptation of a book-chapter published in 2009 (Lachaux and Ossandón, 2009).

3.1 Mechanisms of selective visual attention

Most of what we know about the neural mechanisms underlying attentional selection has been learned from experiments manipulating space-based visual attention in awake behaving monkeys, with micro-electrode recordings from the visual cortex (J. Moran & Desimone, 1985). In such experimental set-ups, experimenters can record the activity of neurons stimulated by visual items presented in their receptive field, and compare this activity when the animal allocates or not attention to that spatial location. Results converge to show that attention acts as a contrast gain control mechanism used to increase the firing rate of neurons whose receptive field is being attended, exactly as if the contrast of the attended object had been increased (Reynolds & Chelazzi, 2004). This mechanism is particularly effective when the animal is confronted with two stimuli shown at different locations, in which case the neural response to the attended stimulus is enhanced relative to the unattended stimulus, hence the attentional selection. This mechanism has now been well-established and observed directly throughout the visual system (reviewed in Reynolds & Chelazzi, 2004). This effect is in fact so strong that it can be measured in humans at the scalp surface with electroencephalography (EEG), as visual stimuli generate a stronger evoked-potential over the visual cortex when they appear within the scope of visual attention (Mangun, Buonocore, Girelli, & Jha, 1998).

This relatively simple and elegant mechanism seemed perfectly adequate and somewhat sufficient to explain the mechanism of attention, at least in sensory cortices. This situation lasted until two puzzling studies found evidence for a complementary mechanism: Steinmetz et al. (Steinmetz et al., 2000) in the somatosensory cortex, and Fries et al (Fries et al., 2001) in the visual cortex of awake behaving monkeys, reported a phenomenon of synchronization linking together in a transient manner, those neurons responding to attended stimuli. As we will see in the forthcoming section, those results, however surprising at first, had in fact been anticipated. To understand why, we will now briefly review some important research on neural synchronization indicating that this phenomenon may be a cornerstone of neural processing.

We cannot follow in this discussion without make ah historical parenthesis about attention. The classic work of Anne Treisman 'A Feature-Integration Theory of Attention'(A. M. Treisman & Gelade, 1980) begins with the following problem: '*when we open our eyes on a familiar scene, we form an immediate impression of recognizable objects, organized coherently in a spatial framework. Analysis of our experience into more elementary sensations is difficult, and appears subjectively to require an unusual type of perceptual activity. In contrast, the physiological evidence suggests that the visual scene is analyzed at an early stage by specialized populations of receptors that respond selectively to such properties as orientation, color, spatial frequency, or movement, and map these properties in different areas of the brain'*. This remark introduces the necessity for a mechanism to integrate, or bind together, those elementary responses to form a unified coherent representation of the perceived object. This mechanism is now referred to as the 'visual binding mechanism'.

In most of their studies, Treisman and colleagues have investigated visual processes with a simple paradigm called Visual Search, which precisely highlights the need for, and properties of, a visual binding mechanism. In the Visual Search paradigm, participants are presented with arrays of objects and are asked to find as quickly as possible one of them, different from the others along individual features, such as color or shape, or defined as a unique combination of such features. This defines a situation very similar to, for instance, looking for a particular face in a crowd, of for a pair of socks in a drawer. Figure 22 illustrates this paradigm: in the left panel, participants are asked to find the item shown on top, which happens to be the only one with a red circle; in the right panel, however, finding the same item requires more effort, because the specificity of the target item now relies in a precise spatial arrangement of colors. In the same way, finding a red pair of socks becomes difficult when we have many red socks, as other factors, such as length or shape must be taken into account simultaneously. Psychophysics experiments have confirmed this, the visual search of basic features (such as colour, size, motion and orientation), as in the left panel, occur in a single step and in parallel way across most of (or all) the visual field: that is, the duration of the search, quantified by the reaction times (RTs) of participants, is independent of the number of items displayed (Wolfe, 2003). On the other hand, search for a particular combination of features, as in the right panel, (the target is the only configuration of its

kind), requires that all the stimuli are processed sequentially, resulting in search duration which increase linearly with the number of items in the display.

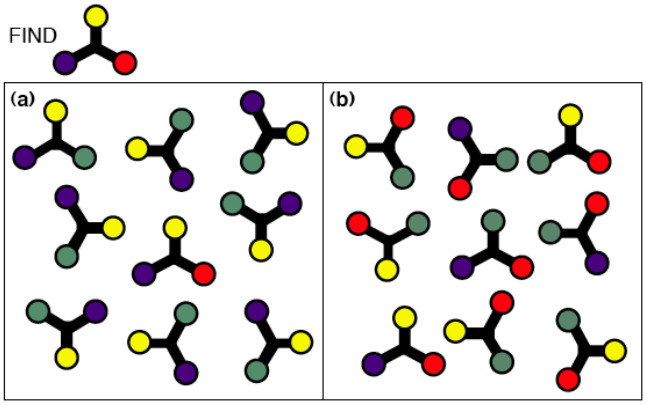

Figure 22: An example of visual search task. Finding the target blue-yellow-red 'molecule' is fast in (a) because the target is the only item with a red component. In contrast, search is slower in (b) because the target is no longer defined by a unique feature, but by a unique conjunction of features. (From (Wolfe, 2003).

Treisman's interpretation of this result is that the search for a unique combination of features requires that visual binding be applied to each individual element in the display, until the target is found, and that this can only be done sequentially, through successive allocation of spatial attention to each item. This proposal, that attention is necessary for correct visual binding, is supported by the illusory conjunction phenomenon, precisely studied by Treisman and collaborators. In this phenomenon, participants are briefly presented with colored letters and must report the color of one of them, experiments show that when the participant's attention is driven away from the display, in 30% of cases, the response will be erroneous and associate the target letter with the color of another letter, in other words, without attention, participants tend to produce illusory associations between shapes and colors (a case of poor binding) (A. Treisman & Sato, 1990; A. Treisman, 1998a).

3.2. On the functional importance of neural synchronization

As in any network, performance in the nervous system relies on efficient coordination between its constitutive elements. The mechanisms underlying the coordination between neurons are certainly multiple and most of them remain unknown. However, evidence accumulated over the last fifteen years points towards one strong candidate: a study by

Gray and Singer (Gray, Konig, Engel, & Singer, 1989) in the primary visual cortex of anesthetized cats showed that neurons had a tendency to fire rhythmically and synchronously at a frequency around 40 Hz (called gamma band) when stimulated by a single coherent moving object; in contrast, they would fire independently of each other when stimulated by multiple, unrelated, visual stimuli. This mechanism allowed for the creation of transient 'resonant' cell assemblies (F. J. Varela, 1995), characterized by synchronous gamma band rhythmic activities, binding together the multiple neural responses to each portion of contour of complex geometrical shapes.

Because of this property, gamma band synchronization was first proposed as a solution to the visual 'binding problem'. The binding problem refers to the problem of how visual objects are 'represented' within the visual system (Roskies, 1999). As we know, visual objects are essentially collections of visual features distributed in space (shapes, colors, etc.), which activate selective, specific, but large and widespread populations of neurons throughout the visual system. When, as in most visual scenes, the visual system is confronted with several, possibly overlapping, objects; a visual binding mechanism is necessary to mark neural activities triggered by the same object and enable scene segmentation, object identification and proper behavior. Because it could be used to create labile neural assemblies, that is, to establish transient relationships between neurons, the synchronization mechanism observed by Gray and Singer was quickly proclaimed as a possible solution to the binding problem (Engel, Roelfsema, Fries, Brecht, & Singer, 1997).

Interestingly, this hypothesis established a strong link between gamma band synchrony and visual attention, because of previous work by Treisman, among others, showing the importance of attention for binding (A. Treisman, 1996, 1998b). Treisman referred to an effect called 'illusory conjunction', which can be described as a failure to bind together the shape and color of an object presented outside the attentional focus: this situation occurs experimentally when participants are instructed to focus their attention on the periphery of a computer screen (while fixating on its center), before colored letters are flashed in the center (say, a red O and a blue X). When asked to report what they have seen, participants often report false associations (or 'illusory conjunctions') between shape and color (a blue O and a red X). This phenomenon illustrated the existence of a visual binding mechanism, its occasional failure, and its dependence on attention. The

necessity of attention for visual binding was also demonstrated by visual search experiments in which participants were asked to search for a specific item embedded in an array of distractors. As I will describe in the method's chapter, I used during my thesis an adaptation of a Treisman's task.

In short, visual binding has been shown to require visual attention. Considering the stream of results initiated by the Singer group, this was enough to build a strong case for a tight connection between attention and gamma band synchrony, one facilitating the other or vice-versa. From a theoretical point of view, neural synchronization also provided an interesting property for attentional selection, in the context of the classic hierarchical model of the visual system. In this model, neurons in early visual areas, such as V1, V2 or V4 project to and activate neurons in higher order visual areas such as the infero-temporal cortex. In this framework, attention facilitation is thought as a mechanism which facilitates the propagation of neural activity, from early to late visual areas within neurons responding to the attended stimulus. Synchrony among neurons responding to the attended object at a given level of the hierarchy would produce the strongest possible impact on neurons responding to the same object at the next level, because the latter would receive simultaneous spikes whose effects add up constructively, as already proposed by others (Fries et al., 2001). Reciprocally, the activity of neurons responding to unattended objects would not propagate so effectively across the hierarchy because they are not synchronous.

For all the previous reasons, the notion that gamma band synchrony and attention were somehow related was 'in the air' even before the two studies mentioned above (Fries et al., 2001; Steinmetz et al., 2000) were published. What was still missing was clear evidence at the neural level.

The first study (Steinmetz et al., 2000) measured the effect in the somatosensory cortex of a shift of attention between the somatosensory and visual modalities. Shifting attention towards somatosensory stimuli produced a clear synchrony increase in the gamma band among neurons of the corresponding sensory cortex, while shifting attention towards visual stimuli had, among those neurons, the opposite effect. In the second study, Fries et al. (Fries et al., 2001) recorded neurons from V4 in monkeys attending to one of two visual stimuli. The effect of attention was also an increase in

gamma band synchrony among neurons responding to the attended stimulus. In contrast, the level of gamma synchrony among neurons selectively activated by the other, unattended stimulus was decreased. Importantly, the firing rate of either group of neurons was unaltered by attention shifts.

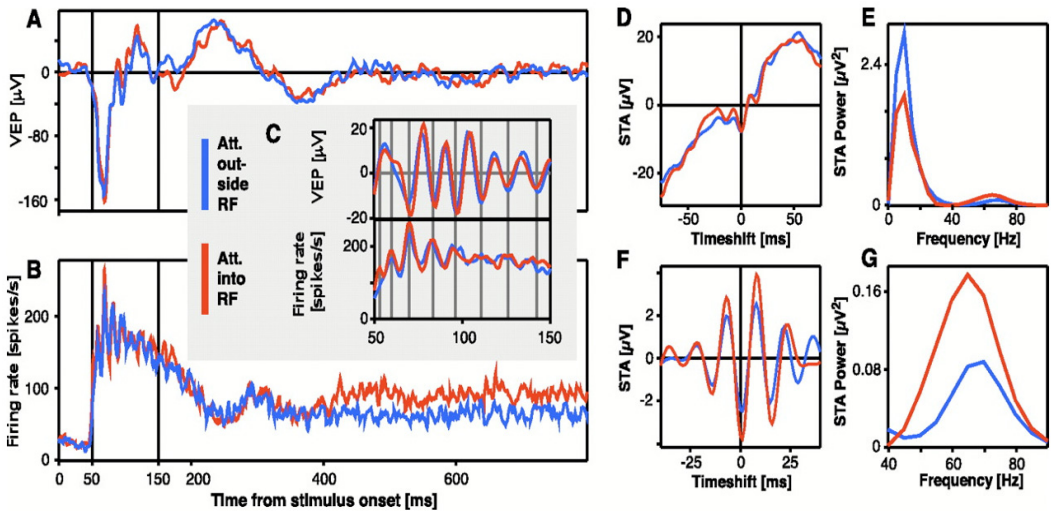

Figure 23: Attention effects in early response. Visual evoked potentials (a) and spike histograms (b) from two separate electrodes as a function of time after stimulus onset. Vertical lines indicate the time period for wish spike-triggered average (STA, d and f) were calculated. The modulation of firing rate by attention starts at about 420 ms after stimulus onset. From 50 to 150 ms after stimulus onset, there are stimulus-locked gamma-frequency oscillations in firing rate synchronized with LFP fluctuations. Gamma-frequency oscillations are shown in detail (c) with the LFP filtered (40 to 90 Hz) and vertical lines indicating peaks of the rhythmic population activity. (g) Power spectrum for STAs for 50 to 150 ms. (From Fries et al., 2001).

In fact, two electrophysiological studies recording intracortical EEG in awake cats had already found much earlier a clear, positive, correlation between the cats' level of attention (as much as it could be interpreted from its behavior) and the level of gamma activity in EEG signals. An increase of EEG power in the gamma band was observed in the parietal and somatosensory cortex when cats observed a mouse (Bouyer, Montaron, & Rougeul, 1981)(Bouyer, Montaron, & Rougeul, 1981); and even before that, Bauer et al. (Bouyer, Dedet, & Konya, 1974) had noticed that cats could be trained to increase the amplitude of gamma oscillations in their visual cortex via a biofeedback device; the result of this training was an seemingly increased attention to their visual environment. Later, studies by the Singer group showed that gamma band synchronization between individual visual neurons was stronger when animals were more vigilant (e.g.

(Herculano-Houzel, Munk, Neuenschwander, & Singer, 1999). Further, an experiment by the same group established a strong link between gamma synchronization and visual awareness (Fries, Roelfsema, Engel, Konig, & Singer, 1997). The study was done in amblyopic cats, stimulated with two simultaneous, contradictory, visual stimuli. Because the cats were amblyopic, and because of the experimental design, cats would perceive at every moment only one of the two stimuli, with a spontaneous alternance between the two. Fries and col. were able to record from a group of neurons responding selectively to one of the two patterns possibly perceived and found an increase of synchrony within this group when the corresponding pattern was actually perceived by the animals.

Those two studies (Fries et al., 2001; Steinmetz et al., 2000) were in agreement with a very active research stream confirming the generality of the synchronization mechanism in a variety of animal species anesthetized or awake. Their particular merit has been to establish more specifically the link with selective attention, and the fact that gamma synchronization could bias competition between sensory stimuli. Since those two studies, several new experiments in awake behaving monkeys have further supported that same mechanism (Bichot, Rossi, & Desimone, 2005; Bichot & Desimone, 2006; Taylor, Mandon, Freiwald, & Kreiter, 2005), and it has even been shown that high levels of synchrony in the gamma band before the stimulus onset are predictive of faster reaction times when monkeys have to respond as fast as possible to the stimulus presentation (Womelsdorf, Fries, Mitra, & Desimone, 2006). This is especially interesting since a shorter reaction time is one of the psychophysical effects defining a high level of attention at the behavioral level (Fan, McCandliss, Fossella, Flombaum, & Posner, 2005). In summary, the manipulation of synchrony to implement attentional bias seems now like a plausible mechanism to complement the gain control mechanism based on firing rate modulation (Jensen, Kaiser, & Lachaux, 2007). As we have seen, even if gamma oscillation does not solve the issue of binding, oscillations in the gamma-frequency range remain a compelling timing/selection mechanism for neuronal communication (Buzsaki, 2006).

3.3. Humans studies on neural synchronization

The existence of large-scale oscillations in the human brain was discovered in the late 20's, as soon as it became possible to record human EEG by Hans Berger (Berger, 1929). It became soon evident that the electrophysiological activity of the human brain, revealed by EEG, was the sum of slow and fast oscillations, ranging approximately, in the waking state, from the delta band (1 to 4 Hz), the theta band (4 to 7 Hz), the alpha band (7 to 14 Hz), the beta band (15 to 30 Hz) and the gamma band (above 30 Hz). Early writers (Adrian, 1941; Berger, 1929) quickly formulated the hypothesis that each frequency band was associated with distinct functional and behavioral correlates, and was the result of synchronization mechanisms between neurons at different spatial scales. But more than seventy years after their discovery, the precise functional role of those oscillations had remained elusive, mainly because their precise understanding required the conjunction of mathematical tools and computer power which has become available only recently.

In the late 90's, the progressive accumulation of evidence of neural synchronization in animals motivated the search for a similar phenomenon in humans, with the current technology to record electrophysiological activity in people, that is scalp EEG. Considering the large differences in spatial resolution between the recording techniques used in humans and animals, the objective was obviously not to observe neural synchronization directly, but to find modulations of the EEG signal, triggered by cognitive tasks, compatible with the effects likely to occur when synchronization emerges within the large populations of neurons producing EEG signals. As we know, with very few exceptions, human electrophysiological recordings do not record the activity of individual neurons. They rather record the average activity of hundreds of millions of them, usually from the scalp surface with scalp EEG electrodes. Still, there is a suspected relationship between neural synchronization in the gamma range and energy modulations in the same frequency range in EEG signals: when a group of neurons establishes synchronization around 40 Hz, an EEG electrode recording the average activity of that population should detect a transient oscillation at the same frequency. Such oscillations can be detected with the application of time frequency analysis techniques to EEG signals. These analyses belong to a family of mathematical transforms which can measure the instantaneous variations of the power spectrum of a

signal. Since the mid 1990's, a variety of techniques, more or less equivalent, have been used for this purpose, such as the Morlet wavelet decomposition, Wigner Transform, Short-Term Fourier analysis and the Matching Pursuit.

At the end of last century, fueled by the progress of computers and mathematical analysis, several groups started to look for gamma oscillations, and for their relation to cognition in humans, using scalp EEG (e.g. (Gruber, Muller, Keil, & Elbert, 1999; Rodriguez et al., 1999; TallonBaudry, Bertrand, Delpuech, & Pernier, 1997). Over the last ten years, human and animal research developed mostly in parallel, to study the mechanisms and functional role of gamma synchronization at two very different spatial scales. Human studies have investigated complex cognitive functions sometimes unique to humans, while animal studies have used much simpler functions, but with incomparably higher spatial resolution.

3.4 Gamma band responses in humans

Since their beginning, the principle of EEG studies on gamma oscillations has remained the same: to evaluate statistically the probability that a cognitive, or motor, event is associated with an increase in gamma band power in the EEG. This involves reproducing the same event many times, for instance the perception of a face in a complex image, and performing statistical analysis on the EEG signals recorded after such events (TallonBaudry et al., 1997). Take the example of a study designed to test whether the perception of a face, embedded in a complex visual stimulus, is associated with gamma band energy increase in the EEG: in such a design, the experimenter shows the subject a series of one hundred pictures (or more), and records the EEG signal in response to each image. The pictures are designed in such as way that the face is hard to detect, so that the experimenter can compare the EEG response when a face is actually detected and when it is not. Time-frequency analysis of each of the hundred EEG signals, for each picture presentation, provides a measure of the EEG spectral energy, at each frequency band, from say 1 to 200 Hz, as a function of the time elapsed since the stimulus was shown. For each time and frequency, it is then possible to compare statistically the hundred energy values measured for each stimulus presentation, with the hundred energy values measured at the same frequency before stimulus presentation (during what is called the baseline level, that is in the absence of the cognitive event of

interest). It is also possible to compare the response to detected vs. non-detected faces. Those statistical comparisons tell the experimenter a) whether, in average, the cognitive processes which followed stimulus presentation were associated with an increased EEG gamma band energy relative to baseline, and b) to which degree such increase depends on the fact that the face is actually detected or not. It becomes then possible to associate specific aspects of the gamma band response with face detection.

This exact procedure was used in a series of EEG studies starting in 1995 to associate such gamma band energy increases (called gamma band responses) with several stages of object perception and memorization (reviewed in (Tallon-Baudry & Bertrand, 1999). In one of them, for instance (TallonBaudry et al., 1997), participants were presented with apparently random patterns of black and white dots, which triggered neither meaningful perception nor significant gamma band response. However, the dots patterns actually hid a Dalmatian dog, which could be clearly seen by the participant after the trick had been explained by the experimenter ("ah, ok, now I see it!"). After this explanation, in a second EEG session presenting the same stimuli, the same images, now interpreted by the subjects as meaningful images, triggered a gamma band response over parietal and occipital electrodes. The difference between the results obtained in the two EEG sessions was explained by the fact that in the second session, subjects had bound together some of the dots of the pictures to create the image of a Dalmatian dog, which is precisely what visual binding is about. This was an elegant demonstration, in humans, that visual binding is associated with increased EEG gamma band activity.

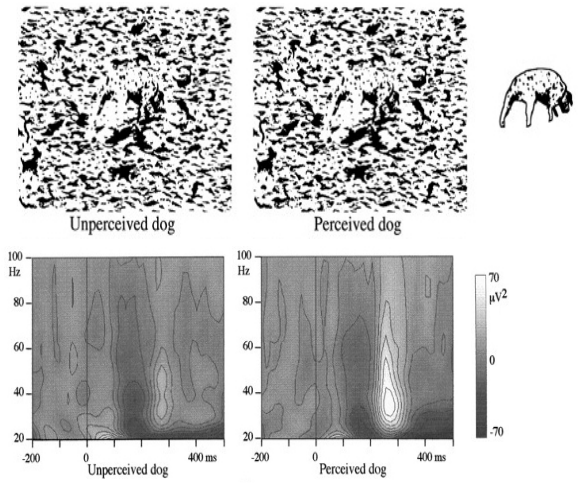

Figure 24: When the stimuli (a Dalmatian, with its head to the right and tail to the left) is unperceived as a dog, because subjects were not instructed of its presence, the response in an occipital electrode (grand average in electrode 01 across the subjects) is not significant in the time-frequency domain. In contrast, an increase of energy between 30 and 70 Hz compared with baseline level can be observed when the Dalmatian is perceived. From Tallon-Baudry et al., 1997.

The same procedure was then used to show EEG gamma band energy increases associated with very diverse cognitive or motor events, including language, memory, and their modulation by attention. Of particular interest for our present topic, several studies showed that EEG gamma band responses were modulated by attention, and always stronger for stimuli attended by the subjects (Gruber et al., 1999; Muller, Gruber, & Keil, 2000), in line with animal data on neural synchronization.

3.4.1. Eye-movements artifacts

Artifectual scalp muscle activity and electromagnetic interference in the high gamma frequency range have further complicated studies with MEG and EEG. Indeed, a recent study may introduce some additional concerns; Yuval-Greenberg and colleagues (2008) showed that during a visual EEG experiment, broadband gamma activity might appear to arise from occipital regions when in fact they are direct manifestations of mini-saccade transients. These authors show that an ocular myoelectric signal, the saccadic spike potential, can be seriously confounded previous EEG studies of induced gamma-band responses (iGBRs) (Yuval-Greenberg et al., 2008; Yuval-Greenberg & Deouell, 2009). The temporal and frequential characteristics of this phenomena, a peak between 150 and 350 ms with a frequency band of 20–90 Hz, has opened a prolific discussion in the interpretation of GBRs measured in sclap-EEG (Yuval-Greenberg et al., 2008; Yuval-Greenberg & Deouell, 2009). It is unclear if this phenomenon extends to MEG, since it may be a consequence of EEG reference electrode placement.

3.5 Intracerebral EEG studies in humans

In very recent years, starting around 2000, research on gamma band synchronization in humans was considerably boosted by new studies using high-resolution intracerebral EEG ('ICE') recordings in humans. Conventional—non invasive—EEG, using electrodes placed on the scalp surface, suffers from some limitations due to weak spatial resolution. In particular, the precise anatomical sources of the effects measured on the scalp surface are unknown, and several distant sources can combine to produce an effect visible at the surface. Also, the neural phenomena observed in scalp EEG in the gamma band are measured at a spatial scale so different from neuron-to-neuron synchronization,

as observed in animal's micro-recordings, that it is not clear how, or even whether, the two are related. In addition, EEG signals are often contaminated by electromyographic activity, mainly from neck and face muscles which produce a strong signal component above 20 Hz. For this reason, the ratio between true gamma band activity of cerebral origin and this noise is often quite low, which complicated the detection of task-induced gamma band synchrony in scalp EEG.

3.5.1 Invasive recordings in epileptic patients

For this reason, several groups initiated collaborations with clinical groups specialized in the treatment of severe epilepsy, to study brain oscillations in humans with invasive, ICE electrodes. Recordings were performed in patients suffering from drug resistant epilepsy, where the only efficient therapy is the surgical resection of brain tissues critically involved in the generation of epileptic seizures. This complex procedure requires in most cases a careful identification of the epileptogenic cortical tissues, which can only be performed with ICE electrodes, positioned under the skull or directly inside the cortex. Compared to scalp EEG, ICE recordings are an order of magnitude more precise, with a spatial resolution on the order of half a centimeter. Therefore, in this range, brain structures generating ICE signals can be identified readily and with no ambiguity. This resolution is in fact comparable to that of fMRI, with the additional millisecond temporal precision of EEG. Also, a very important feature for the study of gamma band synchrony is that ICE signals are not contaminated by electromyographic activity.

The process of identifying the future site of cortical resection takes about two weeks of continuous ICE monitoring, in the patients hospital room. During this time, patients are free to participate in cognitive tasks designed to understand the functional organization of their brain, and of the brain in general. The information that can be derived from such experiments is used to delineate functionally important brain structures that should be sparred by the surgery. This is also a rare opportunity to observe working human brains with a high spatio-temporal precision. Provided that certain precautions are taken to sort between healthy and pathological brain activity, conclusions can be drawn, across several patients, on neural mechanisms underlying human cognition in general

(Lachaux, Rudrauf, & Kahane, 2003b).

3.5.2 Dynamic spectral imaging

Initial ICE studies immediately produced significant improvement in our understanding of gamma band synchrony in humans (Aoki, Fetz, Shupe, Lettich, & Ojemann, 1999; Crone, Miglioretti, Gordon, Sieracki et al., 1998; Lachaux et al., 2000). For instance, it was shown that the sources of the scalp EEG gamma band responses to visual stimuli are multiple and complex. Their latencies, durations and strength largely depend on their anatomical origin, even for very simple cognitive tasks, such as the perception of simple geometrical shapes (Lachaux et al., 2000).

The added-value of this technique was well-illustrated by a study performed in ICE (Lachaux et al., 2005) after the same experiment had been done in scalp EEG (Rodriguez et al., 1999). The task was a face detection task, in which participants had to respond whether briefly flashed stimuli contained a face picture or abstract shapes. The scalp EEG study had revealed a large gamma band response around the 200 ms latency, with a widespread topography over parieto-central electrodes compatible with sources in the visual cortex. The ICE study brought a detailed description of the response networks that had been hypothesized from the scalp EEG analysis: it revealed that face stimuli elicited in fact a mosaic of gamma band responses along the ventral visual pathway involved in object identification, propagating from early visual areas (around 100ms) to higher-order, object-identification regions (around 200 ms); this was followed by responses in parietal regions involved in visual attention in the intraparietal sulcus. Moreover, ICE responses were stronger for pictures of faces in brain regions associated with face perception in fMRI, such as the fusiform gyrus, and in the parietal attentional network where the attention-grabbing effect of face stimuli coincided with gamma band responses in the intraparietal sulcus; another instance of relationship between attention and gamma band synchrony, in our interpretation.

Within a couple of years, ICE studies revealed task-specific gamma band responses in a variety of cognitive processes including not only visual perception, but also auditory (Crone, Boatman, Gordon, & Hao, 2001), and olfactory perception (Jung et al., 2006),

short- and long-term memory (Mainy, Kahane et al., 2007; Sederberg, Kahana, Howard, Donner, & Madsen, 2003; Sederberg et al., 2007) language perception and production (Crone, Hao et al., 2001; Jung et al., 2008; Mainy, Jung et al., 2007) and motor preparation and execution (Aoki et al., 1999; Brovelli, Lachaux, Kahane, & Boussaoud, 2005; Crone, Miglioretti, Gordon, & Lesser, 1998; Lachaux, Hoffmann, Minotti, Berthoz, & Kahane, 2006). The observation of gamma band responses in cognitive tasks is now so common, that, at first glance, it may even seem that such responses are just general reactions of the active brain, with no functional specificity. This view is erroneous though, as the networks of gamma band responses induced by a cognitive task have always been extremely sensitive to the task, both in terms of anatomical and temporal organization. Moreover, it turns out that the networks of gamma band responses triggered by cognitive tasks are very similar to those found with fMRI (Lachaux, Fonlupt et al., 2007). It should also be noted that gamma band activity can be also recorded in the deepest stages of sleep (Le Van Quyen et al.).

The results obtained so far support the models proposed by Singer (Singer, 1999) and Fries (Fries, 2005), which assert that gamma band synchrony is a general mechanism for local communication between nearby neurons. As such, it would be indispensable for cognition: the recruitment of any local population of neurons, specialized in a precise cognitive process, would necessarily involve the establishment of transient but intense communication between those neurons, based on neural synchronization in the gamma band. According to this view, the detection of gamma band synchrony in ICE signals would provide an efficient marker of the spatio-temporal dynamics of the neural networks underlying cognition, with a high spatial, frequency and temporal resolution. For this reason, we called this technique ‘dynamical spectral imaging’ (DSI).

To illustrate the advantages of DSI, let’s consider two recent studies from our group. Recently, we asked whether reading was associated with gamma band synchronization and, if yes, whether it would be possible to associate the various subcomponents of reading, such as grapho-phonological conversion or semantic analysis, with specific gamma band responses. We recorded from ten patients in three experimental conditions (Mainy, Jung et al., 2007): a simple orthographic task in which they were shown consonant strings and had to decide whether those strings contained twice the same letter or not, a phonological task in which they had to mentally pronounce visually

presented pseudowords, and a semantic task in which they had to decide whether visually presented words were living entities or not. Across the ten patients, we had the opportunity to record from most of the temporo-parieto-frontal network associated with reading as revealed by previous fMRI studies (Price, 2000). Our study showed that indeed, visual stimuli elicited a widely distributed network of gamma band responses throughout the reading network including early visual areas, the word form area in the fusiform gyrus, the superior temporal gyrus and Broca's area. In addition, the degree to which these brain regions produced gamma band responses varied across experimental conditions, matching the functional specificity known within this network. For instance, we found a functional dissociation within Broca's area: while the strongest gamma band response in the most anterior part was associated with semantic processing, that elicited in the posterior part correlated with phonological processing.

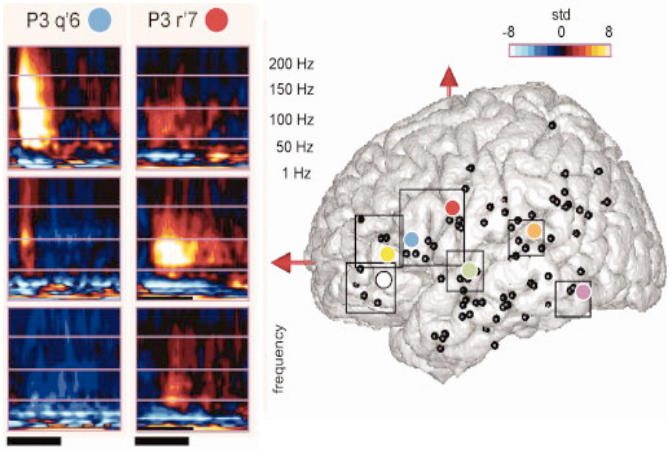

Figure 26: Anatomical and task-sensitivity of gamma-band responses. We can see that electrode q'6, located in the anterior part of Broca's area respond only in the semantic condition, while the electrode r'7, located 2 cm more posterior, respond more strongly in the phonological condition. (From Mainy et al., 2007).

In a second study (Mainy, Kahane et al., 2007), our group investigated whether verbal working memory was also associated with gamma band synchronization. Ten patients were recorded during a classic Sternberg task asking them to memorize a series of five letters, presented one by one in succession. We found that each letter in a series induced gamma band responses in a network comprising both temporal and frontal structures. More interestingly, in some regions like the inferior frontal gyrus, the amplitude of those responses increased linearly with the number of letters stored in working memory, with a weaker response for the first letters in a series and stronger responses for the last ones.

Those results provided a direct neural implementation of the classic model of phonological loop proposed by Baddeley to model verbal working memory (Baddeley, 2003).

3.6 Gamma band synchrony and attention: insights from human ICE studies

The previous results laid the ground for complementary studies and analysis investigating the role of gamma band synchrony in attentional processes in humans. What happens to the gamma band responses observed in humans with ICE, when attention is manipulated? We now have elements to answer that ICE gamma band responses are very sensitive to attention. Let us illustrate this point with three examples, drawn from the studies just reviewed on visual perception, reading and verbal working memory.

3.6.1 Attention and visual perception

As we know now, the presentation of visual items triggers a chain of gamma band responses in the visual system; but how does the duration of those responses vary with the time actually spent by the subjects paying attention to the scene and extracting visual information? If gamma band synchrony is involved in visual attention, then we might expect that a longer search would trigger a longer gamma band response. This can be hypothesized considering a classic result of the psychophysiological literature (A. Treisman, 1998b): when you search for a complex object among many distractors, like a face in a crowd at the train station, there is no other strategy than to shift visual attention in space from face to face, until you eventually find your target. This is generally the case except if the face has a very distinctive feature, like a large mustache, for example, in which case the target pop-out, as previously mentioned. In other words, the search for a specific item in an array of distracters is usually serial, with duration proportional to the number of distracters. Visual search is thus an ideal situation to study the effect of search duration on the timing of gamma band responses. If visual attention requires gamma band synchrony, then we would expect longer gamma band responses to arrays that require longer search. This is precisely what we observed in a recent study (Ossandon et al. in preparation): patients were shown arrays of letters, containing one ‘T’ and 35 ‘L’’s. The

‘T’ was always gray, and was the target to be found in each display. ‘L’s were either gray or black, so that the duration of the search could be manipulated by varying the proportion of ‘L’ with the same color as the target. The results of this study will be shown and discuss in the chapter Results.

3.6.2 Attention and reading

What happens when our attention fluctuates during reading, when we read certain portions of a text attentively, but shift to a forgetful mode for others? We had the opportunity to answer this question in the patients mentioned above, in whom networks of gamma band responses had been identified for several subcomponents of reading (Jung et al., 2008). These patients volunteered to perform an additional reading task, in which they simply had to look at stories, shown word by word on a computer screen. The critical experimental manipulation of the task was that two stories were intermingled, with the words of the first story written in one color, and the words of the other story in another color. Patients had to read only one of the two stories, say, the green story, and ignore the other. However, because words were flashed on screen for only 100 ms, and because patients had no way to guess the color of the upcoming word, each word was actually processed visually in the same way, irrespective of its color, at least at the early stages of the visual system. The only difference was that once a word had been identified as part of the attended story, most likely because of its color, or because of its congruence with that story, it would capture further attentional resources and be processed fully, while words of the non-target story would not. The analysis of the ICE signals in response to attended words showed that they triggered a chain of gamma band responses throughout the reading network which was very similar to what had been observed in the semantic condition of the earlier reading task, (as discussed previously, see Mainly, Jung et al., 2007). This was expected in some sense, as comparably to that previous task, words also benefited from the patients’ attention. But the most striking result was that gamma band responses for unattended words were strongly attenuated compared to attended words. Furthermore, this attenuation, which was quantified by the ratio between the global energy of the ‘unattended’ gamma band response divided by the global energy of the attended response, was stronger for frontal sites than for posterior sites, as if there was a gradient of attenuation from posterior to anterior brain structures. In some high-level

structures such as Broca's area, the gamma band response for unattended words was close to zero, as if the words had not been presented at all. In contrast, the attenuation was weak in visual regions such as the fusiform gyrus.

3.6.3 Attention and memory

Another effect of attention is that it facilitates memorization: it is a well-known fact to every student that we memorize items and facts better when we are attentive. The study on verbal working memory summarized above, which asked subjects to memorize series of letters, investigated this effect. This was done with an experimental condition asking the subjects to pay attention to certain letters only (Mainy, Kahane et al., 2007). In that condition, each letter in a series was presented after a visual cue, a green or red dot, informing the patient that the associated letter was important and had to be attended and remembered. We could then compare the gamma band response to letters tagged as important or unimportant and found an effect similar to the one observed in the attentive reading study: in frontal regions, like the inferior frontal gyrus, gamma band responses followed only attended, and later remembered letters. This showed that the positive effect of attention on memorization manifested itself, at the neural level, as an increase in gamma band synchronization; because only letters which received the full attention of the patient, for the clear purpose of memorizing them, triggered gamma band responses.

The three studies discussed above converge to show amplification by attention of gamma band responses associated with cognitive processing. In other words, when a process is done attentively, the gamma band responses associated with this process are amplified. This was further demonstrated in premotor cortex during a spatial attention task (Brovelli et al., 2005), and in the ventral visual stream during object-based attention (Tallon-Baudry, Bertrand, Henaff, Isnard, & Fischer, 2005). Altogether, the results obtained on attention and gamma band synchrony in ICE studies have extended into high-level cognitive tasks and associative cortical areas the validity of observations made in animals in simple tasks and lower level sensory cortices. They fit the general view that attention and gamma band synchrony go "hand in hand".

What we have learned too, is that this relationship is always limited to very specific brain

structures, completely determined by the task which is being attended. Our general experience is that an average of 10% of the cortical sites we record from generate gamma band responses during a given task, a subset of which are modulated by attention. This was clearly illustrated by the visual search experiment in which the correlation between the duration of the gamma band responses and the time spent scanning the display attentively, was true in early visual areas but not in higher order areas along the ventral visual pathway.

The future will certainly add complexity to this apparently straightforward relationship. To launch the discussion, let us end this section with a thought provoking result: in both the visual search experiment and the attentive experiment, we observed negative gamma band responses to the stimulus presentation (Lachaux et al., 2008); they were found in the ventral lateral prefrontal cortex and had timing similar to the other, positive, gamma band responses found in other cortical sites. The only difference was that they corresponded to decrease in gamma band activity. The question that surge in this point is the following, this decrease in gamma band activity possibly reflecting desynchronization? This is a central point that will be developed in the Discussion of this thesis. In fact, this decrease even brought the gamma band energy below the level measured at rest, before the experiment started. Further, this phenomenon was strongly amplified by attention. The same effect of deactivation was found in the lateral prefrontal cortex in the visual search experiment ('T' and 'L') described above: the duration of this deactivation increased with the duration of the search. As we will observe in the first article of my thesis (Ossandon et al. submitted), this deactivation not only happen in VLPFC, but in the entire DMN, describe above. This suggests that in some brain structures, attention may act not by increasing gamma band activity, but by decreasing it. This does not necessarily contradict the earlier conclusions, since our knowledge of the ventral lateral prefrontal cortex (VLPFC) tells us that it could interfere with reading or visual search processes (Lachaux et al., 2008). Therefore, the negative gamma band response may in fact correspond to the interruption of processes which could interfere with the task at hand, such as constant monitoring for occasional external events with possible general behavioral relevance, as the VLPFC has been suggested to participate in this function (Corbetta & Shulman, 2002). One way to think about this effect is that the relationship between attention and gamma band synchrony may have more degrees of freedom than previously thought, and that attentional bias may take the form of a balance between regional synchronizations

and desynchronizations phenomena in the gamma band.

3.7 Broadband activity reflects synchrony?

3.7.1 Asynchronous neuronal populations can explain narrowband oscillations

As we have seen throughout this chapter, neuronal synchronization has been considered a fundamental step in sensory, motor, and cognitive processing (Buzsaki & Draguhn, 2004; F. Varela, Lachaux, Rodriguez, & Martinerie, 2001). In fact, neural synchronization was detected by explicit cross-correlation between spike trains in several systems (Gray et al., 1989; Marin, Mpodozis, Sentis, Ossandon, & Letelier, 2005; Singer, 1994).

Furthermore, neural synchronization was also inferred by existence of narrowband oscillations in recorded local field potentials (LFPs) (Engel, Fries, & Singer, 2001; F. Varela et al., 2001). This identification is based in the assumption that narrowband oscillations must necessarily reflect the constructive summation of synchronous oscillators. In a recent article, Javier Diaz and colleagues (Diaz, Razeto-Barry, Letelier, Caprio, & Bacigalupo, 2007) study the origin of a beta band oscillation (called Peripheral Wave, PWs[11]), recorded in the olfactory epithelium of catfish. The dominant theoretical notion was that PWs represent intermittent synchronous activity of groups of olfactory receptors neurons (ORNs); however, because there are no established neural connections between ORNs (i.e. interneurons, Gap junctions, or an afferent pathway of fibers) the mechanism for this peripheral synchrony remained unclear. But, according to these authors, properties of this wave can be explained as the superposition of asynchronous oscillators. To reach this conclusion, the authors relied on two main evidences: the pattern of discharge of ORNs is constant in response to the odorants (in the next figure we can see a trace of a single neuron response); and second, each time that the stimulus is applied, the amplitude modulation in PWs is different (random pattern of amplitude-modulated). Using Rayling fading, an interference phenomenon well known in physics, the authors characterized neural signals generated by addition of random phase

[11] A classic case of neural oscillations found in the olfactory epithelium of the vertebrate (Ottoson, 1955).

oscillators[12]. In conclusion, this article shows that neural oscillations, detected in LFPs recordings within a narrow band, do not necessarily originate from synchronization events.

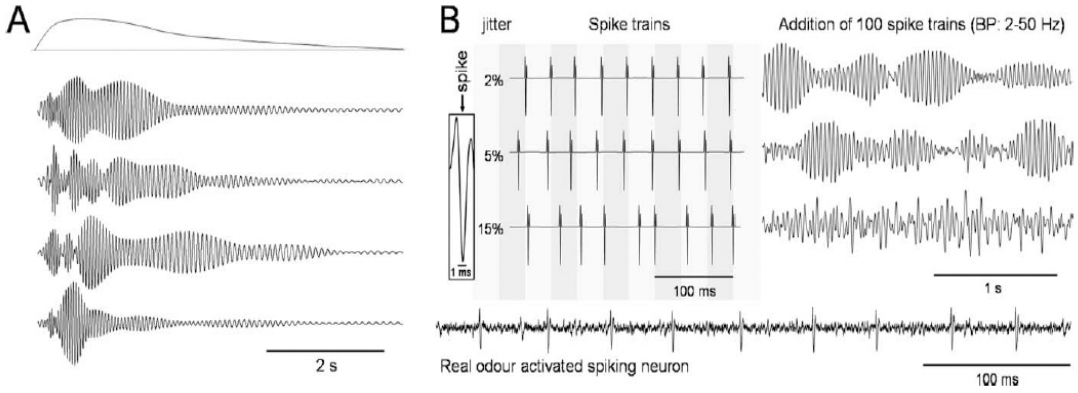

Figure 29: Simulated PWs produced by real neural oscillators. (A) Examples of artificial PWs generated by addition of 25 uncoupled oscillators (top trace depicts the temporal amplitude profile of each elementary oscillators. (B) Artificial PWs generated as the addition of uncorrelated spike trains. One hundred artificial spike trials (left traces) were added and bandpass filtered between 2 and 50 Hz to obtain artificial PW signals (right traces). We can see that high jitter levels destroy the amplitude modulation characteristics of PWs. (From Diaz et al., 2007).

3.7.2 Broadband spectral gamma: synchrony or neural correlate of population firing rate?

The relation between the spiking of individual neurons and the aggregate electrical activity of neuronal ensembles as seen in the local field potentials has become a fundamental question in neuroscience. In a recent article, Manning and colleagues directly examined this relation examining 2030 neurons in widespread brain region from 20 neurosurgical patients (Manning, Jacobs, Fried, & Kahana, 2009). Their primary objective was to examine how the firing rates of individual neurons related to narrowband

[12] This phenomenon has been well studied in physics, especially by the boom of the mobile telephony. Our mobile not only receives a signal, but thousand of signals with the same frequency with random phases. Even counterintuitive, these signals do not cancel one another out; moreover, they form a wave with random amplitude.

changes (i.e., oscillations) and broadband changes in the LFP (see Figure 30). For many of the neurons recorded, narrowband oscillations correlated significantly with the firing rate, especially in the gamma band (30-150 Hz). Nevertheless, the principal finding of these authors is that neuronal spiking is positively correlated with broadband LFP power across all the frequencies. Because this broadband (and also the gamma 30-150) spectra change is correlated with the action potential rate at the LFPs scale, broadband would then dictate the size of neuronal population that the firing rate is being averaged over (Manning et al., 2009; Miller, 2010).

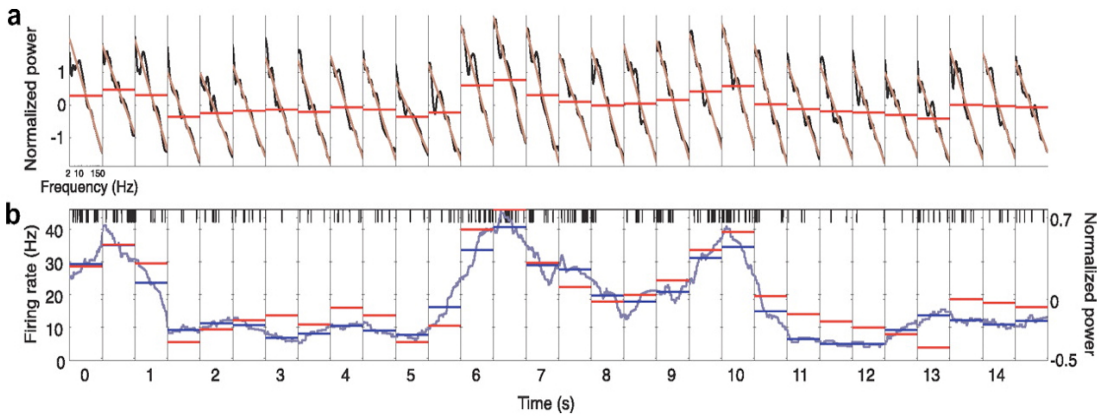

Figure 30: LFP power and neuronal firing rate time series. Each box details the activity in one 500 ms epoch. (a) This panel illustrates how various features of the LFP change over time. In each epoch, the black lines indicate the overall LFP power spectrum, brown lines indicate robust-fit lines, and the horizontal red lines indicate mean broadband powers. (b) Changes in the neuronal firing rate concurrent with changes in the LFP power spectrum. (From Manning et al., 2009).

Beginning with Crone and colleagues (1998), several studies described ICE and ECoG power increases at 50-150 Hz, called high gamma[13](Fries, 2009), when a brain region is active (Jacobs & Kahana, 2010; Manning et al., 2009). The use of the term high gamma implied that this faster signal reflected a true rhythmic oscillation (Jacobs et al., 2010). As we have seen, gamma oscillations can be difficult to distinguish from broadband fluctuations because both phenomena appear at overlapping frequency bands; both exhibits phase-amplitude coupling with theta (4-8 Hz) oscillations; and both correlate with neuronal spiking (Canolty et al., 2006; Jacobs, Kahana, Ekstrom, & Fried, 2007;

[13] This pattern was called 'high gamma' because it appeared to be a faster version of the gamma oscillation, which generally appears as a rhythmic signal at +- 40Hz (Fries, 2009; Jacobs & Kahana, 2010).

Jacobs & Kahana, 2010; Manning et al., 2009). In conclusion, we need be carefully when we talk about gamma oscillation. It is important to distinguish true oscillations from broadband fluctuations because the two phenomena imply distinct underlying physiological processes (Jacobs & Kahana, 2010; Miller, 2010).

3.8 Perspectives

Given that the application of ICE to understand the functional role of gamma band synchrony in attentional processes is relatively new, we will end up this chapter discussing its future, rather than its past. There are several major avenues for future ICE research which can be highlighted.

3.8.1 Long distance synchrony

In this chapter, we have been essentially dealing with one type of synchronization, called local, which binds together neurons belonging to a single, homogeneous, functional structure such a the primary visual cortex, or the posterior part of Broca's area. However, another type of synchronization, linking together widespread neural activities over the whole brain has been evidenced in the recent years, as part of a mechanism of large-scale integration indispensable for cognition. In short, the need for integration mechanisms, which was first described in the visual system to solve the binding problem, is in fact general. Most cognitive acts involve the integration of processes carried out by distinct functional systems, sensory, motor, emotional or cognitive, most of them anatomically widespread. All such aspects must be integrated to produce coherent experience of the world and adapted behavior. This constraint has led to the idea that synchrony, as an integration mechanism, may well be used outside the context of 'simple' sensory integration, as in visual binding, to achieve this large-scale integration across functional systems (F. Varela et al., 2001). Shortly after their first observations of synchrony in cat's area 18, Singer and col. showed that synchrony could occur between neurons in functionally segregated areas (area 18 and 19) (Gray et al., 1989) or between hemispheres (Konig, Engel, & Singer, 1995), providing the first examples of 'non-local' synchrony.

Since then, several studies have found instances of long-distance synchrony in relation to behavior, for instance between parietal and motor cortices in cats involved in a sensory motor discrimination task, or in humans during face perception. It must be said, however, that in most instances long-distance synchrony was found at lower frequencies than local gamma band synchrony—in the alpha and beta range, typically. It remains to be demonstrated, especially with the high anatomical precision of intracranial EEG, that attention facilitates the emergence of large-scale synchronization. We know of no convincing intracranial EEG evidence of large-scale synchrony in the gamma range facilitated by attention; this is the kind of research to watch for carefully in the future.

3.8.2. Other frequency bands

As said earlier, large-scale synchrony has often been found in frequency bands lower than the gamma range, between 8 and 30 Hz. For instance, Tallon-Baudry et al. (Tallon-Baudry, Bertrand, & Fischer, 2001) have found in ICE recordings from the visual system, that the maintenance of abstract shapes in working memory, over a couple of seconds, involves the synchronization of the lateral occipital sulcus with the fusiform gyrus around 20 Hz. Since that study, similar large-scale synchrony, in the same frequency range, has also been found between the ventral and dorsal visual pathways in the ICE study on face perception described above (Lachaux et al., 2005). This clearly indicates that gamma band synchronization is not the whole story. This is also true for local synchrony, as the theta, alpha and beta bands are known to be modulated by cognitive activity: theta oscillations have been shown to be enhanced in the hippocampus mostly during spatial navigation, and across widespread cortical locations during memory tasks (Caplan, Madsen, Raghavachari, & Kahana, 2001; Kahana, Seelig, & Madsen, 2001). The reactivity of the alpha and beta bands has been repeatedly shown to be anti-correlated with the gamma band: in most cognitive situations studied so far, gamma band energy increases have been simultaneous with alpha and beta energy decreases, suggesting the hypothesis that the three phenomena are in fact ‘three sides’ of the same coin (Lachaux et al., 2005). This possible claim should be qualified by the additional observation that the anatomical specificity of alpha and beta decreases is not as precise as for gamma increases. This was perfectly illustrated in a study by Crone et al. (Crone, Miglioretti,

Gordon, & Lesser, 1998), where they localize the alpha, beta and gamma band energy variations induced in the sensorimotor cortex by movements of various body parts: the homunculus drawn from movement-induced gamma band energy increases matched precisely the classic motor homunculus which characterizes the functional organization of the motor cortex. The distribution of alpha and beta decreases, in contrast, was by far less refined spatially, providing only a blurred version of the motor homunculus. Still, alpha, beta, and theta band activities have the advantage over gamma band activities of being much easier to detect at the scalp surface because they involve larger neural populations; for this reason, they provide valuable electrophysiological markers of a number of cognitive processes or states, including attentional states, which can be easily measured non-invasively with scalp EEG and MEG (Jokisch & Jensen, 2007).

3.8.3 Scalp recordings

As precise as they can be, ICE recordings will never replace non invasive EEG/MEG recordings. Because ICE is limited to patients and a handful of clinical centers, this type of recording is bound to remain a minor path of investigation of the human brain. Electrophysiological research in humans across large and healthy populations will rely on scalp EEG and MEG. Therefore, one can reasonably wonder how such non-invasive techniques can benefit from ICE research. There are several possible answers to this question. The first one is that ICE records neural activity at a level of resolution intermediate between micro-recordings in animals and EEG/MEG, therefore constituting a missing link between the two extreme levels. Moreover, ICE studies provide the simplest way to associate EEG/MEG signal components, such as gamma band energy increases, with neural mechanisms observed directly at the neural level in animals. The second contribution of ICE is to reveal the sources of the signals recorded with EEG and MEG at the scalp surface. As we know, an entire field of research has developed to design mathematical techniques to enhance the spatial resolution of EEG and MEG (Sereno, 1998). Most of these techniques aim at reconstructing the cortical sources of EEG and MEG signals, and suffer from the fact that any given set of EEG/MEG signals can be generated by a potentially infinite number of different source configurations. Solutions to the so-called source reconstruction problem require a-priori knowledge about the actual sources, and this is exactly what ICE provides.

We believe that the future of attention research in humans, at least in electrophysiology, should involve studies combining ICE and EEG/MEG. Practically, this means EEG/MEG studies in normal subjects, using attention tasks extensively studied in patients, so that the networks active during those tasks have been previously identified with ICE. EEG/MEG would then be used to validate those results in healthy subjects, refining our understanding of the parameters controlling those networks, with longer versions of the tasks and more control conditions than acceptable in patients. The combination of ICE and EEG/MEG should be particularly fruitful for the development of attention-training paradigms based on real-time EEG analysis, such as BrainTV (Lachaux, Jerbi et al., 2007). With BrainTV, ICE is already providing electrophysiological indexes, with very well-defined anatomical origin and temporality, which correlate tightly with certain dimensions of attention. EEG/MEG research should focus on the specific traces of such indexed at the scalp surface to provide an ensemble of non-invasive attentional markers which could then be used for training aspects of attention in healthy individuals.

4. MATERIAL AND METHODS

4.1. Subjects

Intracranial recordings were obtained from fourteen patients with intractable epilepsy (11 women, mean age: 32 ± 10 years) that were candidates for surgery at the Epilepsy Department of the Grenoble Neurological Hospital (Grenoble, France). All patients were stereotactically implanted with multi-lead EEG depth electrodes (SEEG) simultaneously sampling lateral, intermediate and medial wall structures. Electrode implantation was performed according to routine procedures and all target structures for the presurgical evaluation were selected strictly according to clinical considerations with no reference to the current study. All electrode data exhibiting pathological waveforms were discarded from the present study. All participants provided written informed consent and the experimental procedures were approved by the Institutional Review Board and by the National French Science Ethical Committee (CPPRB). All participants had normal or corrected to normal vision. Patient specific clinical details are provided in Table 1.

Patient	age	gender	epileptogenic zone
S1	46	M	right temporal (antero-mesial)
S2	42	F	left temporal (anterior)
S3	22	F	left frontal (operculum)
S4	21	F	right frontal (prefrontal)
S5	39	F	bifrontal
S6	35	F	right temporo-parietal
S7	45	F	right temporo-occipital
S8	26	F	right frontal (premotor)
S9	37	F	right frontal (premotor)
S10	25	F	right central
S11	32	F	bitemporal
S12	19	F	right temporal (postero-basal)
S13	17	M	left occipital
S14	47	M	left fronto(orbital)-insular

Table 1. Participant description: age, gender and description of epileptogenic focus as determined by the clinical staff (Grenoble Neurological Hospital, France).

Furthermore, for the purpose of additional analysis and comparison, additional data was also obtained from a second pool of 11 patients (6 women, mean age 33 ± 9.5 years) who were implanted using the same procedure at the Lyon Neurological Hospital (Lyon, France). Informed consent and review board approvals were also obtained for this group.

4.2. Stimuli and Experimental Design

The stimuli used in this study are an adaptation of a classical visual search test developed by Treisman and Gelade (1980). Each stimulus consisted of an array of 36 letters (6 x 6 square array with 35 ‘L’s and one ‘T’ randomly arranged). Participants were instructed to find the 'T' as fast as possible via a response button. To dissociate correct from wrong responses the subjects were required to indicate whether the target was located in the upper or lower half of the display by pressing one of two response buttons on a control pad located under their right index or middle finger. The spatial configuration of the buttons in the control pad was such that the target button for upper field targets was above the target button for lower field targets, ruling out any complex spatial remapping processes between visual target and button position. Response latencies for each trial were stored to disc for subsequent offline analysis of reaction time and behavioral performances. In the present study two main experimental conditions were contrasted: an easy search condition and a difficult search condition. The task was always to find a target (the letter ‘T’) presented among 35 distracters (the letter ‘L’). In the EASY condition, the target was gray while all distracters were black. In the DIFFICULT condition, both distracters and target were gray. The difficult and easy condition stimuli were presented randomly for a fixed duration of 3 seconds and with an inter-stimulus interval (ISI) of 1 second. The stimuli were displayed on a 19’’ computer screen located at 60 cm away from the subject. Only data trials with correct target detection were analyzed. Each experiment consisted of 6 runs of 5 minutes recording blocks.

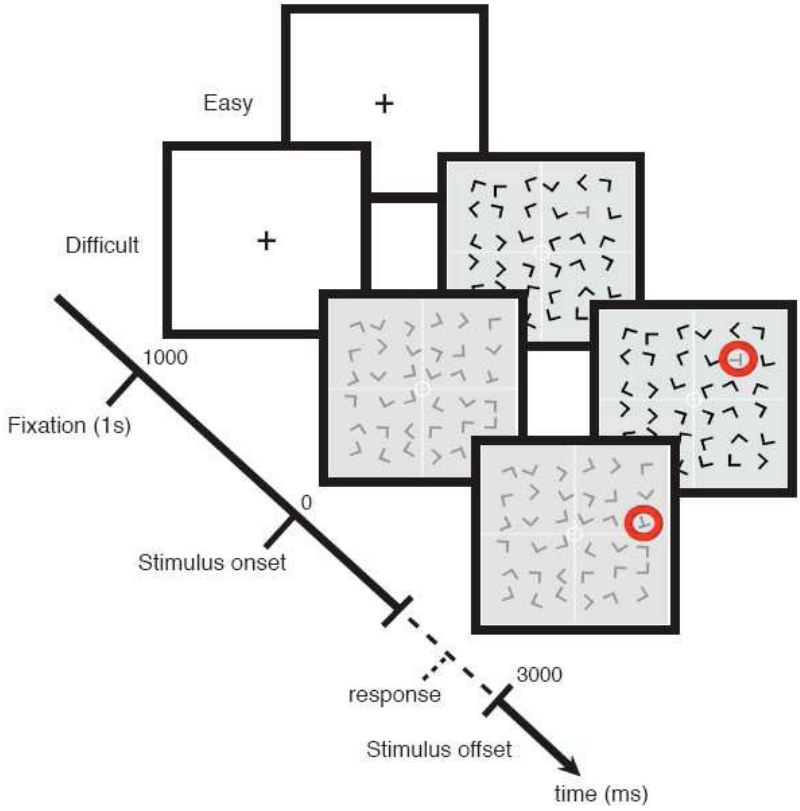

Figure 31: Visual search task description. Subjects were instructed to find the only grey 'T' in an array of 'L's. In the easy condition, all 'L's (the distracters) were black. This made the 'T' easy to spot. In the difficult condition, all 'L's were grey. The conditions were randomly interleaved. Subjects were asked to detect the target as fast as possible via a button press and reaction times (RTs) were stored for offline analysis. The subjects pressed one of two buttons to indicate whether the target was in the upper or lower half of the screen. Each search array was presented for three seconds irrespective of the reaction times of the subjects. The inter-trial interval was one second.

4.3. Data Acquisition

4.3.1. Electrode implantation. Eleven to fifteen semi-rigid multi-lead electrodes were stereotactically implanted in each patient. The stereotactic-EEG (SEEG) electrodes used have a diameter of 0.8 mm and, depending on the target structure, consist of 10 to 15 contact leads 2 mm wide and 1.5 mm apart (DIXI Medical, Besançon, France). All electrode contacts were identified on the patient's individual stereotactic implantation scheme, and were subsequently anatomically localized using Talairach and Tournoux's proportional atlas (2). In addition, computer-assisted matching between a post implantation CT-scan and a pre-implantation 3-D MRI data set (VOXIM R, IVS, Solutions, Germany) allowed for direct visualization of the electrode contacts on the patient's brain anatomy using the ACTIVIS (Software for visualization and analysis of

multi-modal medical images, joint development between INSERM U821, CERMEP and UMR 5230).

4.3.2. SEEG recordings. Intracerebral recordings were conducted using a video-SEEG monitoring system (Micromed, Treviso, Italy), which allowed the simultaneous data recording from 128 depth-EEG electrode sites. The data were bandpass-filtered online from 0.1 to 200 Hz and sampled at 512 Hz in twelve patients (Data from the other two patients were digitized at 1024 Hz). At the time of acquisition the data is recorded using a reference electrode located in white matter, each electrode trace is re-referenced with respect to its direct neighbor (bipolar derivations). This bipolar montage has a number of advantages over common referencing. It helps eliminate signal artifacts common to adjacent electrode contacts (such as the 50 Hz power supply artifact or distant physiological artifacts) and achieves a high local specificity by canceling out effects of distant sources that equally spread to both adjacent sites through volume conduction. The spatial resolution achieved by the bipolar SEEG is on the order of 3mm (Lachaux et al., 2003b). Eye movements were monitored by recording the electrooculogram (EOG) in all sessions.

4.3.3. Specificity of SEEG compared to ECoG

The use of stereotactic EEG (SEEG) is less wide-spread than that of Electrocorticography (ECoG) in the clinical setting of drug-resistance epilepsy treatment. To date, some important differences between these two intracranial EEG techniques remain unknown to the broader community. Some SEEG specificities are crucial with regards to the present study. First of all, by contrast to ECoG which consists of placing grid electrodes (or strips) directly on the cortical surface, SEEG consists of implanting several semi-rigid multi-lead depth electrodes inside the brain. This is achieved via a stereotactic approach developed by Talairach and Bancaud (Talairach & Tounoux, 1993). As a result, SEEG provides direct recordings from deep structures and allows for a sampling of brain activity all the way from the lateral surface to medial wall structures. SEEG electrodes can also records from neural populations located deep within the sulci. Such spatial sampling cannot be achieved with ECoG and represents a major asset for the extensive investigation of distributed brain networks, such as the default-mode network.

Furthermore, the small SEEG inter-electrode distance (1.5 to 4.5 mm inter-electrode distance, compared to 1 cm in standard subdural ECoG grids) in combinations with bipolar derivations guarantees a high spatial specificity and more robustness with respect to signal artifacts.

4.4. DATA ANALYSIS

4.4.1. Time-Frequency Maps (Wavelet analysis)

To quantify signal power modulations across time and frequency we used standard time-frequency (TF) wavelet decomposition (6). The signal $s(t)$ is convoluted with a complex Morlet wavelet (,) 0 *w t f* , which has Gaussian shape in time (*t* s) and frequency (*f* s) around a central frequency 0 *f* and defined by: (,) exp (/2) exp (2) 0 2 t 2 0 *w t f* = *A* -*t* s *i*p*f t* , with *f t* s = 1/ 2ps and a normalization factor 2 / 1) (- = p s *t A* . Throughout this study we used a wavelet family with cycle number set to 7 (i.e. / 7 0 = *f f* s). The square norm of the convolution results in a time-varying representation of spectral power, given by: 2 0 0 $P(t,f) = w(t,f) \cdot s(t)$.

TF maps for each electrode were then computed by averaging TF power maps across trials (and, in the case of cluster-level TF maps, across all electrodes of the cluster). The frequency range extended from 1 to 200 Hz and a pre-stimulus baseline interval was set to be between -400 and -100 ms prior to visual array presentation. All TF maps presented here are given in Z values, as a result of the Wilcoxon signed rank test for emergence (i.e. task-related increases or decreases of power in poststimulus period compared to baseline power values at each frequency). All wavelet-based TF map computations were performed with an in-house software package for electrophysiological signal analysis (ELAN-Pack) developed at INSERM U821 Brain Dynamics & Cognition Lab (Lyon, France).

4.4.2. Estimation of gamma power profiles (Hilbert transform)

In addition to the use of wavelet-based analysis, we also examined the time course of frequency specific amplitude modulations using the Hilbert transform. Applying the Hilbert transform to the continuous recordings splits the data into instantaneous amplitude (i.e. envelope) and phase components in a given frequency interval. In addition to being a convenient measure of instantaneous amplitude modulations in a frequency range of interest, performing spectral analysis using the Hilbert transform was also used to confirm the TF results obtained independently by wavelet analysis. These comparisons provided an additional level of confidence in the results of spectral analysis reported throughout this study. For a comparison of Wavelet decomposition and Hilbert transform see Le Van Quyen et al. (Le Van Quyen et al., 2001).
In the following, we describe the straight-forward procedure followed here to compute task-related amplitude modulations in the high gamma band (60-140 Hz). The same method was used for calculations in other frequency bands.

Step 1 Estimating gamma-band envelope (i.e. time-course of gamma-band power)

Continuous SEEG signals were first band-pass filtered in multiple successive 10Hz-wide frequency bands (e.g. 8 bands from [60 - 70 Hz] to [130 - 140 Hz]). Next, for each band-pass filtered signal we computed the envelope using standard Hilbert transform. The obtained envelope has a time resolution of 64 Hz (time bins every 15,625 ms). Again for each band, this envelope signal (i.e. time-varying amplitude) was divided by its mean across the entire recording session and multiplied by 100. This yields instantaneous envelope values expressed in percent (%) of the mean. Finally, the envelope signals computed for each consecutive frequency bands (e.g. 8 bands of 10-Hz intervals between 60- 140 Hz) were averaged together, to provide one single time-series (the high gamma-band envelope) across the entire session. By construction, the mean value of that time-series across the recording session is equal to 100.

Step 2 Computing task-related time course of % gamma power

As for the wavelet-based TF analysis, we also computed task-related ‘emergence’ (i.e. stimulus related or response-related increases or decreases in the amplitude of the gamma-band envelope). These modulations were computed by contrasting gamma-band

amplitude during visual search to values obtained during the pre-stimulus baseline period (-400 -100). To test for significant increases or decreases we used paired-sample Wilcoxon signed rank test, followed by false discovery rate (FDR) correction across all time samples. The FDR approach yields a corrected threshold for significance (Genovese, Lazar, & Nichols, 2002). Note that for visualization purposes, all power profiles are baseline corrected. Moreover, cluster-level gamma-band time courses were obtained by event-locked time-domain averaging across trials and electrodes of the cluster. Note that strictly speaking, Hilbert transform yields amplitude of a signal envelope, while the waveletbased analysis provides power values. However, given that signal power here is the square of signal amplitude, our findings and their interpretations hold true for power and amplitude and the two concepts are used here interchangeably.

4.5. Mapping intracranial EEG data to standard MNI brain

To obtain an anatomical representation of all significant power modulations for a given frequency band, we mapped pooled data from all subjects onto a standard Montreal Neurological Institute (MNI) brain. The value assigned to each node of the MNI brain represents the average of data from all recording sites located within a distance of maximum 15 mm from the node (For this purpose, all electrode coordinates were transformed from Talairach to common MNI space). The individual data averaged in thus study represent Z values (Wilcoxon test, FDR corrected) for each subject, thereby they represent statistically significant task-related increases or decreases of signal power in a given frequency band (compared to a baseline period, as described above). This data mapping procedure provides, above all, a convenient way to pool and visualize intracerebral EEG data from all subjects on a common MNI brain and is used to identify anatomo-functional regions of interest for more precise analysis at the individual level. Most importantly, all statistical analysis provided throughout this study are based on single electrode or cluster-level statistical analysis based on the estimated band-specific time series at each electrode of each subject (power envelopes obtained with Hilbert transform). In other words, we do not use the interpolated and averaged data represented on the MNI maps for subsequent statistical analysis.

4.6. Definition of anatomo-functional clusters

Mapping significant task-related power increases or decreases to standard MNI brain (as described in previous section) allows for the identification of anatomo-functional clusters of interest. For instance, what we refer to in this study as "deactivation clusters" was obtained by mapping all significant gamma band deactivation (GBD) data from all subjects to the common MNI brain. The result (Fig 2A) represents in blue all brain regions that show a statistically significant suppression of high gamma power (60-140 Hz) during active search compared to the pre-stimulus baseline level (data pooled across all subjects). Using statistical significance of gamma deactivation as functional criterion and its spatial distribution as anatomical criterion the following major anatomo-functional deactivation clusters were obtained: Posterior Cingulate Cortex-Precuneus (PCC), Medial Prefrontal Cortex (MPFC), L and R Ventrolateral Prefrontal Cortex (VLPFC), Temporal Parietal junction (TPJ), Lateral Temporal Cortex (LTC) and Middle Frontal Gyrus (MFG). Table S3 lists all electrodes that define the gamma-band "deactivation cluster" as well as their coordinates and anatomical location (Broadmann areas).

4.7. Computing deactivation onset and duration:

We used signed rank Wilcoxon tests, followed by FDR correction across time samples to assess the statistical significance ($p<0.05$) of event-related increases or decreases in the time course of gamma band power. Gamma-band deactivation (GBD) onset latency and duration were determined on the basis of statistical criteria: The onset of GBD was defined as occurring at the time bin at which the deactivation exceeded the statistical threshold ($p<0.05$, FDR) for the first time and if at least values for 2 consecutive time bins remain below the threshold. We tested for significant differences between GBD onset across clusters using t-test for independent samples ($p<0.01$). The results (as shown in Fig. 2C for example) include pooled data from both the easy and difficult condition since no statistical differences were found between the GBD onset across conditions. As for GBD duration, it was defined as the total duration of statistically significant GBD (FDR, $p<0.05$) occurring in the total time window between deactivation onset and 3000 ms (i.e. end of visual array presentation). We tested for differences in GBD duration between easy and difficult search conditions for each cluster using paired t-test ($p<0.01$). Note that the estimation of onset and duration were performed for task-related power

modulations in other frequency bands (e.g. beta band) in the exact same way as described above for the gamma band.

4.8. Evaluating the relationship between GBD and performance

The link between GBD strength and speed of target detection was examined at two levels: (a) group level analysis across all electrodes of each cluster, and (b) using trial-by-trial correlation analysis in individual subject data.

a) Cluster-level approach

For a given condition (e.g. difficult search), we sorted the trials into two groups: 50 % fastest response trials (short RTs) and 50% slowest response trials (long RTs) trials. We computed mean GBD power separately for each group of trials using data from all electrodes of the deactivation cluster. Note that mean GBD power was obtained by taking the mean of the amplitude over a fixed time window during visual search: [200 700] ms for stimulus-locked analysis (time zero at search array onset) and [-900 -200] for response-locked analysis (time zero at button press). Criteria for GBD time window selection: For stimulus-locked averaging we set the lower bound to 200 ms as this corresponds approximately to the earliest GBD onset across all electrodes and subjects. The upper bound was set to 700 ms, which corresponds to a latency at which no response had yet occurred in 95 % of all trials. The time window for response-locked analysis was set between -900 and -200 ms prior to response (so as not to include data immediately preceding the button-press). In addition, we found that results reported with these windows did not change by shifting the bounds by ±100 ms. Finally, we tested for differences in GBD for the two groups of trials (50 % fastest vs 50% slowest) using paired t-test ($p<0.01$). (e.g. Fig 3A and figure S4 of the firs article).

b) Single-trial analysis

Using single-trial electrode data, we computed the correlation between instantaneous

gamma power and the reaction times of the corresponding trials. This was performed for at each time bin of single trial power envelope resulting in a time-series of correlation coefficients. Scatter plots were then used to illustrate the relationship between reaction times and single-trial gamma power at tmax, the time bin of peak correlation.

4.9. Gamma-band large-scale correlation & anticorrelation analysis

We examined temporal correlations among gamma power envelopes from all recording sites located in task positive (TPN) and task-negative networks (TNN) in each subject. TPN and TNN consist of electrode clusters with significant stimulus-induced gamma-band activation and deactivation respectively (see table S4 for anatomical details). For each pair of electrodes the correlation was computed as follows: For each electrode site a time series was obtained by concatenating multiple 1-s segments of gamma power envelope, one from each trial (from 0 to 1000 ms following stimulus onset). For instance, a data set with 100 trials would yield a 100 s time series of raw gamma power envelope obtained during active task periods. Next, we calculated the cross-correlation between the two signals at various time lags (within +/- 156 ms range) to identify the maximum correlation value (i.e. maximum in terms of absolute value).

Next, we computed correlations obtained with surrogate data sets obtained by recomposing one of the two signals via random shuffling of the trial order within the time-series. This was carried out 99 times for each electrode pair, yielding 99 correlation values. If the original correlation between the two time series is higher (in absolute value) than the 99 surrogates, the correlation between the gamma envelopes at the two sites was considered to be statistically significant at $p<0.01$. Note that the sign of the significant correlation value indicates whether the correlation is positive (“correlated”) or negative (i.e. “anti-correlated”).

After computing all possible correlations between all relevant electrode pairs within each subject, we evaluated the number of significant correlations as a function of the type of electrode-pair group they belong to: *intra-network correlation* (i.e. TPN-TPN and TNA-

TNA electrode pairs), or *inter-network correlation* (i.e. TPN-TNA electrode pairs). The total number of significant positive and negative correlations and their ratio with respect to non-significant correlation was computed as a function of correlation type (inter-network or intra-network correlation). Finally, we used paired t-test across subjects to test whether the negative or rather the positive correlations were predominant in each correlation group (inter-network correlations and intra network correlations). Such analysis allowed us for instance to show that TPN-TNA electrode pairs (inter-network correlation) predominantly exhibit more negative correlations than positive correlations (The inverse was true for the intra-network correlations, where positive correlations were more prominent than negative correlation).

5. First study: Electrophysiological correlates of the default mode network

5.1. Hypothesis and Comments about the study

Our ability to quickly perceive and react to events in the outside world depends on our level of vigilance. Our state of alertness and thus our performance can fluctuate over the course of a day or even over the time span of a few seconds. To date, the neural mechanisms that facilitate or hinder efficient task-engagement are still poorly understood.

As we have seen in the first chapter, converging neuroimaging evidence supports the view that attention-demanding goal-direted behavior is mediated not only by distributed patterns of cerebral activation but, remarkably, also by concurrent suppression of activity in distinct set of brain regions (see Figure 32, Shulman et al. 1997; Corbetta and Shulman, 2002; Fox et al. 2005). Brain regions that show systematic deactivations during task performance collectively form a network known as the default-mode network (DMN) (Raichle et al. 2001; Raichle and Mintun, 2006). Metabolic deactivations in this network during goal-directed behaviors are only the trace of neural mechanisms still unknown.

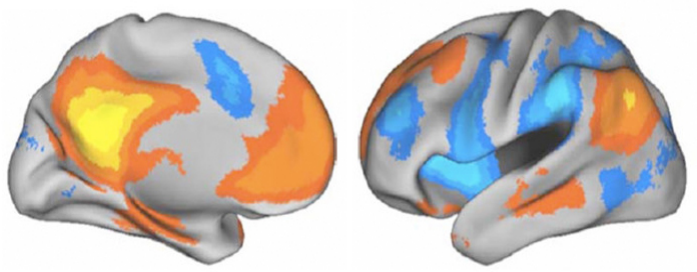

Figure 32: Regions positively correlated with the default mode network (orange). The areas shown in blue are negatively correlated with the DMN and may be described as a goal-directed network. (From Carhart-Harris et al., 2008)

As seen in the previous figure, while task-related activations often involve frontoparietal circuits such as the dorsal attention network, task-negative networks comprise medial and lateral core regions of the DMN, including posterior cingulated cortex (PCC), medial prefrontal cortex (MPFC), lateral temporal cortex (LTC), and temporal parietal junction

(TPJ). Whereas the precise spatial characteristics of the DMN are amenable to imaging studies, its fine-scale temporal properties and its relationship with behavior remain elusive, limiting severely the prospect of fully unraveling the functional role of DMN deactivation.

In this study we address this gap by determining the electrophysiology of the deactivation phenomenon at the population level across the human brain.

Human intracranial recordings were obtained from depth electrodes implanted in epileptic drugs-resistant patients of Grenoble's Hospital, following a standard clinical procedure motivated only by therapeutical considerations, aiming surgical interference with the epileptogenic network (Lachaux et al., 2003a). The spatio-temporal resolution of such recordings is excellent: the temporal resolution of sEEG is on the order of milliseconds (sampling rate of 512 Hz), while the spatial resolution is on the order of a couple of millimetres (see Figure 15), allowing to extract the activity of functionally homogeneous cortical structures. We obtained an unprecedented dense sampling of the human brain by acquiring stereotactic-electroencephalography (SEEG) data from over 1730 intracerebral recording sites in 14 patients.

The stimuli used in this work are an adaptation of classical of visual search test developed by Anne Treisman (A. M. Treisman & Gelade, 1980). Six different stimuli were presented in random order for each patient (figure 5). The stimuli were arrays of 36 letters (6 x 6, 35 'L's and 1 'T') randomly arranged. Participants had to find the grey T to report its position in the display (upper or lower part), as fast as possible, by pressing one of two response buttons on a joystick (located under their right index or middle finger). The spatial configuration of the buttons on the joystick was such that the target button for upper field targets was above the target button for lower field targets, avoiding any necessity for spatial remapping between target and button position. Reaction times for each trial were calculated offline on the PC used for data analysis. There were six different types of display, corresponding to six different conditions, as illustrated in figure 5, and the task was always to find the grey 'T', distractors were always 'L's. In the ONE condition (EASY), all distractors were black, in the TOP condition, 18 black distractors were in the down half of the screen, while 17 grey distractors (and the grey 'T') were in the upper half of the screen. The LEFT and RIGHT conditions were similar to TOP

condition, but the division of screen was made between the left and right halves. In the MIX condition, 19 grey distractors were randomly spaced in the image, the same for the 16 black distractors. In the ALL (DIFFICULT) condition, all distractors were grey. The type of display was changed randomly from one trial to the next; the same display was never presented twice. Each image lasted three seconds with a one second interval. The stimuli were displayed on a 19'' computer screen located at 57 cm of distance. Only the correct answers were analyzed. Each experiment lasted 30 minutes, distributed in 6 blocks of 5 minutes. In order to simplify the data, only two conditions were analyzed: easy (condition ONE) and difficult search (condition ALL).

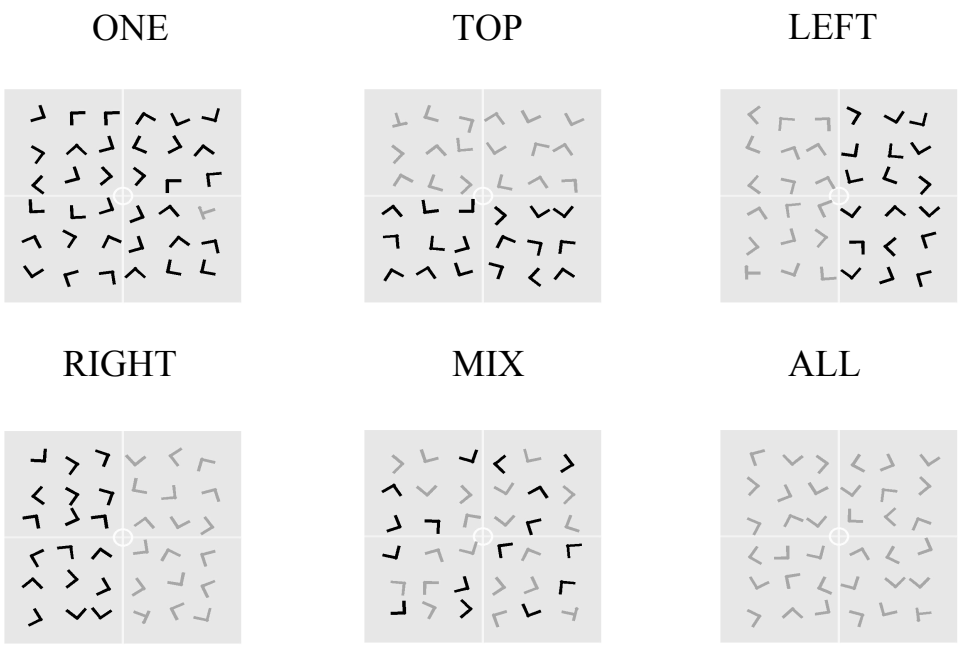

Figure 33 Experimental conditions. Where is the grey T? Task ONE is a good example of easy visual search, because there is an evident feature (in this case grey level) that differentiates the target from distractors (grey 'T' between 35 black 'L's). For the other five tasks the real distractors are the grey 'L's, that increased to 17 (in TOP, LEFT and RIGHT), 19 in MIX and 35 in the task ALL.

As we have see in the first article of this dissertation, our results show that visual search is associated with transient task-induced gamma band suppression (GBS) in posterior cingulate cortex (PPC), medial prefrontal cortex (MPFC), ventrolateral prefrontal cortex (VLPFC), lateral temporal cortex (LTC) and temporal parietal junction (TPJ). The striking spatial correlation between GBD areas and DMN provides evidence in humans

for a direct link between GBS and task-related deactivation as measured with fMRI. Most importantly, our GBS analysis shows that the duration and intensity of gamma suppression is modulated by task complexity. In addition this observation was also found in a second study (Fig. 3) investigating processing of facial expression. **Our data provide novel insights into the electrophysiological correlates of intrinsic brain networks and significantly advance our understanding of the default mode network.**

Behavioral/Systems/Cognitive

Transient Suppression of Broadband Gamma Power in the Default-Mode Network Is Correlated with Task Complexity and Subject Performance

Tomas Ossandón,[1,2] Karim Jerbi,[1,2] Juan R. Vidal,[1,2] Dimitri J. Bayle,[1,2] Marie-Anne Henaff,[1,2] Julien Jung,[1,2] Lorella Minotti,[3,4] Olivier Bertrand,[1,2] Philippe Kahane,[3,4] and Jean-Philippe Lachaux[1,2]

[1]Lyon Neuroscience Research Center, INSERM U1028, CNRS UMR5292, Brain Dynamics and Cognition Team, F-69500 Lyon-Bron, France, [2]Université Claude Bernard Lyon 1, F-69000 Lyon, France, [3]Neurology Department, Grenoble Hospital, F-38043 Grenoble, France, and [4]INSERM U836, Grenoble Institute of Neurosciences, F-38700 Grenoble, France

Task performance is associated with increased brain metabolism but also with prominent deactivation in specific brain structures known as the default-mode network (DMN). The role of DMN deactivation remains enigmatic in part because its electrophysiological correlates, temporal dynamics, and link to behavior are poorly understood. Using extensive depth electrode recordings in humans, we provide first electrophysiological evidence for a direct correlation between the dynamics of power decreases in the DMN and individual subject behavior. We found that all DMN areas displayed transient suppressions of broadband gamma (60–140 Hz) power during performance of a visual search task and, critically, we show for the first time that the millisecond range duration and extent of the transient gamma suppressions are correlated with task complexity and subject performance. In addition, trial-by-trial correlations revealed that spatially distributed gamma power increases and decreases formed distinct anticorrelated large-scale networks. Beyond unraveling the electrophysiological basis of DMN dynamics, our results suggest that, rather than indicating a mere switch to a global exteroceptive mode, DMN deactivation encodes the extent and efficiency of our engagement with the external world. Furthermore, our findings reveal a pivotal role for broadband gamma modulations in the interplay between task-positive and task-negative networks mediating efficient goal-directed behavior and facilitate our understanding of the relationship between electrophysiology and neuroimaging studies of intrinsic brain networks.

Introduction

Our ability to quickly perceive and react to events in the outside world depends on our level of vigilance. Our state of alertness and thus our performance can fluctuate over the course of a day or even over the time span of a few seconds. To date, the neural mechanisms that facilitate or hinder efficient task engagement are still poorly understood. Converging neuroimaging evidence supports the view that attention-demanding, goal-directed behavior is mediated not only by distributed patterns of cerebral activation but, remarkably, also by concurrent suppression of activity in a distinct set of brain areas (Shulman et al., 1997; Corbetta and Shulman, 2002; Fox et al., 2005). Because of their intrinsically elevated activity during rest, these areas collectively form a network known as the default-mode network (DMN) (Raichle et al., 2001; Raichle and Mintun, 2006). While task-related activations often involve frontoparietal circuits such as the dorsal attention network, task-negative networks comprise medial and lateral core regions of the DMN, including posterior cingulate cortex, medial prefrontal cortex, lateral temporal cortex, and temporal parietal junction. Additionally, distinct deactivation patterns have also been reported in inferior parietal and ventrolateral prefrontal cortex areas and are thought to be key components of a ventral attention network (Corbetta et al., 2008). DMN deactivation has been associated with the transition from an interoceptive mode of self-directed cognition (Gusnard and Raichle, 2001; Mason et al., 2007) to an exteroceptive mode of outward attention (Raichle and Mintun, 2006; Raichle, 2009; Spreng et al., 2010). In addition, recent findings suggest that the DMN couples with the frontoparietal network in goal-directed cognition (Spreng et al., 2010). While the precise spatial characteristics of the DMN are amenable to imaging studies, its fine-grained temporal properties and its relationship with behavior remain elusive. As a result, the precise role of DMN deactivations is not fully understood. In this study, we address this issue by monitoring neural population activity directly recorded in human default mode structures and, most importantly, by assessing

Received May 18, 2011; revised Aug. 11, 2011; accepted Aug. 16, 2011.

Author contributions: T.O., M.-A.H., and J.-P.L. designed research; T.O., K.J., J.R.V., D.J.B., L.M., P.K., and J.-P.L. performed research; T.O., K.J., J.R.V., D.J.B., J.J., O.B., P.K., and J.-P.L. analyzed data; T.O., K.J., and J.-P.L. wrote the paper.

Funding was provided by the Ministère de l'Education Nationale et la Recherche (France), the Fondation pour la Recherche Médicale, and the BrainSync FP7 European Project (Grant HEALTH-F2-2008-200728). We thank all patients for their participation, the staff of the Grenoble Neurological Hospital epilepsy unit, and Dominique Hoffmann, Patricia Boschetti, Carole Chatelard, Véronique Dorlin, and Martine Juillard for their support. We are grateful to Dr Bharat Biswal for helpful comments on a previous version of this manuscript.

The authors declare no competing financial interests.

Correspondence should be addressed to Dr. Karim Jerbi, INSERM U1028, Centre de Recherche en Neurosciences de Lyon, Equipe Dynamique Cérébrale et Cognition, Centre Hospitalier le Vinatier, Batiment 452, 95 Boulevard Pinel, F-69500 Lyon-Bron, France. E-mail: karim.jerbi@inserm.fr.

DOI:10.1523/JNEUROSCI.2483-11.2011

 0270-6474/11/3114521-10$15.00/0

its modulation as a function of task engagement and performance. Using extensive brain-wide, intracerebral depth recordings in surgical epilepsy patients performing a visual search task, we found that DMN neural populations display task-related, high-frequency power suppressions in the high gamma range (60–140 Hz). Above all, we reveal for the first time that the fine-scale temporal dynamics of such broadband gamma power suppression in DMN regions are tightly correlated with task demands and subject performance on a trial-by-trial basis. Our findings further suggest that efficient goal-directed behavior is mediated by an intricate interplay between anti-correlated networks of distributed broadband gamma power increases and decreases.

Materials and Methods

Stimuli and experimental design

The stimuli used in this study are an adaptation of a classical visual search test developed by Treisman and Gelade (1980). Each stimulus consisted of an array of 36 letters (6 × 6 square array with 35 Ls and one T randomly arranged). Participants were instructed to search as fast as possible for the "T" and press a response button as soon as they found it. Two main experimental conditions were contrasted: an easy search condition and a difficult search condition (see Fig. 1*B*). In the EASY condition, the target was gray while all distracters were black. To dissociate correct from wrong responses the subjects were required to indicate whether the target was located in the upper or lower half of the display by pressing one of two response buttons. In the DIFFICULT condition, both distracters and target were gray. The difficult and easy condition stimuli were presented randomly for a fixed duration of 3 s and with an interstimulus interval of 1 s. The stimuli were displayed on a 19 inch computer screen located 60 cm away from the subject. Each experiment consisted of 6 runs of 5 min recording blocks.

Participants

Intracranial recordings were obtained from 14 neurosurgical patients with intractable epilepsy (11 women, mean age: 32 ± 10 years) at the Epilepsy Department of the Grenoble Neurological Hospital (Grenoble, France). All patients were stereotactically implanted with multi-lead EEG depth electrodes. All electrode data exhibiting pathological waveforms were discarded from the present study. This was achieved in collaboration with the medical staff and was based on visual inspection of the recordings and by systematically excluding data from any electrode site that was *a posteriori* found to be located within the seizure onset zone. All participants provided written informed consent, and the experimental procedures were approved by the Institutional Review Board and by the National French Science Ethical Committee. Patient-specific clinical details are provided in Table 1.

Table 1. Participant description: age, gender, and description of epileptogenic focus as determined by the clinical staff of Grenoble Neurological Hospital, Grenoble, France

Patient	Age	Gender	Epileptogenic zone
S1	46	M	Right temporal (anteromesial)
S2	42	F	Left temporal (anterior)
S3	22	F	Left frontal (operculum)
S4	21	F	Right frontal (prefrontal)
S5	39	F	Bi-frontal
S6	35	F	Right temporoparietal
S7	45	F	Right temporooccipital
S8	26	F	Right frontal (premotor)
S9	37	F	Right frontal (premotor)
S10	25	F	Right central
S11	32	F	Bi-temporal
S12	19	F	Right temporal (posterobasal)
S13	17	M	Left occipital
S14	47	M	Left fronto (orbital)-insular

Electrode implantation

Eleven to fifteen semi-rigid, multi-lead electrodes were stereotactically implanted in each patient. The stereotactic electroencephalography (SEEG) electrodes used have a diameter of 0.8 mm and, depending on the target structure, consist of 10 to 15 contact leads 2 mm wide and 1.5 mm apart (DIXI Medical Instruments). All electrode contacts were identified on each patient's individual stereotactic implantation scheme and were subsequently localized anatomically using Talairach and Tournoux's proportional atlas (Talairach and Tounoux, 1993). In addition, computer-assisted matching between a post-implantation CT scan and a preimplantation 3-D MRI dataset (VoXim R, IVS Solutions) allowed for direct visualization of the electrode contacts on the patients brain anatomy using ACTIVIS (developed by INSERM U1028, CERMEP, and UMR 5230). Whenever available, we also used a post-implantation MRI to verify electrode localization. Visual inspection of the electrodes superposed on each subject's individual MRI was used to check whether each SEEG electrode was located in gray or white matter.

SEEG recordings

Intracerebral recordings were conducted using a video-SEEG monitoring system (Micromed), which allowed the simultaneous data recording from 128 depth-EEG electrode sites. The data were bandpass filtered online from 0.1 to 200 Hz and sampled at 512 Hz in 12 patients (data from the other two patients were digitized at 1024 Hz). At the time of acquisition the data are recorded using a reference electrode located in white matter, and each electrode trace is subsequently re-referenced with respect to its direct neighbor (bipolar derivations). This bipolar montage has a number of advantages over common referencing. It helps eliminate signal artifacts common to adjacent electrode contacts (such as the 50 Hz mains artifact or distant physiological artifacts) and achieves a high local specificity by cancelling out effects of distant sources that spread equally to both adjacent sites through volume conduction. The spatial resolution achieved by the bipolar SEEG is on the order of 3 mm (Lachaux et al., 2003; Kahane et al., 2006; Jerbi et al., 2009). Both spatial resolution and spatial sampling achieved with SEEG differ slightly from that obtained with subdural grid electrocorticography (Jerbi et al., 2009).

Time–frequency analysis, gamma power, and envelope computations

Task-induced modulations of power across time and frequency were obtained by standard time–frequency (TF) analysis using wavelets (Tallon-Baudry et al., 1997), and instantaneous signal amplitude profiles were computed using the Hilbert transform (Le Van Quyen et al., 2001). All wavelet-based TF map computations were performed with in-house software package for electrophysiological signal analysis (ELAN) developed at INSERM U1028, Lyon, France (Aguera et al., 2011). In addition to the use of wavelet-based analysis, we also examined the time course of frequency-specific signal envelope modulations using the Hilbert transform. Applying the Hilbert transform to the continuous recordings splits the data into instantaneous amplitude (i.e., envelope) and phase components in a given frequency interval. In addition to being a convenient measure of instantaneous amplitude modulations in a frequency range of interest, performing spectral analysis using the Hilbert transform was also used to confirm the TF results obtained independently by wavelet analysis. These comparisons provided an additional level of confidence in the results of spectral analysis reported throughout this study. For a comparison of wavelet decomposition and Hilbert transform, see Le Van Quyen et al. (2001). In the following, we describe the standard procedure used to compute task-related power modulations in the high gamma band (60–140 Hz). The same method was used for calculations in other frequency bands.

Step 1: estimating gamma-band envelope (*i.e., time course of gamma-band amplitude*). Continuous SEEG signals were first bandpass filtered in multiple successive 10 Hz wide frequency bands (e.g., 8 bands from [60–70 Hz] to [130–140 Hz]) using a zero phase shift noncausal finite impulse filter with 0.5 Hz roll-off. Next, for each bandpass filtered signal we computed the envelope using standard Hilbert transform. The obtained envelope has a sampling rate of 64 Hz (i.e., one time sample every 15,625 ms). Again, for each band this envelope signal (i.e., time-varying amplitude) was divided by its mean across the entire recording session

and multiplied by 100. This yields instantaneous envelope values expressed in percentage (%) of the mean. Finally, the envelope signals computed for each consecutive frequency bands (e.g., 8 bands of 10 Hz intervals between 60 and 140 Hz) were averaged together to provide one single time series (the high gamma-band envelope) across the entire session. By construction, the mean value of that time series across the recording session is equal to 100. Note that computing the Hilbert envelopes in 10 Hz sub-bands and normalizing them individually before averaging over the broadband interval allows us to account for a bias toward the lower frequencies of the interval that would otherwise occur due to the $\sim 1/f$ drop-off in amplitude.

Step 2: *computing task-related time course of percentage gamma power modulations*. As for the wavelet-based TF analysis, we also computed task-related "emergence" (i.e., stimulus-related or response-related increases or decreases in the amplitude of the gamma-band envelope). These modulations were computed by contrasting gamma-band amplitude during visual search to values obtained during the prestimulus baseline period (−400 to −100 ms). To test for significant increases or decreases, we used a paired-sample Wilcoxon signed rank test followed by false discovery rate (FDR) correction across all time samples. The FDR approach yields a corrected threshold for significance (Genovese et al., 2002) (e.g., Fig. 3). Note that for visualization purposes, all power profiles are baseline corrected. Moreover, cluster-level gamma-band time courses were obtained by event-locked time domain averaging across trials and electrodes of the cluster (see Table 3 for cluster details).

Mapping intracranial EEG data to standard MNI brain

To obtain an anatomical representation of all significant power modulations for a given frequency band, we mapped pooled data from all subjects onto a standard Montreal Neurological Institute (MNI) brain. The value assigned to each node of the MNI brain represents the average of data from all recording sites located within a maximum distance of 15 mm from the node (for this purpose, all electrode coordinates were transformed from Talairach to common MNI space). The individual data averaged in this study represent *Z* values (Wilcoxon test, FDR corrected) for each subject; thereby they represent statistically significant task-related increases or decreases of signal power in a given frequency band (compared to a baseline period, as described above). This data mapping procedure provides, above all, a convenient way to pool and visualize intracerebral EEG data from all subjects on a common MNI brain and is used to identify anatomo-functional regions of interest for more precise analysis at the individual level. Using statistical significance of gamma power suppression as functional criterion and its spatial distribution as anatomical criterion the following major anatomo-functional deactivation clusters were obtained: posterior cingulate cortex (PCC), medial prefrontal cortex (MPFC), left and right ventrolateral prefrontal cortex (VLPFC), temporal parietal junction (TPJ), lateral temporal cortex (LTC), and middle frontal gyrus (MFG). Table 3 lists the electrodes that define the gamma-band power increase and decrease clusters as well as the coordinates of these ROIs and their anatomical location (Brodmann areas). Most importantly, all statistical analysis provided throughout this study are based on single electrode or cluster-level statistical analysis using the estimated band-specific time series at each electrode of each subject (power envelopes obtained with Hilbert transform). In other words, the interpolated and averaged data represented on the MNI brain maps are used for visualization purposes and not for statistical analysis.

Computing onset and duration of gamma-band power suppressions

We used signed rank Wilcoxon tests, followed by FDR correction (Genovese et al., 2002), across time samples to assess the statistical significance ($p < 0.05$) of event-related increases or decreases in the time course of gamma-band power. Gamma-band power decrease (GBD), onset latency, and duration (see Table 2) were determined from gamma-power envelopes on the basis of statistical criteria (FDR; $p < 0.05$ for the latencies and *t* tests, $p < 0.01$ for the cluster-level inference).

Table 2. Mean duration of significant gamma power suppression in the two experimental conditions (easy and difficult search) computed for all electrodes of each cluster across all 14 participants

	Duration of GBD (ms)				
	LTC	VLPFC	TPJ	PCC	MPFC
Easy search (E)	135 (± 74)	387 (±56)	310 (±114)	178 (±84)	384 (±63)
Difficult search (D)	470 (±72)	689 (±115)	383 (±149)	560 (±117)	1005 (±142)
p value (E vs D)	0.0072225	0.0054465	0.235342	0.006786	0.0003145

The difference between GBD duration in easy and difficult search conditions is statistically significant (paired *t* test, $p < 0.0001$) for all clusters except the TPJ cluster.

Evaluating the relationship between GBD and performance

The link between GBD strength and speed of target detection was examined at two levels, cluster approach and single-trial analysis.

Cluster approach. For a given condition (e.g., difficult search), we sorted the trials into two groups: 50% fastest response trials (short reaction times) and 50% slowest response trials (long reaction times). We computed mean GBD power separately for each group of trials using data from all electrodes of the power suppression cluster (task-negative cluster). Note that mean GBD was obtained by taking the mean of the amplitude over a fixed time window during visual search: [from 200 to 700] ms for stimulus-locked analysis and [from −900 to −200] for response-locked analysis. We tested for differences in GBD for the two groups of trials (50% fastest vs 50% slowest) using a paired *t* test ($p < 0.01$).

Single-trial analysis. Using single-trial electrode data, we computed the correlation between instantaneous gamma power and the reaction times of the corresponding trials. This was performed for each time bin of a single trial power envelope, resulting in a time series of correlation coefficients. Scatter plots were then used to illustrate the relationship between reaction times and single-trial gamma power at $t_{max,}$ the time bin of peak correlation (e.g., Fig. 4*D*).

Gamma-band large-scale correlation and anticorrelation analysis

We examined temporal correlations among gamma power envelopes from all recording sites located in task-positive networks (TPNs) and task-negative networks (TNNs) in each subject. TPN and TNN consist of electrode clusters with significant stimulus induced gamma-band power increases and decreases respectively (see Table 3 for anatomical details). For each pair of electrodes the correlation was computed as follows. For each electrode site a time series was obtained by concatenating multiple 1 s segments of gamma power envelope, one from each trial (from 0 to 1000 ms following stimulus onset). For instance, a dataset with 100 trials would yield a 100 s time series of raw gamma power envelope obtained during active task periods. Next, we calculated the cross-correlation between the two signals at various time lags (within ± 156 ms range) to identify the maximum correlation value (i.e., maximum in terms of absolute value). Next, we computed correlations obtained with surrogate datasets obtained by recomposing one of the two signals via random shuffling of the trial order within the time series. This was carried out 99 times for each electrode pair, yielding 99 correlation values. If the original correlation between the two time series is higher (in absolute value) than the 99 surrogates, the correlation between the gamma envelopes at the two sites was considered to be statistically significant at $p < 0.01$. After computing all possible correlations between all relevant electrode pairs within each subject, we evaluated the number of significant correlations as a function of the type of electrode pair group to which they belong: intranetwork correlation (i.e., TPN-TPN and TNA-TNA electrode pairs) or internetwork correlation (i.e., TPN-TNA electrode pairs). The total number of significant positive and negative correlations and their ratio with respect to nonsignificant correlation was computed as a function of correlation type (internetwork or intranetwork correlation). Finally, we used paired *t* test across subjects to test whether the negative or rather the positive correlations were predominant in each correlation group (internetwork correlations and intranetwork correlations).

Table 3. Anatomical details of the task positive network and the task negative network

	Cluster	Brodmann area(s)	No. of electrode pairs	No. of patients (of 14)	ROI center (right hemisphere)	ROI center (left hemisphere)
TNN	PCC	31	11	5	(−4, −53, 30)	(−4, −53, 30)
TNN	VLPFC	45/47	26	6	(50, 34, 6)	(−49, 37, 6)
TNN	MPFC	32/10	12	5	(10, 45, 4)	(10, 45, 4)
TNN	TPJ	40	7	4	(53, −31, 43)	(−57, 27, 52)
TNN	LTC	21	12	5	(61, −31, −7)	(−61, −34, −4)
TNN	MFG	9	6	3	(43, 8, 40)	(−39, 47, 25)
TPN	DLPFC	46	12	4	(43, 34, 26)	(−50, 11, 16)
TPN	IPS	7	5	2	(23, −50, 49)	n.a.
TPN	IPL	7/40	8	3	(40, −41, 41)	n.a.
TPN	FEF	6	12	3	(12, −10, 56)	(−18, −5, 49)
TPN	SMA/Pre-SMA	6	6	3	(6, −3, 54)	(−10, 4, 49)
TPN	Inf prec gyrus	6/32	35	3	(38, −6, 56)	(−38, −4, 40)
TPN	MT	19/37	51	7	(45, −61, 0)	(−42, −58, −3)
TPN	Orbital gyrus	19/18/23	22	4	(37, −76, 11)	(−24, −72, 0)

Electrodes that show statistically significant decrease or increase in gamma-band power (compared to prestimulus baseline levels) were assigned to the TNN or TPN group respectively (compare Fig. 6). Electrodes within the TNN and TPN were grouped into multiple anatomical clusters. Given the combination of functional (i.e. statistically significant gamma power modulation, Wilcoxon test, $p < 0.05$, FDR correction) and anatomical criteria, the individual clusters within TNN and TPN represent anatomofunctional regions of interest (ROIs). The center of each cluster is obtained by computing the centroid of the Talairach coordinates of all recording sites it includes. Note that the coordinates of PCC, MPFC, and TPJ ROIs are consistent with the coordinates of these DMN structures as reported in the fMRI literature (e.g., Fox et al., 2005). DLPFC, Dorsolateral prefrontal cortex; FEF, frontal eye field; Inf prec gyrus, inferior precentral gyrus; IPL, inferior parietal lobule; IPS intraparietal sulcus; MT, middle temporal cortex; SMA, supplementary motor area.

Results

Transient gamma power suppressions in DMN areas during task performance

We obtained a spatially dense sampling of the human brain by acquiring SEEG data from 1730 intracerebral recording sites in 14 patients who underwent neurosurgical treatment for epilepsy (Fig. 1*A*). Participants were presented with a search array and were instructed to detect a target (a T among the Ls) as fast as possible. We computed task-related spectral power modulations across time and frequency at all recording sites in two experimental conditions: (1) an easy search; and (2) a difficult search (Fig. 1*B*). Remarkably, during visual search a subset of recording sites displayed strong power suppressions in the high-gamma range (60–140 Hz) that was occasionally associated with power increases at lower (<30 Hz) frequencies, as illustrated in Figure 1*C*. To evaluate the spatial distribution of such broadband gamma power suppressions during visual search across the entire brain, we mapped all statistically significant task-related gamma-band decreases, GBDs, from all individuals onto a normalized common brain (see Materials and Methods). The results in Figure 2*A* show that the anatomical distribution of GBD bears a striking similarity with the classical DMN areas (Raichle et al., 2001). In addition to PCC, MPFC, and TPJ, we also observed statistically significant suppressions bilaterally in VLPFC, LTC, and in right MFG.

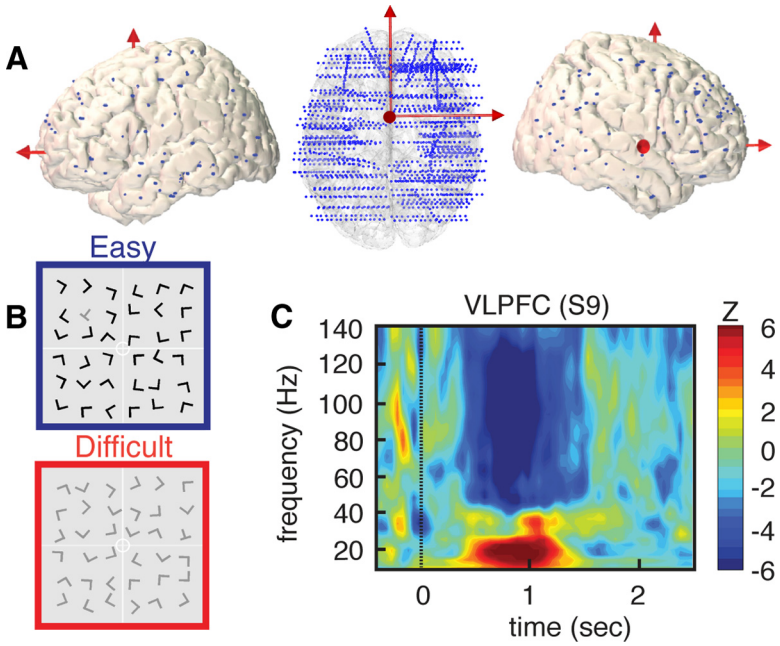

Figure 1. High-density depth electrode recordings during visual search. ***A***, Left, Top and right side views of implanted electrode locations represented on a 3-D reconstruction of a standard (MNI) brain. Blue dots represent the Talairach coordinates for all contacts on all SEEG electrodes for all 14 subjects (total = 1730 recording sites). ***B***, Example of visual search arrays for easy (blue) and difficult (red) conditions (subjects were asked to find the T among the Ls). ***C***, Strong power suppression in broad-band gamma (60–140 Hz) in right VLPFC during visual search. High gamma suppression also coincides with power increases in lower (<30 Hz) frequency range. The illustrative time–frequency map represent increases and decreases in spectral power compared to a prestimulus baseline level (baseline, [from −400 to −100] ms, Wilcoxon *Z* value).

Correlation between subject behavior and gamma power suppression

Analysis of the behavioral data showed that correct target detections (achieved within the fixed 3 s time window) dropped from 91% hits in the easy search to 77% hits in the difficult search. Mean subject reaction times were significantly faster in the easy search (1009 ± 59 ms) than the difficult search (1678 ± 79 ms) conditions ($t = 34.24$, $p < 0.0001$), suggesting longer task engagement during the difficult search. Remarkably, the direct electrophysiological recordings in all the GBD clusters reveal a longer lasting suppression of gamma power in the difficult search condition compared to the easy search condition (see Fig. 2*B*,*D* for cluster results and Fig. 3 for individual electrode data). In other words, the gamma suppression phenomenon lasted longer with higher task complexity and longer task engagement. Furthermore, mean onset times of significant gamma suppression in each cluster were found to indicate that the earliest power de-

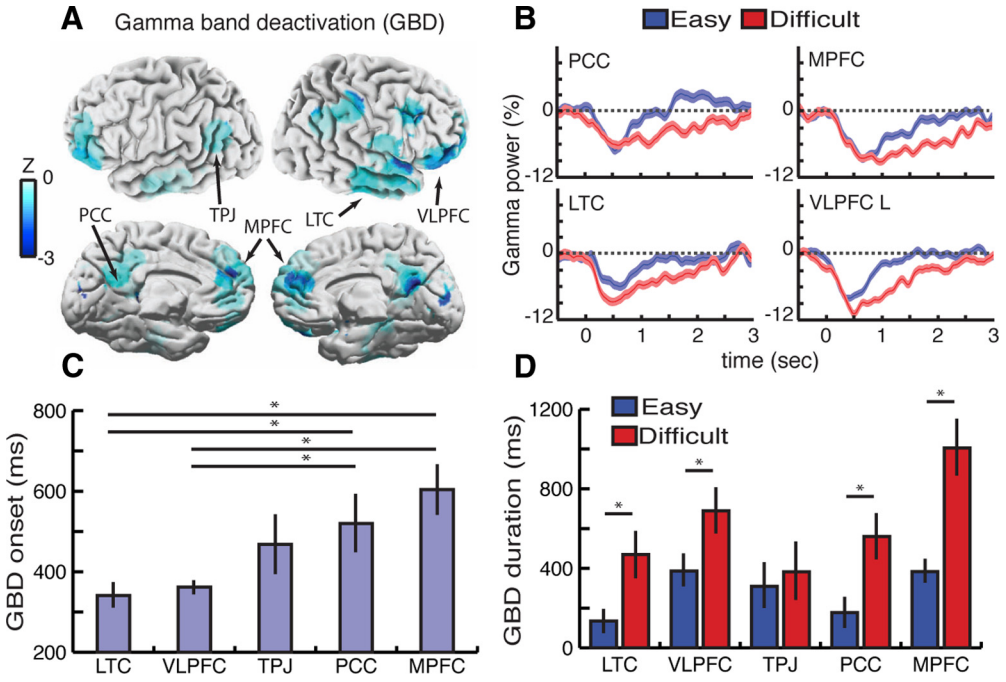

Figure 2. Brain-wide dynamics of gamma-band power decrease, GBD, during visual search. ***A***, Anatomical distribution of statistically significant broad-band gamma (60–140 Hz) suppression obtained by mapping depth electrode data in all subjects ($n = 14$) to a standard brain. The spatial properties of GBD bear a striking resemblance to DMN maps previously reported with fMRI. Data snapshot at $t = 640$ ms following search array presentation (only power decreases are shown here; see Fig. 5 for power increases and decreases and Materials and Methods for details) ***B***, GBD temporal profile during easy (blue) and difficult (red) search for four illustrative clusters: PCC, MPFC, LTC, and VLPFC left (L). Time $t = 0$ ms indicates onset of search array display. ***C***, Mean GBD onset for each cluster. Values represent mean onset latency, i.e., time sample at which deactivation reached statistical significance (group effect $F_{(4,98)} = 6.817$, $p < 0.0001$; Tukey's HSD Test (*) indicates $p < 0.05$). ***D***, Duration of GBD for easy (blue) and difficult (red) visual search conditions. Values represent mean duration of significant deactivation across all electrodes of each cluster (*t* test (*) indicates $t > 2.76$, $p < 0.01$). See Table 2 for the details of task-related GBD duration and associated *p* values and Table 3 for GBD cluster details.

creases occurred in LTC and VLPFC clusters, followed by TPJ, PCC, and eventually MPFC [Fig. 2*C*, group effect $F_{(4,98)} = 6.817$, $p < 0.0001$; Tukey's honestly significant difference (HSD) test, $p < 0.05$]. Interestingly, the chronology of gamma power suppression in these clusters was the same regardless of task difficulty. Next, we addressed the link between the task-related gamma power decrease and behavioral performance by assessing the putative relationship between the strength of gamma suppression and target detection speed. First, when splitting the data recorded in all anatomical clusters into two subgroups of trials, 50% shortest versus 50% longest reaction times, we found quicker target detection to be associated with stronger gamma suppression in MPFC and VLPFC clusters (Fig. 4*A*). The correlation between GBD amplitude and performance (target detection speed) was thus not as ubiquitous across the task-negative network as the correlation between GBD duration and task complexity. Furthermore, the relationship between power suppression and reaction time was also investigated in individual electrode data (e.g., Fig. 4*B–E*). Remarkably, single-trial power analysis in individual electrodes revealed statistically significant correlation between gamma suppression and target detection speed on a trial-by-trial basis (cf. illustrative example in Fig. 2*C-E*, correlation peak rho = 0.34968 at $t = 736$ ms, $p < 0.001$, Spearman's correlation test).

Functional specificity of broadband gamma power suppression

Furthermore, we also computed brain-wide, task-related power modulations across theta (4–7 Hz), alpha (8–12 Hz), beta (13–30 Hz) and low gamma (30–60 Hz) bands. Compared to lower frequencies, task-related (low and high) gamma suppression patterns displayed the closest anatomical match with typical DMN deactivation networks (Fig. 5). Note that power suppressions were also observed in the beta-band in some DMN areas (e.g., PCC). However, by contrast to GBD, beta-band decreases were neither correlated with task complexity nor with subject performance (correlations did not achieve statistical significance, $p > 0.05$). Furthermore, beta-band power suppression was not restricted to DMN structures (see Fig. 5). Modulations of low-gamma (30–60 Hz) power suppression showed statistically longer lasting decreases in MPFC in the difficult compared to the easy search condition as well as stronger reductions in LTC in association with faster responses ($p < 0.01$, *t* test, both $t > 2.73$) (data not shown). Nevertheless, low-gamma modulations failed to achieve the level of significance and consistency across the full DMN network that was observed in the high gamma range (60–140 Hz).

Relationship between task-positive and task-negative gamma modulation networks

In addition to identifying the dynamics of GBD and its relationship with behavior, we also investigated task-related gamma band activation (GBA) and the putative interplay between task-related negative and positive gamma power modulations during visual search. Figure 6*A* depicts the brain-wide spatial distribution of task-related GBD and GBA forming the task-negative network and the task-positive network, respectively. Furthermore, we computed exhaustive pairwise correlation analysis between the time courses of gamma power modulation across both networks. The global correlation results (Fig. 6*B*,*C*) indicate that TPN and TNN are predominantly negatively correlated (i.e., anticorrelated), whereas TNN-TNN and TPN-TPN pairs of sites are predominantly positively correlated (see Materials and Methods for

details). This result matches patterns of correlated and anticorrelated networks of intrinsic brain organization (Fox et al., 2005) revealed using resting-state functional magnetic resonance imaging (fMRI) with the notable difference, however, that here it was obtained during active task performance and by measuring high gamma-band power modulations.

Discussion

This study provides the first direct evidence for a correlation between behavioral parameters and task-related gamma-band suppression dynamics in DMN. Our findings indicate that complex tasks are associated with longer lasting power decreases than easier tasks, and that stronger gamma suppressions in distinct DMN components are correlated with better performances (i.e., faster target detection).

Studies in animals (Logothetis et al., 2001; Niessing et al., 2005) and humans (Mukamel et al., 2005; Lachaux et al., 2007; Nir et al., 2007; He et al., 2008) suggest that increases in hemodynamic responses are not only linked to increases in spiking activity but also to power increases in the gamma-band component of local field potentials (LFPs). Conversely, here we demonstrate, using direct electrophysiological recordings in the human brain, that all DMN areas, which are known to exhibit negative BOLD responses, display suppressions of gamma-band power during task engagement. Critically, our results significantly extend previous invasive studies of task-related gamma power suppressions in humans (Lachaux et al., 2008; Miller et al., 2009; Jerbi et al., 2010; Dastjerdi et al., 2011) and monkeys (Shmuel et al., 2006; Hayden et al., 2009). In addition to probing DMN electrophysiology via an unprecedented large-scale sampling of the human brain (14 subjects, 1730 recording sites), the present study is above all the first to reveal the millisecond temporal features (onset and duration) of cortical gamma power decreases across the entire default-mode network, and it is also the first to report significant correlations between the transient power suppressions and behavior (duration of task engagement and performance). The highly transient nature of the DMN power suppressions reported here and the sequential order of the power drop onset in each of the various nodes of the network highlight the dynamic nature of the network, a feature that is likely to facilitate rapid switching between different attentional states or degrees of engagement with the external world.

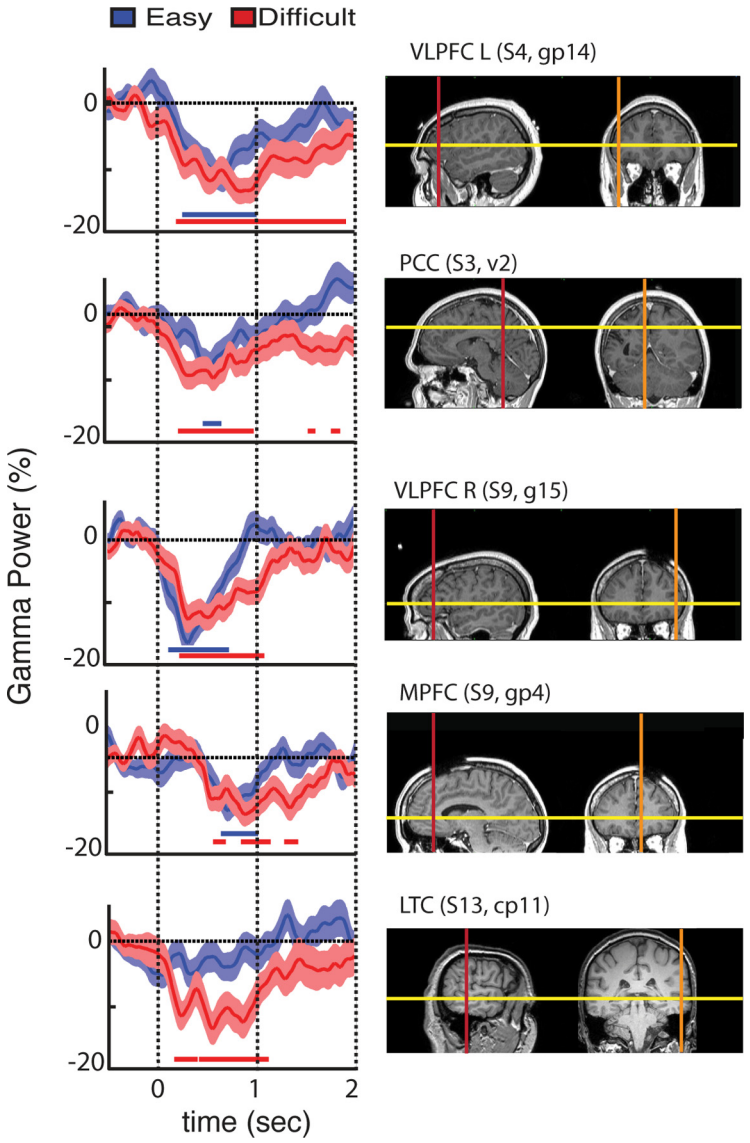

Figure 3. Single electrode data show suppression of gamma-band activity varies with task difficulty. Temporal profile of gamma band (60–140 Hz) power modulations are displayed for the two conditions: easy search (blue) and difficult search (red) for representative sites in the task-negative (i.e., power suppression) network. The displayed data correspond to electrodes located in (from top to bottom): VLPFC left (L), PCC, VLPFC right (R), MPFC, and LTC. Horizontal red and blue lines, beneath the waveforms, indicate statistically significant gamma-band suppressions relative to baseline period ([from −400 to −100] ms). We used signed rank Wilcoxon test and FDR correction ($p < 0.05$). Line upper/lower bounds indicate ± 1 SEM. Note that the anatomical ROI name above each MRI panel is followed by subject number and electrode name.

A significant side result from this study is that it provides additional irrefutable electrophysiological evidence for a neural origin of task-related DMN deactivation in agreement with recent studies (Hayden et al., 2009; Miller et al., 2009; Jerbi et al., 2010). This firmly settles the recurrent controversy sparked by suggestions that deactivations in DMN may arise from non-neuronal signals such as cardiac or respiratory artifacts (Birn et al., 2008) and vascular or metabolic changes (Pasley et al., 2007). Most importantly, our data argue against this claim not only because power suppressions were recorded directly in DMN structures, but also because the duration and amplitude of the power suppressions were correlated with the attentional demands of the task and with subject performance.

Compared to previous noninvasive studies based on scalp electroencephalography or magnetoencephalography (MEG) (Laufs et al., 2003; Mantini et al., 2007; Scheeringa et al., 2008; de Pasquale et al. 2010; Brookes et al., 2011), the direct intracranial recordings used here allow for a higher spatial resolution particularly for deeper structures, and for the detection of electrophysiological correlates of the DMN at higher frequencies (up to 200

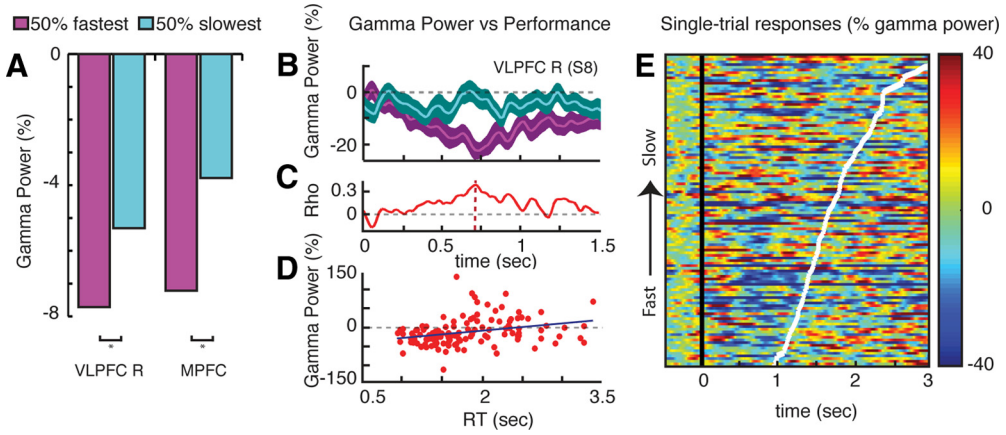

Figure 4. Relationship between gamma-band power decreases and behavioral performance. ***A***, Mean gamma power suppression computed separately for 50% fastest response trials (magenta) and 50% slowest response trials (turquoise). Gamma power suppressions in MPFC and right VLPFC (VLPC R) clusters were stronger for fast target detection than for the slower detections (both $t > 3.11$, $p < 0.01$). Differences were not statistically significant for other GBD clusters (data not shown). Mean power was computed over a [200–700] ms time window following stimulus presentation. ***B***, Profile of mean gamma power (± SE) in a VLPFC R recording site (Talairach coordinates: $x = 55, y = 33, z = 0$) for 50% fastest (magenta) versus 50% slowest (turquoise) response trials. ***C***, Profile of correlation coefficient between single-trial gamma power at this site and the individual reaction times. A peak correlation occurred at $t_{max} = 736$ ms after stimulus onset. ***D***, Trial-by-trial plot of reaction time (RT) versus gamma power at t_{max} depicts the significant correlation between single-trial gamma suppression and behavioral performance (Spearman's correlation test, rho = 0.34968, $p = 0.0000969$). ***E***, Single-trial gamma power plot for same electrode as in ***B***–***D*** with trials sorted according to RTs (fastest to slowest target detection). White line depicts RT (i.e., latency of button press indicating target detection for each trial. Time $t = 0$ corresponds to visual search array onset.

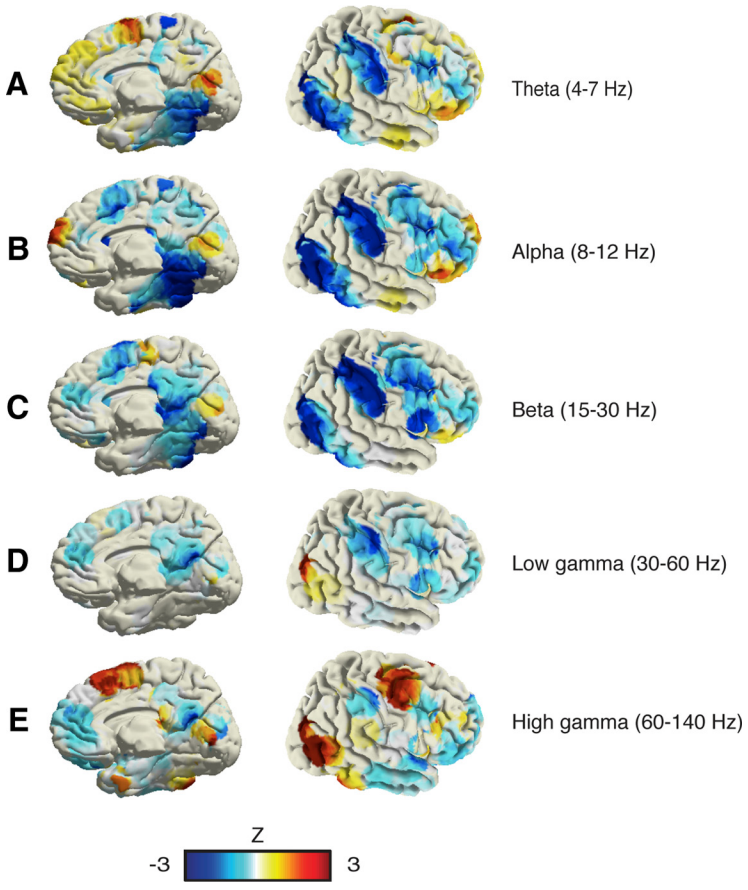

Figure 5. Spatial distribution of task-related power decreases (blue) and increases (red) during visual search in multiple frequency bands. ***A***, Theta (4–7 Hz). ***B***, Alpha band (8–12 Hz). ***C***, Beta band (13–30 Hz). ***D***, Low gamma band (30–60 Hz). ***E***, High gamma band (60–140 Hz). The distribution of task-related gamma power suppressions is the one that most closely matches typical DMN deactivation patterns. Power patterns in theta and alpha bands did not show comparable suppressions in DMN areas. Beta power suppressions were observed in some DMN areas but also in visual and dorsal attention network areas. Unlike gamma suppressions, beta suppressions in the DMN clusters were not significantly correlated with behavior (data not shown).

Hz). Incidentally, these two properties are critical for an optimal investigation of the electrophysiological correlates of DMN (Jerbi et al., 2010). This suggests that intracranial EEG studies might be essential for the reliable study of DMN electrophysiology in humans. Nevertheless, it is important to keep in mind that one major asset of scalp EEG is that it can be acquired simultaneously with fMRI (Laufs et al., 2003; Mantini et al., 2007; Scheeringa et al., 2008; de Pasquale et al. 2010;). We therefore expect fMRI invasive and noninvasive EEG approaches to play increasingly complementary roles to elucidate the neural underpinnings of intrinsic brain networks and to bridge the gap between imaging studies and electrophysiology.

Although the precise role of resting state networks is not yet fully understood, recent fMRI investigations suggest that DMN deactivation is correlated with task demands and behavioral parameters (Weissman et al., 2006; Singh and Fawcett, 2008). Our ability to directly measure task-related neural population activity with electrodes implanted in DMN structures significantly expands on previous investigations of the functional role of DMN. First of all, by contrast to the hemodynamic response that represents an indirect measure of neural activity, the brain-wide, high-resolution depth electrode recordings reported here allow for a direct assessment of the electrophysiological basis of the DMN phenomenon in humans. Second, the high signal-to-noise ratio of intracerebral recordings allowed

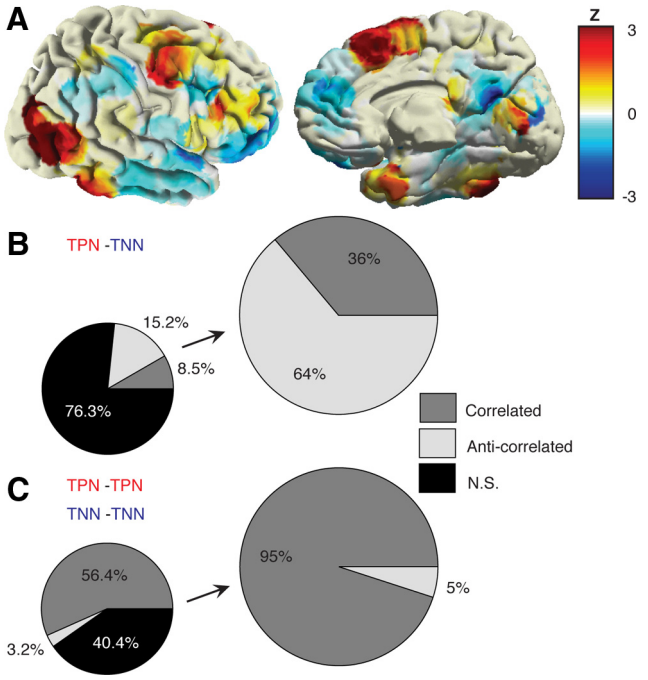

Figure 6. Correlated and anticorrelated gamma-band task networks. ***A***, Spatial distribution of task-related gamma decreases (blue) and increases (red) during visual search, representing a task negative network and a task positive network, respectively. While TNN closely matches DMN and ventral attention network areas, TPN depicts concurrent activations in visual and dorsal attention network areas (data represent a snapshot of gamma power modulation at $t =$ 640 ms as compared to baseline level). ***B***, Anticorrelated gamma networks. These measure correlation among TPN-TNN by assessing correlation between single-trial data from all electrodes of TPN ROIs and TNN ROIs. ***C***, Correlated gamma networks. These are the same as in ***B***, but electrode pairs for the correlation analysis were always from the same type of network i.e., TPN-TPN and TNN-TNN correlations (TPN and TNN anatomical regions and electrode details are provided in Table 3).

us to perform trial-by trial data analysis revealing, for the first time, a significant correlation between an electrophysiological feature of DMN dynamics and subject performance on a trial-by-trial basis. Third, our study unravels the profile of DMN power suppression with a temporal resolution, allowing us to precisely determine the onset times and duration of the power decrease across the full DMN network. Remarkably, this fine-grained evaluation of DMN temporal dynamics as a function of task complexity unraveled the strikingly transient nature of the reduction in DMN gamma power. In fact, the high temporal resolution of intracerebral EEG may be key to fine-tuning the functional dissociation between the DMN and the ventral frontoparietal network structures in goal-directed behavior (Corbetta et al., 2008; Spreng et al., 2010). As a matter of fact, our finding that task engagement induced neural power suppression first in LTC, VLPFC, and TPJ structures before it occurred in PCC and MPFC. This observation could be taken as an indication that the ventral attention network is deactivated before the canonical DMN structures in this visual search task. Whether this fine temporal dissociation between the two networks holds true for other attention-demanding tasks is an exciting question for future intracranial EEG studies.

Moreover, accumulating evidence supports a direct relationship between broadband gamma and spiking activity (Nir et al., 2007; Ray et al., 2008; Manning et al., 2009; Ray and Maunsell, 2011). Remarkably, electrophysiological recordings in the macaque have shown that gamma-band suppression in LFP signals is associated with a decrease in neuronal firing (Shmuel et al., 2006; Hayden et al., 2009). Taken in conjunction with these reports, our results suggest that DMN deactivation in humans is also likely to coincide with transient task-related drops in neuronal firing. Beyond uncovering a key role for broadband gamma activity in the electrophysiological mechanisms underlying DMN power suppression, our results have direct implications on the functional interpretation of task-related neural deactivation. The correlation we found between the decrease in DMN power and subject behavior suggests that beyond indicating a switch from an inattentive or introspective state to an attentive exteroceptive mode, the extent and duration of DMN suppression actually encode the quality of this transition, i.e., the efficiency and extent of our engagement with the external world. Critically, the remarkably transient nature of broadband gamma suppression in the default mode and ventral attention networks indicates that task-related reduction in cortical power is followed by a rapid return to baseline levels immediately after completion of task processing. As shown in Table 2, the mean duration of task-related gamma suppression was as short as 135 ms in LTC (easy search) and could last up to 1005 ms in MPFC (difficult search).

Additionally, our results point toward a prominent role for the network interplay between task-specific gamma increases and task-unspecific gamma decreases in mediating goal-directed behavior. Incorporating these findings in future research will further narrow the gap between fMRI studies and electrophysiology and will advance our knowledge of large-scale neural synchronization in the gamma band (Varela et al., 2001; Lakatos et al. 2008; Fries, 2009; Luo et al., 2010). In particular, our findings suggest that modulations of broadband gamma activity can be observed locally by task-related enhancement or suppression of power, but also through task-related, long-range, amplitude–amplitude correlations and anticorrelations in the same frequency range. Our understanding of the functional architecture of the human brain is being reshaped by resting-state fMRI studies that show how multiple brain areas form distinct, large-scale, coherent networks (Biswal et al., 1995, 2010). Investigating the electrophysiological correlates of spontaneous coherent fluctuations with the techniques used in this study will provide critical insights into the neural mechanisms mediating fMRI functional connectivity. In particular, applying coupling measures to direct electrophysiological recordings obtained simultaneously from multiple DMN nodes will be critical to unravel the frequency characteristics and directionality of large-scale slow correlated oscillations and their putative relationship with broadband gamma amplitude fluctuations (Jensen and Colgin, 2007; Lakatos et al. 2008; Dalal et al., 2011).

Because we did not have the possibility to acquire functional MRI data from the patients we examined here, we cannot completely rule out that the properties of the DMN in some of these subjects might have been directly or indirectly affected by epilepsy. Indeed, previous studies have reported possible alterations of the DMN in some epilepsy patients (e.g., Broyd et al., 2009, Laufs et al., 2007; Sakurai et al., 2010, Zhang et al., 2010). Future studies that combine fMRI and intracranial EEG exploration of the DMN in the same population will be key to distinguishing the physiological and pathological aspects of the electrophysiological underpinnings of the DMN. In the present study, we minimize the effect of epilepsy-related activity by excluding data from any electrode site that showed epileptic discharges or that was identified as being part of the seizure onset zone.

Finally, our data suggest that broadband gamma modulations could prove to be an efficient electrophysiological biomarker, complementing resting-state fMRI approaches, to investigate the

pathophysiology of neurological diseases that involve DMN dysfunction. These include attention deficit hyperactivity disorders, autism, depression, Alzheimer's disease, and schizophrenia (Greicius et al., 2004; Garrity et al., 2007; Castellanos et al., 2008; Broyd et al., 2009; Uhlhaas and Singer, 2010). For such a perspective to become clinical routine, the challenge remains to localize broadband gamma brain signals using noninvasive methods (e.g., MEG or EEG) with sufficiently high spatial and temporal resolution (Jerbi et al., 2009) to warrant the type of DMN assessment achieved here with intracerebral recordings.

References

Aguera PE, Jerbi K, Caclin A, Bertrand O (2011) ELAN: a software package for analysis and visualization of MEG, EEG, and LFP signals. Comput Intell Neurosci 2011:158970.

Birn RM, Murphy K, Bandettini PA (2008) The effect of respiration variations on independent component analysis results of resting state functional connectivity. Hum Brain Mapp 29:740–750.

Biswal BB, Mennes M, Zuo XN, Gohel S, Kelly C, Smith SM, Beckmann CF, Adelstein JS, Buckner RL, Colcombe S, Dogonowski AM, Ernst M, Fair D, Hampson M, Hoptman MJ, Hyde JS, Kiviniemi VJ, Kötter R, Li SJ, Lin CP, et al. (2010) Toward discovery science of human brain function. Proc Natl Acad Sci U S A 107:4734–4739.

Biswal B, Yetkin FZ, Haughton VM, Hyde JS (1995) Functional connectivity in the motor cortex of resting human brain using echo-planar MRI. Magn Reson Med 34:537–541.

Brookes MJ, Wood JR, Stevenson CM, Zumer JM, White TP, Liddle PF, Morris PG (2011) Changes in brain network activity during working memory tasks: a magnetoencephalography study. Neuroimage 55:1804–1815.

Broyd SJ, Demanuele C, Debener S, Helps SK, James CJ, Sonuga-Barke EJ (2009) Default-mode brain dysfunction in mental disorders: a systematic review. Neurosci Biobehav Rev 33:279–296.

Castellanos FX, Margulies DS, Kelly C, Uddin LQ, Ghaffari M, Kirsch A, Shaw D, Shehzad Z, Di Martino A, Biswal B, Sonuga-Barke EJ, Rotrosen J, Adler LA, Milham MP (2008) Cingulate-precuneus interactions: A new locus of dysfunction in adult attention-deficit/hyperactivity disorder. Biol Psychiatry 63:332–337.

Corbetta M, Shulman GL (2002) Control of goal-directed and stimulus-driven attention in the brain. Nat Rev Neurosci 3:201–215.

Corbetta M, Patel G, Shulman GL (2008) The reorienting system of the human brain: From environment to theory of mind. Neuron 58:306–324.

Dalal SS, Vidal JR, Hamamé CM, Ossandón T, Bertrand O, Lachaux JP, Jerbi K (2011) Spanning the rich spectrum of the human brain: slow waves to gamma and beyond. Brain Struct Funct 216:77–84.

Dastjerdi M, Foster BL, Nasrullah S, Rauschecker AM, Dougherty RF, Townsend JD, Chang C, Greicius MD, Menon V, Kennedy DP, Parvizi J (2011) Differential electrophysiological response during rest, self-referential, and non-self-referential tasks in human posteromedial cortex. Proc Natl Acad Sci U S A 108:3023–3028.

de Pasquale F, Della Penna S, Snyder AZ, Lewis C, Mantini D, Marzetti L, Belardinelli P, Ciancetta L, Pizzella V, Romani GL, Corbetta M (2010) Temporal dynamics of spontaneous MEG activity in brain networks. Proc Natl Acad Sci U S A 107:6040–6045.

Fox MD, Snyder AZ, Vincent JL, Corbetta M, Van Essen DC, Raichle ME (2005) The human brain is intrinsically organized into dynamic, anticorrelated functional networks. Proc Natl Acad Sci U S A 102:9673–9678.

Fries P (2009) Neuronal gamma-band synchronization as a fundamental process in cortical computation. Annu Rev Neurosci 32:209–224.

Garrity AG, Pearlson GD, McKiernan K, Lloyd D, Kiehl KA, Calhoun VD (2007) Aberrant "default mode" functional connectivity in schizophrenia. Am J Psychiat 164:450–457.

Genovese CR, Lazar NA, Nichols T (2002) Thresholding of statistical maps in functional neuroimaging using the false discovery rate. Neuroimage 15:870–878.

Greicius MD, Srivastava G, Reiss AL, Menon V (2004) Default-mode network activity distinguishes Alzheimer's disease from healthy aging: evidence from functional MRI. Proc Natl Acad Sci U S A 101:4637–4642.

Gusnard DA, Raichle ME (2001) Searching for a baseline: functional imaging and the resting human brain. Nat Rev Neurosci 2:685–694.

Hayden BY, Smith DV, Platt ML (2009) Electrophysiological correlates of default-mode processing in macaque posterior cingulate cortex. Proc Natl Acad Sci U S A 106:5948–5953.

He BJ, Snyder AZ, Zempel JM, Smyth MD, Raichle ME (2008) Electrophysiological correlates of the brain's intrinsic large-scale functional architecture. Proc Natl Acad Sci U S A 105:16039–16044.

Jensen O, Colgin LL (2007) Cross-frequency coupling between neuronal oscillations. Trends Cogn Sci 11:267–269.

Jerbi K, Ossandón T, Hamamé CM, Senova S, Dalal SS, Jung J, Minotti L, Bertrand O, Berthoz A, Kahane P, Lachaux JP (2009) Task-related gamma-band dynamics from an intracerebral perspective: review and implications for surface EEG and MEG. Hum Brain Mapp 30:1758–1771.

Jerbi K, Vidal JR, Ossandon T, Dalal SS, Jung J, Hoffmann D, Minotti L, Bertrand O, Kahane P, Lachaux JP (2010) Exploring the electrophysiological correlates of the default-mode network with intracerebral EEG. Front Syst Neurosci 4:27.

Kahane P, Landre E, Minotti L, Francione S, Ryvlin P (2006) The Bancaud and Talairach view on the epileptogenic zone: a working hypothesis. Epileptic Disord 8 [Suppl 2]:S16–S26.

Lachaux JP, Rudrauf D, Kahane P (2003) Intracranial EEG and human brain mapping. J Physiol Paris 97:613–628.

Lachaux JP, Fonlupt P, Kahane P, Minotti L, Hoffmann D, Bertrand O, Baciu M (2007) Relationship between task-related gamma oscillations and BOLD signal: New digits from combined fMRI and intracranial EEG. Hum Brain Mapp 28:1368–1375.

Lachaux JP, Jung J, Mainy N, Dreher JC, Bertrand O, Baciu M, Minotti L, Hoffmann D, Kahane P (2008) Silence is golden: transient neural deactivation in the prefrontal cortex during attentive reading. Cereb Cortex 18:443–450.

Lakatos P, Karmos G, Mehta AD, Ulbert I, Schroeder CE (2008) Entrainment of neuronal oscillations as a mechanism of attentional selection. Science 320:110–113.

Laufs H, Krakow K, Sterzer P, Eger E, Beyerle A, Salek-Haddadi A, Kleinschmidt A (2003) Electroencephalographic signatures of attentional and cognitive default modes in spontaneous brain activity fluctuations at rest. Proc Natl Acad Sci U S A 100:11053–11058.

Laufs H, Hamandi K, Salek-Haddadi A, Kleinschmidt AK, Duncan JS, Lemieux L (2007) Temporal lobe interictal epileptic discharges affect cerebral activity in "Default mode" brain regions. Hum Brain Mapp 28:1023–1032.

Le Van Quyen M, Foucher J, Lachaux J, Rodriguez E, Lutz A, Martinerie J, Varela FJ (2001) Comparison of Hilbert transform and wavelet methods for the analysis of neuronal synchrony. J Neurosci Methods 111:83–98.

Logothetis NK, Pauls J, Augath M, Trinath T, Oeltermann A (2001) Neurophysiological investigation of the basis of the fMRI signal. Nature 412:150–157.

Luo L, Rodriguez E, Jerbi K, Lachaux JP, Martinerie J, Corbetta M, Shulman GL, Piomelli D, Turrigiano GG, Nelson SB, Joëls M, de Kloet ER, Holsboer F, Amodio DM, Frith CD, Block ML, Zecca L, Hong JS, Dantzer R, Kelley KW, Craig AD (2010) Ten years of Nature Reviews Neuroscience: insights from the highly cited. Nat Rev Neurosci 11:718–726.

Manning JR, Jacobs J, Fried I, Kahana MJ (2009) Broadband shifts in local field potential power spectra are correlated with single-neuron spiking in humans. J Neurosci 29:13613–13620.

Mantini D, Perrucci MG, Del Gratta C, Romani GL, Corbetta M (2007) Electrophysiological signatures of resting state networks in the human brain. Proc Natl Acad Sci U S A 104:13170–13175.

Mason MF, Norton MI, Van Horn JD, Wegner DM, Grafton ST, Macrae CN (2007) Wandering minds: the default network and stimulus-independent thought. Science 315:393–395.

Miller KJ, Weaver KE, Ojemann JG (2009) Direct electrophysiological measurement of human default network areas. Proc Natl Acad Sci U S A 106:12174–12177.

Mukamel R, Gelbard H, Arieli A, Hasson U, Fried I, Malach R (2005) Coupling between neuronal firing, field potentials, and FMRI in human auditory cortex. Science 309:951–954.

Niessing J, Ebisch B, Schmidt KE, Niessing M, Singer W, Galuske RA (2005) Hemodynamic signals correlate tightly with synchronized gamma oscillations. Science 309:948–951.

Nir Y, Fisch L, Mukamel R, Gelbard-Sagiv H, Arieli A, Fried I, Malach R (2007) Coupling between neuronal firing rate, gamma LFP, and BOLD fMRI is related to interneuronal correlations. Curr Biol 17:1275–1285.

Pasley BN, Inglis BA, Freeman RD (2007) Analysis of oxygen metabolism

implies a neural origin for the negative BOLD response in human visual cortex. Neuroimage 36:269–276.
Raichle ME (2009) A paradigm shift in functional brain imaging. J Neurosci 29:12729–12734.
Raichle ME, Mintun MA (2006) Brain work and brain imaging. Annu Rev Neurosci 29:449–476.
Raichle ME, MacLeod AM, Snyder AZ, Powers WJ, Gusnard DA, Shulman GL (2001) A default mode of brain function. Proc Natl Acad Sci U S A 98:676–682.
Ray S, Maunsell JH (2011) Different origins of gamma rhythm and high-gamma activity in macaque visual cortex. PLoS biology 9:e1000610.
Ray S, Crone NE, Niebur E, Franaszczuk PJ, Hsiao SS (2008) Neural correlates of high-gamma oscillations (60–200 Hz) in macaque local field potentials and their potential implications in electrocorticography. J Neurosci 28:11526–11536.
Sakurai K, Takeda Y, Tanaka N, Kurita T, Shiraishi H, Takeuchi F, Nakane S, Sueda K, Koyama T (2010) Generalized spike-wave discharges involve a default mode network in patients with juvenile absence epilepsy: a MEG study. Epilepsy Res 89:176–184.
Scheeringa R, Bastiaansen MC, Petersson KM, Oostenveld R, Norris DG, Hagoort P (2008) Frontal theta EEG activity correlates negatively with the default mode network in resting state. Int J Psychophysiol 67:242–251.
Shmuel A, Augath M, Oeltermann A, Logothetis NK (2006) Negative functional MRI response correlates with decreases in neuronal activity in monkey visual area V1. Nat Neurosci 9:569–577.
Shulman GL, Fiez JA, Corbetta M, Buckner RL, Miezin FM, Raichle ME, Petersen SE (1997) Common blood flow changes across visual tasks. II. Decreases in cerebral cortex. J Cogn Neurosci 9:648–663.
Singh KD, Fawcett IP (2008) Transient and linearly graded deactivation of the human default-mode network by a visual detection task. Neuroimage 41:100–112.
Spreng RN, Stevens WD, Chamberlain JP, Gilmore AW, Schacter DL (2010) Default network activity, coupled with the frontoparietal control network, supports goal-directed cognition. Neuroimage 53:303–317.
Talairach J, Tounoux P (1993) Referentially oriented cerebral MRI anatomy: an atlas of stereotaxic anatomical correlations for gray and white matter. New York: Thieme.
Tallon-Baudry C, Bertrand O, Delpuech C, Permier J (1997) Oscillatory gamma-band (30–70 Hz) activity induced by a visual search task in humans. J Neurosci 17:722–734.
Treisman AM, Gelade G (1980) Feature-integration theory of attention. Cogn Psychol 12:97–136.
Uhlhaas PJ, Singer W (2010) Abnormal neural oscillations and synchrony in schizophrenia. Nat Rev Neurosci 11:100–113.
Varela F, Lachaux JP, Rodriguez E, Martinerie J (2001) The brainweb: phase synchronization and large-scale integration. Nat Rev Neurosci 2:229–239.
Weissman DH, Roberts KC, Visscher KM, Woldorff MG (2006) The neural bases of momentary lapses in attention. Nat Neurosci 9:971–978.
Zhang Z, Lu G, Zhong Y, Tan Q, Liao W, Wang Z, Wang Z, Li K, Chen H, Liu Y (2010) Altered spontaneous neuronal activity of the default-mode network in mesial temporal lobe epilepsy. Brain Res 1323:152–160.

SUPPLEMENTARY NOTES

Note on the specificity of SEEG compared to ECoG.

The use of stereotactic EEG (SEEG) is less wide-spread than that of Electrocorticography (ECoG) in the clinical setting of drug-resistance epilepsy treatment. To date, some important differences between these two intracranial EEG techniques remain unknown to the broader community. Some SEEG specificities are crucial with regards to the present study. First of all, by contrast to ECoG which consists of placing grid electrodes (or strips) directly on the cortical surface, SEEG consists of implanting several semi-rigid multi-lead depth electrodes inside the brain. This is achieved via a stereotactic approach developed by Talairach and Bancaud35. As a result, SEEG provides direct recordings from deep structures and allows for a sampling of brain activity all the way from the lateral surface to medial wall structures. SEEG electrodes can also records from neural populations located deep within the sulci. Such spatial sampling cannot be achieved with ECoG and represents a major asset for the extensive investigation of distributed brain networks, such as the default-mode network. Furthermore, the small SEEG inter-electrode distance (1.5 to 4.5 mm inter-electrode distance, compared to 1 cm in standard subdural ECoG grids) in combinations with bipolar derivations guarantees a high spatial specificity and more robustness with respect to signal artifacts34.

Note on the definition of anatomo-functional clusters.

Mapping significant task-related power increases or decreases to standard MNI brain (as described in previous section) allows for the identification of anatomo-functional clusters of interest. For instance, what we refer to in this study as “deactivation clusters” was obtained by mapping all significant gamma band deactivation (GBD) data from all subjects to the common MNI brain. The result (Fig 2a) represents in blue all brain regions that show a statistically significant suppression of high gamma power (60-140 Hz) during active search compared to the pre-stimulus baseline level (data pooled across all subjects).

Using statistical significance of gamma deactivation as functional criterion and its spatial distribution as anatomical criterion the following major anatomo-functional deactivation clusters were obtained: Posterior Cingulate Cortex (PCC), Medial Prefrontal Cortex (MPFC),

93

L and R Ventrolateral Prefrontal Cortex (VLPFC), Temporal Parietal junction (TPJ), Lateral Temporal Cortex (LTC) and Middle Frontal Gyrus (MFG). Supplementary Table 3 lists all electrodes that define the gamma-band "deactivation cluster" as well as their coordinates and anatomical location (Brodmann areas).

Note on excluding epilepsy-related data from the study.

We followed our routine procedures to ensure that all the analysis in this paper was performed using recordings that originate from healthy cortical tissue and that the interpretations of the data are not biased by pathological traces related to epileptic activity. This is achieved using several procedures. First, we use automatic identification of electrodes that contain epileptic spikes based on straight-forward amplitude thresholds. In addition, we visually scan all the data obtained in each subject in search for artefactual and pathological traces, assisted by expertise from the neurologists. All electrodes that contain pathological traces are excluded from the study even if the abnormal activity was present on a small segment of the recordings. Furthermore, after surgery is performed in order to remove the identified focus of the seizure, we double-check that none of the sites kept for our analysis were part of the resected area. Finally, any effects of residual isolated pathological events is further systematically minimized by the type of data analysis we use: First, the task-related nature of our cross-trial averaging analysis cancels out any effects that are not induced or evoked by the stimulus. Second, outliers such as a particularly strong interictal events may show up on the averaged map across trials but would not achieve statistical significance across trials. Finally, single-trial analysis (e.g. single-trial gamma-band plots used in this study) shows the robustness and consistency of the data across trials.

94

6.1. Context of the second article:

Neuroscience and psychology have been converging on the idea that cognitive tasks, including attention, that are carried out by networks of neural areas extending over much of the brain, but involve localized computation involved in the task (Varela et al, 2001; Corbetta et al, 2008). Findings from neuroimaging that cognitive tasks involve a number of different anatomical areas has led to an emphasis on tracing the time dynamics of these areas. Because shifts of attention can be so rapid, it is difficult to follow them with hemodynamic imaging. To fill this role, different algorithms have been developed to relate the scalp distribution of brain electrical activity, recorded from high-density electrical or magnetic sensors on or near the skull, to brain areas active during hemodynamic imaging. This combination between spatial localization with hemodynamic imaging and temporal precision from electrical or magnetic skill recordings has provided an approach to measure the networks underlying goal directed behaviors. Nevertheless, our understanding of the precise neural mechanisms underlying attention within these networks remains fragmented, primarily because the imaging techniques used to describe the functional organization of the human brain, fMRI and PET, measure only metabolic changes induced by neural activity, with low temporal resolution, and not the actual, fast-changing behavior of the neural networks themselves.

To date, the only data sufficiently precise to reveal these mechanisms have been obtained in animals, with invasive intracranial microelectrodes recording from groups of individual neurons. Results converge to show that attention acts as a 'contrast gain control mechanism' used to increase the firing rate of neurons whose receptive field is being attended, exactly as if the contrast of the attended object had been increased (Reynolds & Chelazzi, 2004). On the other hand, data obtained principally from event-related electrical brain potentials in humans suggest that voluntary attentional orienting is initiated by medial portions of frontal cortex, which then recruit medial parietal areas. Together, these areas sensitise the region-specific visual-sensory cortex to facilitate the processing of upcoming stimuli (Grent-t-Jong & Woldorff., 2007). These and other studies have substantiated the notion of top-down processes (Sarter et al., 2001) by demonstrating sequential activation of frontal-parietal-sensory regions, including decreases in task-irrelevant sensory regions, and the modulation of neuronal activity in sensory and sensory-associational areas (Desimone and Duncan, 1995; Hopfinger et al., 2000; kastner et al., 2000; Grent-t-Jong and Woldorff, 2007).

95

To solve this problem of the gap between local and large scale measures, one can use an intermediate level of recording, the local field potential, which includes both post-synaptic potentials and integrative activity occurring at the soma. This is constituted principally by a stimulus-induced fast oscillation in the range 30-150 Hz, (Logothetis et al, 2001). Increasing evidence suggest that gamma-band response (GBR, >40 Hz) might be a particularly efficient marker of functional mapping. A recent series of intracranial EEG studies showing that broadband energy increase of neural signals (50–150 Hz, the so-called gamma-band) constitutes a precise marker identifying neural recruitment during cognitive processing (Jensen et al., 2007; Jerbi et al., 2009; Lachaux et al., 2003). Such gamma-band responses (GBRs) have been used to map the large-scale cortical networks underlying several major cognitive functions, including language processing (Jung et al., 2008; Mainy et al., 2008), attention (Jensen et al., 2007), and top–down processes (Engel et al., 2001; Kahana, 2006). Those results are in line with a possible role of gamma-band neural synchronization in local and large-scale neural communication (Fries et al., 2007; Lee, 2003; Singer, 1999; Varela et al., 2001). Further, recent studies combining electrophysiological and BOLD measures using fMRI have found a strong correlation between GBRs and the BOLD signal (Lachaux et al., 2007; Logothetis et al., 2001; Mukamel et al., 2005).

Beginning with Crone and colleagues (1998), several studies describe transient intracranial and ECoG power increases at 50-150 Hz (tGBRs), related to stimuli processing (Crone et al, 1998, Jacobs & Kahana, 2010; Manning et al., 2009; Lachaux et al., 2005). In contrast to the transient GBRs, observed principally in primary sensory cortices, power increases in the gamma band can be sustained when they are modulated by intrinsic sources (Engel et al, 2001). These top-down influences include the activity of systems involved in goal definition, action planning, working memory or selective attention (Corbetta et al, 2002; Varela et al, 2001).

The main objective of this article is to distinguish transient neural responses elicited by stimuli properties, from sustained responses elicited by intrinsic modulations. To test this prediction in the most direct fashion, we used unprecedented brain-wide intracerebral depth recordings in 19 surgical patients performing a visual search task.

96

Second Article

Efficient 'Pop-Out' Visual Search Elicits Sustained Broadband Gamma Activity in the Dorsal Attention Network

Tomas Ossandón*[1], Juan R Vidal*[1], Carolina Ciumas[4,5], Karim Jerbi[1], Carlos M. Hamamé[1], Sarang S. Dalal[1,3], Olivier Bertrand[1], Lorella Minotti[2], Philippe Kahane[2] and Jean-Philippe Lachaux[1].

[1] INSERM U1028 - CNRS UMR5292, Brain Dynamics and Cognition Team, Lyon Neuroscience Research Center; University Claude Bernard, Lyon 1, France

[2] CHU Grenoble and Dept. Neurology, INSERM U704, Grenoble, France

[3] Zukunftskolleg and Department of Psychology, University of Konstanz, Germany

[4] Translational and Integrative Group in Epilepsy Research (TIGER), Lyon, France

[5] Institute for Child and Adolescent with Epilepsy (IDEE), Lyon, France

*these authors contributed equally to this work

Running Title: Sustained broadband gamma reflects top-down processing

Corresponding authors: Tomas Ossandon or Juan R. Vidal

E-mail: tomas.ossandon@inserm.fr or juan.vidal@inserm.fr

Tel: 00 33 4 72 13 89 00

Fax: 00 33 4 72 13 89 01

Keywords: ECoG, broadband gamma activity, visual search, top-down, bottom-up, attention, epilepsy

97

Conflict of interest statement

The authors declare no competing financial interests.

Acknowledgements

We thank all patients for their participation; the staff of the Grenoble Neurological Hospital epilepsy unit; Dominique Hoffmann, Patricia Boschetti, Carole Chatelard, Véronique Dorlin and Martine Juillard for their support. Funding was provided by the Fondation pour la Recherche Médicale (FRM) and by the BrainSync FP7 European Project (Grant HEALTH-F2-2008-200728).

98

Abstract

An object that differs markedly from its surrounding – for example, a red cherry among green leaves – seems to pop out effortlessly in our visual experience. The rapid detection of salient targets, independently of the number of other items in the scene, is thought to be mediated by efficient search brain mechanisms. It is not clear, however, whether efficient search is actually an 'effortless' bottom-up process or if it also involves regions of the prefrontal cortex generally associated with top-down sustained attention. We addressed this question with a combined fMRI/intracerebral EEG study designed to identify brain regions underlying a classic visual search task in healthy subjects (fMRi) and correlate neural activity with target detection latencies on a trial-by-trial basis with high temporal precision recordings of these regions in epileptic patients (iEEG). The spatio-temporal dynamics of single-trial spectral analysis of iEEG recordings revealed sustained energy increases in a broad gamma band (50-150 Hz) throughout the duration of the search process in the entire dorsal attention network both in efficient and inefficient search conditions. By contrast to extensive theoretical and experimental indications that efficient search relies exclusively on transient bottom-up processes in visual areas, we found that efficient search is mediated by sustained gamma activity in the dorsal lateral prefrontal cortex and the anterior cingulate cortex, alongside the superior parietal cortex and the frontal eye field. Our findings support the hypothesis that active visual search systematically involves the frontal-parietal attention network and therefore, executive attention resources, irrespective of target saliency.

Introduction

When searching for a specific object in a crowded visual scene, search duration depends on the dissimilarity between that object and its surroundings. Current theories distinguish between efficient search, when the target spontaneously captures attention because it differs from its background along a simple dimension (e.g., a red cherry ‘pops out’ among green leaves) and inefficient search, when the search requires attention to be shifted serially across the entire display to recognize the target (Wolfe, 2003; Wolfe et al., 2011). A frontal-parietal network, comprising the frontal eye fields (FEF) and the superior parietal lobule (SPL), drive those attentional shifts exerting a continuous top-down influence on the visual cortex (Bisley and Goldberg, 2003; Moore and Armstrong, 2003; Buschman and Miller, 2007; Bressler et al., 2008; Bisley and Goldberg, 2010). Both regions contain priority maps that guide attention towards task-relevant and/or salient items (Shulman et al., 2002; Bichot et al., 2005; Buschman and Miller, 2007; Kalla et al., 2008; Zhou and Desimone, 2011). The action of the FEF and SPL is guided by the dorsal lateral prefrontal cortex (DLPFC) and the dorsal anterior cingulate cortex (dACC). The DLPFC is actively involved in executive aspects of working memory, attention and decision making (Barcelo et al., 2000; Rowe et al., 2000; Procyk and Goldman-Rakic, 2006; Heekeren et al., 2008; Kalla et al., 2009), which are crucial to identify and discard non-relevant distractors when compared to the memorized target template (Duncan and Humphreys, 1989). The dACC is thought to control the general engagement of attention in the task until the target has been found (Cole and Schneider, 2007). However, while those four regions have been identified to participate of inefficient search, their role during efficient 'pop-out' search remains controversial. Predominant views suggest that the capture of attention by targets that ‘pop-out’ is mainly a bottom-up process (Treisman

and Gelade, 1980; Desimone and Duncan, 1995; Corbetta and Shulman, 2002) with little or no involvement of the aforementioned network. Indeed, theories on saliency maps have provided efficient and purely bottom-up models solving efficient search (Itti and Koch, 2001). However, alternative models suggest the need for top-down processes to guide attention towards the target and perform categorical decision-making, even during efficient search (Joseph et al., 1997; Cole and Schneider, 2007). Therefore, current theories suggest two alternatives scenarios: (i) efficient search might rely exclusively on transient bottom-up processes mediating the capture of attention by salient targets, with no top-down contributions from frontal cortical areas, or (ii) efficient and inefficient search would both require the continuous action of the same fronto-parietal attentional network, presumably facilitated by bottom-up capture processes during efficient search. To dissociate between those two scenarios, we compared the timing of neural activation with search duration on a trial-by-trial basis during efficient vs. inefficient search in key structures of the human fronto-parietal network defined by a parallel fMRI study: FEF, SPL, DLPFC and dACC.

In line with previous visual attention studies in primates and humans (Fries et al., 2001; Vidal et al., 2006; Buschman and Miller, 2007; Wyart and Tallon-Baudry, 2008), we found that deployment of visual attention is concomitant with sustained energy increase of local field potentials in the high-frequency band (50 - 150 Hz): broadband gamma activity was observed in the DLPFC, FEF, SPL and dACC and were sustained throughout the search process at the single-trial level, during both efficient and inefficient search. Altogether, our results support the view that both efficient and inefficient search require active top-down processes from frontal executive regions.

Materials and Methods

Stimuli and Experimental Design. Stimuli and paradigm were adapted from Treisman and Gelade (1980). Each stimulus consisted of an array of 36 letters (6 x 6 square array with 35 distractors 'L's and one target 'T' randomly arranged) and participants were instructed to find a target (present in all trials) as fast as possible (Figure 1A). To dissociate correct from incorrect responses, subjects indicated whether the target was located in the upper or lower half of the display by pressing on a control pad, with their right index (upper button) or middle finger (lower button) respectively. The initial experimental design consisted of 6 conditions with varying distractor layout (contrast and quantity) in the displays. 11 out of 24 subjects performed this experiment, while the remaining 13 subjects performed a simplified design consisting of only two of the six conditions. In this study we focus on two conditions, efficient and inefficient visual search, defined as follows: in the efficient condition a gray target was presented among black distractors while in the inefficient condition, all letters were gray (Figure 1A). Both conditions were presented randomly for a fixed duration of 3 seconds and with an inter-stimulus interval (ISI) of 1 second. The stimuli were displayed on a 19'' computer screen located at 60 cm away from the subject. Only data from trials with correct target detection were analyzed. Each experimental block lasted 5 minutes, interleaved with short inter-block pauses.

Participants. Intracranial recordings were obtained from 24 neurosurgical patients with intractable epilepsy (16 women, mean age: 34 ± 12 years) at the Epilepsy Department of the Grenoble University Hospital. All subjects were stereotactically

implanted with multi-lead EEG depth electrodes simultaneously sampling lateral, intermediate and medial wall structures. Electrode implantation was performed according to routine procedures and all target structures for the presurgical evaluation were selected strictly according to clinical considerations with no reference to the current study. All recorded electrophysiological data exhibiting pathological activity were discarded from the present study. All participants provided written informed consent and the experimental procedures were approved by the Institutional Review Board and by the National French Science Ethical Committee (CPPRB). All participants had normal or corrected to normal vision.

Electrode implantation. Eleven to fifteen semi-rigid multi-lead electrodes were stereotactically implanted in the brain of each patient. These stereotactic-EEG electrodes have a diameter of 0.8 mm and, depending on the target structure, consist of 10 to 15 contact leads 2 mm wide and 1.5 mm apart (DIXI Medical, Besançon, France). Electrode contacts were identified on the patient's individual stereotactic implantation scheme, and were anatomically localized using Talairach and Tournoux's proportional atlas (Talairach and Tounoux, 1993). Computer-assisted matching between a post-implantation CT-scan and a pre-implantation 3-D MRI data set (VOXIM R, IVS, Solutions, Germany) allowed for direct visualization of the electrode contacts on the patient's brain anatomy using the ACTIVIS (Aguera et al., 2011).

iEEG recordings. Intracerebral recordings were conducted using a video-iEEG monitoring system (Micromed, Treviso, Italy), which allowed the simultaneous data recording from 128 depth-EEG electrode sites. The data was bandpass-filtered online

from 0.1 to 200 Hz and sampled at 512 Hz in 22 subjects and 1024 Hz in the remaining two. During the acquisition the data was recorded using a reference electrode located in white matter. For subsequent analyses, each electrode trace was referenced with respect to its direct neighbor by bipolar derivation. This final electrode montage eliminates signal artifacts common to adjacent recording sites (such as the 50 Hz power supply artifact or distant physiological artifacts) and achieves a high local specificity by canceling out effects of distant sources that equally spread to both adjacent sites through volume conduction (Lachaux et al., 2003; Jerbi et al., 2009a,b). The spatial resolution achieved by this bipolar iEEG montage is on the order of 3 mm. Eye movements were monitored by recording the electro-oculogram (EOG) in all sessions.

Intracranial recordings: Spectral analysis and statistical measures. We used two analysis techniques to assess spectral responses from neural recordings. Initially, we computed a standard time-frequency (TF) wavelet decomposition, which allows identifying major TF components of interest across all trials at each recording site. This was carried out with the software package for electrophysiological analysis (ELAN-pack) developed at the laboratory INSERM U1028 (Aguera et al., 2011). The frequency range extended from 1 to 200 Hz and the time interval included a 300 ms pre-stimulus baseline, from -400 ms to -100 ms, and lasted until stimulus offset (3000 ms). We estimated significant power responses compared to average baseline with the Wilcoxon signed rank test (see Figure 1.C). Based on these results we determined a frequency range of interest which was used to compute the Hilbert transform, to evaluate the significance of this neural response with a lower degree of complexity and thus with a higher statistical power. Applying the Hilbert transform to the

continuous recordings splits the data into instantaneous amplitude (i.e., envelope) and phase components in a given frequency interval (Le Van Quyen et al., 2001). In addition to being a convenient measure of instantaneous amplitude modulations in a frequency range of interest, performing spectral analysis using the Hilbert transform was also used to confirm the TF results obtained independently by wavelet analysis. These comparisons provided an additional level of confidence in the results of spectral analysis reported throughout this study. Hilbert transform and subsequent envelope calculations were done with Matlab software (Mathworks Inc. Natick, MA, USA).

Continuous iEEG signals were first band-pass filtered in multiple successive 10 Hz-wide frequency bands (e.g., 10 bands, beginning with 50-60 Hz up to 140-150 Hz). Next, for each band-pass filtered signal we computed the envelope using standard Hilbert transform. The obtained envelope had a time resolution of 15.625 ms. Again, for each band, this envelope signal (i.e., time-varying amplitude) was divided by its mean across the entire recording session and multiplied by 100. This yields instantaneous envelope values expressed in percent of the mean. Finally, the envelope signals computed for each consecutive frequency bands (e.g., 10 bands of 10-Hz intervals between 50-150 Hz) were averaged together, to provide one single time-series (the high gamma-band envelope) across the entire session. By construction, the mean value of that time-series across the recording session is equal to 100.

To estimate the significance of the amplitude responses across time (post-stimulus) we compared each post-stimulus time-bin (0 ms to 3000ms) to an average pre-stimulus baseline amplitude value (-400ms to -100ms) with a Wilcoxon signed rank test followed by false discovery rate (FDR) correction (Genovese et al., 2002) across

all time samples. We used a non-parametric Kruskal-Wallis test to compare baseline-corrected post-stimulus amplitude responses between efficient and inefficient search followed by false discovery rate (FDR) correction across all time samples.

Mapping intracranial EEG data to standard MNI brain.

The anatomical representation of all significant amplitude modulations for a given frequency band were obtained by pooling data from all subjects and mapping it onto a standard Montreal Neurological Institute (MNI) brain based on the localization of each electrode. The value assigned to each node of the MNI brain represents the average of data from all recording sites located within a distance maximum 15 mm from the node. The individual data averaged in this study represents the change in amplitude (in %) compared to pre-stimulus baseline period (more detailed methods in Ossandon et al, in press; Vidal et al., 2010). This data mapping procedure allows visualizing intracerebral EEG data from all subjects on a common MNI brain and is used to identify anatomo-functional regions of interest for further detailed analyses.

fMRI recordings

13 healthy controls (5 female subjects; mean age 31 years) were recorded in the same visual search paradigm in a parallel fMRI experiment to define Regions of Interest (ROIs) for the iEEG analysis.

fMRI Data Acquisition

MRI was performed on a 3-Tesla unit (Philips Achieva, Netherlands), equipped with an 8-channel head coil. fMRI data were acquired using a whole-brain blood oxygen level-dependent (BOLD) echo-planar imaging sequence, with repetition time 2.5 s, echo time 30 ms, field of view (FOV) 92 x 90 mm, 0.4 mm adjacent transverse slices, and 124 volumes per acquisition. For anatomic reference, a T_1-weighted three-dimensional (3D) turbo field echo was acquired with the following parameters: TR 6.9 ms, TE 3.1 ms, flip angle 8°, voxel size 1.10 × 1.10 × 1.20 mm, duration 10.53 ms.

1. Experimental Design

The experiment consisted of 3 blocks of each of the two stimulus types. Each block consisted of presentations of 10 consecutive images, each of 2.5 s duration, giving resulting in a total block length of 25 s. We used the same images described for the iEEG recordings (efficient and inefficient visual search) with the target being located in the left or right hemi field of the array. Subjects were instructed to press the button on the left or right depending on the visual hemi field where the target letter appeared. Block presentation was randomized, so that no two consecutive blocks contained the same stimulus type. Each block was followed by a rest period of 25 s to allow recovery of the hemodynamic response during which the subjects were looking at a fixation cross.

2. fMRI Data Analysis

fMRI data analysis was carried out using statistical parametric mapping (SPM 5, Wellcome Department of Cognitive Neurology, London, UK), implemented in

Matlab. The first 4 volumes were discarded to allow for T1 equilibration effects. All images underwent slice timing, realignment across all two runs, spatial normalization to the MNI template using a 4th Degree B-spline interpolation, and smoothing using an isotropic 8-mm^3 Full-Width-Half maximum kernel. Each individual data set was then carefully screened for data quality via inspection for image artifacts and excessive head motion (> 3 mm head motion or 2° head rotation). fMRI responses were modeled using the General Linear Model (GLM) across all two runs modeled as separate blocks with a canonical hemodynamic response function (HRF) convolved for the length of each block, normalized to the global signal across the whole brain across the entire session, and high-pass filtered (less than 128 s).

Second level random-effects analyses were performed using one-sample t-tests to explore the main effect of each task condition during the experimental phase (between task performance and baseline and between efficient and inefficient visual search task). Statistical thresholds for one-sample t-tests were set at $p < 0.05$, with false discovery rate (FDR).

Results

Behavioral results

Reaction times (RTs) in patients were shorter and performance higher during efficient compared with inefficient search (RT: efficient: 1003 ms ± 70 s.e.m., inefficient: 1705 ms ± 138 s.e.m.; $t = 17.05$, $p<0.001$, see Figure 1B; performance: efficient: 95.3 %correct, inefficient 84.3 %correct; $t=5.66$, $p<0.001$). Similar results were obtained in healthy control subjects during the fMRI session (efficient: 1006 ms ± 96 s.e.m., inefficient: 1415 ms ± 81 s.e.m.; $t=5.53$, $p<0.001$; efficient: 98.4%, inefficient 92.2%

of correct responses; t=2.78, p<0.01). Healthy controls had better performance on the inefficient search condition (t = 2.04, p < 0.05), but both groups performed the efficient search equally well.

Three distinct temporal profiles in the gamma band

iEEG data were collected from a total of 2413 intracerebral recording sites across 24 patients. TF statistical analysis revealed a significant post-stimulus spectral power increase in a broad frequency range covering the low and high gamma-bands (50 – 150 Hz) in 352 sites (14.6% of all sites). This frequency range of interest (50 – 150 Hz) was used to compute the Hilbert transform (see Methods for details; Wilcoxon test vs. baseline after Hilbert transformation, p<0.05, corrected for multiple comparisons).

Among the significant sites, the post-stimulus broadband gamma activity (BGA) amplitude was significant either for (i) the efficient search (16 sites), (ii) the inefficient search (25 sites), or for both conditions (309 sites, see Figure 1B). Visual inspection of those broadband gamma responses revealed a dissociation between short transient responses time-locked to stimulus onset (type I), sustained energy increases lasting the entire search process (type II) and late energy increases time-locked to the motor response (type III) (Figure 2B). Our main question was whether type II responses could be observed during efficient search and if so, in which brain structures. To address this question, we defined this response type more precisely as follows: any significant post-stimulus energy increase between 50 Hz and 150 Hz which duration was correlated with reaction time on a single-trial basis; $p < 0.05$, Spearman correlation, corrected). The duration of the increase was defined as the

number of samples during the 3 seconds following stimulus onset (the time of the stimuli presentation) with an energy value higher than baseline ($p<0.05$, Wilcoxon test, corrected). Trials in which responses occurred after 3 seconds were not analyzed (less than 1% of trials). Such type II responses, called task-related BGA thereafter, were found in 112 sites overall, mostly located in the frontal lobes (see Figure 2B). Of the remaining 240 responsive sites, 72 had responses time-locked to the motor response (i.e., a significant correlation between the latency of the response maximum and the reaction time on a single-trial basis, Spearman correlation, corrected $p<0.01$; see Figure 2B) located principally along the precentral and postcentral gyrus.

Finally, 123 sites had transient responses time-locked to stimulus onset, in which the duration of BGA was completely independent of reaction times across the trials (90 of which were located in the temporal lobes). 45 additional sites (13% overall) were responsive but could not categorized as type I, II or III.

ROI identification with fMRI

Our strategy was to compare the strength and timing of type II responses during efficient vs. inefficient search in the fronto-parietal network supporting visual search. In order to achieve a spatial identification of the involved networks, in line with previous neuroimaging studies, we also conducted an fMRI study in 13 healthy participants during the same visual search conditions. As shown in figure 2A, inefficient search elicited bilateral activation in the DLPFC, premotor cortex, inferior frontal gyri (including Broca's area), an extended parietal activation including the superior parietal lobule, occipital and anterior cingulate gyrus. Efficient search

activated a smaller network, comprising only the occipital gyri, and in the left inferior parietal lobule. See Figure 2A for comparison of fMRI and iEEG activation maps in the inefficient vs. efficient search conditions.

Based on the fMRI study, the analysis of iEEG responses focused on four anatomical ROIs (Figure 2A): DLPFC (bilateral, center coordinates*:* [43, 39, 22] and [-39, 28, 25], Talairach space), dACC (center coordinate: [-4, 16, 44]), SPL (bilateral, center coordinates: [32, -50, 46] and [-36, -56, 45]) – and right and left *intersection* line between *precentral sulcus* and middle frontal gyrus (PrCS/MFG, center coordinates [44, -1, 39] and [-42, -2, 43]), including the proposed location of the human FEF (Blanke et al., 2000; Lobel et al., 2001).

Task effects

63 of the 112 task-related BGA (type II) were located in one of these four ROIs (Figure 3A). 19 in the DLPFC (7 patients), 20 in the PrCS/MFG (7 patients), 12 in the SPL (6 patients), 12 in the dACC (4 patients). In all four ROIs, the majority of BGA responses (85%) had no significant amplitude difference between the efficient and inefficient search conditions (see Figure 3B, time windows: 100 to 600 ms after stimulus presentation; $p > 0.05$, Kruskal-Wallis test, FDR corrected) (DLPFC: 17/19; PrCS/MFG: 14/20; SPL: 11/12; dACC: 11/12).

The overall energy of the BGA was higher in the inefficient than in the efficient search condition, but mostly because of longer reaction times, yielding longer responses in the former condition (3 seconds, see Figure 1C and 3A). When considering only trials with equivalent reaction time distributions (i.e., shortest

inefficient search vs. longest efficient search trials), we found that most (53 out of 63) recording sites produced BGA responses with equivalent energy (Kruskal-Wallis test, FDR corrected, $p>0.05$. At least 27 trials by condition were compared). In half of the 10 remaining sites, the energy of the average response over trials with matched duration was higher in the efficient search condition. Overall, all four ROIs were characterized by increases in broadband gamma activity that were sustained throughout the duration of each trial, from stimulus onset to target detection. Most importantly this was observed both for the pop-out (efficient search) and the more complex (inefficient search) tasks with no significant difference in mean energy between the two conditions.

Discussion

To the best of our knowledge, this study is the first to reveal a significant trial-by-trial correlation between neuronal activity and behavioral paremeters during a visual search task in humans. Significant correlations between reaction times and the duration of sustained gamma-band responses provide clear evidence that the dorsal attention network provide clear evidence that the dorsal attention network supported by the dorsal ACC and the DLPFC in the frontal lobe, and by the SPL is equally active during efficient and inefficient visual search. Differences in search duration across the two conditions accounted for longer neural responses during inefficient search, but onset latencies and response amplitudes were similar in both types of search in the majority of frontal and parietal recording sites.

Sustained frontal activation during efficient visual search

Our results support the view that efficient and inefficient visual search rely on the same network, despite previous models showing that salient targets can be detected by purely bottom-up processes in the visual cortex (Treisman and Gelade, 1980; Itti and Koch, 2001). In fact, the temporal dynamics of sustained broadband gamma activity (BGA) increases accompanying efficient search is more compatible with top-down influences than with bottom-up processes, which are usually characterized by early and transient neural responses following stimulus onset.

The findings we report here need to be considered and incorporated into a previous literature that supports the view that prefrontal areas, and especially the DLPFC, are not necessary for efficient search. For instance, in an fMRI study, Leonards et al. (2000) found that although the networks underlying efficient and inefficient search overlapped almost completely, the DLPFC was active only during inefficient search. This was later confirmed by Anderson et al. (2007), who reported no fMRI activation in the DLPFC when participants searched for singletons – a typical efficient search condition. One possible explanation might be that search durations are too short in the efficient condition to elicit a BOLD response in the DLPFC that is sufficiently long to be detected with fMRI. This would amount to a simple technical limitation of fMRI, which is its low temporal resolution compared to electrophysiological recordings such intracranial EEG, an interpretation which is compatible with the absence of significant prefrontal activation in our own fMRI study during the efficient search condition. However, the failure to detect prefrontal activations during efficient search is not unique to fMRI studies. Kalla et al. (2009) reached similar conclusions with Transcranial Magnetic Stimulation: TMS pulses delivered to the DLPFC did not

impair the participants' ability to detect the presence of singletons in a crowded display. This led them to conclude that this region is not necessary for efficient search (Kalla et al., 2009). As recently summarized, and in fact questioned by Wardak et al. (2010) in a monkey study, the classical view remains that efficient search involves solely, or mainly, low-level preattentive processes.

Yet, there are reasons to believe that the DLPFC should be active during any kind of visual search, be it efficient or inefficient. Several functions have been attributed to the DLPFC: not only the guidance, control and monitoring of spatial attention but also decision-making and response selection processes (Heekeren et al., 2004; Heekeren et al., 2008), and working-memory, including the maintenance of a memory trace of the task-set and the attention-set which define the task-at-hand (Corbetta and Shulman, 2002; Sakai, 2008). In direct contradiction with the previously mentioned fMRI and TMS studies, our results support the view that at least a subset of those processes also occurs during efficient search, in parallel with low-level detection processes. This finding might be explained by the fact that our 'efficient search' condition required that participants actually find the target and identify its spatial location, which clearly involves decision-making and a working memory component, to maintain the attention-set which defines the target.

In the three studies previously mentioned (Leonards et al., 2000; Anderson et al., 2007; Kalla et al., 2009), participants simply had to report whether a singleton was present or absent in the visual display. This might constitute an exceptionally easy task for the visual system, which can be performed without any memory requirement. The perceptual decision might amount to a simple low-level categorical scene

interpretation (Hochstein and Ahissar, 2002) discriminating between two general configurations of displays: spatially homogeneous vs. inhomogeneous. Therefore, their task would not necessarily require an actual search process per se, that is, the localization of a pre-identified item embedded within a crowded visual environment, but simply the detection that 'the display looks odd and inhomogeneous'. When the search is, indeed, a search, we argue that the prefrontal cortex is actively involved even when the target is a salient target. This view is reminiscent of earlier claims by Joseph et al. (1997) that even simple search tasks, including searching for simple features, require central attentional resources and are disrupted when attention is diverted away by a secondary task.

We propose that, during efficient search, bottom-up influences act in parallel with top-down search processes to orient attention to the salient target and terminate the search early. During the search process, sustained neural activity in the DLPFC, the FEF and the SPL might reflect top-down influences from frontal areas to continuously update saliency/priority maps in the parietal lobe (Bisley and Goldberg, 2010). We further propose that top-down influences guide attention deployment as soon as participants search for a pre-specified target, be it salient or not. In addition, the dorsal ACC would drive and sustain the attentional effort until task-completion, again independently of search condition (Dosenbach et al., 2006).

Gamma-band activity in the DLPFC, dACC and to a lesser extent the FEF would therefore be characteristic of 'active vision': the search for task-relevant information in a visual scene (Henderson, 2003). Therefore, we suggest that any search condition necessarily activates the frontal executive system, as soon as search instructions define that some items are 'task-relevant', which must then be maintained in an

attention-set and searched for. In other words, 'searching' inevitably contains an active component that would be indissociable from active top-down frontal control, in direct agreement with recent models of visual search (Wolfe, 2003). Purely bottom-up attentional capture – free of frontal influences - would only occur in passive viewing conditions, with no pre-specified target or when participants make an explicit effort to adopt a passive cognitive strategy and let the target pop-out. In fact, a recent eye-tracking study (Watson et al., 2010) showed that during an easy visual search, participants had the natural tendency to react to the display onset with an immediate and active visual exploration. However, it was possible to instruct participants to hold their exploratory behavior and let the target pop-out, before making their first saccade. This more passive strategy proved to be a more efficient extraction of visual information. The study by Watson et al. (2010) is not in contradiction with the results we report here. It rather indicates that 'active search' – involving the dorsal attention network – might be just one option during efficient search, the most natural but not necessarily the most efficient one, and another example that participants do not spontaneously use the most efficient attentional strategy to perform easy tasks, as suggested by several recent studies (Slagter et al., 2007; Slagter et al., 2009).

Sustained gamma-band responses during attentive search

That BGA increases during 'active vision' is an observation reminiscent of earlier proposals that neural synchronization in the gamma-band might mediate attentional selection (Murthy and Fetz, 1996; Fries, 2005, 2009). However, the frequency bandwidth of the iEEG gamma band responses reported here extends well beyond the narrow frequency band found in monkey studies (Fries et al., 2001; Buschman and

Miller, 2007) and might therefore correspond to a different mechanism. An alternative, and possibly non-exclusive, interpretation, is that broadband gamma responses reflect a global enhancement of the firing rate of the underlying neural population, observed as a "spike bleed-through" in the field power spectra (Manning et al., 2009; Ray and Maunsell, 2011). Indeed, recent studies combining multi-unit recordings with iEEG in humans (Manning et al., 2009) or LFP in macaque monkeys (Ray and Maunsell, 2011) have clearly demonstrated strong positive correlations between BGA and co-occurring spike rates at the population level. Based on those studies, we support the view that BGA can, at least, be understood as a proxy of the global discharge rate – and therefore activity level – of the neural populations recorded with iEEG, which is consistent with the tight relationship between BGA and the BOLD signals measured with fMRI (Logothetis et al., 2001; Mukamel et al., 2005; Niessing et al., 2005; Lachaux et al., 2007; Nir et al., 2007; Conner et al., 2011).

A comparison of BOLD and BGA responses during visual search

The strong correlation reported in the litterature between BGA and BOLD signals must then be reconciled with the fact that our fMRI study did not reveal significant frontal activations during efficient search (Leonards et al., 2000; Nobre et al., 2003). As mentioned earlier, one possibility might be that frontal haemodynamic responses are too short-lived to be detected with fMRI, in contrast with the more sustained responses characteristic of the inefficient search condition. However, fMRI detected equally short responses in the visual cortex, in the easy search condition, maybe

because their amplitude was stronger. Future studies, combining simultaneous fMRI and iEEG recordings, will be needed to resolve that issue (Vulliemoz et al., 2011).

References

Aguera PE, Jerbi K, Caclin A, Bertrand O (2011) ELAN: A Software Package for Analysis and Visualization of MEG, EEG, and LFP Signals. *Computational Intelligence and Neuroscience* 2011:11.

Anderson EJ, Mannan SK, Husain M, Rees G, Sumner P, Mort DJ, McRobbie D, Kennard C (2007) Involvement of prefrontal cortex in visual search. *Exp Brain Res* 180:289-302.

Barcelo F, Suwazono S, Knight RT (2000) Prefrontal modulation of visual processing in humans. *Nat Neurosci* 3:399-403.

Bichot NP, Rossi AF, Desimone R (2005) Parallel and serial neural mechanisms for visual search in macaque area V4. *Science* 308:529-534.

Bisley JW, Goldberg ME (2003) Neuronal activity in the lateral intraparietal area and spatial attention. *Science* 299:81-86.

Bisley JW, Goldberg ME (2010) Attention, intention, and priority in the parietal lobe. *Annu Rev Neurosci* 33:1-21.

Blanke O, Spinelli L, Thut G, Michel CM, Perrig S, Landis T, Seeck M (2000) Location of the human frontal eye field as defined by electrical cortical stimulation: anatomical, functional and electrophysiological characteristics. *Neuroreport* 11:1907-1913.

Bressler SL, Tang W, Sylvester CM, Shulman GL, Corbetta M (2008) Top-down control of human visual cortex by frontal and parietal cortex in anticipatory visual spatial attention. *J Neurosci* 28:10056-10061.

Buschman TJ, Miller EK (2007) Top-down versus bottom-up control of attention in the prefrontal and posterior parietal cortices. *Science* 315:1860-1862.

Cole MW, Schneider W (2007) The cognitive control network: Integrated cortical regions with dissociable functions. *Neuroimage* 37:343-360.

Conner CR, Ellmore TM, Pieters TA, Disano MA, Tandon N (2011) Variability of the Relationship between Electrophysiology and BOLD-fMRI across Cortical Regions in Humans. *J Neurosci* 31:12855-12865.

Corbetta M, Shulman GL (2002) Control of goal-directed and stimulus-driven attention in the brain. *Nat Rev Neurosci* 3:201-215.

Desimone R, Duncan J (1995) Neural mechanisms of selective visual attention. *Annu Rev Neurosci* 18:193-222.

Dosenbach NU, Visscher KM, Palmer ED, Miezin FM, Wenger KK, Kang HC, Burgund ED, Grimes AL, Schlaggar BL, Petersen SE (2006) A core system for the implementation of task sets. *Neuron* 50:799-812.

Duncan J, Humphreys GW (1989) Visual search and stimulus similarity. *Psychol Rev* 96:433-458.

Fries P (2005) A mechanism for cognitive dynamics: neuronal communication through neuronal coherence. *Trends Cogn Sci* 9:474-480.

Fries P (2009) Neuronal Gamma-Band Synchronization as a Fundamental Process in Cortical Computation. *Annual Review of Neuroscience* 32:209-224.

Fries P, Reynolds JH, Rorie AE, Desimone R (2001) Modulation of oscillatory neuronal synchronization by selective visual attention. *Science* 291:1560-1563.

Genovese CR, Lazar NA, Nichols T (2002) Thresholding of statistical maps in functional neuroimaging using the false discovery rate. *Neuroimage* 15:870-878.

Heekeren HR, Marrett S, Ungerleider LG (2008) The neural systems that mediate human perceptual decision making. *Nat Rev Neurosci* 9:467-479.

Heekeren HR, Marrett S, Bandettini PA, Ungerleider LG (2004) A general mechanism for perceptual decision-making in the human brain. *Nature* 431:859-862.

Henderson JM (2003) Human gaze control during real-world scene perception. *Trends Cogn Sci* 7:498-504.

Hochstein S, Ahissar M (2002) View from the top: hierarchies and reverse hierarchies in the visual system. *Neuron* 36:791-804.

Itti L, Koch C (2001) Computational modelling of visual attention. Nat Rev Neurosci 2:194-203.

Jerbi K, Ossandon T, Hamame CM, Senova S, Dalal SS, Jung J, Minotti L, Bertrand O, Berthoz A, Kahane P, Lachaux JP (2009a) Task-related gamma-band dynamics from an intracerebral perspective: review and implications for surface EEG and MEG. *Hum Brain Mapp* 30:1758-1771.

Jerbi K, Freyermuth S, Dalal S, Kahane P, Bertrand O, Berthoz A, Lachaux JP (2009b) Saccade related gamma-band activity in intracerebral EEG: dissociating neural from ocular muscle activity. *Brain Topogr* 22:18-23.

Joseph JS, Chun MM, Nakayama K (1997) Attentional requirements in a 'preattentive' feature search task. *Nature* 387:805-807.

Kalla R, Muggleton NG, Cowey A, Walsh V (2009) Human dorsolateral prefrontal cortex is involved in visual search for conjunctions but not features: a theta TMS study. *Cortex* 45:1085-1090.

Kalla R, Muggleton NG, Juan CH, Cowey A, Walsh V (2008) The timing of the involvement of the frontal eye fields and posterior parietal cortex in visual search. *Neuroreport* 19:1067-1071.

Lachaux JP, Rudrauf D, Kahane P (2003) Intracranial EEG and human brain mapping. Journal of Physiology-Paris 97:613-628.

Lachaux JP, Fonlupt P, Kahane P, Minotti L, Hoffmann D, Bertrand O, Baciu M (2007) Relationship between task-related gamma oscillations and BOLD signal: New digits from combined fMRI and intracranial EEG. *Human Brain Mapping* 28:1368-1375.

Le Van Quyen M, Foucher J, Lachaux JP, Rodriguez E, Lutz A, Martinerie J, Varela FJ (2001) Comparison of Hilbert transform and wavelet methods for the analysis of neuronal synchrony. *Journal of Neuroscience Methods* 111:83-98.

Leonards U, Sunaert S, Van Hecke P, Orban GA (2000) Attention mechanisms in visual search -- an fMRI study. *J Cogn Neurosci* 12 Suppl 2:61-75.

Lobel E, Kahane P, Leonards U, Grosbras M, Lehericy S, Le Bihan D, Berthoz A (2001) Localization of human frontal eye fields: anatomical and functional findings of functional magnetic resonance imaging and intracerebral electrical stimulation. *J Neurosurg* 95:804-815.

Logothetis NK, Pauls J, Augath M, Trinath T, Oeltermann A (2001) Neurophysiological investigation of the basis of the fMRI signal. *Nature* 412:150-157.

Manning JR, Jacobs J, Fried I, Kahana MJ (2009) Broadband Shifts in Local Field Potential Power Spectra Are Correlated with Single-Neuron Spiking in Humans. *J Neurosci* 29:13613-13620.

Moore T, Armstrong KM (2003) Selective gating of visual signals by microstimulation of frontal cortex. Nature 421:370-373.

Mukamel R, Gelbard H, Arieli A, Hasson U, Fried I, Malach R (2005) Coupling between neuronal firing, field potentials, and FMRI in human auditory cortex. *Science* 309:951-954.

Murthy VN, Fetz EE (1996) Synchronization of neurons during local field potential oscillations in sensorimotor cortex of awake monkeys. *J Neurophysiol* 76:3968-3982.

Niessing J, Ebisch B, Schmidt KE, Niessing M, Singer W, Galuske RA (2005) Hemodynamic signals correlate tightly with synchronized gamma oscillations. *Science* 309:948-951.

Nir Y, Fisch L, Mukamel R, Gelbard-Sagiv H, Arieli A, Fried I, Malach R (2007) Coupling between neuronal firing rate, gamma LFP, and BOLD fMRI is related to interneuronal correlations. *Curr Biol* 17:1275-1285.

Nobre AC, Coull JT, Walsh V, Frith CD (2003) Brain activations during visual search: contributions of search efficiency versus feature binding. *Neuroimage* 18:91-103.

Ossandón T, Jerbi K, Vidal JR, Bayle DJ, Henaff MA, Jung J, Minotti L, Bertrand O, Kahane P, Lachaux JP. (2011) Transient Suppression of Broadband Gamma Power in the Default-Mode Network Is Correlated with Task Complexity and Subject Performance. *J Neurosci,* In Press

Procyk E, Goldman-Rakic PS (2006) Modulation of dorsolateral prefrontal delay activity during self-organized behavior. J Neurosci 26:11313-11323.

Ray S, Maunsell JH (2011) Different origins of gamma rhythm and high-gamma activity in macaque visual cortex. *PLoS Biol* 9:e1000610.

Rowe JB, Toni I, Josephs O, Frackowiak RS, Passingham RE (2000) The prefrontal cortex: response selection or maintenance within working memory? *Science* 288:1656-1660.

Sakai K (2008) Task set and prefrontal cortex. *Annu Rev Neurosci* 31:219-245.

Shulman GL, Tansy AP, Kincade M, Petersen SE, McAvoy MP, Corbetta M (2002) Reactivation of networks involved in preparatory states. *Cereb Cortex* 12:590-600.

Slagter HA, Lutz A, Greischar LL, Nieuwenhuis S, Davidson RJ (2009) Theta phase synchrony and conscious target perception: impact of intensive mental training. *J Cogn Neurosci* 21:1536-1549.

Slagter HA, Lutz A, Greischar LL, Francis AD, Nieuwenhuis S, Davis JM, Davidson RJ (2007) Mental training affects distribution of limited brain resources. *PLoS Biol* 5:e138.

Talairach J, Tounoux P (1993) Referentially Oriented Cerebral MRI Anatomy: An Atlas of Stereotaxic Anatomical Correlations for Gray and White Matter: Thieme Medical Publishers, New York.

Treisman AM, Gelade G (1980) Feature-Integration Theory of Attention. *Cognitive Psychology* 12:97-136.

Vidal JR, Chaumon M, O'Regan JK, Tallon-Baudry C (2006) Visual grouping and the focusing of attention induce gamma-band oscillations at different frequencies in human magnetoencephalogram signals. *J Cogn Neurosci* 18:1850-1862.

Vidal JR, Ossandon T, Jerbi K, Dalal SS, Minotti L, Ryvlin P, Kahane P, Lachaux JP (2010) Category-Specific Visual Responses: An Intracranial Study Comparing Gamma, Beta, Alpha, and ERP Response Selectivity. *Front Hum Neurosci* 4:195.

Vulliemoz S, Carmichael DW, Rosenkranz K, Diehl B, Rodionov R, Walker MC, McEvoy AW, Lemieux L (2011) Simultaneous intracranial EEG and fMRI of interictal epileptic discharges in humans. *Neuroimage* 54:182-190.

Wardak C, Vanduffel W, Orban GA (2010) Searching for a salient target involves frontal regions. Cereb Cortex 20:2464-2477.

Watson MR, Brennan AA, Kingstone A, Enns JT (2010) Looking versus seeing: Strategies alter eye movements during visual search. *Psychon Bull Rev* 17:543-549.

Wolfe JM (2003) Moving towards solutions to some enduring controversies in visual search. *Trends Cogn Sci* 7:70-76.

Wolfe JM, Vo ML, Evans KK, Greene MR (2011) Visual search in scenes involves selective and nonselective pathways. *Trends Cogn Sci* 15:77-84.
Wyart V, Tallon-Baudry C (2008) Neural dissociation between visual awareness and spatial attention. *J Neurosci* 28:2667-2679.
Zhou H, Desimone R (2011) Feature-Based Attention in the Frontal Eye Field and Area V4 during Visual Search. *Neuron* 70:1205-1217.

Figures

Figure 1.

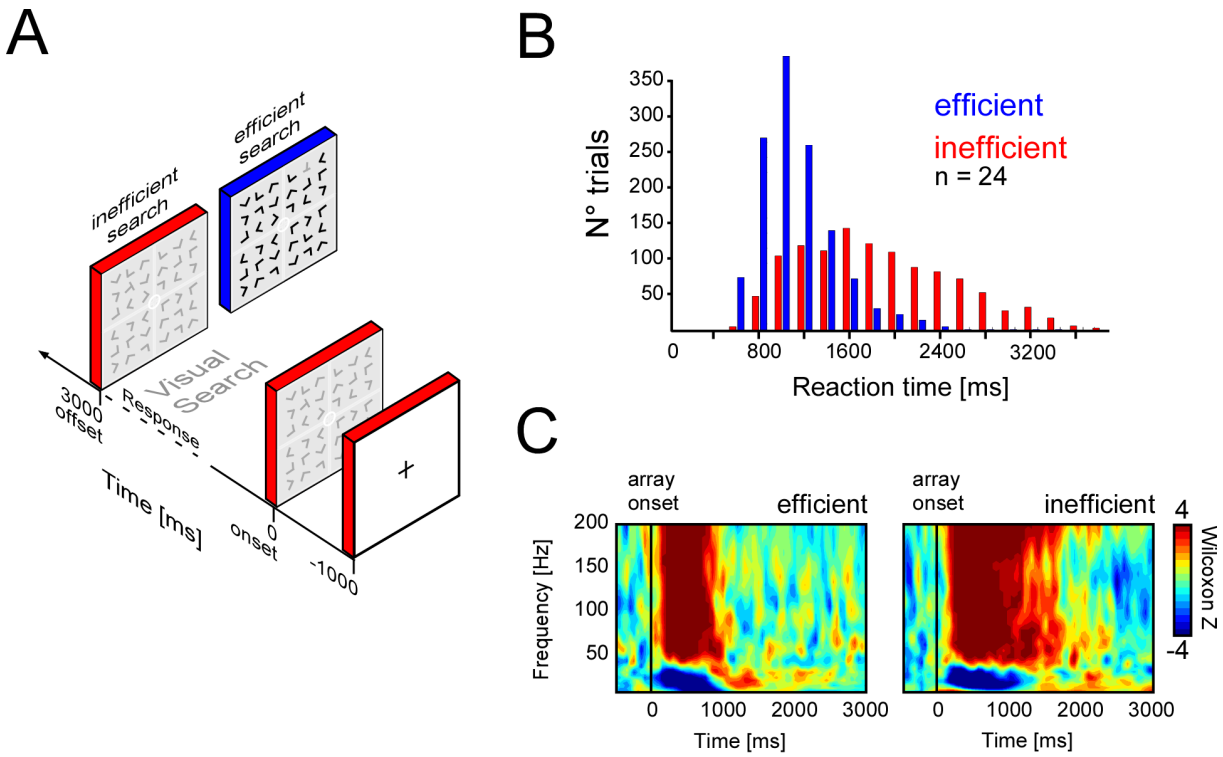

Figure 2.

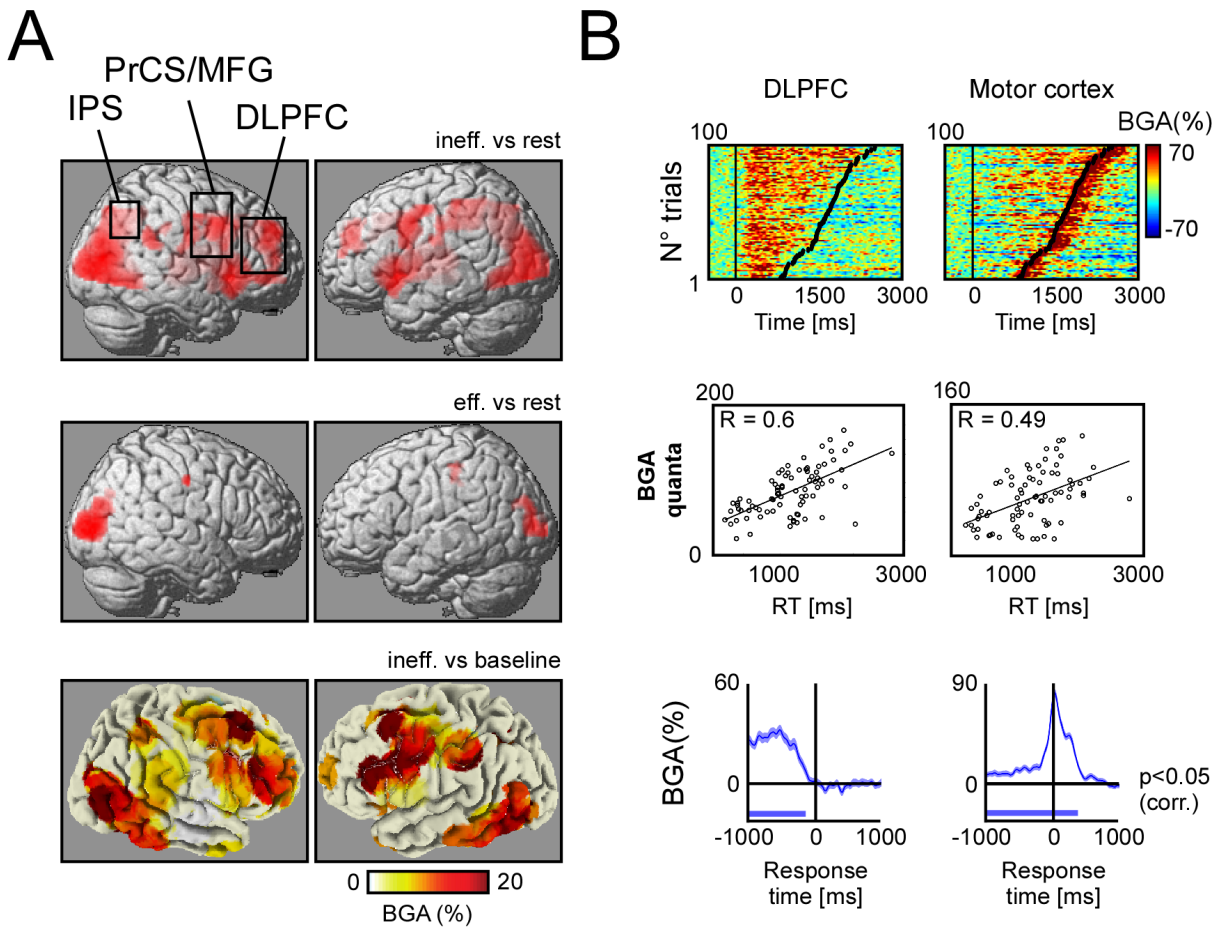
A
PrCS/MFG
IPS
DLPFC
ineff. vs rest
eff. vs rest
ineff. vs baseline
0
20
BGA (%)
B
DLPFC
Motor cortex
BGA(%)
70
-70
100
1
N° trials
0
1500
3000
Time [ms]
200
160
R = 0.6
R = 0.49
BGA quanta
0
1000
3000
RT [ms]
60
90
BGA(%)
-1000
1000
Response time [ms]
p<0.05 (corr.)

Figure 3.

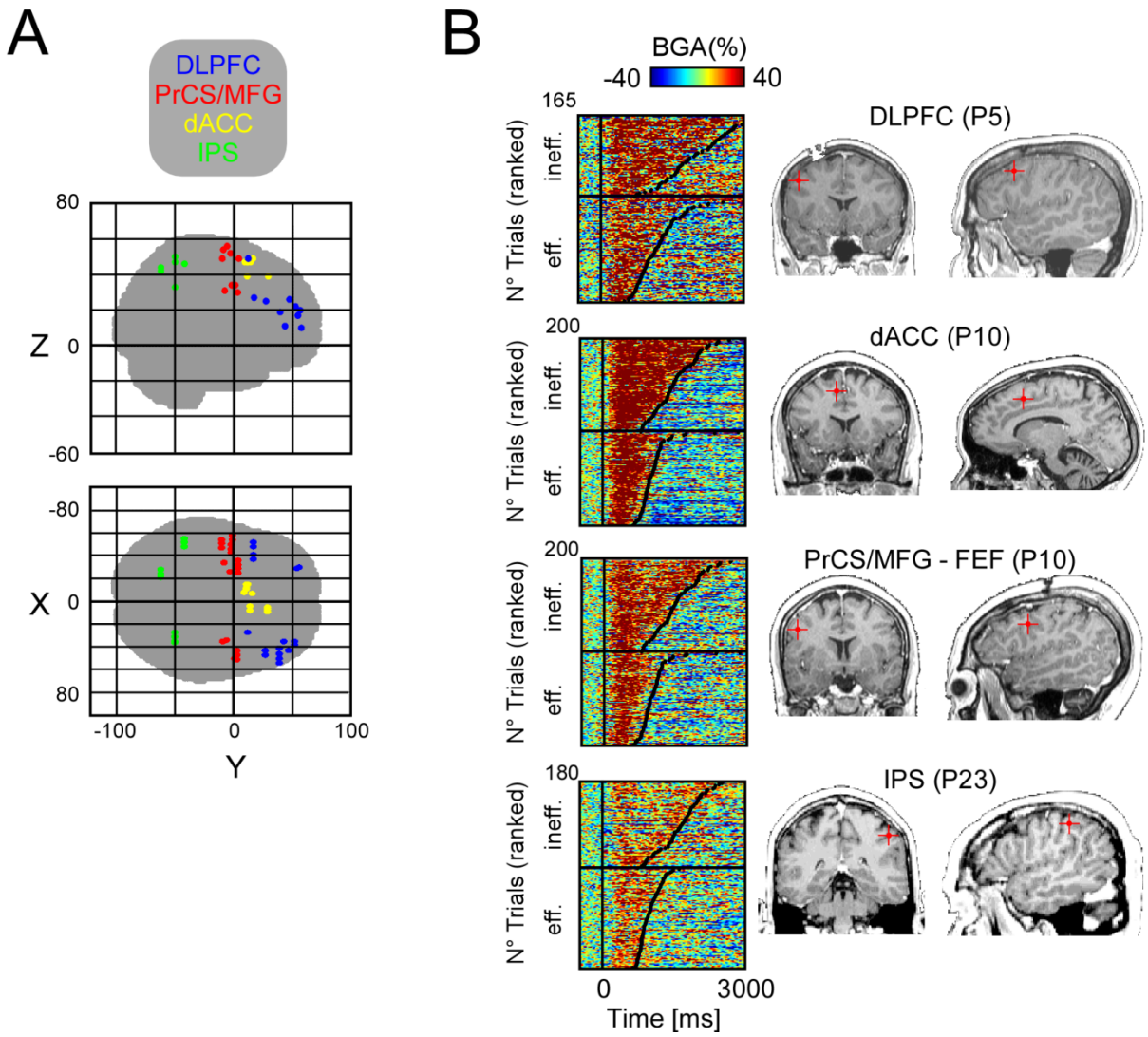
A
DLPFC
PrCS/MFG
dACC
IPS
80
Z 0
-60
-80
X 0
80
-100
0
100
Y
B
BGA(%)
-40
40
165
N° Trials (ranked)
ineff.
eff.
DLPFC (P5)
200
dACC (P10)
200
PrCS/MFG - FEF (P10)
180
IPS (P23)
0
3000
Time [ms]

Figure Legends

Figure 1. Experimental conditions, behaviour and time-frequency responses. ***A,*** The experimental design. After 1000 ms ISI a visual array is presented for 3000 ms. When the target is detected, subjects press a button to indicate in which quadrant of the array (upper or lower) it is located. In the inefficient search condition (in red), target and distractors have the same color. In the efficient search condition (in blue), the target has a different contrast than the distractors. ***B***, Reaction time distribution for efficient (blue) and inefficient visual search (red). ***C***, Statistical time-frequency maps (Wilcoxon Z, FDR corrected) for efficient (left panel) and inefficient (right panel) visual search from a recording site (patient 10; Talairach coordinates: [-43 -3 34]), located in dorsolateral prefrontal cortex.

Figure 2. BOLD response contrasts and broadband gamma activity response patterns during visual search. ***A,*** *Upper panel*, BOLD response contrast between inefficient search and rest conditions. *Middle panel*, BOLD response contrast between efficient search and rest conditions. *Lower panel*, broadband gamma response topography across all recording sites and all patients, plotted on a "glass brain" in MNI coordinates. ***B,*** Upper panel, single-trial BGA responses recorded from DLPFC (left, Talairach coordinates [-37 17 27]) and primary motor cortex (right, Talairach coordinates: [-57 -28 48]) from patient 23 in the inefficient search condition. Middle panel, scatterplot of single-trial BGA quanta versus reaction times. A BGA quantum is a significant time-sample of BGA response versus baseline power evaluated between stimulus onset and offset (Wilcoxon test, FDR corrected). Left and right

panels correspond to upper panel BGA responses. ***C,*** Average BGA responses aligned to the response (button-press). Left and right panel correspond to upper panel BGA responses.

Figure 3. Single-trial gamma-band responses to efficient and inefficient visual search from frontal-parietal recording sites. ***A,*** Recording sites located in glass brain (Talairach). ***B,*** Four illustrative examples (MRI, right panels) of single-trial gamma-band responses to efficient (eff) and inefficient (ineff) visual search (left panels) recorded within 4 regions of interest of the frontal-parietal network: DLPFC (patient 5, Talairach coordinates [-58 -1 34]), dACC (patient 10, Talairach coordinates [-12 11 47]), PrCS/MFG putative FEF (patient 10, Talairach coordinates [-46 -2 34]) and IPS (patient 23, Talairach coordinates [-52 -42 46]).

7. Discussion

7.1 General discussion

Imagine sitting on a hammock, watching the stars, and lost in your own thoughts. While you are in this state, a shooting star crosses the horizon. As you might have experienced, your attention suddenly becomes focused on the shooting star; yet some seconds later your thoughts return to their previous state. What was going on in your brain after the shooting star? And what was going on just before? Many neuroscientists have long assumed that much of the neural activity at rest matches your subdued, somnolent mood (Raichle, 2010). In this view, the activity in the resting brain represents nothing more than random noise, similar to the snowy pattern on the television screen when a station is not broadcasting (Raichle, 2010). Nevertheless, recent analysis produced by neuroimaging techniques has revealed something quite remarkable: a great deal of meaningful activity is occurring in the brain when a person is sitting back and doing nothing at all.

As we have seen throughout this work, neuroscience has traditionally been dominated by an empiricist approach that partly stems from the influential work of Sherrington (Raichle, 2009; Yuste, MacLean, Smith, & Lansner, 2005). In an extreme empiricist view, the nervous system is considered to remain inactive until it is engaged by sensory input, at which point it would process the sensory information and generate an appropriate output (Yuste et al., 2005). This reflexive view of the brain has proven to be a very useful model and has greatly improved our understanding of neural circuits, not only in sensory regions, but also more generally with respect to overall brain function (Yuste et al., 2005; Raichle, 2010). It has also inspired fundamental concepts such as receptive field.

Nevertheless, a fundamental observation reported by Barath Biswal and colleagues in 1995 regarding the metabolic patterns of brain activity was able to change several assumptions about the brain at rest. These authors showed that even while a subject remained motionless, the baseline activity in the left precentral gyrus, specifically in the homunculus activated with right hand movement, fluctuating in unison with

similar activity in the area on the opposite side of the brain associated with left hand movement (Biswal et al., 1995). As we have seen before, similar characteristics have been found in multiple highly specific functional anatomical networks, known as Resting State Networks (RSNs), coming to the conclusion that **spontaneous slow fluctuations appear to reflect a fundamental aspect of brain organization**.

One of these networks, the Default Mode Network (DMN), has taken an important place in our field, principally because it has been associated to higher level cognitive functions in humans, that by definition are difficult to access, like episodic and prospective memory, self-projection, propioception, social cognition, and the prospective thought (Buckner and Carroll, 2007). At the moment, the DMN is defined only from metabolic data obtained by neuroimaging methods. Therefore, the metabolic deactivations in this network during goal-directed behaviors are the only potential trace of neural mechanisms still poorly understood. The first objective of my dissertation was to answer this question in the human brain.

In this dissertation, we have used an adaptation of a classical visual search task, developed by Triesmann and Gelade in 1980. The use of this task was not haphazard. Using this task, we can control easily the level of difficulty. The brain regions implicated have been well studied, and principally, we can compare two models of visual search, contrasting essentially the parallel search for a single and salient feature with a sequential visual search. Our goal was two-fold. The first main objective was to find the neural correlate of the task-related deactivation across the DMN and its relation with several markers of task engagement, such as performance. The second main objective was to study with a high temporal and spatial resolution the bottom-up and top-down components of a visual search, using unprecedented brain-wide intracerebral depth recordings in surgical patients.

7.2. Electrophysiological correlate of the Default Mode Network

As we have said, one of the main problems in neuroimaging techniques, is the poorly temporal resolution. For the same reason, several characteristics of the DMN are still unknown. While we know the brain regions that participate in this network, the

neural basis of the characteristic deactivation, its relation with behavioural parameters and the temporal order of the deactivations were unclear.

Our first study provides undisputable conceptual advance over previous fMRI research into DMN whit the major difference originating the fact that was based on direct electrophysiological recordings in DMN structures. This is a fundamental difference. By contrast to fMRI, the human intracerebral recordings we used provide a direct measure of neural activity, a millisecond temporal precision, and a signal quality that allows for trial-by-trial correlation analysis between neural activity and behaviour. These key differences lead to a radically different level of functional and physiological interpretation of the role of the DMN. Here's how each of these three key differences lead to unique achievement in our study:

1) We directly measured the neural basis of the DMN deactivation: by contrast to the BOLD signal measured in fMRI, which is only an indirect measure of neural activity, we directly recorded population neural activity. This allow us to unravel the neural basis of the DMN phenomenon and to rule out confounding factors that pose a challengue to fMRI studies of DMN goal-directed deactivation, such as vascular or metabolic changes (Pasley, Inglis, & Freeman, 2007) as well as cardiac and respiratory artefacts (Birn, Murphy, & Bandettini, 2008; Pasley et al., 2007) which can affect the BOLD signal.

2) DMN timing at a previously unattained precision: our study unravels DMN dynamics at a previously unprecedented temporal scale. This allowed us to determinate neural deactivation onset times (e.g. separation between VAN and DMN onsets) and duration across the full DMN network and correlate them with task complexity. This level of temporal resolution and the link it reveals with task-demands is unprecedented and only feasible with electrophysiology.
3) Trial-by-trial analyses reveal correlations between DMN deactivation and subject performance: our study benefited from the outstanding signal-to-noise ratio (SNR) of intracerebral electrode recordings. In combination with behavioural measures (such as reaction times) this high SNR of our recordings allowed us to perform trial-by-trial data analysis revealing, for the first time, a

significant correlation between DMN neural deactivation and subject performance on trial-to-trial basis.

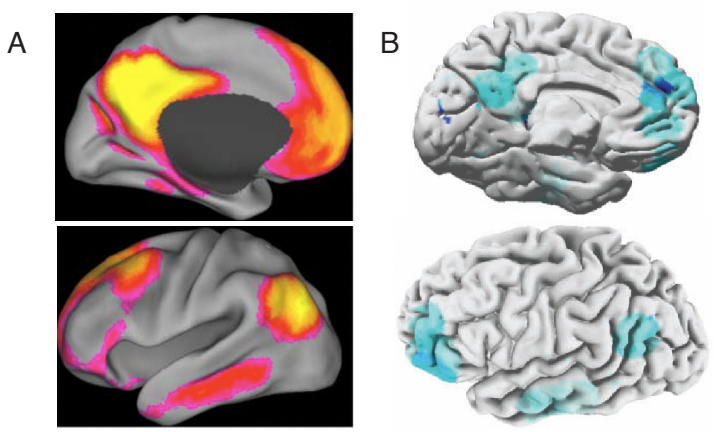

Figure 34: Metabolic and electrophysiological deactivation of the default mode network during goal-directed behavior. Comparison between BOLD deactivation (in red, from Gusnard & Raichle, 2001) and the brain-wide dynamics of Gamma-Band Deactivation (in blue, GBD) during visual search (b). We can observe that spatial properties of GBD bear a striking resemblance to DMN maps previously reported with fMRI (a).

In addition to the key points described above that differentiate our study from previous fMRI work, our manuscript represents a 'global' qualitative leap forward, compared to all previous DMN research: it provides the most complete and extensive study, to date, that probes the **neural basis of the DMN phenomenon and -critically- its relation with behavior**. The investigation of task-related modulation of frequency components in neural responses and trial-by-trial correlation analysis, with the level of combined temporal, spatial and spectral precision provided by our study, **cannot be achieved with any other technique** than the extensive invasive measurements reported in our manuscript.

The neural basis of DMN deactivation (especially broadband gamma suppression), the transient characteristics of task-related suppressions, and finally the relationship between DMN dynamics and behavior revealed by our study are all unprecedented and highlight the increasingly pivotal role that electrophysiological investigations will

play in understanding the function (and alteration by disease) of the DMN and more generally all so-called intrinsic or resting state networks.

In a very recent review by Northoff et al. published in Trends in Neurosciences (Northoff et al., 2010), entitled "Rest-stimulus interaction in the brain: a review", the authors end the review with the following statement: "Methodologically, most of the results described above *(i.e. 'Rest-Stimulus and stimulus-rest interaction in the brain')* rely on human imaging and more specifically on fMRI. However, because the BOLD response in fMRI is rather sluggish, clear-cut experimental separation between RSA and stimulus-induced activity changes can be difficult. Hence, techniques other than fMRI could be more suitable for RSA studies" (Northoff et al, TINS, 33, 277-284, 2010)."

The view expressed here by Northoff and colleagues in this recent review and shared by many scientists in the field is that a lot has been learned about resting state networks (including the default-mode) via fMRI studies, but that we have now come to a point where the next major advances in the field will need novel insights from electrophysiological assessments of these networks in order to fully elucidate their functional role and physiological basis.

7.3. Clinical implications of our first study

It should be noted that this work is framed in a clinical context, and the implantation of the electrodes has as principal objective to find the origin of the epileptic activity. In this sense, we think that the study of the DMN could be important for the understanding and the treatment of the epilepsy for three reasons:

a) Many patients report that their seizures often occur at the precise moment when attention is relaxed at the end of a demanding activity, such as driving or any form of intellectual work. The facts that this moment coincides with a sudden increase in the activity of the DMN (i.e. when the patients found the target) suggest a possible link between this network and the onset of crises, at least in some cases. This relationship has hardly

ever been studied until now (Laufs, Walker, & Lund, 2007), principally by our lack of understanding of the neural phenomena that occur in the DMN.

b) Second, because several neuroimaging studies have established a clear link between the activation of DMN and a state of 'decoupling' between the brain and its environment, called 'Mind Wandering' (Zacks, Speer, Swallow, Braver, & Reynolds, 2007), during which attention is no longer available to process the information from the outside world. Again, these phases of distraction are often observed in patients with epilepsy, especially in children. A disorganization of the DMN in some forms of epilepsy, even the influence of drugs on the network can be advanced. But again, only the study of neural activity within the DMN may allow progress in this line of research.

c) Finally, surgery for drug-resistant epilepsy is always preceded by a phase tracking to both, identify the epileptogenic network and to locate the near brain regions, still functional, that must be saved by surgery. This decision is now, in most cases, based in a procedure of intracerebral electrical stimulation, whose principle is to trigger behavioural manifestations, positive or negative, such as a temporary stopping of the speech (Afif, Minotti, Kahane, & Hoffmann, 2010). This procedure is not suitable to identify regions of the DMN, which by definition are silent. Then, the risk to include parts of this network still healthy in the surgical resection is high. Several studies have shown that a disruption of the DMN may lead to serious neurological and psychiatric disorders, ranging from depression to schizophrenia (Broyd et al., 2009). It is therefore desirable, even imperative to have a technique of anatomical tracing of the DMN, in the pre-surgical phase of epileptic patients.

In conclusion, the work done has allowed us to determine an experimental setting which can identify regions of the DMN in the pre-surgical phase with few constraints. We have shown that activity decreases in the DMN are sometimes fast (about 500 ms), and not always visible in fMRI. Therefore, we will adapt this framework to define a procedure faster and accurate to inform the clinical team the location of

DMN in each patient. This information would then tailor the surgery to limit its impact on the DMN.

7.4. Transient and sustained gamma bans responses

As stated in the third chapter, visual search (Treinsman and Gelade, 1980) has been a model task for investigating the operations of selective attention in crowded and unpredictable environments (Nobre et al, 2002). The mechanisms for selection targets during visual search remain under intensive discussion. According to one influential model (Treisman and Gelade, 1980), the visual search of basic features (such as colour, size, motion and orientation), occur in a single step and in parallel way across most of (or all) the visual field: that is, the duration of the search, quantified by the reaction times (RTs) of participants, is independent of the number of items displayed (Wolfe, 2003). On the other hand, search for a particular combination of features, requires that all the stimuli are processed sequentially, resulting in search duration which increase linearly with the number of items in the display.

The mechanisms for selecting targets with a particular combination of features (search) remain under intensive discussion. According to Treisman, serial deployment of attention to spatial locations is required to integrate components features of stimuli. Others have argued that the sloped RT functions during search do not necessary imply a serial mechanism. Instead, target detection may proceed via parallel neural computations that take longer to resolve with interference from increasing number of distractor stimuli (Duncan and Humphreys, 1989; Nobre et al, 2002). Finally, some have suggested that a combination of parallel and serial mechanisms is required for selecting targets from interfering displays (Wolfe, 1993, 2003).

A novel lecture of neural mechanisms of visual attention (Desimone & Duncan, 1995a) proposes that both visual pop-out tasks and active search tasks would involve bottom-up and top-down neural mechanisms, and that these mechanisms would enable to differentiate the target from a background made of the distractors.

This model of attention, named Biased Competition theory (BC, Desimone and

Duncan, 1995), suggests that neuronal responses are determined by competitive interactions. A central assumption of the BC account is that visual input elicits activity, in parallel, in several areas of the brain, each of which is specialized for the analysis of different stimulus attributes, e.g. shape, color or motion. Selection for further processing of a certain object is achieved by the integration of competitive activity across multiple areas. This selection is, however, not achieved by competition of independent objects. Rather, features of the same object reinforce each other while suppressing activations of other objects, thus forming a stable state of activations belonging to one object over a time course of several hundred milliseconds. Concerning selection mechanisms in visual search, the biased competition account proposes two main sources of attentional control: stimulus-driven (’bottom-up’) information from stimuli presented in the scene and ’top-down’ feedback mechanisms that arise from current behavioral goals (Desimone & Duncan, 1995). The latter gain influence by (a) increasing the maintained activity of visual cortical neurons or by (b) an increase in sensory-evoked responses. Further, competition of object features can be modulated independent of spatial constraints: Processing can be biased in favor of stimuli possessing a specific characteristic (e.g., colour, shape, etc.) in parallel throughout the visual field as well as occupying a specific spatial location (e.g. made relevant by task instruction, in our case searching for a gray letter ‘T’ amongst gray or black ‘L’s). However, competition between two stimuli is assumed to be strongest when the two stimuli are at the same location and, thus, activate cells in the same local region of cortex (Desimone, 1998). The biased competition approach has been influential particularly with regard to mechanisms that might underlie neglect or other neuropsychological deficits of attention (Mahn, 2005).

In short, this theory has these assumptions: given the limits of our ability to process several stimuli simultaneously, visual objects compete for representational resources, and only one or a small number of stimuli can be represented at one time. As the neural representations of visual stimuli are highly distributed, competitive processing occurs in many of the brain areas sensitive to visual inputs. Second, the competition would integrate across several areas, such that the neural populations that represent different aspects of a single object interact in a mutually facilitatory fashion. The gain in response to the selected object is accompanied by a suppression of the processes in the neural populations representing features of competing objects. Therefore, as a

'winner' emerges in one system, the same object becomes dominant across the distributed network (see also (Kanwisher & Wojciulik, 2000a)). This way, the principal difference between a visual pop-out and top-down neural mechanisms would be in the space and the time where this competition would occur (a extensive review about the localization of bottom-up and top-down networks activities was published recently (Corbetta & Shulman, 2002b)).

As we have seen in the second paper presented in this dissertation, our criterion to separate bottom-up of top-down processes was related with the temporal characteristics of responses, in the broadband gamma-band responses (GBR). When the activity of each trial was transient and only dependent to the onset of visual stimuli (and not related to the trial's duration), the electrodes were classified as bottom-up. In contrast, when the duration of GBR was related to the task processing (GBR sustained), we assumed that the activity reflect a top-down processing. We can see in the next figure these two types of responses.

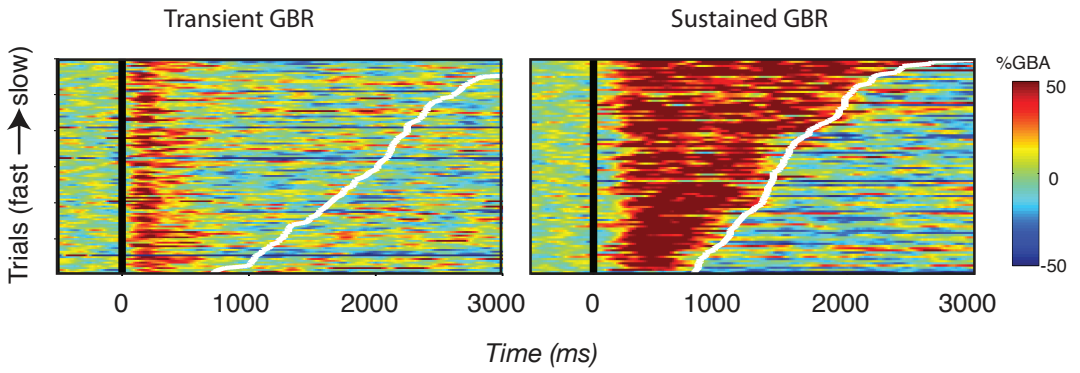

Figure 35: transient vs. sustained gamma band responses. We represent here the two main types of GBRs for the same task (difficult visual search). While latency of transient GBR (left panel) is not related with the searching time (RTs are plotted in white), duration of the GBR in sustained contacts is time-dependent (right panel).

How shall we understand those results? If we see the map presented before (in complement to Figure 3 of the second article) we can conclude two principal ideas: first, while the transients responses were highly concentrated in the occipital and temporal lobe, sustained responses are widespread across several regions, but principally grouped in the frontal lobe. Second, the brain regions implicated in both

pop-out and visual search condition are practically the same. This result is consistent with Desimone and Duncan's theory, in the sense that both visual pop-out and active search tasks would involve bottom-up and top-down neural mechanism[1] (Desimone and Duncan, 1995). Several studies revealed an extensive overlap in the brain areas involved in both visual searches, in special posterior parietal and visual areas. Nevertheless, active visual search would activate parietal and visual areas more strongly than visual pop-out search (Leonards et al., 2000). Our results are in accord with the first assumption (overlap in the brain areas involved in both visual searches). In contrast, and as we can see in Figure 2 and 3 of the second paper, the pop-out condition elicit a strongly activation in parietal areas related to search condition. We can see the same effect in the some contacts located in the occipital and temporal lobe. Our interpretation of these results is that normally, and principally by methodological constraints, we take a grand average across large neuronal populations, with multiple types of responses (i.e. EEG and ECoG recordings). Then, if a subgroup of neurons responds in a sustained form (as we can see in figure 2, there are some contacts with this type of GBR in the occipital lobe, especially located in V3 and V4), the difference in favour of the second type of visual search will be only the reflex of this subgroup. Interestingly, left intra-parietal sulcus was the only brain regions where the GBR is only specific for the pop-out condition. This result is according with literature, in the sense of that spatial orientation becomes more relevant for this condition (the question in the task was: Where is the gray letter 'T'?) (Pessoa et al, 2009 Brain Res; Kristjánsson, 2007 C Cortex). In contrast, this process of spatial orientation becomes relevant only after finding the target in the second condition (active search). For this reasons, activation can be spread over time in this region.

On the other side, our results about the sites with sustained GBRs were consistent with the existing literature on the role of prefrontal cortex in attention. Task –related sites (GBR sustained) in both experimental conditions are spread out through several

1

We use the terms *bottom up* and *top down* to refer to the perspectives in which dynamics of visual processing is task independent or task dependent, respectively. Bottom up simply implies that processing is guided from the outside world, and top down implies that processing is guided from higher cortical regions.

frontal regions: Anterior cingulate cortex, midline frontal cortex, dorsolateral prefrontal cortex, as well as supplementary motor area. According with Posner and Peterson (1990), these areas could form the 'anterior attention system', known to be particularly involved in target detection.

Another implication that reinforces our results is that parietal and frontal cortex are evidently involved in pop-out searches. Within psychology and the behavioral literature, processing of pop-out stimuli was traditionally thought to be strictly 'preattentive' (e.g. Treisman & Gelade, 1980), rather than to involve attentional mechanisms as indicated here. More recent behavioral work had suggested possible attentional involvement in pop-out (see, for example discussion in Nakayama & Joseph, 1998), though some controversies still exist concerning this (e.g. Donner et al. 2005). Our findings provide unequivocal new evidence that the neural substrates underlying modulation of visual search for pop-out targets by repetition do in fact involve some of the parietal and frontal areas long implicated in attention control.

Finally, to elucidate if the difference between activities in both task was not related simply to the time of processing, we compare the GBRs for trials with the same reaction times of the two experimental conditions. Surprisingly, in most of the trials (90%) GBR does not allow differentiating between both conditions. Interestingly, in one of the exceptions, the left and right DLPFC, the pattern of GBR is bimodal. GBR is related is stimulus-related in the pop-out condition, while is task-related for the search condition, as shown in the next figure.

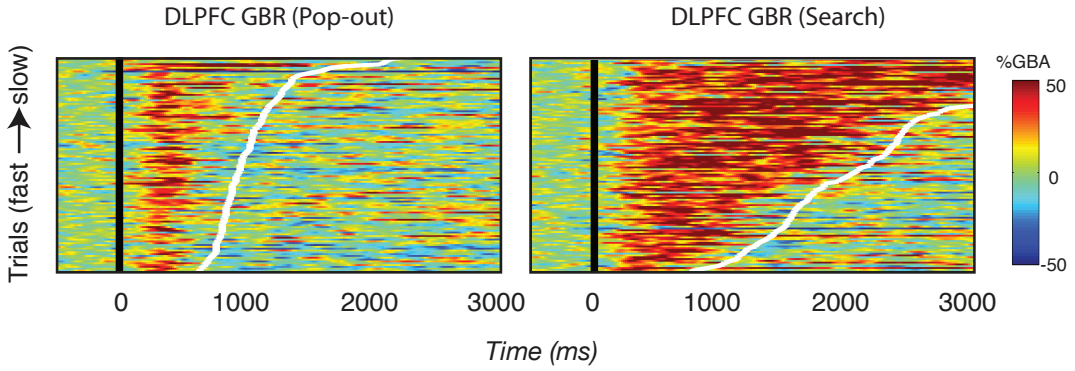

Figure 36: Bimodal GBR in DLPFC. While GBR is transient for the pop-out condition, GBR is task-related in the search condition in an electrode located in the left DLPFC of patient 3.

Summarizing, our results show that is possible to differentiate two types of responses during a goal directed task: a transient and sustained. These responses could reflect a marker of the two major ways of neural processing, bottom-up and top-down. As we have said repeatedly, these processing pathways have been studied mainly in two scales. While the microscale reflect the activity of a small neuronal population, the macroscale reflect: the metabolic activity of a brain region with high-spatial and low-temporal resolution (PET and fMRI) or the electric or magnetic (EEG and MEG) fields reflected the temporal evolution of a collective response from millions of neurons on a millisecond scale (low spatial resolution). The intermediate level of recording (LFP) used during this work, could explain the gap between the two scales.

Finally, our results suggest that new models of attention may be required, based on temporally coherent or in the temporal dynamics of neural activity rather than neural amplification (Niebur et al., 2002). Is difficult to explain this results using standard models of attention that rely solely on gain-based changes, or even on gain/spectral-sensitivity hybrid models (Okamoto et al., 2007). Alternatively, a more arguable theory of neural mechanisms underlying the role of top-down attention in the buildup of perceptual streams would involve top-down projections acting in conjunction with the physical stimulus as regulators or clocks for the firing patterns of neuronal

populations in visual cortex that present sustained responses (Elhieali, 2009). The neural support of this bottom-up/top-down interaction are likely to mediate changes in the response profiles of cortical neurons, via mechanisms of synaptic and receptive field plasticity which have been shown to be gated by attention; whereby attention plays a crucial role in shifting cortical circuits from one state to another depending on behavioral demands (Fritz, Elhilali, & Shamma, 2005). We speculate that temporal patterns of neuronal firings are crucial in any goal-directed task to resolve the competition between attended and unattended objects, hence, delimiting the cognitive border between different streams.

7.5. Conclusion:

During this dissertation, our goal was two-fold. The first main objective was to find the neural correlate of the task-related deactivation across the default-mode network (DMN) and its relation with several markers of task engagement, such as performance. The second main objective was to study with a high temporal and spatial resolution the bottom-up and top-down components of a visual search, using unprecedented brain-wide intracerebral depth recordings in surgical patients.

The role of DMN deactivation remains enigmatic because its electrophysiological correlates, temporal dynamics and link to behavior are poorly understood. Using extensive depth electrode recordings in humans, we provide electrophysiological evidence for a direct correlation between DMN neural deactivation dynamics and individual subject behavior. We found that all DMN areas displayed transient suppressions of gamma (60-140 Hz) power during task performance and, critically, the duration and extent of this broadband suppression were correlated with task complexity and subject performance. Furthermore, trial-by-trial correlations revealed that spatially distributed gamma activations and deactivations formed distinct anticorrelated networks. These findings facilitate our understanding of the relationship between electrophysiology and neuroimaging studies in humans and indicate that neural deactivations encode the duration and efficiency of our engagement with the external world.

By the other hand, findings from neuroimaging that cognitive tasks involve a number of different anatomical areas has led to an emphasis on tracing the time dynamics of these areas. Because shifts of attention can be so rapid, it is difficult to follow them with hemodynamic imaging. For this reason, the principal objective of the second article was to distinguish transient neural responses elicited by stimuli properties (bottom-up), from sustained responses elicited by intrinsic modulations (top-down). While the transient responses were highly focalized in the occipital and temporal lobe, sustained responses are widespread across several regions, but primarily localized in the frontal lobe. During this dissertation, we have used an adaptation of a classical visual search task, developed by Triesmann and Gelade in 1980. As we have said, the use of this task was not haphazard. Using this task, we can control easily the level of difficulty, the brain regions implicated have been well studied, and principally, we can compare two models of visual search, contrasting essentially the parallel search for a single and salient feature with a sequential visual search. The brain regions implicated in both pop-out and visual search condition are practically the same. Several studies revealed an extensive overlap in the brain areas involved in both visual searches, in special posterior parietal and visual areas. Together, these findings support a view of a tightly coupled interaction between the lower-level neural representation and the higher-level cognitive representation of visual objects (Elihaly et al., 2009).

Finalizing, the findings revealed during this dissertation reinforces the idea of the pivotal role for broadband gamma modulations in the interplay between activation and deactivation networks mediating efficient goal-directed behavior. In this sense, the next logical step is to investigate the interaction between these two phenomena.

Bibliography

Adrian ED: Afferent discharges to the cerebral cortex from peripheral sense organs. J Physiol 100:159-191, 1941.

Afif A, Minotti L, Kahane P, et al.: Middle short gyrus of the insula implicated in speech production: intracerebral electric stimulation of patients with epilepsy. Epilepsia 51:206-213, 2010.

Andreasen NC, O'Leary DS, Cizadlo T, et al.: Remembering the past: two facets of episodic memory explored with positron emission tomography. Am J Psychiatry 152:1576-1585, 1995.

Andrews-Hanna JR, Reidler JS, Huang C, et al.: Evidence for the default network's role in spontaneous cognition. J Neurophysiol 104:322-335.

Aoki F, Fetz EE, Shupe L, et al.: Increased gamma-range activity in human sensorimotor cortex during performance of visuomotor tasks. Clin Neurophysiol 110:524-537, 1999.

Baddeley A: Working memory: looking back and looking forward. Nat Rev Neurosci 4:829-839, 2003.

Berger H: Über das Elektrenkephalogramm des Menschen. Arch. Psychiatr. Nervenkr 87:527–570, 1929.

Bichot NP, Rossi AF, Desimone R: Parallel and serial neural mechanisms for visual search in macaque area V4. Science 308:529-534, 2005.

Bichot NP, Desimone R: Finding a face in the crowd: parallel and serial neural mechanisms of visual selection. Prog Brain Res 155:147-156, 2006.

Binder JR, Frost JA, Hammeke TA, et al.: Conceptual processing during the conscious resting state. A functional MRI study. J Cogn Neurosci 11:80-95, 1999.

Birn RM, Murphy K, Bandettini PA: The effect of respiration variations on independent component analysis results of resting state functional connectivity. Human Brain Mapping 29:740-750, 2008.

Biswal B, Yetkin FZ, Haughton VM, et al.: Functional connectivity in the motor cortex of resting human brain using echo-planar MRI. Magn Reson Med 34:537-541, 1995.

Biswal BB, Mennes M, Zuo XN, et al.: Toward discovery science of human brain function. Proceedings of the National Academy of Sciences of the United States of America 107:4734-4739, 2010.

Bouyer JJ, Dedet L, Konya A: [Convergence of 3 thalamo-cortical rhythmic systems on the somesthetic area in the normal cat and baboon]. Rev Electroencephalogr Neurophysiol Clin 4:397-406, 1974.

Bouyer JJ, Montaron MF, Rougeul A: Fast fronto-parietal rhythms during combined focused attentive behaviour and immobility in cat: cortical and thalamic localizations. Electroencephalogr Clin Neurophysiol 51:244-252, 1981.

Brovelli A, Lachaux JP, Kahane P, et al.: High gamma frequency oscillatory activity dissociates attention from intention in the human premotor cortex. Neuroimage 28:154-164, 2005.

Brown GG, Eyler LT: Methodological and conceptual issues in functional magnetic resonance imaging: applications to schizophrenia research. Annu Rev Clin Psychol 2:51-81, 2006.

Brown TG: On the nature of the fundamental activity of the nervous centres; together with an analysis on the conditioning rhythmic activity in progression, and a theory of the evolution of function in the nervous systems. Proc. Amer. Phil. Soc. L:19-44, 1911.

Broyd SJ, Demanuele C, Debener S, et al.: Default-mode brain dysfunction in mental disorders: a systematic review. Neurosci Biobehav Rev 33:279-296, 2009.

Buckner RL, Carroll DC: Self-projection and the brain. Trends Cogn Sci 11:49-57, 2007.

Buckner RL, Andrews-Hanna JR, Schacter DL: The brain's default network: anatomy, function, and relevance to disease. Ann N Y Acad Sci 1124:1-38, 2008.

Burdette JH, Durden DD, Elster AD, et al.: High b-value diffusion-weighted MRI of normal brain. J Comput Assist Tomogr 25:515-519, 2001.

Burgess PW, Dumontheil I, Gilbert SJ: The gateway hypothesis of rostral prefrontal cortex (area 10) function. Trends Cogn Sci 11:290-298, 2007.

Buzsaki G, Draguhn A: Neuronal oscillations in cortical networks. Science 304:1926-1929, 2004.

Canolty RT, Edwards E, Dalal SS, et al.: High gamma power is phase-locked to theta oscillations in human neocortex. Science 313:1626-1628, 2006.

Castellanos FX, Margulies DS, Kelly C, et al.: Cingulate-precuneus interactions: A new locus of dysfunction in adult attention-deficit/hyperactivity disorder. Biological Psychiatry 63:332-337, 2008.

Cavada C, Goldman-Rakic PS: Posterior parietal cortex in rhesus monkey: II. Evidence for segregated corticocortical networks linking sensory and limbic areas with the frontal lobe. J Comp Neurol 287:422-445, 1989.

Cavanna AE, Trimble MR: The precuneus: a review of its functional anatomy and behavioural correlates. Brain 129:564-583, 2006.

Corbetta M, Shulman GL: Control of goal-directed and stimulus-driven attention in the brain. Nat Rev Neurosci 3:201-215, 2002a.

Corbetta M, Shulman GL: Control of goal-directed and stimulus-driven attention in the brain. Nature Reviews Neuroscience 3:201-215, 2002b.

Corbetta M, Patel G, Shulman GL: The reorienting system of the human brain: From environment to theory of mind. Neuron 58:306-324, 2008.

Crone NE, Miglioretti DL, Gordon B, et al.: Functional mapping of human sensorimotor cortex with electrocorticographic spectral analysis. II. Event-related synchronization in the gamma band. Brain 121 (Pt 12):2301-2315, 1998.

Crone NE, Miglioretti DL, Gordon B, et al.: Functional mapping of human sensorimotor cortex with electrocorticographic spectral analysis. I. Alpha and beta event-related desynchronization. Brain 121 (Pt 12):2271-2299, 1998.

Crone NE: Functional mapping with ECoG spectral analysis. Adv Neurol 84:343-351, 2000.

Crone NE, Boatman D, Gordon B, et al.: Induced electrocorticographic gamma activity during auditory perception. Brazier Award-winning article, 2001. Clin Neurophysiol 112:565-582, 2001.

Crone NE, Hao L, Hart J, Jr., et al.: Electrocorticographic gamma activity during word production in spoken and sign language. Neurology 57:2045-2053, 2001.

Crone NE, Sinai A, Korzeniewska A: High-frequency gamma oscillations and human brain mapping with electrocorticography. Prog Brain Res 159:275-295, 2006.

D'Argembeau A, Collette F, Van der Linden M, et al.: Self-referential reflective activity and its relationship with rest: a PET study. Neuroimage 25:616-624, 2005.

D'Argembeau A, Stawarczyk D, Majerus S, et al.: The neural basis of personal goal processing when envisioning future events. J Cogn Neurosci 22:1701-1713, 2010.

Dandekar S, Ales J, Carney T, et al.: Methods for quantifying intra- and inter-subject variability of evoked potential data applied to the multifocal visual evoked potential. J Neurosci Methods 165:270-286, 2007.

Desimone R, Duncan J: Neural Mechanisms of Selective Visual-Attention. Annual Review of Neuroscience 18:193-222, 1995a.

Desimone R, Duncan J: Neural mechanisms of selective visual attention. Annu Rev Neurosci 18:193-222, 1995b.

Diaz J, Razeto-Barry P, Letelier JC, et al.: Amplitude modulation patterns of local field potentials reveal asynchronous neuronal populations. J Neurosci 27:9238-9245, 2007.

Doron G, Moulding R: Cognitive behavioral treatment of obsessive compulsive disorder: a broader framework. Isr J Psychiatry Relat Sci 46:257-263, 2009.

Egeth HE, Yantis S: Visual attention: control, representation, and time course. Annu Rev Psychol 48:269-297, 1997.

Elhilali M, Xiang J, Shamma SA, et al.: Interaction between attention and bottom-up saliency mediates the representation of foreground and background in an auditory scene. PLoS Biol 7:e1000129, 2009.

Engel AK, Roelfsema PR, Fries P, et al.: Role of the temporal domain for response selection and perceptual binding. Cereb Cortex 7:571-582, 1997.

Engel AK, Fries P, Singer W: Dynamic predictions: oscillations and synchrony in top-down processing. Nat Rev Neurosci 2:704-716, 2001.

Engell AD, McCarthy G: Selective attention modulates face-specific induced gamma oscillations recorded from ventral occipitotemporal cortex. J Neurosci 30:8780-8786, 2010.

Esposito F, Bertolino A, Scarabino T, et al.: Independent component model of the default-mode brain function: Assessing the impact of active thinking. Brain Res Bull 70:263-269, 2006.

Fan J, McCandliss BD, Fossella J, et al.: The activation of attentional networks. Neuroimage 26:471-479, 2005.

Fox MD, Snyder AZ, Vincent JL, et al.: The human brain is intrinsically organized into dynamic, anticorrelated functional networks. Proc Natl Acad Sci U S A 102:9673-9678, 2005.

Fox MD, Corbetta M, Snyder AZ, et al.: Spontaneous neuronal activity distinguishes human dorsal and ventral attention systems. Proc Natl Acad Sci U S A 103:10046-10051, 2006.

Fox PT, Raichle ME: Focal physiological uncoupling of cerebral blood flow and oxidative metabolism during somatosensory stimulation in human subjects. Proc Natl Acad Sci U S A 83:1140-1144, 1986.

Fransson P: Spontaneous low-frequency BOLD signal fluctuations: an fMRI investigation of the resting-state default mode of brain function hypothesis. Hum Brain Mapp 26:15-29, 2005.

Fransson P: How default is the default mode of brain function? Further evidence from intrinsic BOLD signal fluctuations. Neuropsychologia 44:2836-2845, 2006.

Fries P, Roelfsema PR, Engel AK, et al.: Synchronization of oscillatory responses in visual cortex correlates with perception in interocular rivalry. Proc Natl Acad Sci U S A 94:12699-12704, 1997.

Fries P, Reynolds JH, Rorie AE, et al.: Modulation of oscillatory neuronal synchronization by selective visual attention. Science 291:1560-1563, 2001.

Fries P: A mechanism for cognitive dynamics: neuronal communication through neuronal coherence. Trends Cogn Sci 9:474-480, 2005.

Fries P: Neuronal Gamma-Band Synchronization as a Fundamental Process in Cortical Computation. Annual Review of Neuroscience 32:209-224, 2009.

Friston KJ, Frith CD, Liddle PF, et al.: Functional connectivity: the principal-component analysis of large (PET) data sets. J Cereb Blood Flow Metab 13:5-14, 1993.

Frith CD, Frith U: Interacting minds--a biological basis. Science 286:1692-1695, 1999.

Fritz JB, Elhilali M, Shamma SA: Differential dynamic plasticity of A1 receptive fields during multiple spectral tasks. J Neurosci 25:7623-7635, 2005.

Genovese CR, Lazar NA, Nichols T: Thresholding of statistical maps in functional neuroimaging using the false discovery rate. Neuroimage 15:870-878, 2002.

Giambra LM: A laboratory method for investigating influences on switching attention to task-unrelated imagery and thought. Conscious Cogn 4:1-21, 1995.

Gilbert SJ, Dumontheil I, Simons JS, et al.: Comment on "Wandering minds: the default network and stimulus-independent thought". Science 317:43; author reply 43, 2007.

Gray CM, Konig P, Engel AK, et al.: Oscillatory responses in cat visual cortex exhibit inter-columnar synchronization which reflects global stimulus properties. Nature 338:334-337, 1989.

Greicius MD, Krasnow B, Reiss AL, et al.: Functional connectivity in the resting brain: a network analysis of the default mode hypothesis. Proc Natl Acad Sci U S A 100:253-258, 2003.

Greicius MD, Supekar K, Menon V, et al.: Resting-state functional connectivity reflects structural connectivity in the default mode network. Cereb Cortex 19:72-78, 2009.

Gruber T, Muller MM, Keil A, et al.: Selective visual-spatial attention alters induced gamma band responses in the human EEG. Clin Neurophysiol 110:2074-2085, 1999.

Gujar N, Yoo SS, Hu P, et al.: The unrested resting brain: sleep deprivation alters activity within the default-mode network. J Cogn Neurosci 22:1637-1648.

Gusnard DA, Akbudak E, Shulman GL, et al.: Medial prefrontal cortex and self-referential mental activity: relation to a default mode of brain function. Proc Natl Acad Sci U S A 98:4259-4264, 2001.

Gusnard DA, Raichle ME: Searching for a baseline: functional imaging and the resting human brain. Nat Rev Neurosci 2:685-694, 2001.

Haxby JV, Horwitz B, Ungerleider LG, et al.: The functional organization of human extrastriate cortex: a PET-rCBF study of selective attention to faces and locations. J Neurosci 14:6336-6353, 1994.

Hayden BY, Smith DV, Platt ML: Electrophysiological correlates of default-mode processing in macaque posterior cingulate cortex. Proc Natl Acad Sci U S A 106:5948-5953, 2009.

He BJ, Snyder AZ, Zempel JM, et al.: Electrophysiological correlates of the brain's intrinsic large-scale functional architecture. Proc Natl Acad Sci U S A 105:16039-16044, 2008.

Herculano-Houzel S, Munk MH, Neuenschwander S, et al.: Precisely synchronized oscillatory firing patterns require electroencephalographic activation. J Neurosci 19:3992-4010, 1999.

Hikosaka O, Wurtz RH: Visual and oculomotor functions of monkey substantia nigra pars reticulata. I. Relation of visual and auditory responses to saccades. J Neurophysiol 49:1230-1253, 1983.

Howard MW, Rizzuto DS, Caplan JB, et al.: Gamma oscillations correlate with working memory load in humans. Cereb Cortex 13:1369-1374, 2003.

Huettel SA, Song AW, McCarthy G: Functional Magnetic Resonance Imaging: Sinauer Associates, 2008.

Ingvar DH: "Hyperfrontal" distribution of the cerebral grey matter flow in resting wakefulness; on the functional anatomy of the conscious state. Acta Neurol Scand 60:12-25, 1979.

Jacobs J, Kahana MJ, Ekstrom AD, et al.: Brain oscillations control timing of single-neuron activity in humans. J Neurosci 27:3839-3844, 2007.

Jacobs J, Kahana MJ: Direct brain recordings fuel advances in cognitive electrophysiology. Trends Cogn Sci 14:162-171, 2010.

Jensen O, Kaiser J, Lachaux JP: Human gamma-frequency oscillations associated with attention and memory. Trends Neurosci 30:317-324, 2007.

Jerbi K, Ossandon T, Hamame CM, et al.: Task-related gamma-band dynamics from an intracerebral perspective: review and implications for surface EEG and MEG. Hum Brain Mapp 30:1758-1771, 2009.

Jerbi K, Vidal JR, Ossandon T, et al.: Exploring the electrophysiological correlates of the default-mode network with intracerebral EEG. Frontiers in Systems Neuroscience 4:5, 2010.

Jung J, Hudry J, Ryvlin P, et al.: Functional significance of olfactory-induced oscillations in the human amygdala. Cereb Cortex 16:1-8, 2006.

Jung J, Mainy N, Kahane P, et al.: The neural bases of attentive reading. Hum Brain Mapp 29:1193-1206, 2008.

Kanwisher N, Wojciulik E: Visual attention: Insights from brain imaging. Nature Reviews Neuroscience 1:91-100, 2000a.

Kanwisher N, Wojciulik E: Visual attention: insights from brain imaging. Nat Rev Neurosci 1:91-100, 2000b.

Konig P, Engel AK, Singer W: Relation between oscillatory activity and long-range synchronization in cat visual cortex. Proc Natl Acad Sci U S A 92:290-294, 1995.

Lachaux JP, Rodriguez E, Martinerie J, et al.: A quantitative study of gamma-band activity in human intracranial recordings triggered by visual stimuli. Eur J Neurosci 12:2608-2622, 2000.

Lachaux JP, Rudrauf D, Kahane P: Intracranial EEG and human brain mapping. Journal of Physiology-Paris 97:613-628, 2003a.

Lachaux JP, Rudrauf D, Kahane P: Intracranial EEG and human brain mapping. J Physiol Paris 97:613-628, 2003b.

Lachaux JP, George N, Tallon-Baudry C, et al.: The many faces of the gamma band response to complex visual stimuli. Neuroimage 25:491-501, 2005.

Lachaux JP, Hoffmann D, Minotti L, et al.: Intracerebral dynamics of saccade generation in the human frontal eye field and supplementary eye field. Neuroimage 30:1302-1312, 2006.

Lachaux JP, Fonlupt P, Kahane P, et al.: Relationship between task-related gamma oscillations and BOLD signal: New digits from combined fMRI and intracranial EEG. Human Brain Mapping 28:1368-1375, 2007.

Lachaux JP, Jerbi K, Bertrand O, et al.: A blueprint for real-time functional mapping via human intracranial recordings. PLoS ONE 2:e1094, 2007.

Lachaux JP, Jung J, Mainy N, et al.: Silence is golden: transient neural deactivation in the prefrontal cortex during attentive reading. Cereb Cortex 18:443-450, 2008.

Lachaux JP, Ossandon T: Intracortical recordings during attentional tasks, in From attention to goal-directed behavior: neurodynamical, methodological and clinical trends. Edited by Aboitiz F, Cosmelli D. Berlin, Springer, 2008, pp. 29-49.

Lachaux JP, Ossandon T: Intracortical recordings during attentional tasks, in From attention to goal-directed behavior: neurodynamical, methodological and clinical trends. Edited by Aboitiz F, Cosmelli D. Berlin, Springer, 2009, pp. 29-49.

Laufs H, Krakow K, Sterzer P, et al.: Electroencephalographic signatures of attentional and cognitive default modes in spontaneous brain activity fluctuations at rest. Proc Natl Acad Sci U S A 100:11053-11058, 2003.

Laufs H, Walker MC, Lund TE: 'Brain activation and hypothalamic functional connectivity during human non-rapid eye movement sleep: an EEG/fMRI study'--its limitations and an alternative approach. Brain 130:e75; author reply e76, 2007.

Le Van Quyen M, Staba R, Bragin A, et al.: Large-scale microelectrode recordings of high-frequency gamma oscillations in human cortex during sleep. J Neurosci 30:7770-7782.

Le Van Quyen M, Foucher J, Lachaux JP, et al.: Comparison of Hilbert transform and wavelet methods for the analysis of neuronal synchrony. Journal of Neuroscience Methods 111:83-98, 2001.

Leichnetz GR: Connections of the medial posterior parietal cortex (area 7m) in the monkey. Anat Rec 263:215-236, 2001.

Leonards U, Singer W: Conjunctions of colour, luminance and orientation: the role of colour and luminance contrast on saliency and proximity grouping in texture segregation. Spat Vis 13:87-105, 2000.

Leopold DA, Murayama Y, Logothetis NK: Very slow activity fluctuations in monkey visual cortex: implications for functional brain imaging. Cereb Cortex 13:422-433, 2003.

Lettvin JY, Maturana HR, McCulloch WS, et al.: What the frog's eye tells the frog's brain. Proc. Inst. Radio Engr 47:140-1951, 1959.

Logothetis NK, Pauls J, Augath M, et al.: Neurophysiological investigation of the basis of the fMRI signal. Nature 412:150-157, 2001.

Lowe MJ, Mock BJ, Sorenson JA: Functional connectivity in single and multislice echoplanar imaging using resting-state fluctuations. Neuroimage 7:119-132, 1998.

Mainy N, Jung J, Baciu M, et al.: Cortical dynamics of word recognition. Hum Brain Mapp, 2007.

Mainy N, Kahane P, Minotti L, et al.: Neural correlates of consolidation in working memory. Hum Brain Mapp 28:183-193, 2007.

Mangun GR, Buonocore MH, Girelli M, et al.: ERP and fMRI measures of visual spatial selective attention. Hum Brain Mapp 6:383-389, 1998.

Manning JR, Jacobs J, Fried I, et al.: Broadband Shifts in Local Field Potential Power Spectra Are Correlated with Single-Neuron Spiking in Humans. Journal of Neuroscience 29:13613-13620, 2009.

Mantini D, Perrucci MG, Del Gratta C, et al.: Electrophysiological signatures of resting state networks in the human brain. Proc Natl Acad Sci U S A 104:13170-13175, 2007.

Maquet P: Positron emission tomography studies of sleep and sleep disorders. J Neurol 244:S23-28, 1997.

Marin G, Mpodozis J, Sentis E, et al.: Oscillatory bursts in the optic tectum of birds represent re-entrant signals from the nucleus isthmi pars parvocellularis. J Neurosci 25:7081-7089, 2005.

Mason MF, Norton MI, Van Horn JD, et al.: Wandering minds: the default network and stimulus-independent thought. Science 315:393-395, 2007.

McGuire PK, Paulesu E, Frackowiak RS, et al.: Brain activity during stimulus independent thought. Neuroreport 7:2095-2099, 1996.

McKiernan KA, Kaufman JN, Kucera-Thompson J, et al.: A parametric manipulation of factors affecting task-induced deactivation in functional neuroimaging. J Cogn Neurosci 15:394-408, 2003.

McKiernan KA, D'Angelo BR, Kaufman JN, et al.: Interrupting the "stream of consciousness": an fMRI investigation. Neuroimage 29:1185-1191, 2006.

Miller KJ, Weaver KE, Ojemann JG: Direct electrophysiological measurement of human default network areas. Proc Natl Acad Sci U S A 106:12174-12177, 2009.

Miller KJ: Broadband spectral change: evidence for a macroscale correlate of population firing rate? J Neurosci 30:6477-6479, 2010.

Minoshima S, Giordani B, Berent S, et al.: Metabolic reduction in the posterior cingulate cortex in very early Alzheimer's disease. Ann Neurol 42:85-94, 1997.

Moran J, Desimone R: Selective attention gates visual processing in the extrastriate cortex. Science 229:782-784, 1985.

Moran JM, Lee SM, Gabrieli JD: Dissociable Neural Systems Supporting Knowledge about Human Character and Appearance in Ourselves and Others. J Cogn Neurosci, 2010.

Mukamel R, Gelbard H, Arieli A, et al.: Coupling between neuronal firing, field potentials, and FMRI in human auditory cortex. Science 309:951-954, 2005.

Muller MM, Gruber T, Keil A: Modulation of induced gamma band activity in the human EEG by attention and visual information processing. Int J Psychophysiol 38:283-299, 2000.

Niebur E, Hsiao SS, Johnson KO: Synchrony: a neuronal mechanism for attentional selection? Curr Opin Neurobiol 12:190-194, 2002.

Niessing J, Ebisch B, Schmidt KE, et al.: Hemodynamic signals correlate tightly with synchronized gamma oscillations. Science 309:948-951, 2005.

Nir Y, Fisch L, Mukamel R, et al.: Coupling between neuronal firing rate, gamma LFP, and BOLD fMRI is related to interneuronal correlations. Curr Biol 17:1275-1285, 2007.

Northoff G, Qin P, Nakao T: Rest-stimulus interaction in the brain: a review. Trends Neurosci 33:277-284, 2010.

Ogawa S, Tank DW, Menon R, et al.: Intrinsic signal changes accompanying sensory stimulation: functional brain mapping with magnetic resonance imaging. Proc Natl Acad Sci U S A 89:5951-5955, 1992.

Okamoto H, Stracke H, Wolters CH, et al.: Attention improves population-level frequency tuning in human auditory cortex. J Neurosci 27:10383-10390, 2007.

Ottoson D: Analysis of the electrical activity of the olfactory epithelium. Acta Physiol Scand Suppl 35:1-83, 1955.

Pardo JV, Pardo PJ, Raichle ME: Neural correlates of self-induced dysphoria. Am J Psychiatry 150:713-719, 1993.

Pasley BN, Inglis BA, Freeman RD: Analysis of oxygen metabolism implies a neural origin for the negative BOLD response in human visual cortex. Neuroimage 36:269-276, 2007.

Posner MI, Petersen SE: The attention system of the human brain. Annu Rev Neurosci 13:25-42, 1990.

Price CJ: The anatomy of language: contributions from functional neuroimaging. J Anat 197 Pt 3:335-359, 2000.

Raichle ME, MacLeod AM, Snyder AZ, et al.: A default mode of brain function. Proc Natl Acad Sci U S A 98:676-682, 2001.

Raichle ME, Mintun MA: Brain work and brain imaging. Annual Review of Neuroscience 29:449-476, 2006.

Raichle ME, Snyder AZ: A default mode of brain function: a brief history of an evolving idea. Neuroimage 37:1083-1090; discussion 1097-1089, 2007.

Raichle ME: A Paradigm Shift in Functional Brain Imaging. Journal of Neuroscience 29:12729-12734, 2009.

Raichle ME: Two views of brain function. Trends Cogn Sci 14:180-190, 2010.

Reynolds JH, Chelazzi L: Attentional modulation of visual processing. Annu Rev Neurosci 27:611-647, 2004.

Ries ML, Schmitz TW, Kawahara TN, et al.: Task-dependent posterior cingulate activation in mild cognitive impairment. Neuroimage 29:485-492, 2006.

Robinson D, Milanfar P: Fundamental performance limits in image registration. IEEE Trans Image Process 13:1185-1199, 2004.

Rodriguez E, George N, Lachaux JP, et al.: Perception's shadow: long-distance synchronization of human brain activity. Nature 397:430-433, 1999.

Roskies AL: The binding problem. Neuron 24:7-9, 111-125, 1999.

Scannell JW, Young MP: Neuronal population activity and functional imaging. Proc Biol Sci 266:875-881, 1999.

Sederberg PB, Kahana MJ, Howard MW, et al.: Theta and gamma oscillations during encoding predict subsequent recall. J Neurosci 23:10809-10814, 2003.

Sederberg PB, Schulze-Bonhage A, Madsen JR, et al.: Hippocampal and neocortical gamma oscillations predict memory formation in humans. Cereb Cortex 17:1190-1196, 2007.

Selemon LD, Goldman-Rakic PS: Common cortical and subcortical targets of the dorsolateral prefrontal and posterior parietal cortices in the rhesus monkey: evidence for a distributed neural network subserving spatially guided behavior. J Neurosci 8:4049-4068, 1988.

Sereno MI: Brain mapping in animals and humans. Curr Opin Neurobiol 8:188-194, 1998.

Shannon BJ, Buckner RL: Functional-anatomic correlates of memory retrieval that suggest nontraditional processing roles for multiple distinct regions within posterior parietal cortex. J Neurosci 24:10084-10092, 2004.

Sheline YI, Price JL, Yan Z, et al.: Resting-state functional MRI in depression unmasks increased connectivity between networks via the dorsal nexus. Proc Natl Acad Sci U S A 107:11020-11025, 2010.

Sherrington C: The integrative action of the nervous system. New Haven, CT: Yale University Press;, 1906.

Shmuel A, Augath M, Oeltermann A, et al.: Negative functional MRI response correlates with decreases in neuronal activity in monkey visual area V1. Nat Neurosci 9:569-577, 2006.

Shu SY, Wu YM, Bao XM, et al.: Interactions among memory-related centers in the brain. J Neurosci Res 71:609-616, 2003.

Shulman GL, Corbetta M, Buckner RL, et al.: Top-down modulation of early sensory cortex. Cereb Cortex 7:193-206, 1997.

Shulman GL, Fiez JA, Corbetta M, et al.: Common blood flow changes across visual tasks .2. Decreases in cerebral cortex. Journal of Cognitive Neuroscience 9:648-663, 1997.

Shulman GL, Astafiev SV, McAvoy MP, et al.: Right TPJ deactivation during visual search: functional significance and support for a filter hypothesis. Cereb Cortex 17:2625-2633, 2007.

Simpson JR, Jr., Snyder AZ, Gusnard DA, et al.: Emotion-induced changes in human medial prefrontal cortex: I. During cognitive task performance. Proc Natl Acad Sci U S A 98:683-687, 2001.

Singer W: Coherence as an organizing principle of cortical functions. Int Rev Neurobiol 37:153-183; discussion 203-157, 1994.

Singer W: Neuronal synchrony: a versatile code for the definition of relations? Neuron 24:49-65, 111-125, 1999.

Singh KD, Fawcett IP: Transient and linearly graded deactivation of the human default-mode network by a visual detection task. Neuroimage 41:100-112, 2008.

Sokoloff L, Mangold R, Wechsler RL, et al.: The effect of mental arithmetic on cerebral circulation and metabolism. J Clin Invest 34:1101-1108, 1955.

Sonuga-Barke EJ, Castellanos FX: Spontaneous attentional fluctuations in impaired states and pathological conditions: a neurobiological hypothesis. Neurosci Biobehav Rev 31:977-986, 2007.

Sperry RW: Effecr of 180 degree rotation of the retinal field on visuomotor coordination. The Journal of Experimental Zoology 92:263-279, 1943.

Sporns O, Tononi J: Structural determinants of functional brain dynamics, in Handbook of Brain Activity, Vol. Complexity. Edited by Jirsa VK, McIntosh AR, Springer, 2008.

Steinmetz PN, Roy A, Fitzgerald PJ, et al.: Attention modulates synchronized neuronal firing in primate somatosensory cortex. Nature 404:187-190, 2000.

Szpunar KK, Chan JC, McDermott KB: Contextual processing in episodic future thought. Cereb Cortex 19:1539-1548, 2009.

Talairach J, Tounoux P: Referentially Oriented Cerebral MRI Anatomy: An Atlas of Stereotaxic Anatomical Correlations for Gray and White Matter: Thieme Medical Publishers, New York, 1993.

Tallon-Baudry C, Bertrand O: Oscillatory gamma activity in humans and its role in object representation. Trends Cogn Sci 3:151-162, 1999.

Tallon-Baudry C, Bertrand O, Henaff MA, et al.: Attention Modulates Gamma-band Oscillations Differently in the Human Lateral Occipital Cortex and Fusiform Gyrus. Cereb Cortex 15:654-662, 2005.

TallonBaudry C, Bertrand O, Delpuech C, et al.: Oscillatory gamma-band (30-70 Hz) activity induced by a visual search task in humans. Journal of Neuroscience 17:722-734, 1997.

Taylor K, Mandon S, Freiwald WA, et al.: Coherent oscillatory activity in monkey area v4 predicts successful allocation of attention. Cereb Cortex 15:1424-1437, 2005.

Treisman A, Sato S: Conjunction Search Revisited. Journal of Experimental Psychology-Human Perception and Performance 16:459-478, 1990.

Treisman A: The binding problem. Curr Opin Neurobiol 6:171-178, 1996.

Treisman A: Feature binding, attention and object perception. Philosophical Transactions of the Royal Society of London Series B-Biological Sciences 353:1295-1306, 1998a.

Treisman A: Feature binding, attention and object perception. Philos Trans R Soc Lond B Biol Sci 353:1295-1306, 1998b.

Treisman AM, Gelade G: Feature-Integration Theory of Attention. Cognitive Psychology 12:97-136, 1980.

van Eimeren T, Monchi O, Ballanger B, et al.: Dysfunction of the default mode network in Parkinson disease: a functional magnetic resonance imaging study. Arch Neurol 66:877-883, 2009.

Varela F, Lachaux JP, Rodriguez E, et al.: The brainweb: phase synchronization and large-scale integration. Nat Rev Neurosci 2:229-239, 2001.

Varela FJ: Resonant cell assemblies: a new approach to cognitive functions and neuronal synchrony. Biol Res 28:81-95, 1995.

Vincent JL, Patel GH, Fox MD, et al.: Intrinsic functional architecture in the anaesthetized monkey brain. Nature 447:83-86, 2007.

Vogt BA, Laureys S: Posterior cingulate, precuneal and retrosplenial cortices: cytology and components of the neural network correlates of consciousness. Prog Brain Res 150:205-217, 2005.

Wolfe JM: Moving towards solutions to some enduring controversies in visual search. Trends in Cognitive Sciences 7:70-76, 2003.

Womelsdorf T, Fries P, Mitra PP, et al.: Gamma-band synchronization in visual cortex predicts speed of change detection. Nature 439:733-736, 2006.

Yuste R, MacLean JN, Smith J, et al.: The cortex as a central pattern generator. Nat Rev Neurosci 6:477-483, 2005.

Yuval-Greenberg S, Tomer O, Keren AS, et al.: Transient induced gamma-band response in EEG as a manifestation of miniature saccades. Neuron 58:429-441, 2008.

Yuval-Greenberg S, Deouell LY: The broadband-transient induced gamma-band response in scalp EEG reflects the execution of saccades. Brain Topogr 22:3-6, 2009.

Zacks JM, Speer NK, Swallow KM, et al.: Event perception: a mind-brain perspective. Psychol Bull 133:273-293, 2007.

Zhang D, Snyder AZ, Fox MD, et al.: Intrinsic functional relations between human cerebral cortex and thalamus. J Neurophysiol 100:1740-1748, 2008.

Zhang DY, Raichle ME: Disease and the brain's dark energy. Nature Reviews Neurology 6:15-28, 2010.

Journal Club

Editor's Note: These short, critical reviews of recent papers in the *Journal*, written exclusively by graduate students or postdoctoral fellows, are intended to summarize the important findings of the paper and provide additional insight and commentary. For more information on the format and purpose of the Journal Club, please see http://www.jneurosci.org/misc/ifa_features.shtml.

Role of Posterior Parietal Gamma Activity in Planning Prosaccades and Antisaccades

Karim Jerbi,[1,2] Carlos M. Hamamé,[3] Tomás Ossandón,[1,4] and Sarang S. Dalal[1]

[1]INSERM U821, Dynamique Cérébrale et Cognition, 69500 Lyon, France, [2]Laboratoire de Physiologie de la Perception et de l'Action, UMR 7152, Collège de France, CNRS, 75005 Paris, France, [3]Programa de Doctorado en Ciencias Biomédicas, Instituto de Ciencias Biomédicas, Facultad de Medicina, Universidad de Chile, Santiago 8380453, Chile, and [4]École Doctorale Neurosciences et Cognition, Université Claude Bernard Lyon I, 69622 Villeurbanne cedex, France

Review of Van Der Werf et al. (http://www.jneurosci.org/cgi/content/full/28/34/8397)

Although the components of the cerebral network mediating saccade preparation in humans have been extensively outlined by numerous functional magnetic resonance imaging (fMRI) studies (e.g., Schluppeck et al., 2006; Curtis and Connolly, 2008), the fine temporal and spectral dynamics of its underlying electrophysiology and their relationship to findings reported in animal studies still remain poorly understood. The delayed saccade paradigm explored by Van Der Werf et al. (2008) using the high temporal precision of magnetoencephalography (MEG) reveals unprecedented evidence in humans that gamma-band activity recorded in posterior parietal cortex (PPC) during the delay period is associated with the encoding of forthcoming saccades.

The main finding in the article is the emergence of sustained direction-selective high-frequency gamma activity over posterior parietal regions during planning of saccades. Using a delayed saccade paradigm, the authors set out to separate the brain activity involved in visual perception (the "stimulus component") from activity representing a motor goal (the "goal component"). The basic assumption behind this design is that saccades toward the memorized location (prosaccade condition) and away from it (antisaccade condition) have the same stimulus component but an opposite goal component. The participants were asked to memorize the position of a stimulus that was flashed peripherally for 0.1 s while they maintained central fixation. After a delay of 1.5 s, the fixation cross disappeared, instructing the subjects to perform a prosaccade or an antisaccade depending on the experimental condition. By contrasting the topographies of MEG signal power for left versus right prosaccades across frequencies, the authors found significant sustained parietal gamma activity contralateral to target location [Van Der Werf et al. (2008), their Fig. 2 (http://www.jneurosci.org/cgi/content/full/28/34/8397/F2)]. Next, by comparing these results to the outcome of the same analysis obtained in the antisaccade condition [Van Der Werf et al. (2008), their Fig. 3 (http://www.jneurosci.org/cgi/content/full/28/34/8397/F3)], two temporally distinct gamma components were distinguishable. An early broadband (40–120 Hz) component was modulated by stimulus location but not by the spatial target of the motor goal. In contrast, ~500 ms after stimulus presentation, a second narrowband gamma component (85–105 Hz) appeared to be selective to the direction of the upcoming saccade [Van Der Werf et al. (2008), their Fig. 4 (http://www.jneurosci.org/cgi/content/full/28/34/8397/F4)]. Compared with the widespread spatial distribution of the transient stimulus-related activity, the cortical sources showing goal-related modulations were found more focally in PPC [Van Der Werf et al. (2008), their Fig. 5*A*,*B* (http://www.jneurosci.org/cgi/content/full/28/34/8397/F5)]. Finally, the dissociation between the two components was not found for frequencies <30 Hz, suggesting that it is indeed specific to the gamma range [Van Der Werf et al. (2008), their Fig. 7 (http://www.jneurosci.org/cgi/content/full/28/34/8397/F7)].

One possible confound in the attempt to separate stimulus and motor components in delayed saccade paradigms with a short response delay period is the coactivation of neural networks involved in visual persistence (i.e., afterimages). This phenomenon produces an optical illusion in which an image remains perceived after the true visual stimulus has ended. Although most theories explain afterimages through the adaptation of different retinal cell populations to the properties of the inducing stimulus [e.g., chromatic characteristics, luminance, or contrast as in the study by Wede and Francis (2006)],

Received Oct. 10, 2008; revised Nov. 4, 2008; accepted Nov. 5, 2008.

This work was supported by European Community Research Program NeuroProbes (FP6-IST 027017) to K.J., the EC Marie Curie Fellowship (FP7–221097) to S.S.D., the Comisión Nacional de Investigación Científica y Tecnológica (Chile) Doctoral Fellowship to C.M.H., and a doctoral fellowship from the Ministère de l'Education Nationale et la Recherche (France) to T.O.

Correspondence should be addressed to Dr. Karim Jerbi, INSERM U821, Dynamique Cérébrale et Cognition, 69500 Lyon, France. E-mail: karim.jerbi@inserm.fr.

DOI:10.1523/JNEUROSCI.4896-08.2008

 0270-6474/08/2813713-03$15.00/0

they also recognize an important role of cortical structures. Afterimage-related activity has been observed as occipital and temporal scalp event-related potentials (Kobayashi et al., 2002) as well as gamma oscillations over occipital and parietal sensors using MEG (Tikhonov et al., 2007). So can the persistent parietal gamma activity identified by the authors after the offset of the peripheral stimulus be interpreted as a neural correlate of visual persistence of the stimulus? The inversion of hemispheric bias that was found for the late-gamma component (>500 ms) between prosaccade and antisaccades [Van Der Werf et al. (2008), their Fig. 2 (http://www.jneurosci.org/cgi/content/full/28/34/8397/F2) and Fig. 3 (http://www.jneurosci.org/cgi/content/full/28/34/8397/F3)] argues against this. Furthermore, results of a previous MEG study by the same group with a delayed double-step saccade task only show high parietal gamma enhancement preceding the saccade "go" signal but not after the first cue (Medendorp et al., 2007). An explanation of the sustained gamma solely on the account of afterimages can therefore be ruled out.

Another critical factor that might require additional investigation is the putative link between the reported gamma activity and visuospatial attention orienting. Clearly, subjects planning a saccade attend to the target location during the delay. In the case of a prosaccade, this is the same location as the stimulus, but for an antisaccade, subjects likely shift and maintain their attention to the opposite side of the screen. The authors note that this explanation is unlikely given the tendency of the sustained gamma activity to increase closer toward saccade execution. It is conceivable, however, that purely attentional neural processes might also be enhanced closer toward the onset of a planned movement and thereby account at least partially for the observed increase. This question is worth pursuing in future studies using a modified delayed saccade paradigm that explicitly controls for spatial attention. Most importantly, the endeavor to elucidate whether high-gamma activity in human PPC is specifically related to intention or to attention is part of a longstanding debate on the separability of neural representations of motor goals and spatial attention (preceding movement execution). Indeed, saccade planning and the allocation of spatial attention have been shown to be mediated by overlapping neural substrates (Kowler et al., 1995). This is an intuitively appealing idea given that visual attention and saccades both mediate the selection of a portion of the visual scene. Nevertheless, several studies have also provided evidence in favor of a putative segregation between goal representation and spatial attention across parietal and frontal areas (Colby and Goldberg, 1999; Juan et al., 2004; Quian Quiroga et al., 2006). Clearly, the attempt to fully dissociate the neural correlates of the two processes carries the inherent risk of misrepresenting the intricate interaction between them. However, recent findings, including the present study by Van Der Werf et al. (2008), suggest that the fine-scale spatial and temporal resolution of gamma-band activity might be particularly helpful in linking the findings of animal and human studies exploring the overlap and segregation between attention and intention (Pesaran et al., 2002; Brovelli et al., 2005).

Many variants of the delayed saccade task have been reported in the literature. As described above, the paradigm implemented by Van Der Werf et al. (2008) requires visuospatial processing and memorization of a flashed stimulus position (or its mirror location) in addition to motor planning. One way to probe the neural processes underlying oculomotor intention while minimizing the effect of target location is to place the visual stimulus instructing saccade direction at the center of the screen, e.g., as an arrow pointing left or right toward targets that remain visible throughout the experiment (Khonsari et al., 2007; Milea et al., 2007). Such delayed saccade paradigms significantly reduce lateralized perceptual and visuospatial memory demands because the instruction is provided centrally, and the peripheral targets are not flashed but remain present (cf. Curtis and Connolly, 2008). This places the emphasis during the delay on the motor goal and visuomotor transformation rather than the visual stimulus location. Whether such a paradigm reveals gamma patterns comparable with those reported by Van Der Werf et al. (2008) still remains to be shown.

A further important issue which could impact the interpretation of the findings reported by Van Der Werf et al. (2008) is the fact that scalp muscle activity and electromagnetic interference can contaminate MEG and EEG data yielding artifactual activity in the high-gamma frequency range. Indeed, a recent study may introduce some additional concerns; Yuval-Greenberg et al. (2008) showed that with a visual EEG experiment, broadband gamma activity may appear to arise from occipital regions when in fact they are direct manifestations of miniature saccade transients. Therefore, given that microsaccades have been shown to be modulated by shifts of spatial attention (Engbert and Kliegl, 2003), it is important to rule out that the gamma-band activity detected by Van Der Werf et al. (2008) is of artifactual origin. Such an explanation is unlikely for several reasons: First, it is unclear if the miniature saccade artifact phenomenon extends to MEG. In EEG recordings, such an artifact may be a consequence of reference electrode placement (Yuval-Greenberg et al., 2008); in contrast, MEG may not be susceptible to this problem because it is inherently reference-free. Additionally, the beamforming source reconstruction method provides a degree of protection from artifacts arising from outside the brain. Beamforming estimates either the time course or power modulations of neural activity over the brain volume using adaptive spatial filters (Van Veen et al., 1997). This method does not require a priori assumptions about the location or number of sources and so does not assume sources are restricted to the brain. Sources of ocular origin would therefore be localized near the eyes rather than projected to distant parts of the brain (Bardouille et al., 2006). A third argument in favor of a cortical origin of the reported gamma activity findings is that they are in agreement with results from direct recordings in monkeys at several levels. For instance, the reported hemisphere-specific contralateral selectivity of spectral power for an upcoming saccade is in line with findings obtained with gamma-range components of local field potentials recorded in monkey PPC (Pesaran et al., 2002). Furthermore, the timing of gamma power modulation shift from stimulus processing to goal encoding appears to coincide with the average inversion time of lateral intraparietal neurons remapping from stimulus location to goal encoding as reported in a memory-delayed saccade task in monkeys (Zhang and Barash, 2004). Finally, the significance of the parietal high-gamma findings is further enhanced by a growing body of evidence linking population-level gamma activity to the blood oxygenation level-dependent signal recorded in fMRI, both in monkeys (Logothetis et al., 2001) and in humans (Lachaux et al., 2007).

The authors propose that parietal gamma-band activity reflects visuomotor encoding mechanisms that determine the saccade goal. Given that the neural network involved in oculomotor planning and execution spreads across multiple ce-

rebral areas, including parietal and frontal regions, one might have expected to also find comodulations of gamma activity in frontal areas, including dorsolateral prefrontal cortex or frontal and supplementary eye fields (Lachaux et al., 2006). The absence of such findings in this study could either be attributable to the experimental design used (trial number, delay latency, etc.), or to important differences in amplitude between parietal and frontal gamma activity, or alternatively to the dependency of MEG source estimation on various properties of the underlying generators such as the orientation and size of the activated patch of cortex.

To conclude, although much still needs to be done to fully disentangle the neural correlates of visuomotor processing, spatial attention and motor goal encoding in PPC, the study by Van Der Werf et al. (2008) brings us one step closer toward elucidating the role of high-gamma activity in these processes and provides fundamental findings that help bridge the gap between electrophysiological recordings in monkeys and humans during visually guided motor behavior.

References

Bardouille T, Picton TW, Ross B (2006) Correlates of eye blinking as determined by synthetic aperture magnetometry. Clin Neurophysiol 117:952–958.

Brovelli A, Lachaux JP, Kahane P, Boussaoud D (2005) High gamma frequency oscillatory activity dissociates attention from intention in the human premotor cortex. Neuroimage 28:154–164.

Colby CL, Goldberg ME (1999) Space and attention in parietal cortex. Annu Rev Neurosci 22:319–349.

Curtis CE, Connolly JD (2008) Saccade preparation signals in the human frontal and parietal cortices. J Neurophysiol 99:133–145.

Engbert R, Kliegl R (2003) Microsaccades uncover the orientation of covert attention. Vision Res 43:1035–1045.

Juan CH, Shorter-Jacobi SM, Schall JD (2004) Dissociation of spatial attention and saccade preparation. Proc Natl Acad Sci U S A 101:15541–15544.

Khonsari RH, Lobel E, Milea D, Lehéricy S, Pierrot-Deseilligny C, Berthoz A (2007) Lateralized parietal activity during decision and preparation of saccades. Neuroreport 18:1797–1800.

Kobayashi Y, Yoshino A, Ogasawara T, Nomura S (2002) Topography of evoked potentials associated with illusory motion perception as a motion aftereffect. Brain Res Cogn Brain Res 13:75–84.

Kowler E, Anderson E, Dosher B, Blaser E (1995) The role of attention in the programming of saccades. Vision Res 35:1897–1916.

Lachaux JP, Hoffmann D, Minotti L, Berthoz A, Kahane P (2006) Intracerebral dynamics of saccade generation in the human frontal eye field and supplementary eye field. Neuroimage 30:1302–1312.

Lachaux JP, Fonlupt P, Kahane P, Minotti L, Hoffmann D, Bertrand O, Baciu M (2007) Relationship between task-related gamma oscillations and BOLD signal: new insights from combined fMRI and intracranial EEG. Hum Brain Mapp 28:1368–1375.

Logothetis NK, Pauls J, Augath M, Trinath T, Oeltermann A (2001) Neurophysiological investigation of the basis of the fMRI signal. Nature 412:150–157.

Medendorp WP, Kramer GF, Jensen O, Oostenveld R, Schoffelen JM, Fries P (2007) Oscillatory activity in human parietal and occipital cortex shows hemispheric lateralization and memory effects in a delayed double-step saccade task. Cereb Cortex 17:2364–2374.

Milea D, Lobel E, Lehéricy S, Leboucher P, Pochon JB, Pierrot-Deseilligny C, Berthoz A (2007) Prefrontal cortex is involved in internal decision of forthcoming saccades. Neuroreport 18:1221–1224.

Pesaran B, Pezaris JS, Sahani M, Mitra PP, Andersen RA (2002) Temporal structure in neuronal activity during working memory in macaque parietal cortex. Nat Neurosci 5:805–811.

Quian Quiroga R, Snyder LH, Batista AP, Cui H, Andersen RA (2006) Movement intention is better predicted than attention in the posterior parietal cortex. J Neurosci 26:3615–3620.

Schluppeck D, Curtis CE, Glimcher PW, Heeger DJ (2006) Sustained activity in topographic areas of human posterior parietal cortex during memory-guided saccades. J Neurosci 26:5098–5108.

Tikhonov A, Händel B, Haarmeier T, Lutzenberger W, Thier P (2007) Gamma oscillations underlying the visual motion aftereffect. Neuroimage 38:708–719.

Van Der Werf J, Jensen O, Fries P, Medendorp WP (2008) Gamma-band activity in human posterior parietal cortex encodes the motor goal during delayed prosaccades and antisaccades. J Neurosci 28:8397–8405.

Van Veen BD, van Drongelen W, Yuchtman M, Suzuki A (1997) Localization of brain electrical activity via linearly constrained minimum variance spatial filtering. IEEE Trans Biomed Eng 44:867–880.

Wede J, Francis G (2006) The time course of visual afterimages: data and theory. Perception 35:1155–1170.

Yuval-Greenberg S, Tomer O, Keren AS, Nelken I, Deouell LY (2008) Transient induced gamma-band response in EEG as a manifestation of miniature saccades. Neuron 58:429–441.

Zhang M, Barash S (2004) Persistent LIP activity in memory antisaccades: working memory for a sensorimotor transformation. J Neurophysiol 91:1424–1441.

MINI-REVIEW

Task-Related Gamma-Band Dynamics From an Intracerebral Perspective: Review and Implications for Surface EEG and MEG

Karim Jerbi,[1,2] Tomás Ossandón,[1] Carlos M. Hamamé,[3] S. Senova,[1,2] Sarang S. Dalal,[1] Julien Jung,[1] Lorella Minotti,[4] Olivier Bertrand,[1] Alain Berthoz,[2] Philippe Kahane,[4] and Jean-Philippe Lachaux[1]*

[1]*INSERM, U821, Brain Dynamics and Cognition; Université Claude Bernard, Lyon 1, Lyon, France*
[2]*CNRS, UMR 7152, Physiology of Perception and Action Laboratory, Collège de France, Paris, France*
[3]*Instituto de Ciencias Biomédicas, Universidad de Chile, Santiago, Chile*
[4]*Neurology Department, Grenoble Hospital, Grenoble, France*

Abstract: Although non-invasive techniques provide functional activation maps at ever-growing spatio-temporal precision, invasive recordings offer a unique opportunity for direct investigations of the fine-scale properties of neural mechanisms in focal neuronal populations. In this review we provide an overview of the field of intracranial Electroencephalography (iEEG) and discuss its strengths and limitations and its relationship to non-invasive brain mapping techniques. We discuss the characteristics of invasive data acquired from implanted epilepsy patients using stereotactic-electroencephalography (SEEG) and electrocorticography (ECoG) and the use of spectral analysis to reveal task-related modulations in multiple frequency components. Increasing evidence suggests that gamma-band activity (>40 Hz) might be a particularly efficient index for functional mapping. Moreover, the detection of high gamma activity may play a crucial role in bridging the gap between electrophysiology and functional imaging studies as well as in linking animal and human data. The present review also describes recent advances in real-time invasive detection of oscillatory modulations (including gamma activity) in humans. Furthermore, the implications of intracerebral findings on future non-invasive studies are discussed. *Hum Brain Mapp 00:000–000, 2009.* © 2009 Wiley-Liss, Inc.

Key words: stereotactic electroencephalography (SEEG); electrocorticography (ECoG); oscillations; gamma-band activity; real-time electrophysiology; functional mapping; invasive human recordings; epilepsy

INTRODUCTION

Shortly after Berger [1929] reported the first electroencephalography (EEG) measurements in humans using electrodes placed on the scalp the technique was adapted by neurosurgeons to directly acquire intracerebral signals from patients. Such recordings proved to be of great interest for pre-surgical brain mapping allowing for clinical assessments with an unprecedented spatial precision [Jasper and Penfield, 1949; Ward and Thomas, 1955]. These early studies marked the birth of a new field that would

Additional Supporting Information may be found in the online version of this article.

*Correspondence to: Jean-Philippe Lachaux, INSERM – U821, Brain Dynamics and Cognition, Centre Hospitalier Le Vinatier, Bâtiment 452, 95 Boulevard Pinel, 69500 Bron, France.
E-mail: jp.lachaux@inserm.fr

Received for publication 13 November 2008; Revised 19 January 2009; Accepted 20 January 2009

DOI: 10.1002/hbm.20750

Published online in Wiley InterScience (www.interscience.wiley.com).

expand beyond its clinical application to the field of brain research. Indeed, more than fifty years later, intracranial electroencephalography (iEEG) has become an essential component of the pre-surgical routine procedures for a wide range of neurological diseases including drug-resistant epilepsy, Parkinson disease, essential tremor, brain tumors, while providing unique insights into brain function [Engel et al., 2005]. Early observations that changes in iEEG recordings were correlated with the patient's environment or behavior [Jasper and Penfield, 1949] gradually laid the foundations for a new research field bringing together clinicians and neuroscientists and advancing our understanding of the neural mechanisms underlying human cognition. Despite a number of restrictions inherent to the therapeutic context of its application, iEEG has grown into a field of its own, yielding a steady stream of seminal observations ranging from the functional organization of the human visual system [Allison et al., 1999; Halgren et al., 1994] to response properties of individual neurons during mental imagery in the anterior temporal lobe [Kreiman et al., 2000] to name but a few examples of iEEG's important input to neuroscience.

In this review, we provide a short overview of iEEG and discuss its advantages and its limitations for cognitive neuroscience as well as its relationship to non-invasive brain mapping techniques. A comprehensive review of invasive recordings in a range of clinical conditions including movement disorders such as Parkinson's disease can be found in Engel et al. [2005]. Here, we restrict the discussion to invasive recordings acquired from implanted epilepsy patients either with stereotactic-electroencephalography (SEEG) or electrocorticography (ECoG) and focus on current topics in invasive functional mapping based on the detection of task-related modulations of cortical oscillations. In particular, we discuss the efficiency of detecting gamma-band activity (>40 Hz) using offline and online analysis for invasive functional mapping [Crone et al. 2006; Jensen et al. 2007], and its putative role in bridging the gap between electrophysiology and functional imaging studies as well as linking animal and human data. In addition, we aim to dispel certain misconceptions about the significance and interpretability of human invasive recordings by outlining their unique advantages and explicitly describing their inherent limitations. Finally, we also address the relationship and complementarities between iEEG and non-invasive electrophysiological studies.

INVASIVE RECORDINGS IN EPILEPSY

Intracerebral recordings in humans are performed using a wide range of techniques tailored to the neurological disorder and therapeutic strategy at hand. Depth recordings are for instance used during positioning of a deep brain stimulation (DBS) electrode in Parkinson's disease [Benazzouz et al., 2002; Engel et al., 2005]. Furthermore, invasive recordings are used in patients with intractable epilepsy in order to simultaneously and chronically probe the neural activity in multiple brain structures during a pre-surgical evaluation period.

The Clinical Setting

In patients with pharmacologically resistant epilepsy, iEEG is used to identify cortical regions critical for seizure onset and identify others that need to be spared at the time of surgery [e.g., Kahane et al., 2004]. The intracerebral electrodes sometimes stay in place for more than two weeks in order to localize the origin of fast electrophysiological rhythms that precede seizure onset and that are at the core of the epileptogenic network. Surgical resection of the focus of the seizure has been shown to yield up to 70% success rates for drug-resistant temporal lobe epilepsy [Engel, 1996]. Intracranial EEG is used to test one or several hypothesis regarding the anatomical organization of the epileptogenic network. This sometimes implies that intra-cerebral electrodes are positioned in widely distributed brain regions that might include pathological but also healthy tissue. Therefore, such a clinical context can also provide a unique opportunity to study fundamental questions about neural coding and cognition. The rest of this review is dedicated to iEEG data acquired in the clinical context of epilepsy.

Stereotactic-EEG and Electrocorticography: Two Intracranial Recording Techniques

Although microelectrodes have been used in humans to acquire single-neuron spiking data [Fried et al., 1997; Heit et al., 1988; Ojemann et al., 2002; Ward and Thomas, 1955], clinical recordings in epilepsy patients are generally performed using macroelectrodes that measure coherent activity of local neuronal populations in the vicinity of the recording site. The most common choice in the clinical routine is to use either stereotactic-electroencephalography (SEEG) or electrocorticography (ECoG) which acquire intracranial data using multilead depth electrodes or subdural grid electrodes respectively (see Fig. 1). Subdural grids consist of 2D arrays (or sometimes one-dimensional strips) of electrodes positioned directly on the lateral surface of the brain, with a typical inter-electrode distance of 1 cm [Engel et al., 2005]. In contrast, depth electrodes are semi-flexible one-dimensional linear arrays, shaped as narrow needles that penetrate deep into the brain. Such depth electrode implantations are often referred to as Stereotactic EEG because a stereotactic technique developed by Talairach and Bancaud is used to localize the electrodes [Kahane et al., 2006]. While subdural grids provide widespread cortical coverage and cortical maps of gyral activity, the multilead depth electrodes record from both sulci and gyri and go beneath the cortical surface to probe deep cortical structures, such as the cingulate gyrus, and occasionally subcortical structures, such as the lateral geniculate nucleus [Krolak-Salmon et al., 2003] or the nucleus

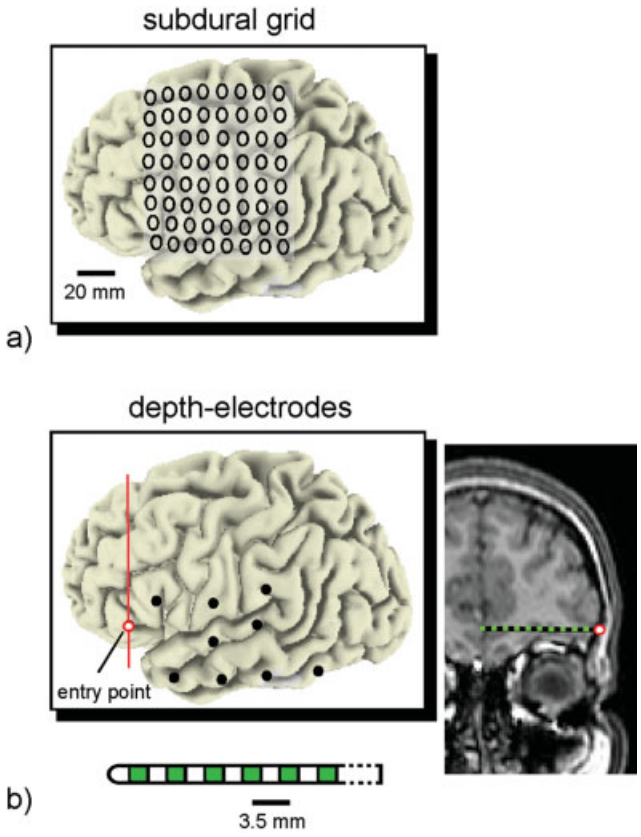

Figure 1.

Subdural grids vs. depth electrodes. (**a**) Representation of electrocorticographic (ECoG) subdural grid electrodes. Open circles indicate recording sites on a 8-by-8 matrix covering the lateral surface of the somatosensory cortex. (**b**) Example of implantation with stereotactic encephalography (SEEG) electrodes. Black dots represent the entry points of ten depth electrodes. Each electrode consists of 5–15 contact sites (green squares). In most cases, SEEG electrodes are inserted orthogonal to the interhemispheric plane as shown on coronal MRI slice.

acumbens [Münte et al., 2008]. A further difference between SEEG and ECoG is that while depth electrodes require small burr holes for implantation the implantation of two-dimensional subdural grids involves a larger craniotomy.

Converging evidence suggests that both grid [Menon et al., 1996] and depth-electrodes recordings [Lachaux et al., 2003] provide sufficient spatial resolution to localize neural activity at the gyral level, a precision that is as good as, if not better, than what is achieved with fMRI. In addition, the spatial precision of the analysis also depends on the accuracy of electrode localization [Dalal et al., 2008a] and choice of reference electrode. In SEEG data, the local precision is highest when each recording site is referenced to its nearest neighbor (bipolar montage) than when one remote site is used as reference for all channels (common reference) [Lachaux et al., 2003].

Unless otherwise stated in the manuscript, the experiments performed by our group that are reported in this review were carried out using multi-channel video-EEG acquisition and monitoring system (Micromed, Treviso, Italy) that simultaneously records the intracerebral activity from up to 128 depth-EEG electrodes (up to 1024 Hz sampling rate and a 0.1–200 Hz bandpass filter). As a general rule, twelve to fourteen semi-rigid multi-lead electrodes are stereotactically implanted in each patient. The stereotactic-EEG (SEEG) electrodes used have a diameter of 0.8 mm and, depending on the target structure, consist of 5–18 contact leads 2 mm wide and 1.5 mm apart (Alcys, Besançon, France).

Strengths and Limitations of iEEG Research

At first sight, iEEG can be seen as combining the best of two worlds: the spatial resolution of fMRI and the temporal accuracy of MEG/EEG. In addition, given that the recording sites are within the brain, iEEG signals are immune to a large range of external artifacts (e.g., eye blinks, face and neck muscles contractions). However, it is important to bear in mind two significant limitations: first, the data acquired report on patients with epileptic disorders and, second, the invasive electrodes only provide a limited coverage of the brain.

Indeed, in recent years, iEEG research has begun to establish a set of methods and specific practices to limit the risk of making physiological interpretations based on phenomena that actually reflect the pathological condition of the patients. It is common iEEG practice to discard signal epochs that show any type of epileptiform activity. Furthermore, most iEEG studies include post-surgical information about the spatial organization of the epileptogenic network and do not report on task-related responses within that network. Also, when possible, an additional caution is to only report observations that are reproducible across several patients with different types of epileptogenic networks and anticonvulsant medication [Fell et al., 2002; Halgren et al., 1994]. Nevertheless, an important body of iEEG research provides evidence that such issues can indeed be overcome to an extent that warrants the physiological significance of the physiological insights and novel hypotheses drawn from the data [Axmacher et al., 2008b; Brovelli et al., 2005; Canolty et al., 2006; Crone et al., 1998a, 2006; Fell et al., 2002; Jung et al., 2008; Lachaux et al., 2003, 2005, 2006a; Lakatos et al., 2008; Mainy et al., 2007].

The second limitation of many iEEG investigations is the fact that the electrode implantation scheme only provides a restricted sampling of selected cerebral structures. A complete 3D coverage of the brain with a spatial resolution of 3.5 mm has been estimated to require about 10,000 recording sites [Halgren et al., 1998], that is roughly 100 times more than the number of sites we actually record (approx. 100). A more comprehensive view of the large-

scale networks involved in various cognitive tasks would therefore require combining data from multiple subjects with both overlapping and complementary electrode positions. In practice, collecting data from comparable anatomical origin across several patients is of non-negligible difficulty since the target structures for intracerebral electrodes placement is determined in each patient individually and independently of research objectives. The standards of invasive and non-invasive research are thus inherently different. Furthermore, to a certain extent, iEEG studies share some common aspects with monkey electrophysiology studies. The latter report in most cases on two or three animals with recordings in comparable regions and with a particularly high signal-to-noise ratio. In addition, the limited extent of probed cerebral structures (spatial coverage) and the question of generalization to the healthy human brain are undoubtedly two issues that are also relevant to findings reported invasively in monkey studies. Animal studies provide valuable observations and hypotheses that ultimately need to be explored and validated in humans. Similarly, the results of iEEG studies in human patients may be further validated in healthy subject by non-invasive techniques such as MEG and EEG.

SPECTRAL COMPONENTS OF iEEG DATA

Oscillatory brain responses are not perfectly phase-locked with respect to experimental stimuli and are thus discarded by the time-domain averaging of the data typically used to compute event-related potentials (ERPs). Therefore, with the advent of enhanced computing power, novel time-frequency domain approaches were applied to assess such activations, described as *induced responses*, by contrast to the phase-locked activations known as *evoked responses* [Tallon-Baudry and Bertrand, 1999]. As an example, using time-frequency analysis intracranial data in humans have reported that motor behavior is associated with spatially focal increases in high frequency (>40 Hz) activity and widespread decreases in lower frequencies (8–30 Hz) in the motor cortex [Aoki et al., 1999; Crone et al., 1998a; Lachaux et al., 2006a; Mehring et al., 2004; Pfurtscheller et al., 2003; Pistohl et al., 2008; Szurhaj et al., 2005].

Gamma-Band Activity Modulations: A Robust Correlate of Local Neural Activation

Several early animal microelectrode studies pointed towards the putative functional importance of synchronized neural oscillations at high frequencies (>40 Hz), i.e., within the gamma band [Eckhorn et al., 1988; Freeman, 1978; Gray et al., 1989; Rougeul-Buser et al., 1975]. Neural synchronization in the gamma band has been proposed as a fundamental mechanism for neural communication underlying both perceptual and motor processes [Murthy and Fetz, 1992; Singer and Gray, 1995]. In addition, several scalp EEG studies reported task-related responses in the gamma band in a variety of visual paradigms [Gruber et al., 1999; Tallon-Baudry et al., 1996] suggesting a link to the neural synchronization phenomenon recorded invasively in animals.

Forty years after Chatrian's seminal report [Chatrian et al., 1960], task-related gamma band increases were observed in direct recordings of the human brain using tightly controlled experimental paradigms and advanced signal processing analysis [Crone et al., 1998a; Lachaux et al., 2000]. Ever since, an increasing number of iEEG studies in humans (epilepsy patients for the large part) report gamma-range activations in various brain structures and in various experimental conditions. Interestingly, although research into the functional significance of gamma activity is still in its early days, converging findings from these studies point to a number of properties of gamma-band responses (GBRs) that appear to be reproducible across a variety of brain structures and in various experimental conditions. Previous work including numerous ECoG and SEEG studies by our group and others suggest that these common characteristics could be tentatively summarized as follows:

1. Broad frequency extent: gamma-band responses (GBR) consist of spectral power increases (or suppressions) that are time-locked to sensory or motor events, in a broad range of frequencies (40– 200 Hz). Note also that task-related gamma-band suppressions (GBS) have recently been reported with iEEG [Lachaux et al., 2008].
2. Functional specificity: the fine spatial organization of GBRs strongly depends on the cognitive process at hand. For example, Figure 2 illustrates this specificity within Broca's area during a word recognition task (semantic versus phonological processing). Similarly, we have also reported using SEEG in an implanted subject performing an auditory experiment, that switching the auditory stimulus from speech to music causes a seven millimeters shift in the focus of the GBR locus in the Superior temporal gyrus [Lachaux et al., 2007a].
3. Spatial specificity: Although sources of GBRs have been found across distributed brain areas, each GBR source per se generally shows spatially focal activation. This contrasts with the wider spatial distribution of power modulations in lower frequency bands such as the alpha (8–13 Hz) or beta (15–30 Hz) bands. This general observation has been shown to be particularly clear in the sensorimotor cortex [Crone et al., 1998b], but is also visible during visual search tasks for instance (cf. Fig. 3).
4. Generalization: large-scale networks exhibiting GBRs have been found in a large variety of cognitive tasks involving working memory [Axmacher et al., 2008b; Howard et al., 2003; Mainy et al., 2008], declarative memory [Axmacher et al., 2008a; Fell et al., 2001, 2002, 2008; Sederberg et al., 2007], reading [Mainy

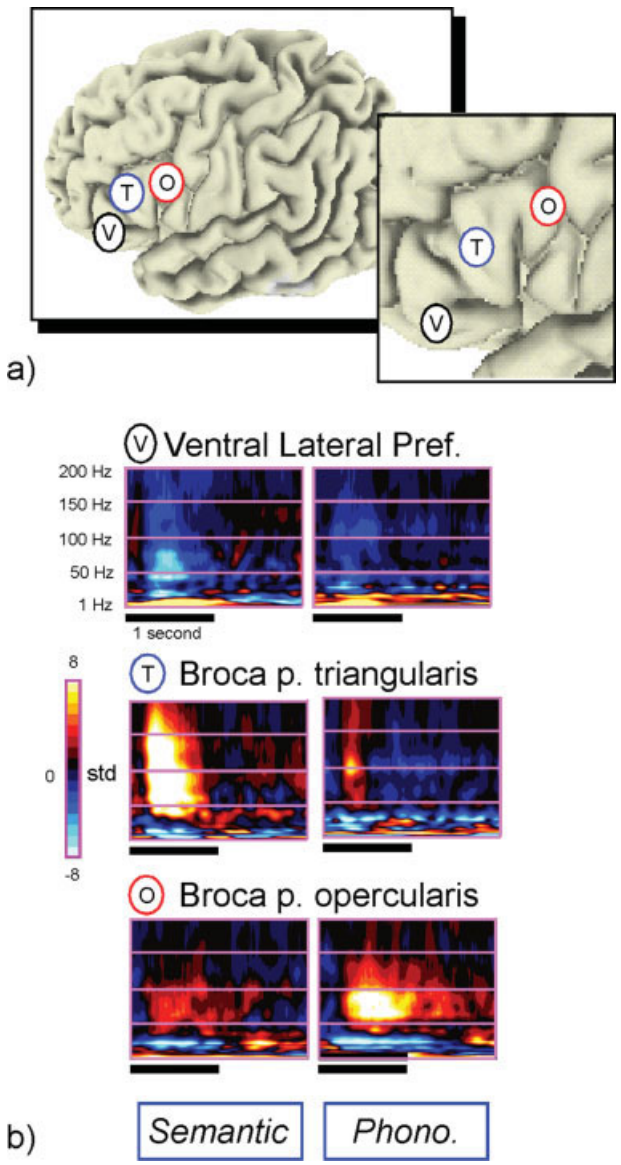

Figure 2.

Illustration of the functional specificity of gamma-band activity in a word recognition task. Patients had to perform either an animacy decision on written words (Semantic task) or rhyme detection on visually presented pseudo-words (Phonological task). Time-frequency (TF) representations show energy increases and decreases relative to pre-stimulus baseline across the two conditions in three distinct regions: Broca pars triangularis ('T'), Broca pars opercularis ('O') and Ventral Lateral Prefrontal Cortex ('V') (response is shown for 2 seconds after stimulus onset). Energy increases above 50 Hz clearly differentiate between task conditions in Broca ('T' and 'O'). Enhanced gamma-band responses in Broca coincide with gamma-band suppression in the VLPFC (V). TF maps also display a clear Broca power suppression in all conditions below 30 Hz, i.e., in the alpha and beta bands.

et al., 2008], speech perception and production [Crone et al., 2001b], attention [Brovelli et al., 2005; Jensen et al., 2007; Jung et al., 2008; Ray et al., 2008], visual [Lachaux et al., 2005; Tanji et al., 2005], auditory [Bidet-Caulet and Bertrand, 2005; Crone et al., 2001a; Edwards et al., 2005], somatosensory [Aoki et al., 1999] and olfactory perception [Jung et al., 2006], motor processes [Crone et al., 1998a; Lachaux et al., 2006].

Although the above properties should by no means convey the impression that GBRs provide by themselves a comprehensive view of task-related neural dynamics, they do highlight, in our opinion, the importance of exploring the functional significance of gamma range activity. Whether GBRs represent a phenomenon that is intrinsic to cognition is still debated. A theoretical framework which draws upon single-unit recordings in animal studies suggests that gamma-band synchronization facilitates neural communication [Fries, 2005; Singer, 1999]. Compared to a resting baseline level, gamma-band activity recorded within a neural population would increase when its neurons are recruited by a cognitive process, and conversely, gamma power might be expected to decrease when the population is no longer necessary or when its activity is inhibited [Lachaux et al., 2008]. The view that engagement in a cognitive act triggers a large-scale network of distributed and spatially focal enhancements and suppressions (i.e., positive and negative modulations) of gamma-band responses compared to the resting state provides an attractive framework for comparison with fMRI studies. Indeed, recent studies both in animals and in humans report prominent spatial overlap between the networks of gamma-band activations and those of the BOLD signal suggesting a direct relationship between the two [Kayser et al., 2004; Lachaux et al., 2007b; Logothetis et al., 2001; Niessing et al., 2005; Nishida et al., 2008].

Oscillatory Modulations in Lower Frequency Bands

In addition to GBRs, time-frequency analysis of iEEG data has also revealed robust task-related response patterns in lower frequency bands, mostly in the theta (4–7 Hz), alpha (7–14 Hz) and beta (15–30 Hz) bands. Results obtained with iEEG are largely in line with reports from scalp recordings, and often reveal alpha and beta power suppressions during the task compared to the baseline period. For instance, such findings were reported in the sensori-motor cortex and described as event-related mu and beta desynchronization [Crone et al., 1998b; Pfurtscheller et al., 2003] as well as in the parieto-occipital cortex [e.g., Adrian, 1941]. Furthermore, alpha and beta suppressions often occur simultaneously with GBRs. Although there has been, to our knowledge, no extensive iEEG data meta-analysis that specifically explores this relationship, it has often been reported in humans with iEEG studies [Crone et al., 1998a,b; Lachaux et al., 2005] and MEG recordings [de Lange et al., 2008] as well as in animal studies [e.g., Rickert

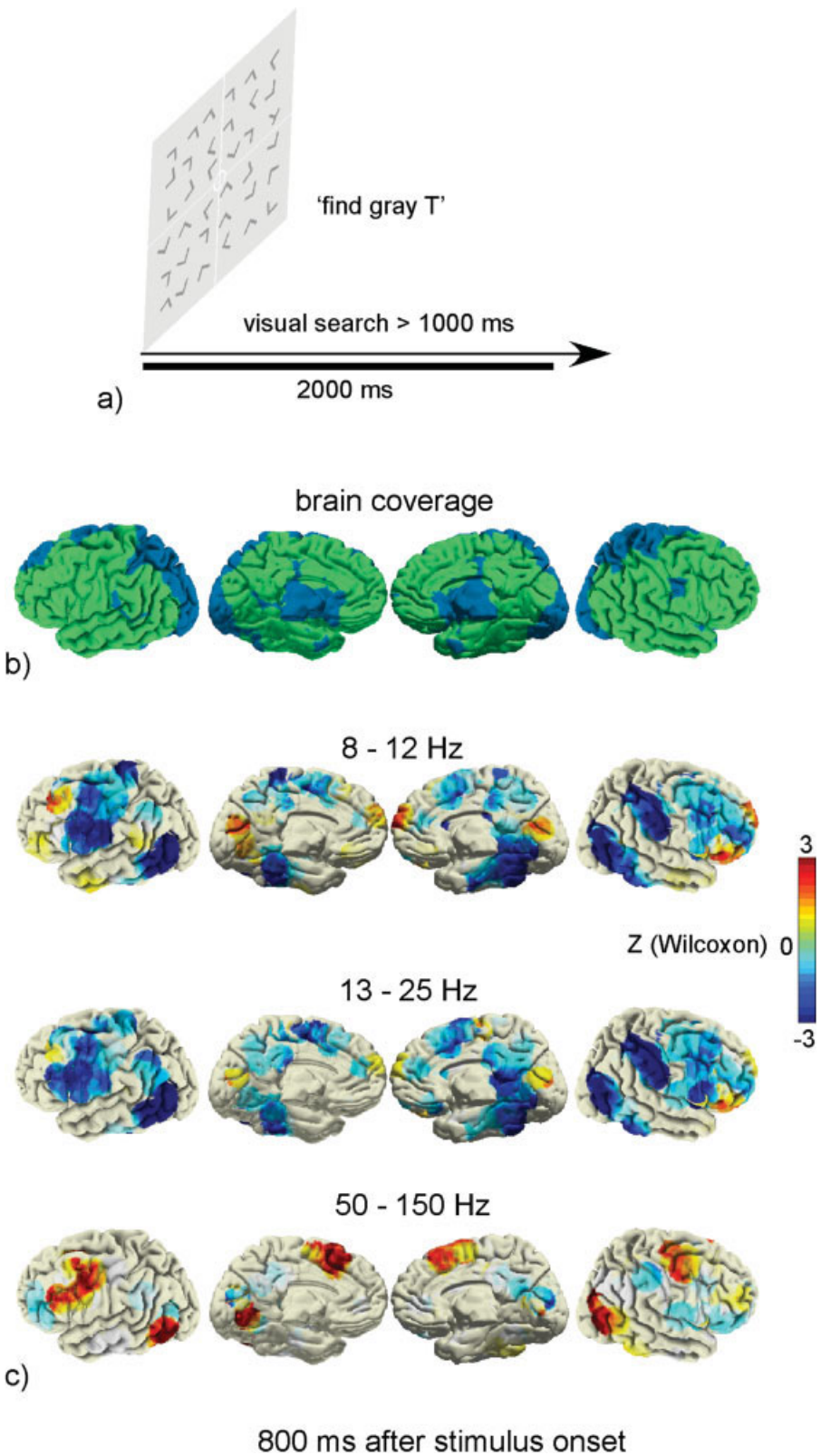

Figure 3.
The spatial distribution of alpha, beta, and gamma-band responses during a visual search task. (**a**) Paradigm: The patients were asked to search for a gray 'T' within an array of distracters (gray 'L's'). (**b**) Cortical areas within direct vicinity of electrode sites across all ten patients (green). (**c**) Following the same convention as in Supplementary Figure 1b, 3D brain reconstructions show the distribution of alpha (8–12 Hz), beta (13–25 Hz) and gamma (50–150 Hz) responses 800 ms after stimulus onset, i.e., while patients are actively searching for the target. Response is expressed in energy variation relative to pre-stimulus baseline (Wilcoxon *Z* score, FDR corrected).

et al., 2005]. Additionally, alpha and beta desynchronizations have been found to occur across cortical areas that often include, but also extend beyond the origin sites of GBR. Figure 3 shows an illustration of this pattern in a visual search task. This has also been reported in the motor cortex, where the spatial organization of movement-related GBR provides a precise focal spatial mapping, while alpha and beta suppressions yield spatially smoothed maps [Crone et al., 1998a]. As shown in Figure 2, such a reversal between high and low frequency activation patterns is also visible in a word recognition paradigm contrasting semantic and phonological processing [Mainy et al., 2008].

Modulations of theta (4–7 Hz) activity have also been consistently reported in iEEG [Kahana et al., 2001; Raghavachari et al., 2001]. In contrast to alpha and beta activity, and much like the gamma band, theta activity appears to be a rhythm often observed to increase in amplitude during active involvement in a task. For instance, theta power increases have been reported in the hippocampus during spatial navigation [Ekstrom et al., 2005] and with memory load during the delay of a verbal working memory task in multiple frontal, temporal and parietal areas [Raghavachari et al., 2001]. The observation that both gamma and theta power increases during cognitive processing may suggest that the two rhythms interact with each other. Indeed, theta–gamma interactions have been reported in animals and in humans [Canolty et al., 2006; Jensen and Colgin, 2007].

Intracranial Event-Related Potentials

Event-related potentials measured at the intracerebral level have been explored extensively by numerous fundamental iEEG studies. A detailed review of this literature is beyond the scope of this review. Interestingly, however, ERPs and cerebral oscillations are often investigated separately. Only a few studies have sought to establish links between the two [Karakas et al., 2000; Mazaheri and Jensen, 2008; Nikulin et al., 2007]. A handful of studies have compared the task-sensitivity and spatial organization of ERPs and gamma-band responses and revealed a degree of overlap between the two systems. For instance, in a paradigm that required participants to detect faces hidden in high-contrast figures, the presented stimuli triggered both ERPs and gamma-band responses in the same region of the fusiform area [Lachaux et al., 2005]. However, this particular study did also reveal that, on some instances, the ERP was identical whether the face was actually detected or not, while GBR was stronger for detected faces. This is in line with other iEEG results that report functional dissociations between ERPs and gamma-band responses [Tallon-Baudry et al., 2005].

An illustrative iEEG example: ERPs and GBR in early visual areas

In a matched to sample task, subjects were instructed to compare two complex and simultaneously presented stimuli and decide whether they are the same or different. Subjects were allowed to freely explore both stimuli as long as they wanted before giving a behavioral response. The differences between the stimuli were hard to detect and a decision required multiple saccades back and forth between the two (see Fig. 4a). By contrast to surface recordings, the saccades that precede each fixation on the left or right stimulus did not elicit signal artifacts. A key question in this study was therefore to investigate the neural activity related to fixation (gaze immobilization at the end of each saccade). Visual ERPs and GBRs were obtained from the neural signal acquired in multiple sites in the occipital lobe of two patients.

In order to describe the propagation of neural activity in early visual areas, we considered two electrodes one located in primary visual cortex and the other in latero-occipital area. The first peak latency of the ERPs was identified and used to describe the direction of neural activity propagation. In primary visual area the average latency for each subject was 32 and 29 ms, while in latero-occiptal area the average latencies were 165 and 155 ms, for subjects one and two respectively. Time-frequency analysis revealed GBR (50-150 Hz) with onset latency around 38 and 44 ms (Fig. 4c) which were only observed in the primary visual area, not in the lateral-occipital sites (see Fig. 4d).

The ability to align the analysis on the end of a saccade when using direct recordings from the cortex allows for the investigation of brain activity in humans during a free viewing experiment. Our observations suggest that the onset of foveal vision following a saccade to an already existing object elicits ERPs and high gamma responses in primary visual areas. Most interestingly this activity starts earlier than latencies one might have expected from previous reports [Poghosyan and Ioannides, 2007; Schmolesky et al., 1998]. We propose that this probably related to the fact that previous experiments used stimuli that were flashed in the visual fixation point of the subject. Here, stimuli were present on the screen throughout the entire duration of the trial and so the time-zero of the ERPs and GBR was set to be at the end of a saccade (fixation onset). Hence the interval between fixation and the time the visual information reaches the primary visual cortices might be shorter than the interval between stimulus onset and primary visual activity in a classical central fixation paradigm. However, further investigations will be needed to validate these interpretations.

Statistical Considerations for iEEG Data Analysis and Interpretations

Intracranial EEG data analysis is complicated by the fact that populations are often small, and the recording sites are highly variable across patients. As a consequence, group statistics, as they are commonly used in MEG/EEG studies, are not suitable to many iEEG studies. Instead, task-related effects can be shown at the individual level and localized precisely on the cortical anatomy of each patient. The attempt to represent statistically significant task-related modulations of iEEG data across subjects,

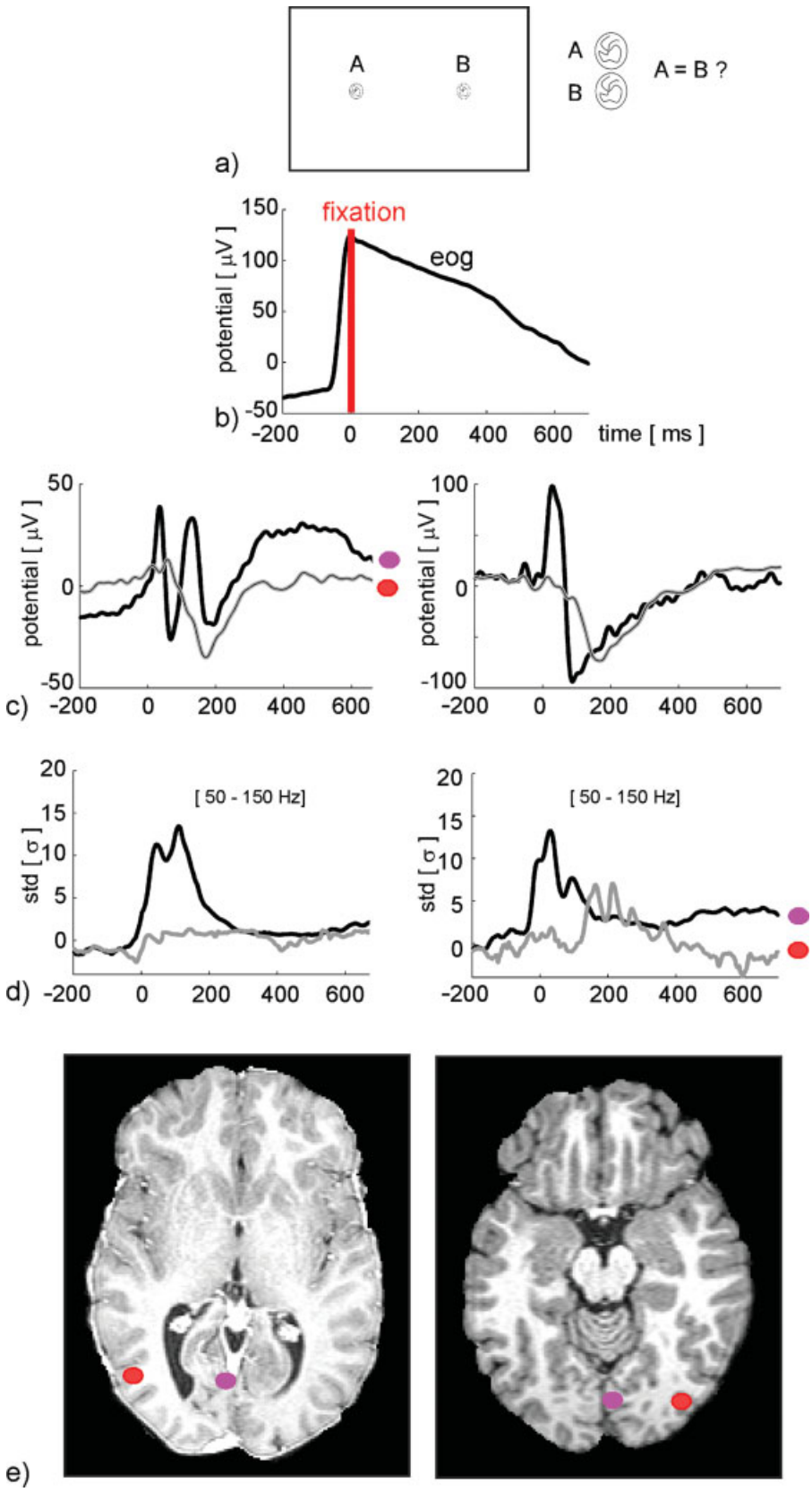

Figure 4.

Example study. Free viewing in human early visual areas. (**a**) Schematic representation of the behavioral task. Stimuli were separated from each other by 10 degrees, centered on the middle of the screen, and had a diameter of 1 degree. Both stimuli were present during the entire trial, which was ended by a behavioral response of "same" or "different" made through a computer mouse. (**b**) Electroculogram (EOG) recording showing the method used to determine the end of a saccade (fixation onset). (**c**) ERPs and (**d**) GBRs as recorded in two electrodes for two patients. Black and gray traces represents the activation recorded from primary visual and latero-occipital areas. Left and right panels correspond to patient one and two. (**e**) Magnetic resonance images of a horizontal cut from brains of each patient. Red and magenta dots show the location of the electrode contacts.

time, space and frequency is in itself quite a unique neuroimaging challenge. One approach used in our group to deal with this complexity consists of the following three-step procedure: First, a statistical comparison is performed between experimental conditions at the individual level, on each recording site, to identify regions of interest with task-related neural responses. This includes a correction for multiple comparisons and may involve either a direct comparison between two conditions or a comparison between the task and a pre-stimulus resting baseline. The second step is the identification of brain regions of interest which show similar effects across several patients. The third step is to display the individual data for each region of interest, displaying the task-related effect on each patient's anatomical MRI. The above steps are illustrated in Supporting Information Figure 1. Such a procedure has proven to be particularly well-suited for analyzing depth-electrode recordings in populations of ten to twenty patients [Jung et al., 2008; Mainy et al., 2007].

ONLINE MONITORING OF INTRACRANIAL OSCILLATORY ACTIVITY (BRAIN TV)

In a recent implementation, we proposed an iEEG real-time system that computes and displays the variations of ongoing alpha, beta and gamma-band activations at each recording site [Lachaux et al., 2007a]. The system, dubbed *Brain TV*, allows the experimenter, clinical staff as well as the patient to visualize the immediate effect of his behavior on brain oscillations. As an example, while monitoring iEEG activity in the superior temporal gyrus in one patient with the real-time system, a selective reactivity of the gamma activity to certain aspects of speech perception was suspected (such as perceiving a change of speaker). The hypothesis was then confirmed and fine-tuned using follow-up experiments tailor-designed to probe the observed phenomenon [Lachaux et al., 2007a]. A similar approach has also been used to map the motor cortex [Miller et al., 2007]. More importantly, the *Brain TV* set-up holds the potential of revealing previously unsuspected correlations between various mental events and the online display of oscillatory activity. Such events may also be covert cognitive operations and part of the patient's subjective experience.

Figure 5 shows an illustrative example of the application of the *Brain TV* platform. While monitoring the power of ongoing alpha oscillations measured by one specific electrode, the patient reported that a decrease in the displayed activity appeared to be associated with vision, in particular to focused vision. The monitored electrode position turned out to be in the superior parietal lobule (SPL, BA 7) and when cued to switch between a visual attention state and an auditory attention state systematic alternations between alpha suppression and enhancement were visible on the Brain TV set-up (Fig. 5b). These qualitative online observations provide single-trial evidence that alpha modulations in the SPL are modulated by visual attention.

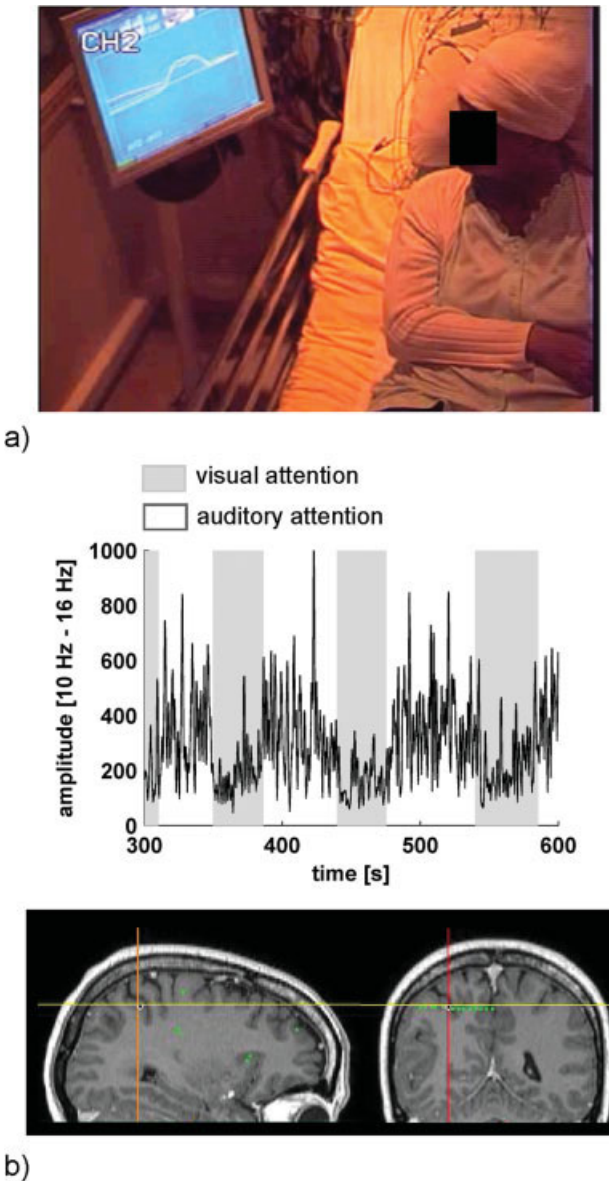

Figure 5.

Online measurements of visual attention with *Brain TV.* (**a**) The *Brain TV* set-up allows patients to visualize ongoing alpha, beta or gamma-band activity measured in real-time in specific regions of their brain. (**b**) Using the set-up, one patient was able to achieve online control of the activity recorded in her superior parietal lobe within the 10-16 Hz frequency range. She reported her ability to modulate the activity by focusing her attention on distant visual objects. The subject was then cued to switch between auditory and visual attention. The graph depicts the online variations of the activity as she shifted her attention back and forth between vision (in gray) and audition (in white). These online observations of alpha ERD during visual attention are inline with previous offline studies.

Beyond investigating the functional role of neural oscillations, the online system also has immediate applications as a clinical tool for pre-surgical mapping (as a complement to electrocortical stimulation) [Lachaux et al., 2007a] and can be directly used in explorative investigations for the development of novel brain computer interface (BCI) strategies [Jerbi et al., 2007, in press].

IMPLICATIONS FOR MEG AND EEG

Invasive EEG recordings are restricted to a number of clinical conditions that require the surgical implantation of intracerebral recordings. Therefore, while it is fortunate that access to such data is sometimes possible for research purposes, it is clearly an exceptional setting. It is therefore important to ask whether the findings obtained via access to such fine-scale recordings in humans has implications on investigations based on non-invasive electrophysiological techniques such as MEG and scalp-EEG. Indeed, findings of iEEG would almost invariably benefit from a validation in a large population of healthy subjects. Of course, this assumes that the phenomena reported invasively can also be detected using non-invasive techniques. In particular, it is unclear to which extent the growing body of evidence on high gamma activity (60–200 Hz) reported with iEEG can be replicated using EEG and MEG. The detection of gamma-band activity in EEG and MEG signals is complicated by several factors related in one way or another to a low SNR at this high frequency range. EEG and MEG sensors inherently measure the summed activity from multiple neural populations. While the skull is assumed to have similar impedance at both low and high frequencies, active patches of cortex can exhibit large phase variability, and the resulting polyphasic summation effectively results in lowpass filtering [Pfurtscheller and Cooper, 1975]. As discussed above, the spatial extent of oscillatory power modulations in the high gamma range is generally more focal than in the lower alpha and beta frequencies [Crone et al. 1998a; Edwards et al. 2005], which implies less signal reaches the scalp since the active patch may be relatively small. A further issue that limits the detectability of high gamma activity is the presence of artifacts. EEG and MEG signals can be contaminated by EMG signals from oculomotor and head muscles with spectral characteristics similar to that of physiological gamma-band activity [Yuval-Greenberg et al., 2008].

Despite these limitations, several studies have reported gamma-band activity using MEG or EEG in a variety of experimental conditions, including motor [Ball et al., 2008; Cheyne et al., 2008; Dalal et al., 2008b; de Lange et al., 2008; Gonzalez et al., 2006; Pfurtscheller et al., 1993; Salenius et al., 1996], oculomotor [Jerbi et al., 2008; Medendorp et al., 2007; Van der Werf et al., 2008], sensory [Hoogenboom et al., 2006; Tecchio et al., 2008], visual [Chaumon et al., 2008; Muthukumaraswamy and Singh, 2008a; Rodriguez et al., 1999; Tanji et al., 2005] behavior as well as in decision making [Guggisberg et al., 2007] pain [Gross et al., 2007] and attention [Schurger et al., 2008; Vidal et al., 2006] processes.

In general, the increasing number of reports of widely distributed networks of high gamma activity detected with iEEG in various experiments and across numerous structures suggests that increasing sensitivity to high frequency oscillations might be a priority for future research with non-invasive techniques. This may be achieved by optimizing three distinct aspects of non-invasive studies: (1) Adapted experimental design: one way to compensate for the low SNR of high gamma activity is to ensure a large number of trials (e.g., 200 trials or more) per condition. In addition, the design should be carefully adapted to the source estimation procedure that will be subsequently used. This might involve ensuring sufficiently long epochs to improve the estimation of signal and noise covariance. Furthermore, block design experiments, if suitable to the investigated question, might help drive the neural networks into a sustained activation state, which could positively affect the SNR, compared to that associated with transient neural phenomena. (2) Improving artifact detection and rejection: As discussed above, disambiguating physiological and artifactual gamma range activity is a non-negligible concern. This can be enhanced by systematic and accurate monitoring of the possible source of artifact. Electromyograms and electrooculograms (EOG) should be used systematically and the respective traces should be used both for visual inspection and automatic or semi-automatic artifact detection. Independent component analysis may also be used for artifact removal. Furthermore, in the light of recent concerns linking miniature saccades and gamma components of the EEG [Yuval-Greenberg et al., 2008], accurate monitoring of eye movements using dedicated eye-tracking systems might become critical for future studies. Note however, that although this issue might be of direct relevance to scalp-EEG studies, it may be less critical issue for MEG which is reference-free. Indeed the artifact was shown to be prominent for nose-referenced EEG data which re-injects the microsaccadic activity into distant occipital electrodes. Nevertheless, the susceptibility of MEG to contamination by microsaccade artifacts requires further investigation. As a matter of fact, we have recently shown that even iEEG, which is predominantly immune to saccade artefacts, can display artifactual gamma power increases at depth electrodes located close to the extra-ocular eye muscles [Jerbi et al., 2009]. (3) Using source reconstructions: source reconstruction techniques may potentially prove to be crucial for the detection of task-related high gamma activity that is not readily detectable at the sensor level. Source estimation based on minimum norm solutions or on beamforming have successfully been used in the past to detect high gamma (>60 Hz) activity in MEG data [Cheyne et al., 2008; Dalal et al., 2008b; Van Der Werf et al., 2008]. Insights into optimizing source estimation techniques to increase sensitivity to high gamma activity will definitely benefit from recent studies of simultaneous acquisitions of iEEG and MEG recordings

in the same patient (Dalal et al., in press; Lachaux et al., 2007c]. Moreover, source estimation of such high frequency activity may also be improved by the use of data from iEEG as a source of a priori constraints for EEG/MEG source analysis. Additionally, granted that future studies firmly establish that BOLD and gamma-band activity are indeed tightly linked, then fMRI studies could also be used to provide a priori knowledge of the origin of gamma-band responses and be used for EEG/MEG source localization. Finally, investigating the correspondence between lower frequency findings in invasive and non-invasive recordings is equally crucial. For instance, the discrepancy between the spatial and functional specificity of alpha versus beta motor rhythms reported in MEG [Salmelin et al., 1995] and the lack thereof in some iEEG studies will have to be resolved.

CONCLUSION

Albeit being sometimes faced with a fair share of skepticism or, at times, with excessive fascinations, intracranial recordings in humans has grown into a field of its own providing a steady stream of novel observations that have advanced our understanding of brain function. Intracerebral recordings, especially of gamma activity, may play a pivotal role in providing a means to better understand the links to data reported in animal electrophysiology and to findings of neuroimaging studies. In addition, advances in non-invasive electrophysiological recordings will be key to validating and possibly extending findings of invasive studies. Future trends include increased direct sampling of single-unit neural activity in the human brain via various microelectrode recording techniques [Neves and Ruther, 2007; Ulbert et al., 2001]. Combining microelectrode data and population level recordings will be crucial in order to elucidate the neural mechanisms that encode information processing and communication within local and large-scale cerebral networks. This said, the increasing scientific appeal of invasive human recordings will also have to be associated with enhanced vigilance to questions of ethics and patient safety.

ACKNOWLEDGMENTS

Support provided in part by the EC research program NeuroProbes (FP6-IST 027017) to K.J., the EC Marie Curie Fellowship (FP7-221097) to S.S.D., the CONICYT (Chile) doctoral fellowship to C.M.H., and a doctoral fellowship from the Ministère de l'Education Nationale et la Recherche (France) to T.O. is acknowledged.

REFERENCES

Adrian ED (1941): Afferent discharges to the cerebral cortex from peripheral sense organs. J Physiol 100:159–191.

Allison T, Puce A, Spencer DD, McCarthy G (1999): Electrophysiological studies of human face perception. I. Potentials generated in occipitotemporal cortex by face and non-face stimuli. Cereb Cortex 9:415–430.

Aoki F, Fetz EE, Shupe L, Lettich E, Ojemann GA (1999): Increased gamma-range activity in human sensorimotor cortex during performance of visuomotor tasks. Clin Neurophysiol 110:524–537.

Axmacher N, Elger CE, Fell J (2008a): Ripples in the medial temporal lobe are relevant for human memory consolidation. Brain 131:1806–1817.

Axmacher N, Schmitz DP, Wagner T, Elger CE, Fell J (2008b): Interactions between medial temporal lobe, prefrontal cortex, and inferior temporal regions during visual working memory: A combined intracranial EEG and functional magnetic resonance imaging study. J Neurosci 28:7304–7312.

Ball T, Demandt E, Mutschler I, Neitzel E, Mehring C, Vogt K, Aertsen A, Schulze-Bonhage A (2008): Movement related activity in the high gamma range of the human EEG. Neuroimage 41:302–310.

Benazzouz A, Breit S, Koudsie A, Pollak P, Krack P, Benabid AL (2002): Intraoperative microrecordings of the subthalamic nucleus in Parkinson's disease. Mov Disord 17 (Suppl 3):S145–S149.

Berger H (1929): Über das Elektrenkephalogramm des Menschen. Arch Psychiatr Nervenkr 87:527–570.

Bidet-Caulet A, Bertrand O (2005): Dynamics of a temporo-fronto-parietal network during sustained spatial or spectral auditory processing. J Cogn Neurosci 17:1691–1703.

Brovelli A, Lachaux JP, Kahane P, Boussaoud D (2005): High gamma frequency oscillatory activity dissociates attention from intention in the human premotor cortex. Neuroimage 28:154–164.

Canolty RT, Edwards E, Dalal SS, Soltani M, Nagarajan SS, Kirsch HE, Berger MS, Barbaro NM, Knight RT (2006): High gamma power is phase-locked to theta oscillations in human neocortex. Science 313:1626–1628.

Chatrian GE, Bickford RG, Uihlein A (1960): Depth electrographic study of a fast rhythm evoked from the human calcarine region by steady illumination. Electroencephalogr Clin Neurophysiol 12:167–176.

Chaumon M, Schwartz D, Tallon-Baudry C (2008): Unconscious learning versus visual perception: Dissociable roles for gamma oscillations revealed in MEG. J Cogn Neurosci. (in press).

Cheyne D, Bells S, Ferrari P, Gaetz W, Bostan AC (2008): Self-paced movements induce high-frequency gamma oscillations in primary motor cortex. Neuroimage 42:332–342.

Crone NE, Sinai A, Korzeniewska A (2006): High-frequency gamma oscillations and human brain mapping with electrocorticography. Prog Brain Res 159:275–295.

Crone NE, Miglioretti DL, Gordon B, Lesser RP (1998a): Functional mapping of human sensorimotor cortex with electrocorticographic spectral analysis. II. Event-related synchronization in the gamma band. Brain 121 (Part 12):2301–2315.

Crone NE, Boatman D, Gordon B, Hao L (2001a): Induced electrocorticographic gamma activity during auditory perception. Brazier Award-winning article, 2001. Clin Neurophysiol 112:565–582.

Crone NE, Miglioretti DL, Gordon B, Sieracki JM, Wilson MT, Uematsu S, Lesser RP (1998b): Functional mapping of human sensorimotor cortex with electrocorticographic spectral analysis. I. Alpha and beta event-related desynchronization. Brain 121 (Part 12):2271–2299.

Crone NE, Hao L, Hart J Jr, Boatman D, Lesser RP, Irizarry R, Gordon B (2001b): Electrocorticographic gamma activity during word production in spoken and sign language. Neurology 57:2045–2053.

Dalal SS, Edwards E, Kirsch HE, Barbaro NM, Knight RT, Nagarajan SS (2008a): Localization of neurosurgically implanted electrodes via photograph-MRI-radiograph coregistration. J Neurosci Methods 174:106–115.

Dalal SS, Guggisberg AG, Edwards E, Sekihara K, Findlay AM, Canolty RT, Berger MS, Knight RT, Barbaro NM, Kirsch HE, Nagarajan SS (2008b): Five-dimensional neuroimaging: Localization of the time-frequency dynamics of cortical activity. Neuroimage 40:1686–1700.

Dalal SS, Baillet S, Adam C, Ducorps A, Jerbi K, Bertrand O, Garnero L, Martinerie J, Lachaux J-P: Simultaneous MEG and intracranial EEG recordings during attentive reading. NeuroImage (in press).

de Lange FP, Jensen O, Bauer M, Toni I (2008): Interactions between posterior gamma and frontal alpha/beta oscillations during imagined actions. Front Hum Neurosci 2:7.

Eckhorn R, Bauer R, Jordan W, Brosch M, Kruse W, Munk M, Reitboeck HJ (1988): Coherent oscillations: A mechanism of feature linking in the visual cortex? Multiple electrode and correlation analyses in the cat. Biol Cybern 60:121–130.

Edwards E, Soltani M, Deouell LY, Berger MS, Knight RT (2005): High gamma activity in response to deviant auditory stimuli recorded directly from human cortex. J Neurophysiol 94:4269–4280.

Ekstrom AD, Caplan JB, Ho E, Shattuck K, Fried I, Kahana MJ (2005): Human hippocampal theta activity during virtual navigation. Hippocampus 15:881–889.

Engel AK, Moll CK, Fried I, Ojemann GA (2005): Invasive recordings from the human brain: Clinical insights and beyond. Nat Rev Neurosci 6:35–47.

Engel J (1996): Surgery for seizures. N Engl J Med 334:647–652.

Fell J, Klaver P, Elger CE, Fernandez G (2002): The interaction of rhinal cortex and hippocampus in human declarative memory formation. Rev Neurosci 13:299–312.

Fell J, Ludowig E, Rosburg T, Axmacher N, Elger CE (2008): Phase-locking within human mediotemporal lobe predicts memory formation. Neuroimage 43:410–419.

Fell J, Klaver P, Lehnertz K, Grunwald T, Schaller C, Elger CE, Fernandez G (2001): Human memory formation is accompanied by rhinal-hippocampal coupling and decoupling. Nat Neurosci 4:1259–1264.

Freeman WJ (1978): Spatial properties of an EEG event in the olfactory bulb and cortex. Electroencephalogr Clin Neurophysiol 44:586–605.

Fried I, MacDonald KA, Wilson CL (1997): Single neuron activity in human hippocampus and amygdala during recognition of faces and objects. Neuron 18:753–765.

Fries P (2005): A mechanism for cognitive dynamics: Neuronal communication through neuronal coherence. Trends Cogn Sci 9:474–480.

Gonzalez SL, Grave de Peralta R, Thut G, Millan Jdel R, Morier P, Landis T (2006): Very high frequency oscillations (VHFO) as a predictor of movement intentions. Neuroimage 32:170–179.

Gray CM, Konig P, Engel AK, Singer W (1989): Oscillatory responses in cat visual cortex exhibit inter-columnar synchronization which reflects global stimulus properties. Nature 338:334–337.

Gross J, Schnitzler A, Timmermann L, Ploner M (2007): Gamma oscillations in human primary somatosensory cortex reflect pain perception. PLoS Biol 5:e133.

Gruber T, Muller MM, Keil A, Elbert T (1999): Selective visual–spatial attention alters induced gamma band responses in the human EEG. Clin Neurophysiol 110:2074–2085.

Guggisberg AG, Dalal SS, Findlay AM, Nagarajan SS (2007): High-frequency oscillations in distributed neural networks reveal the dynamics of human decision making. Front Hum Neurosci 1:14.

Halgren E, Marinkovic K, Chauvel P (1998): Generators of the late cognitive potentials in auditory and visual oddball tasks. Electroencephalogr Clin Neurophysiol 106:156–164.

Halgren E, Baudena P, Heit G, Clarke JM, Marinkovic K, Clarke M (1994): Spatio-temporal stages in face and word processing. I. Depth-recorded potentials in the human occipital, temporal and parietal lobes [corrected]. J Physiol Paris 88:1–50.

Heit G, Smith ME, Halgren E (1988): Neural encoding of individual words and faces by the human hippocampus and amygdala. Nature 333:773–775.

Hoogenboom N, Schoffelen JM, Oostenveld R, Parkes LM, Fries P (2006): Localizing human visual gamma-band activity in frequency, time and space. Neuroimage 29:764–773.

Jasper H, Penfield W (1949): Electrocorticograms in man: Effect of voluntary movement upon the electrical activity of the precentral gyrus. Arch Psychiatr Nervenkr 183:162–174.

Jensen O, Colgin LL (2007): Cross-frequency coupling between neuronal oscillations. Trends Cogn Sci 11:267–269.

Jensen O, Kaiser J, Lachaux JP (2007): Human gamma-frequency oscillations associated with attention and memory. Trends Neurosci 30:317–324.

Jerbi K, Freyermuth S, Minotti L, Kahane P, Berthoz A, Lachaux JP: Watching brain TV and playing brain ball: Exploring novel BCI strategies using real-time analysis of human intracranial data. Int Rev Neurobiol (in press).

Jerbi K, Bertrand O, Schoendorff B, Hoffmann D, Minotti L, Kahane P, Berthoz A, Lachaux JP (2007): Online detection of gamma oscillations in ongoing intracerebral recordings: From functional mapping to brain computer interfaces. In: Joint Meeting of the 6th International Symposium on Noninvasive Functional Source Imaging of the Brain and Heart and the International Conference on Functional Biomedical Imaging, 2007. NFSI-ICFBI 2007, Hangzhou. pp 330–333.

Jerbi K, Freyermuth S, Dalal SS, Kahane P, Bertrand O, Berthoz A, Lachaux JP (2009): Saccade related gamma-band activity in intracerebral EEG: Dissociating neural from ocular muscle activity. Brain Topogr (in press).

Jerbi K, Hamamé CM, Ossandón T, Dalal SS (2008): Role of posterior parietal gamma activity in planning prosaccades and antisaccades. J Neurosci 28:13713–13715.

Jung J, Hudry J, Ryvlin P, Royet JP, Bertrand O, Lachaux JP (2006): Functional significance of olfactory-induced oscillations in the human amygdala. Cereb Cortex 16:1–8.

Jung J, Mainy N, Kahane P, Minotti L, Hoffmann D, Bertrand O, Lachaux JP (2008): The neural bases of attentive reading. Hum Brain Mapp 29:1193–1206.

Kahana MJ, Seelig D, Madsen JR (2001): Theta returns. Curr Opin Neurobiol 11:739–744.

Kahane P, Minotti L, Hoffmann D, Lachaux J, Ryvlin P (2004): Invasive EEG in the definition of the seizure onset zone: Depth electrodes. In: Rosenow F, Lüders HO, editors. Handbook of Clinical Neurophysiology. Pre-Surgical Assessment of the Epilepsies With Clinical Neurophysiology and Functional Neuroimaging. Amsterdam; Boston: Elsevier Science.

Kahane P, Landre E, Minotti L, Francione S, Ryvlin P (2006): The Bancaud and Talairach view on the epileptogenic zone: A working hypothesis. Epileptic Disord 8 Suppl 2:S16–S26.

Karakas S, Erzengin OU, Basar E (2000): The genesis of human event-related responses explained through the theory of oscillatory neural assemblies. Neurosci Lett 285:45–48.

Kayser C, Kim M, Ugurbil K, Kim DS, Konig P (2004): A comparison of hemodynamic and neural responses in cat visual cortex using complex stimuli. Cereb Cortex 14:881–891.

Kreiman G, Koch C, Fried I (2000): Imagery neurons in the human brain. Nature 408:357–361.

Krolak-Salmon P, Henaff MA, Tallon-Baudry C, Yvert B, Guenot M, Vighetto A, Mauguiere F, Bertrand O (2003): Human lateral geniculate nucleus and visual cortex respond to screen flicker. Ann Neurol 53:73–80.

Lachaux JP, Rudrauf D, Kahane P (2003): Intracranial EEG and human brain mapping. J Physiol Paris 97:613–628.

Lachaux JP, Hoffmann D, Minotti L, Berthoz A, Kahane P (2006a): Intracerebral dynamics of saccade generation in the human frontal eye field and supplementary eye field. Neuroimage 30:1302–1312.

Lachaux JP, Rodriguez E, Martinerie J, Adam C, Hasboun D, Varela FJ (2000): A quantitative study of gamma-band activity in human intracranial recordings triggered by visual stimuli. Eur J Neurosci 12:2608–2622.

Lachaux JP, Jerbi K, Bertrand O, Minotti L, Hoffmann D, Schoendorff B, Kahane P (2007a): A blueprint for real-time functional mapping via human intracranial recordings. PLoS ONE 2: e1094.

Lachaux JP, Fonlupt P, Kahane P, Minotti L, Hoffmann D, Bertrand O, Baciu M (2007b): Relationship between task-related gamma oscillations and BOLD signal: New insights from combined fMRI and intracranial EEG. Hum Brain Mapp 28:1368–1375.

Lachaux JP, George N, Tallon-Baudry C, Martinerie J, Hugueville L, Minotti L, Kahane P, Renault B (2005): The many faces of the gamma band response to complex visual stimuli. Neuroimage 25:491–501.

Lachaux JP, Baillet S, Adam C, Ducorps A, Jerbi K, Bertrand O, Garnero L, Martinerie J (2007c): A simultaneous MEG and intracranial EEG study of task-related brain oscillations. In: New Frontiers in Biomagnetism. Proceedings of the 15th International Conference on Biomagnetism, Vancouver, BC, Canada, August 21–25, 2006. International Congress Series, Elsevier. 1300:421–424.

Lachaux JP, Jung J, Mainy N, Dreher JC, Bertrand O, Baciu M, Minotti L, Hoffmann D, Kahane P (2008): Silence is golden: Transient neural deactivation in the prefrontal cortex during attentive reading. Cereb Cortex 18:443–450.

Lakatos P, Karmos G, Mehta AD, Ulbert I, Schroeder CE (2008): Entrainment of neuronal oscillations as a mechanism of attentional selection. Science 320:110–113.

Logothetis NK, Pauls J, Augath M, Trinath T, Oeltermann A (2001): Neurophysiological investigation of the basis of the fMRI signal. Nature 412:150–157.

Mainy N, Kahane P, Minotti L, Hoffmann D, Bertrand O, Lachaux JP (2007a): Neural correlates of consolidation in working memory. Hum Brain Mapp 28:183–193.

Mainy N, Jung J, Baciu M, Kahane P, Schoendorff B, Minotti L, Hoffmann D, Bertrand O, Lachaux JP (2008): Cortical dynamics of word recognition. Hum Brain Mapp 29:1215–1230.

Mazaheri A, Jensen O (2008): Asymmetric amplitude modulations of brain oscillations generate slow evoked responses. J Neurosci 28:7781–7787.

Medendorp WP, Kramer GF, Jensen O, Oostenveld R, Schoffelen JM, Fries P (2007): Oscillatory activity in human parietal and occipital cortex shows hemispheric lateralization and memory effects in a delayed double-step saccade task. Cereb Cortex 17:2364–2374.

Mehring C, Nawrot MP, de Oliveira SC, Vaadia E, Schulze-Bonhage A, Aertsen A, Ball T (2004): Comparing information about arm movement direction in single channels of local and epicortical field potentials from monkey and human motor cortex. J Physiol Paris 98:498–506.

Menon V, Freeman WJ, Cutillo BA, Desmond JE, Ward MF, Bressler SL, Laxer KD, Barbaro N, Gevins AS (1996): Spatio-temporal correlations in human gamma band electrocorticograms. Electroencephalogr Clin Neurophysiol 98:89–102.

Miller KJ, denNijs M, Shenoy P, Miller JW, Rao RP, Ojemann JG (2007): Real-time functional brain mapping using electrocorticography. Neuroimage 37:504–507.

Münte TF, Heldmann M, Hinrichs H, Marco-Pallares J, Krämer UM, Sturm V, Heinze H (2008): Nucleus accumbens is involved in human action monitoring: Evidence from invasive electrophysiological recordings. Front Hum Neurosci 1:11.

Murthy VN, Fetz EE (1992): Coherent 25- to 35-Hz oscillations in the sensorimotor cortex of awake behaving monkeys. Proc Natl Acad Sci USA 89:5670–5674.

Muthukumaraswamy SD, Singh KD (2008a): Functional decoupling of BOLD and gamma-band amplitudes in human primary visual cortex. Hum Brain Mapp.

Muthukumaraswamy SD, Singh KD (2008b): Spatiotemporal frequency tuning of BOLD and gamma band MEG responses compared in primary visual cortex. Neuroimage 40:1552–1560.

Neves HP, Ruther P (2007): The NeuroProbes Project. Conf Proc IEEE Eng Med Biol Soc 2007:6443–6445.

Niessing J, Ebisch B, Schmidt KE, Niessing M, Singer W, Galuske RA (2005): Hemodynamic signals correlate tightly with synchronized gamma oscillations. Science 309:948–951.

Nikulin VV, Linkenkaer-Hansen K, Nolte G, Lemm S, Muller KR, Ilmoniemi RJ, Curio G (2007): A novel mechanism for evoked responses in the human brain. Eur J Neurosci 25:3146–3154.

Nishida M, Juhasz C, Sood S, Chugani HT, Asano E (2008): Cortical glucose metabolism positively correlates with gamma-oscillations in nonlesional focal epilepsy. Neuroimage 42:1275–1284.

Ojemann GA, Schoenfield-McNeill J, Corina DP (2002): Anatomic subdivisions in human temporal cortical neuronal activity related to recent verbal memory. Nat Neurosci 5:64–71.

Pfurtscheller G, Cooper R (1975): Frequency dependence of the transmission of the EEG from cortex to scalp. Electroencephalogr Clin Neurophysiol 38:93–96.

Pfurtscheller G, Neuper C, Kalcher J (1993): 40-Hz oscillations during motor behavior in man. Neurosci Lett 164:179–182.

Pfurtscheller G, Graimann B, Huggins JE, Levine SP, Schuh LA (2003): Spatiotemporal patterns of beta desynchronization and gamma synchronization in corticographic data during self-paced movement. Clin Neurophysiol 114:1226–1236.

Pistohl T, Ball T, Schulze-Bonhage A, Aertsen A, Mehring C (2008): Prediction of arm movement trajectories from ECoG-recordings in humans. J Neurosci Methods 167:105–114.

Poghosyan V, Ioannides AA (2007): Precise mapping of early visual responses in space and time. Neuroimage 35:759–770.

Raghavachari S, Kahana MJ, Rizzuto DS, Caplan JB, Kirschen MP, Bourgeois B, Madsen JR, Lisman JE (2001): Gating of human theta oscillations by a working memory task. J Neurosci 21:3175–3183.

Ray S, Niebur E, Hsiao SS, Sinai A, Crone NE (2008): High-frequency gamma activity (80–150 Hz) is increased in human cortex during selective attention. Clin Neurophysiol 119:116–133.

Rickert J, Oliveira SC, Vaadia E, Aertsen A, Rotter S, Mehring C (2005): Encoding of movement direction in different frequency ranges of motor cortical local field potentials. J Neurosci 25:8815–8824.

Rodriguez E, George N, Lachaux JP, Martinerie J, Renault B, Varela FJ (1999): Perception's shadow: Long-distance synchronization of human brain activity. Nature 397:430–433.

Rougeul-Buser A, Bouyer JJ, Buser P (1975): From attentiveness to sleep. A topographical analysis of localized "synchronized" activities on the cortex of normal cat and monkey. Acta Neurobiol Exp (Wars) 35:805–819.

Salenius S, Salmelin R, Neuper C, Pfurtscheller G, Hari R (1996): Human cortical 40 Hz rhythm is closely related to EMG rhythmicity. Neurosci Lett 213:75–78.

Salmelin R, Hamalainen M, Kajola M, Hari R (1995): Functional segregation of movement-related rhythmic activity in the human brain. Neuroimage 2:237–243.

Schmolesky MT, Wang Y, Hanes DP, Thompson KG, Leutgeb S, Schall JD, Leventhal AG (1998): Signal timing across the macaque visual system. J Neurophysiol 79:3272–3278.

Schurger A, Cowey A, Cohen JD, Treisman A, Tallon-Baudry C (2008): Distinct and independent correlates of attention and awareness in a hemianopic patient. Neuropsychologia 46:2189–2197.

Sederberg PB, Schulze-Bonhage A, Madsen JR, Bromfield EB, McCarthy DC, Brandt A, Tully MS, Kahana MJ (2007): Hippocampal and neocortical gamma oscillations predict memory formation in humans. Cereb Cortex 17:1190–1196.

Singer W (1999): Neuronal synchrony: A versatile code for the definition of relations? Neuron 24:49–65. See also pp. 111–125.

Singer W, Gray CM (1995): Visual feature integration and the temporal correlation hypothesis. Annu Rev Neurosci 18:555–586.

Szurhaj W, Bourriez JL, Kahane P, Chauvel P, Mauguiere F, Derambure P (2005): Intracerebral study of gamma rhythm reactivity in the sensorimotor cortex. Eur J Neurosci 21:1223–1235.

Tallon-Baudry C, Bertrand O (1999): Oscillatory gamma activity in humans and its role in object representation. Trends Cogn Sci 3:151–162.

Tallon-Baudry C, Bertrand O, Delpuech C, Pernier J (1996): Stimulus specificity of phase-locked and non-phase-locked 40 Hz visual responses in human. J Neurosci 16:4240–4249.

Tallon-Baudry C, Bertrand O, Henaff MA, Isnard J, Fischer C (2005): Attention modulates gamma-band oscillations differently in the human lateral occipital cortex and fusiform gyrus. Cereb Cortex 15:654–662.

Tanji K, Suzuki K, Delorme A, Shamoto H, Nakasato N (2005): High-frequency gamma-band activity in the basal temporal cortex during picture-naming and lexical-decision tasks. J Neurosci 25:3287–3293.

Tecchio F, Zappasodi F, Porcaro C, Barbati G, Assenza G, Salustri C, Rossini PM (2008): High-gamma band activity of primary hand cortical areas: A sensorimotor feedback efficiency index. Neuroimage 40:256–264.

Ulbert I, Halgren E, Heit G, Karmos G (2001): Multiple microelectrode-recording system for human intracortical applications. J Neurosci Methods 106:69–79.

Van Der Werf J, Jensen O, Fries P, Medendorp WP (2008): Gamma-band activity in human posterior parietal cortex encodes the motor goal during delayed prosaccades and antisaccades. J Neurosci 28:8397–8405.

Vidal JR, Chaumon M, O'Regan JK, Tallon-Baudry C (2006): Visual grouping and the focusing of attention induce gamma-band oscillations at different frequencies in human magnetoencephalogram signals. J Cogn Neurosci 18:1850–1862.

Ward AA, Thomas LB (1955): The electrical activity of single units in the cerebral cortex of man. Electroencephalogr Clin Neurophysiol 7:135–136.

Yuval-Greenberg S, Tomer O, Keren AS, Nelken I, Deouell LY (2008): Transient induced gamma-band response in EEG as a manifestation of miniature saccades. Neuron 58:429–441.

Brain Responses to Success and Failure: Direct Recordings from Human Cerebral Cortex

Julien Jung,[1,2]* Karim Jerbi,[1,3] Tomas Ossandon,[1] Philippe Ryvlin,[1,2] Jean Isnard,[1,4] Olivier Bertrand,[1] Marc Guénot,[4,5] François Mauguière,[2,4] and Jean-Philippe Lachaux[1]

[1]*Brain Dynamics and Cognition, INSERM U821, Lyon, France*
[2]*Department of Epileptology and Functional Neurology, Neurological Hospital, Lyon, France*
[3]*Physiology of Perception and Action Laboratory, CNRS, UMR 7152, Collège de France, Paris, France*
[4]*Sensory Integration of Pain, INSERM U879, Lyon, France*
[5]*Department of Neurosurgery, Neurological Hospital, Lyon, France*

Abstract: Evaluating the outcome of our own actions is a fundamental process by which we adapt our behavior in our interaction with the external world. fMRI and electrophysiological studies in monkeys have found feedback-specific responses in several brain regions, unveiling facets of a large-scale network predominantly distributed in the frontal lobes. However, a consensus has yet to be reached regarding the exact contribution of each region. The present study benefited from intracerebral EEG recordings in epileptic patients to record directly the neural activity in each of those frontal structures in response to positive and negative feedback. Both types of feedback induced a sequence of high-frequency responses (>40 Hz) in a widespread network involving medial frontal cortex, dorsolateral prefrontal cortex (DLPFC), orbitofrontal cortex (OFC), and insular cortex. The pre-supplementary motor area (pre-SMA), DLPFC, and lateral OFC showed higher activation in response to negative feedback, while medial OFC and dorsal anterior cingulate cortex (dACC) were more responsive to positive feedback. Responses in the medial prefrontal cortex (pre-SMA and dACC) were sustained (lasting more than 1,000 ms), while responses in the DLPFC, insula, and the OFC were short lasting (less than 800 ms). Taken together, our findings show that evaluating the outcome of our actions triggers γ-range activity modulations in several frontal and insular regions. Moreover, we found that the timing and amplitude of those γ-band responses reveal fine-scale dissociations between the neural dynamics of positive versus negative feedback processing. *Hum Brain Mapp 00:000–000, 2010.* © 2010 Wiley-Liss, Inc.

Key words: γ-band oscillations; intracranial EEG; performance monitoring; epilepsy; executive functions

INTRODUCTION

"... We regret to inform you that we cannot recommend your manuscript for publication ...". Whether you are a researcher reading such a notification or an NBA player witnessing the fraction of a second your ball bounces backwards off the rim of the basketball, your interaction with the outside world is a constant source of feedback evaluating your actions on multiple time scales.

Additional Supporting Information may be found in the online version of this article.

Contract grant sponsor: NeuroProbes (EU Research Program); Contract grant number: FP6-IST 027017 (to KJ); Contract grant sponsor: NeuroBotics (EU Research Program); Contract grant number: FET FP6-IST-001917 (to KJ).

*Correspondence to: Julien Jung, MD, PhD, Brain Dynamics and Cognition, INSERM - Unité 821, Centre Hospitalier Le Vinatier, Bâtiment 452, 95 Boulevard Pinel, 69500 Bron, France. E-mail: julien.jung@inserm.fr

Received for publication 9 January 2009; Revised 28 July 2009; Accepted 28 September 2009

DOI: 10.1002/hbm.20930

Published online in Wiley InterScience (www.interscience.wiley.com).

Our ability to use this feedback to adapt our behavior is critical in all aspects of our life. Lesion studies and the effect of pathologies have shown that this capacity depends critically on the frontal cortex (Alexander et al., 2007; Polli et al., 2008; Thakkar et al., 2008)

In the last 15 years, electrophysiological and neuroimaging studies have provided a more detailed understanding of how the frontal cortex respond to negative (or positive) feedback. Human event-related potential (ERP) studies have shown that negative feedback signals generate an enhanced negative component, as compared to positive feedback, peaking over frontocentral electrodes with a latency of 300 ms (Miltner et al., 1997) and referred to as "feedback-related negativity (FRN)" [but see Holroyd et al. (2008) for alternative interpretation]. Several EEG studies using Source localization have identified the anterior cingulate cortex (dACC) as the most likely generator of the FRN (Gehring and Willoughby, 2002; Luu et al., 2003; Miltner et al., 1997; Ruchsow et al., 2002). In accordance, several fMRI studies have shown increased dACC activation when subjects receive negative feedback (Holroyd et al., 2004; Ullsperger and von Cramon, 2003) despite some discrepancies across studies (Cools et al., 2002; Nieuwenhuis et al., 2005; van Veen et al., 2004).

Moreover, fMRI studies have shown that feedback evaluation activates not only the dACC but also several brain regions including medial prefrontal cortex (Ullsperger and von Cramon, 2003), dorsolateral prefrontal cortex (DLPFC) (Zanolie et al., 2008), orbitofrontal cortex (OFC) (Walton et al., 2004; Zanolie et al., 2008), and insula (Zanolie et al., 2008), depending on the studies.

Single-cell recordings in nonhuman primates indicate that feedback evaluation leads to modulations of neuronal firing in several structures within that frontal network including the dACC (Ito et al., 2003; Michelet et al., 2007; Quilodran et al., 2008), the DLPFC (Matsumoto et al., 2007), and the OFC (Wallis, 2007).

Clearly, feedback stimuli elicit distributed neural responses in a brain network that seems to be more complex than what was initially suggested by source localization of the FRN in human ERP studies. fMRI studies, backed up by monkey electrophysiology, have shown that this network might involve not only the medial frontal cortex including the dACC and pre-supplementary motor area (pre-SMA), but also the DLPFC, the OFC, and the insula. However, to our knowledge, all previous studies have reported only piecewise activations of that network, the exact extent of which remains undetermined. Moreover, the timing of activation of those structures during feedback evaluation remains largely unknown.

The objective of the present study was to clarify the neural bases of feedback evaluation by recording the response to feedback stimuli in all previous structures in humans, with direct neural recordings. Direct electrophysiological recordings can be achieved in epileptic patients with intracerebral electrodes implanted for therapeutic purposes (Lachaux et al., 2003), to record neural activity with a spatial resolution comparable to fMRI, and millisecond temporal resolution. In particular, stereo-encephalography (SEEG), using linear-electrode areas recording from both lateral and mesial structures, from both gyri and sulci, provides a unique opportunity to investigate all regions assumed to participate in feedback monitoring, such as the DLPFC and the dACC.

The present work was triggered by a recent series of intracranial EEG studies showing that broadband energy increase of neural signals (50–150 Hz, the so-called γ-band) constitutes a precise marker identifying neural recruitment during cognitive processing (Jensen et al., 2007; Jerbi et al., 2009; Lachaux et al., 2003). Such γ-band responses (GBRs) have been used to map the large-scale cortical networks underlying several major cognitive functions, including language processing (Jung et al., 2008; Mainy et al., 2008), memory (Mainy et al., 2007), attention (Jensen et al., 2007), and top–down processes (Engel et al., 2001; Kahana, 2006). Those results are in line with a possible role of γ-band neural synchronization in local and large-scale neural communication (Fries et al., 2007; Lee, 2003; Singer, 1999; Varela et al., 2001). Further, recent studies combining electrophysiological and BOLD measures using fMRI have found a strong correlation between GBRs and the BOLD signal (Lachaux et al., 2007; Logothetis et al., 2001; Mukamel et al., 2005). Based on those results, we predicted that feedback stimuli would trigger GBRs in several brain structures activated during fMRI studies, including the medial frontal wall, the DLPFC, the OFC, and the insula. Moreover, we anticipated that possible differences in timing would help delineate functional dissociations within that network.

MATERIALS AND METHODS

Participants

Nine subjects (six females and three males, aged 19–56 years, mean = 36 years) participated in this study. They all suffered from drug-resistant partial epilepsy and were candidates for surgery. They had normal or corrected-to-normal vision and were not colorblind. Because the location of the epileptic focus could not be identified using noninvasive methods, the patients underwent intracerebral EEG recordings by means of stereotactically implanted multilead depth electrodes (SEEG) [for a complete description of the rationale of electrode implantation, see Isnard et al. (2000)]. The selection of the sites to implant was made entirely for clinical purposes with no reference to the present experimental protocol. Patients who took part in this study were selected, because their implantation included various regions of the frontal lobe or insular cortex. The activated sites reported in the Results section were always outside of the seizure onset zone of the patients. The patients performed the task 2 days after the implantation of the electrodes. In agreement with French regulations relative to invasive investigations with a direct

TABLE I. Overview of anatomical regions exhibiting significant GBRs induced by feedback stimuli

	Pre-SMA	dACC	DLPFC	Mesial OFC	Lateral OFC	Insula
No. of sites recorded	9	11	15	9	9	10
No. of significant GBRs (% sites)	5 (55)	2 (18)	4 (27)	4 (44)	2 (22)	6 (60)
No. of nonspecific GBRs (% significant GBRs)	0 (0)	0 (0)	1 (25)	0 (0)	0 (0)	0 (0)
No. of positive feedback (% significant GBRs)	0 (0)	2 (100)	0 (0)	4 (100)	0 (0)	1 (17)
No. of negative feedback (% significant GBRs)	5 (100)	0 (0)	3 (75)	0 (0)	2 (100)	5 (83)

Feedback stimuli induced statistically significant GBRs clustered in a well-defined set of anatomical structures across patients. For each cluster, the total number of recording sites and the number and the percentage of sites with significant GBRs is provided. The number and percentage of sites with a feedback preference to error (negative), correct (positive), or nonspecific for each cluster is given.

individual benefit, patients were fully informed about electrode implantation, stereotactic EEG (SEEG), evoked potential recordings, and cortical stimulation procedures used to localize the epileptogenic and eloquent cortical areas, and the patients gave their informed consent.

Electrode Implantation and Coregistration

The electrodes used consisted of one-dimensional arrays implanted orthogonal to the interhemispheric plane using the Talairach's stereotactic grid. Brain activity was recorded in 5–15 contact sites along each electrode. Spacing between consecutive sites was 3.5 mm (center-to-center), which correspond to the estimated spatial resolution of the recordings (Lachaux et al., 2003). The electrodes were left chronically in place for up to 15 days. The electrode positions were reconstructed onto individual MRI through the superposition of the computed tomography scan images showing the electrodes, the angiography, and the patient's structural MRI slices (using the software Activis package, Lyon, France).

To compare electrode position and summarize brain activations across patients, electrode coordinates were also converted from the individual Talairach space to the normalized Talairach space (Talairach and Tournoux, 1988). Coordinates provided in this study are in the normalized Talairach space. In addition, those coordinates were further converted into the Montreal Neurological Institute (MNI) standard brain space for visualization purpose onto 3D renderings of the single-subject MNI brain. Cortical surface segmentations were performed with the BrainVisa package (CEA, France).

Spatial Sampling

Across the nine patients, we recorded from a total of 59 one-dimensional depth electrodes in the frontal and insular cortex (see Supporting Information Fig. 1 showing all recording sites in the frontal lobes). The total number of recording contacts was 917, distributed in both gray and white matter. For clarity, sites found active in the present paradigm were grouped into distinct anatomical clusters (see Tables I and II for a list of those clusters). Because of the interindividual anatomical variability, the cluster definition was not based on proximity in the Talairach space. Rather, sites were pooled into the same cluster if they belonged to the same anatomical structure, defined on the individual MRI by anatomical (gyri and sulci) or functional landmarks well established in the literature [e.g., the distinction between SMA and pre-SMA (Picard and Strick, 1996)].

Experiment

All participants performed two distinct tasks on the same day. The main experiment consisted of a time-estimation task involving performance monitoring (PM) via visual feedback. This experiment was preceded by a simple visual oddball task, which was used as a control condition [control task (CT)].

PM task

We implemented a paradigm very similar to the one used by Miltner et al. (1997) in a seminal EEG study reporting feedback-related potentials. Participants played a classic time-estimation game in which the aim was to press twice on a button with an interval of exactly 1 s (see Fig. 1). Each trial started with the presentation of a white fixation cross at the center of a black screen. After 500 ms, the color of the cross switched to blue to instruct the participant to play (GO signal). When ready, the participant would press the same joystick button twice to produce a 1-s interval. The performance for this trial was defined as the absolute difference between the actual duration of that interval and the target duration (1,000 ms). Three seconds after the second button press, the central fixation cross was replaced with a small square (FEEDBACK signal) the color of which indicated "success" or "failure." A green square indicated that the performance was below the tolerated margin of error (positive feedback), while a red square indicated that the performance was above the margin (negative feedback). Three seconds after the feedback signal, the actual quantitative performance was displayed (e.g. "−236 ms") for 1 s to allow behavioral adjustment in the next trial. Finally, each trial ended with a 1-s display of the overall score obtained by the participant; starting at 0 at the beginning of a block, the score increased by steps of 1 or 2 with each successful trial, depending on

TABLE II. Talairach coordinates for the recording sites exhibiting different GBRs for positive and negative feedback and presented in Figures 3–6

Cluster	Patient no.	Electrode	x (mm)	y (mm)	z (mm)	Side
Pre-SMA	P2	s2	7	2	52	R
	P3	q′2	−9	1	57	L
	P6	s2	8	2	52	R
	P7	s2	6	10	50	R
	P9	s2	11	4	50	R
dACC	P3	w′3	−11	17	32	L
	P6	k3	8	32	25	R
DLPFC	P3	w′10	−37	17	32	L
	P4	f′11	−37	58	13	L
	P7	f′11	−44	32	31	L
OFC	P1	k7	26	54	7	R
	P1	o11	40	40	−3	R
	P2	e7	27	31	7	R
	P3	e′8	−32	40	−7	L
	P3	e′12	−42	40	−7	L
	P5	o6	25	42	−11	R
Insula	P1	i6	34	10	1	R
	P1	p3	30	16	15	R
	P3	p′2	−33	6	16	L
	P3	t′3	−40	−3	0	L
	P5	t2	33	14	−7	R
	P6	n3	54	−15	19	R

Twenty-three sites across the nine patients exhibited GBRs that differed between positive and negative feedback. x, y, and z refer to the Talairach coordinates (not the MNI coordinates) of the sites (in millimeters). The implanted hemisphere for each site is provided (L = left, R = right). These values were converted to MNI coordinates for display onto the MNI single subject MRI.

performance (see paragraph below). The challenge was to reach a total score of 14 in as few trials as possible, at which point the block ended. Each block was ended after a maximum of 20 trials even if the score of 14 had not been reached. According to the patients' verbal reports, using reduction of the duration of the experiment as a reward for good performance proved to be an efficient way of motivating them.

One critical parameter of the task was the margin of error tolerated in each trial. Because we intended to compare neural responses to positive and negative feedback, we designed the experiment to balance the number of wins and losses. For this purpose, the margin was adjusted to performance on a trial-to-trial basis. Margin was initially set to 200 ms, which meant that any interval between 800 and 1,200 ms was evaluated as "correct." The tolerated margin for each new trial was continuously adapted to the performance in all previous trials since the beginning of the experiment: if e_i is the error at trial i (interval between button the two presses minus 1,000 ms), then the margin was the standard deviation of all previous e_i values. A successful trial was then defined by an error less than the standard deviation of all previous trials (score increased by 1). To further increase motivation, the participants were rewarded with an additional point if their error was less than half the tolerated margin (the score increased by 2).

Each participant performed a total of 16 blocks (yielding between 172 and 213 trials) and was told that the aim was to finish the experiment by reaching the target score (14 points) as quickly as possible and that the accuracy of his performance would be rewarded by an increase of the score. The total duration of the experiment varied with participant's performance and ranged between 1 and 1.5 h.

Control task

The CT used the same visual stimuli as those used in the PM task in a neutral context with no feedback value (a detailed description of the CT is given in Supporting Information Procedures).

Participants responded by pressing a joystick button with their right index finger. The experimental procedure took place in patient's hospital room. Stimuli were presented to the participants on a 17″ computer screen at a 56 cm viewing distance using the stimulus software presentation (Neurobehavioral Systems). Square stimuli subtended a horizontal and vertical angle of ∼4°.

Recording and Data Analysis

Intracerebral recordings were conducted using an audio-video-EEG monitoring system (Micromed, Treviso, Italy),

which allowed for simultaneous acquisition of data from upto 128 depth-EEG channels sampled at 512 Hz (0.1–200 Hz bandwidth) during the experimental paradigm. All signals were rereferenced to their nearest neighbor on the same electrode, 3.5 mm away before analysis (bipolar montage). Recording sites showing epileptiform activities were excluded from the analysis, and among the remaining sites, bipolar data were systematically inspected, and any trial showing epileptic spikes in any of those traces was discarded. All signals analyzed in this study were recorded from sites far from the a posteriori revealed seizure focus.

Data Analysis

We analyzed the acquired data in time–frequency (TF) domain to address three specific questions: First, are there any feedback-induced neural power modulations compared to a prestimulus baseline period? Second, are such activations (if any exist) distinguishable from responses elicited by the mere presentation of the same stimuli in the control condition (irrespective of feedback context)? Third, are those neural responses differentially modulated by the valence of the feedback (positive vs. negative)?

For each stimulus category ("positive" or "correct" vs. "negative" or "error"), the data were segmented into windows extending from 3,000 ms before stimulus onset to 3,000 ms after stimulus onset. Next, individual data segments were transformed into TF power representations, following our routine procedure (Jung et al., 2006): for each single trial, bipolar derivations computed between adjacent electrode contacts were analyzed in the TF domain by convolution with complex Gaussian Morlet's wavelet (Tallon-Baudry et al., 1997) thus providing a TF power map $P(t,f) = |w(t,f)*s(t)|^2$, where $w(t,f)$ was for each time t and frequency f; a complex Morlet's wavelet $w(t,f) = A \exp(-t^2/2\sigma_t^2)\exp(2i\pi ft)$, with $A = (\sigma\sqrt{\pi})^{-1/2}$, $\sigma_t = 1/(2\pi\sigma_f)$, and σ_f a function of the frequency f: $\sigma_f = f/7$. The result of this procedure is a TF map for each recording site and for each epoch presenting the signal power as a function of time (from −3,000 to 3,000 ms relative to stimulus onset) and frequency (from 1 to 150 Hz). See Supporting Information Figure 2 for an overview of the TF analysis. Additionally, to determine whether oscillatory responses were phase-locked to the stimulus, we computed TF maps of the phase-locking factor (Tallon-Baudry et al., 1997) and compared the values obtained after the stimulation with the values during the baseline.

The effect of the stimulus on TF power can then be evaluated at each frequency by comparing statistically pre- and post-stimulus power values. This comparison was done with Wilcoxon nonparametric tests that compared across epochs, the total power in a given TF tile, with that of a tile of similar frequency extent, but covering a [−500:0 ms] prestimulus baseline period. For each recording site, we performed 2,280 Wilcoxon tests to cover a set of [100 ms × 4 Hz] TF tiles covering a [−3,000:3,000 ms] × [1:150 Hz] TF domain. Statistical threshold was set to $P < 0.05$, corrected for multiple comparisons across tiles and recording sites with the false discovery rate method (Genovese et al., 2002). This procedure was used to identify sites with significant feedback-related power changes in the PM task and with no significant response to the same stimuli in the CT. In such sites, characterized by responses related and specific to feedback, TF power was compared between positive and negative feedback. This comparison was done on the power measured in a global TF domain covering the significant responses to feedback stimuli. More precisely, for each type of feedback, and for each site, the TF extent of the response could be defined as the collection of all contiguous TF tiles with significantly higher or lower power than baseline (using Wilcoxon test). The global TF domain used for this comparison was the smallest TF domain that covers the TF response to both positive and negative feedbacks. The statistical test used a Mann–Whitney U test to compare across epochs the average power value measured in that TF domain between positive and negative feedbacks. Note that P values were corrected for multiple comparisons with the Bonferroni method.

Note that Figure 2 displays the envelope of γ-band energy in response to feedback signals, averaged across trials and recording sites for each cluster. That is, all epochs recorded within a cluster (and corresponding to different sites and patients) were considered as if recorded from one single recording site in a single patient. Raw signals were band-pass-filtered in ten consecutive frequency bands [from (50–60 Hz) to (140–150 Hz), by steps of 10 Hz], and for each band, the envelope of the band-pass-filtered signal was computed with a Hilbert transform. For each band, this envelope signal was divided by its mean value across the entire recording session and multiplied by 100 so that envelope values are expressed in percent of that mean value. Finally, the envelope signals computed for each of the ten frequency bands were averaged together, to provide one single time-series (the γ-band envelope) for the entire session. By construction, the mean value of that time-series across the recording session is equal to 100. Figure 2 displays the average and standard error of the mean of that γ-band envelope, across trials, expressed in percent of increase or decrease relative to 100. For each type of feedback and each cluster, the mean peak amplitude (±standard error of the mean) and mean peak latency of the GBRs were measured on those γ-band envelopes.

Note that that visualization has the advantage of summarizing the most prominent responses, but does not fully capture the intersubject variability of the responses. It should thus be qualified by results shown at the individual level, shown in the remaining figures.

ERP Analysis

ERPs were measured by averaging data segments across epochs in the time domain. Comparison between ERPs to positive and negative feedback were done with a nonparametric Mann–Whitney U test on consecutive 20 ms

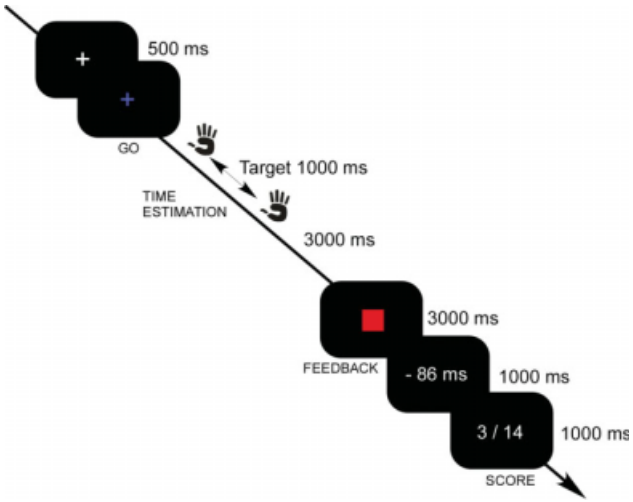

Figure 1.

PM paradigm. Each trial started with the presentation of a white central fixation cross at the center of a black screen. The cross turned blue 500 ms later (GO signal) instructing the participants to generate a 1-s duration via two consecutive joystick button presses. A colored square was displayed as feedback on performance 3,000 ms after the second button press. The square was either green (correct/postive feedback) or red (error/negative feedback) and remained visible for 3,000 ms. This qualitative feedback was then followed by a quantitative feedback (millisecond estimation error, e.g., "−86 ms") presented for 1,000 ms and followed by an overall score update. Task difficulty was adapted on-line to balance the number of positive and negative feedback stimuli (see Materials and Methods). [Color figure can be viewed in the online issue, which is available at www.interscience.wiley.com.]

overlapping windows (1 ms step). All EEG signals were evaluated with the software package for electrophysiological analysis (ELAN-Pack) developed in the INSERM U821 Laboratory and with custom MATLAB (The MathWorks) code.

RESULTS

Behavioral Results

Overall, the intervals measured differed from the intended duration by 265 ms (±191 ms). But since the tolerated error margin was adjusted during the course of the experiment (see Materials and Methods for details), there was no significant difference between the number of correct (87 ± 31) and incorrect trials (89 ± 31) (Mann–Whitney U test, $P > 0.05$). Subject performance improved over time, suggesting that the participants did indeed use the feedback information to adapt their behavior. A statistical analysis showed that estimation errors were larger in the first third of the experiment (first 33% trials) than in the last third (384 > 181 ms, Wilcoxon signed rank test, $P < 0.001$).

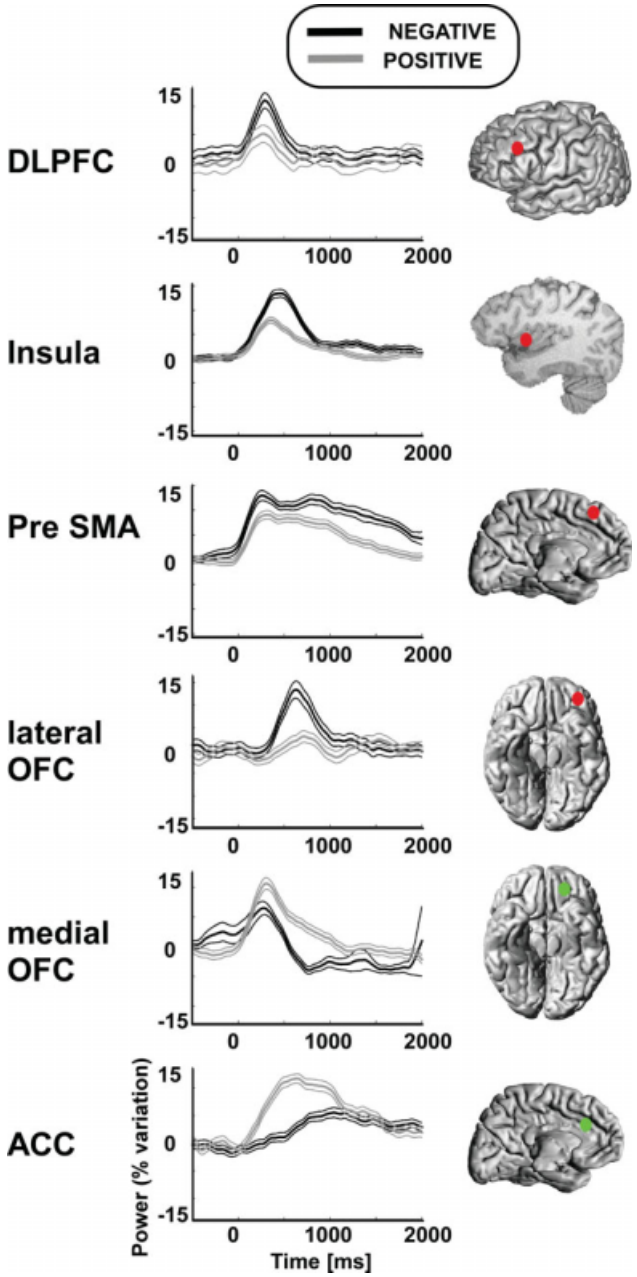

Figure 2.

Overview of the dynamics of the high-frequency responses induced by feedback stimuli. Six anatomical clusters exhibit significant GBRs in response to feedback stimuli. For each cluster, the envelope of GBRs (with standard error of the mean) was averaged across patients and the average response is presented for "error" (i.e., negative feedback, black line) and "correct" (i.e., positive feedback, gray line). Time 0 is the onset of visual feedback. [Color figure can be viewed in the online issue, which is available at www.interscience.wiley.com.]

The Neural Bases of PM: Frontoinsular Neural Network Generating GBRs to Feedback Stimuli

A full-band TF analysis of neural responses to feedback was performed for all recording sites, and it revealed that the most reproducible responses across individuals were in the high-frequency γ-band (>40 Hz) (see however Supporting Information Fig. 3 for examples of TF responses in other frequency bands).

During the PM task, 88 bipolar derivations (out of 917 in nine patients) had a significant energy modulation above 40 Hz after feedback stimuli (Wilcoxon comparison with prestimulus baseline, corrected $P < 0.05$). When several contiguous active bipolar derivations explored the same anatomical structure in the same patient (for example, four sites exploring the dACC), they were further considered as exploring one single site [explaining the total number of active sites (23) shown in Tables I and II].

Those GBRs were induced, and not evoked, by the stimulus; in other words, they were not phase-locked to the stimulus (as indicated by a phase-locking factor analysis).

As responses to feedback in the PM task could theoretically be simply related to visual processing of the stimuli, a CT was performed by all patients. The CT used the same stimuli in a neutral context with no feedback value (a detailed description of the CT is given in Supporting Information Procedures). The CT and the PM task use the same stimuli, but with a different meaning. The comparison between the responses triggered by red/green squares in the PM task and the CT reveals which response components are associated with the particular meaning of those stimuli, as performance feedback. Supporting Information Figure 4 illustrates the striking difference in brain activation induced by meaning alone: as soon as 300 ms after stimulus presentation, the visual stimuli ignite the frontal cortex only in the PM condition, that is, only when they contain meaningful information about feedback. The comparison between the CT and PM task was therefore a way to isolate feedback-specific responses: in the remaining section, any frontal site that also responded to the red/green squares in this neutral control context (example in Supporting Information Fig. 5) was considered nonspecifically feedback-related and was therefore excluded from the analysis and discussions below.

Although the overall spatial coverage of the frontal lobe across the nine patients was extensive, high-frequency responses were found only in spatially restricted anatomical clusters (see Tables I and II for a list of anatomical clusters). Feedback-related GBRs were detected in five regions: (a) the pre-SMA of the frontal medial cortex [Brodmann's area (BA) 6 , superior frontal gyrus rostral to the VAC plane, defined as the vertical plane passing through the anterior commissure, with $0 < y < 20$ mm], (b) the dACC (BA 24/32/33), (c) the middle and inferior frontal gyrus exploring the DLPFC (BA 9/46), (d) the OFC (BA 11/12/13/14), and (e) in the anterior (ventral or dorsal) part of the insula.

The time course of the GBRs varied across the various anatomical structures. Figure 2 provides a summary of the time course of GBRs with respect to the presentation of feedback stimuli by pooling results from electrode sites belonging to the same anatomical cluster across all participants. Compared to positive feedback, negative feedback on performance triggered GBRs that were stronger in the pre-SMA, DLPFC, lateral OFC, and insula. The shortest latencies of activation were found in the DLPFC (peak of the response around 300 ms), followed by insula (peak latency around 500 ms), and lateral OFC (peak latency around 700 ms). In these three clusters, the duration of the responses lasted less than 1,000 ms. By contrast, the responses of the pre-SMA were sustained and lasted almost 2,000 ms. Positive feedback triggered GBRs in the medial OFC and dACC. In the medial OFC, the peak latency of the responses was around 500 ms and activation lasted less than 1,000 ms, while dACC activation was more gradual and sustained more than 1,000 ms. These findings provide an overview of the spatiotemporal properties of the positive versus negative feedback processing network. We will now describe the detected responses in more detail for each anatomical component of the network.

Pre-supplementary motor area

We observed GBRs to feedback stimuli in the pre-SMA of five patients (see Fig. 3). Those responses were found in spatially tightly confined regions ($7 < \text{abs}(x) < 11$; $2 < y < 10$; $50 < z < 54$ in Talairach space), in both right (four sites) and left (one site) hemispheres. On the individual MRI, all sites were located rostral to the VCA line and thus precisely in the pre-SMA (Picard and Strick, 1996). Although GBRs also occurred in response to positive feedback, the responses were significantly stronger for negative feedback ($P < 0.05$ for each site, Mann–Whitney U test). The time profile of the responses consisted of a sustained energy increase between 500 and 2,000 ms or more. The peak amplitude of GBRs in the pre-SMA was 13.0 ± 1 (SEM) for negative feedback and 9.1 (± 0.8) for positive feedback. The peak latency of GBRs in the pre-SMA was 860 ms for negative feedback and 840 ms for positive feedback.

Anterior cingulate cortex (BA 24/32/33)

Among electrodes present in dACC, two sites responded to feedback in the dACC (two patients, Fig. 3). Both were located in the dorsal portion of the anterior cingulate gyrus ($17 < y < 32$, Talaraich space) and had enhanced high-frequency responses to positive feedback ($P < 0.05$ for each site, Mann–Whitney U test), although negative feedback also triggered a high-frequency response. Both responses were gradual energy increases peaking around 800 ms and lasting 1,500 ms. The peak amplitude of GBRs in the dACC was 5.4 ± 0.7 for negative feedback and 11.7 ± 0.8 for positive feedback. The peak latency of GBRs in the dACC was 1,064 ms for negative feedback and 640 ms for positive feedback.

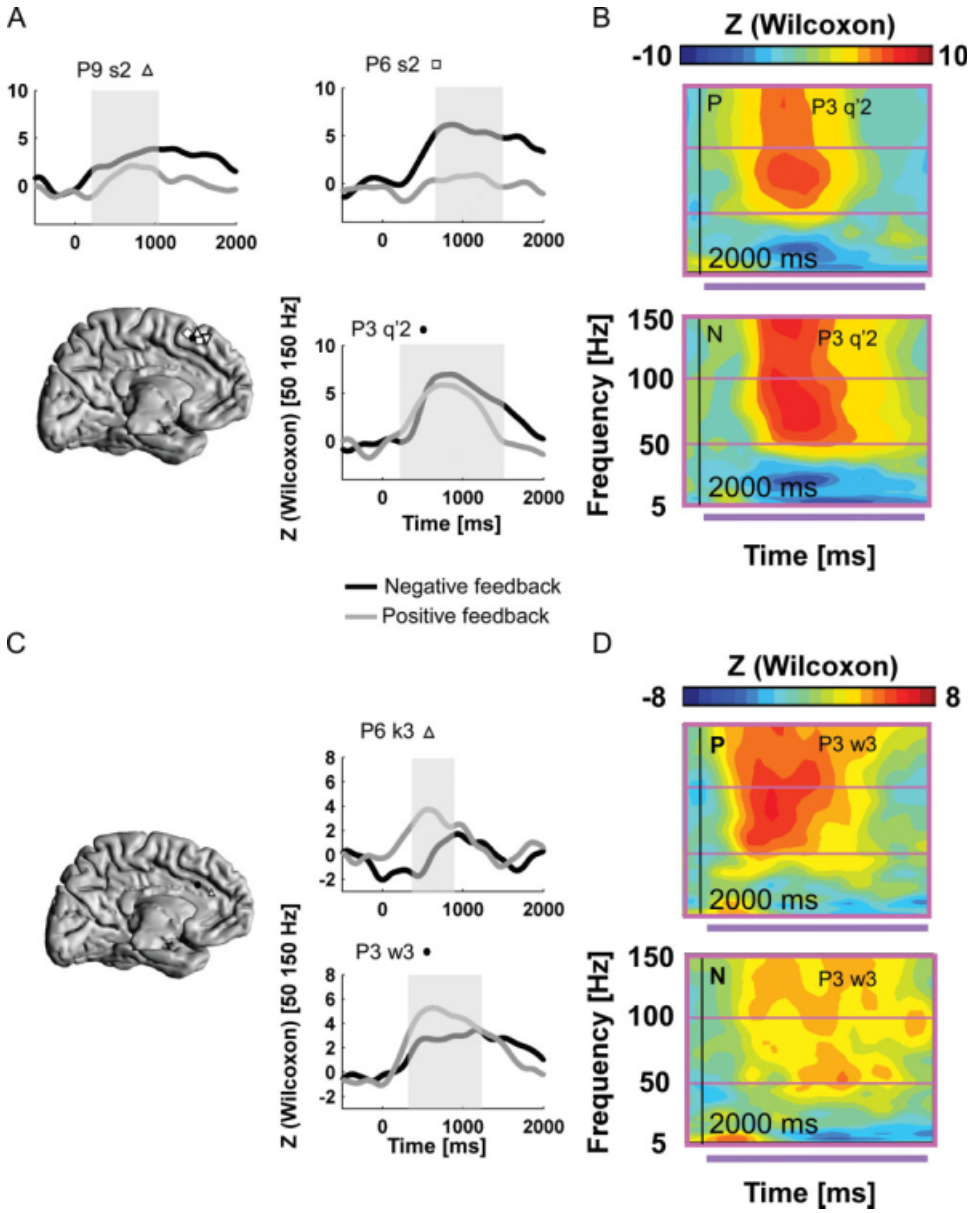

Figure 3.

GBRs in the medial frontal wall in the PM task. (**A**) and (**B**) show responses in the pre-SMA, while (**C**) and (**D**) show responses in the anterior cingulate gyrus (dACC). (A, C) The anatomical picture shows the locations of the corresponding sites reconstructed onto the MNI single-subject MRI. The time course of GBRs (50–150 Hz) for the two types of feedback is displayed, and segments with statistically significant differences between positive and negative feedback are shown as shaded regions. Three typical responses are shown for the pre-SMA (A) and two for the dACC (C). (B, D) Two representative examples of GBRs for one site in the pre-SMA (P3 q′2) and one site in the dACC (P3 w3) are shown on the right with TF maps for positive (upper map) and negative feedback (lower map). [Color figure can be viewed in the online issue, which is available at www.interscience.wiley.com.]

Middle frontal gyrus—DLPFC (BA 9/46)

As shown in Figure 4, responses to feedback were also found in the DLPFC (a total of four sites in four patients). GBRs were found both in response to positive feedback and negative feedback. Although one site in the right hemisphere had similar responses to both types of feedback (not shown in the Fig. 4), the three remaining sites, in the left hemisphere, had significantly stronger responses to negative feedback ($P < 0.05$, Mann–Whitney U test).

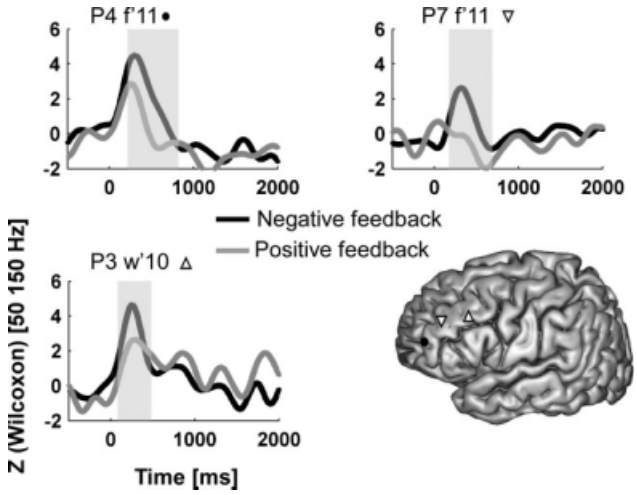

Figure 4.

GBRs in the DLPFC in the PM task. Anatomical locations of DLPFC sites are shown for three participants onto the MNI single-subject 3D MRI reconstruction. The time course of GBRs (50–150 Hz) for the two types of feedback is displayed, and segments with statistically significant differences between positive and negative feedback are shown as shaded regions.

The three left hemispheric responses were all characterized by a sudden short-lasting (less than 600 ms) energy increase in the first 300 ms following feedback presentation.

The peak amplitude of GBRs in the DLPFC was 11.0 ± 1.4 for negative feedback and 5 ± 1.5 for positive feedback. The peak latency of GBRs in the DLPFC was 281 ms for negative feedback and 281 ms for positive feedback.

Orbitofrontal cortex (BA 10/11/12/13/14)

Two anatomically and functionally distinct clusters in the OFC were found to generate feedback-specific γ-range activity (see Fig. 5). In a first, medial cluster (four sites), GBRs were stronger for positive feedback ($P < 0.05$, Mann–Whitney U test), while in a second, lateral cluster, responses were stronger for negative feedback (two sites). The two groups were well-separated anatomically: medial responses were all located in the medial OFC, more precisely in-between the lateral orbital sulcus and the gyrus rectus ($25 < \text{abs}(x) < 32$, Talairach space), while lateral sites were more lateral than the lateral orbital sulcus ($40 < \text{abs}(x) < 42$). In the medial OFC, the response was mostly a progressive energy increase within 400 ms and a gradual return to baseline after 1,000 ms (P1 k7, P3 e'8, P2 e7), although one site (P5 o6) had faster dynamics. Lateral OFC responses were shorter than 1,000 ms, with a sharp energy increase in the first 500 ms.

The peak amplitude of GBRs in the medial OFC was 6.5 ± 1.1 for negative feedback and 10.6 ± 0.9 for positive feedback. The peak latency of GBRs in the medial was 281 ms for negative feedback and 312 ms for positive feedback. The peak amplitude of GBRs in the lateral OFC was 13.3 ± 2.0 for negative feedback and 1.8 ± 1.0 for positive feedback. The peak latency of GBRs in the lateral OFC was 640 ms for negative feedback and 750 ms for positive feedback.

Insular γ-range activity during feedback processing

The remaining cluster was in the insula (see Fig. 6), where both types of feedback elicited γ-band energy increase in six sites (across four patients). In the anterior part of the insula (four sites), the response was fast, short, and stronger for negative feedback (within the first 1,000 ms with a peak around 500 ms). In the two remaining sites, located in the posterior part of insula for one site and in the ventral part of the insula for the other, the response was more gradual. One site in the ventral site had stronger response for positive feedback (P3 t'3). The peak amplitude of GBRs in the insula was 13.4 ± 0.7 for negative feedback and 7.9 ± 0.6 for positive feedback. The peak latency of GBRs in the insula was 437 ms for negative feedback and 359 ms for positive feedback.

γ Deactivations Induced by Feedback Stimuli in the PM Task

In addition to the poststimulus power increases reported above, we also observed that feedback induced power decreases in the same frequency range (high γ-band) along the medial frontal wall (12 sites in eight patients). γ-band energy suppressions were all located in the medial frontal cortex rostral to the pre-SMA or in the gyrus rectus (most medial part of the OFC) (see Fig. 7). Most suppression patterns (eight sites) were comparable for positive and negative feedback, but in four sites, the suppression occurred only in response to one type of feedback: either positive (two sites, P9 f2 and P9 w3) or negative (two sites, P2 f2 and P3 e'2). The time profile of deactivation was fairly reproducible across sites and participants and consisted of a sharp decrease of energy in the first 500 ms followed by a gradual return to baseline level within 1,000–1,500 ms.

Evoked Potentials and θ-Band Activity in the Anterior Cingulate in Response to Feedback Stimuli

Both negative and positive feedback generated ERPs in a large number of frontal sites. However, the ERPs were complex, with multiple positive and negative peaks, and extremely variable from site to site, and from patient to patient, even within the same region. We could not extract reproducible patterns and meaningful information from the ERPs. For this reason, we chose to keep the focus of this report on the robust and consistent GBRs rather than

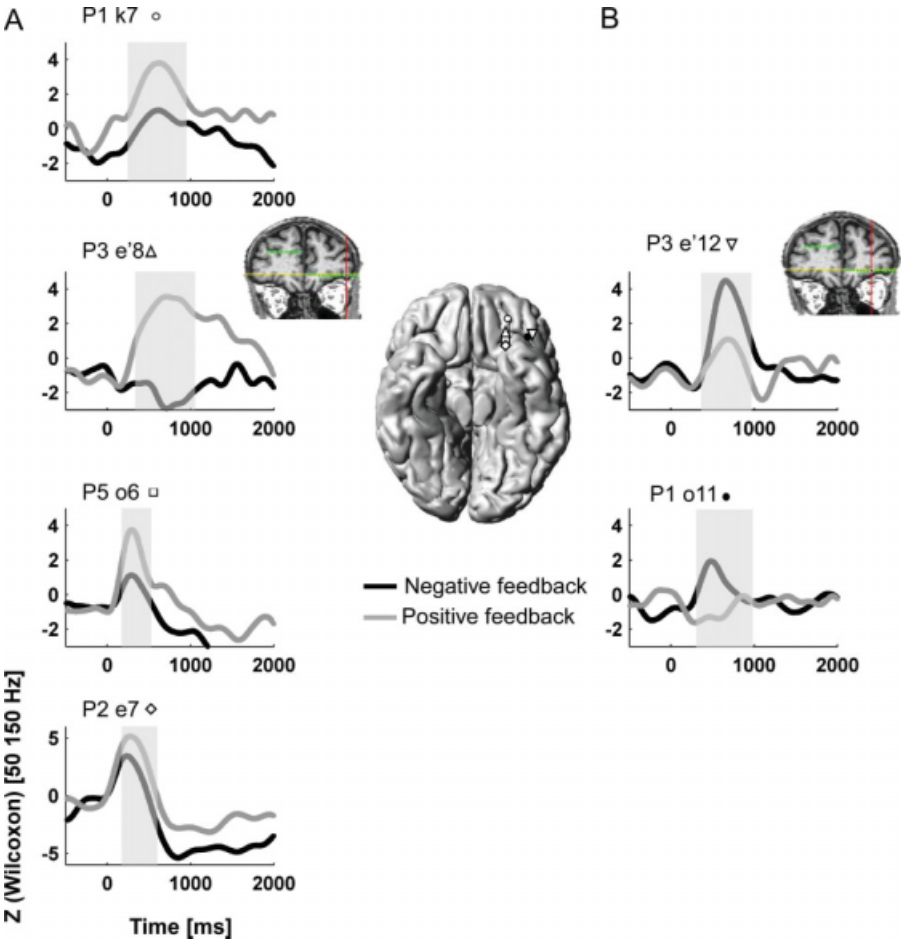

Figure 5.
GBRs in the OFC in the PM task. Anatomical locations of OFC sites are shown for six participants onto the standard MNI single-subject 3D MRI reconstruction. (**A**) For the four sites in the medial OFC, GBRs were stronger for positive feedback than negative feedback. The time course of GBRs (50–150 Hz) for the two types of feedback is displayed, and segments with statistically significant differences between positive and negative feedback are shown as shaded regions. (**B**) By contrast, for the two sites in the lateral OFC, GBRs were stronger for negative feedback than positive feedback. The time course of GBRs (50–150 Hz) for the two types of feedback is displayed, and segments with statistically significant differences between positive and negative feedback are shown as shaded regions. Note that for a particular patient, a stringent dissociation between lateral and medial OFC responses was found (medial P3 e′8 and lateral P3 e′12) and the anatomical locations of those two sites are displayed on the patient's MRI. [Color figure can be viewed in the online issue, which is available at www.interscience.wiley.com.]

to perform a detailed description of ERPs generated by the feedback stimuli. However, since noninvasive EEG studies in humans have consistently reported generators of a specific ERP, the FRN, in the anterior cingulate gyrus, we investigated ERPs specifically in that region. Out of 11 sites in the dorsal dACC, we found ERPs to feedback stimuli in six sites (see Fig. 8) around 300 ms, out of which four differed between types of feedback: a larger amplitude for negative feedback ($P < 0.05$, Kruskal–Wallis test) was found at those four sites at specific latency ranges (P3 k′2 between 620 and 940 ms, P3 w′3 between 400 and 640 ms, P8 i2 between 500 and 600 ms, and P9 z2 between 300 and 620 ms) ($P < 0.05$, Kruskal–Wallis test). Our ERP results are therefore consistent with the hypothesis that the dACC generates a response to negative feedback in a late-latency window after 300 ms. This late component, peaking later than the typical scalp latency of the FRN, might possibly constitute an intracranial correlate of the scalp P300 or Pe (Herrmann et al., 2004; Polich, 2007). We did not find any evidence of a specific response to negative feedback between 200 and 300 ms, that is in the latency range of the scalp FRN. Lastly, since recent work suggests that the FRN may be considered as a θ-band (4–7 Hz) oscillation (Luu et al., 2003), we looked for task-related θ-band activity modulations in the dACC. Out of 11 sites exploring the dACC, only two sites generated short-lasting (<600 ms) θ-band activity modulations in response to feedback stimuli (P3 w′3 and P6 k3). An example of feedback-induced θ-band activity modulation is shown in Supporting Information Figure 6. Note that those two sites also generated GBRs in response to feedback stimuli.

DISCUSSION

The present study is, to our knowledge, the first to assess the large-scale neural dynamics of PM using direct neural recordings of high γ-range neural activity in humans. By combining an unprecedented spatiotemporal resolution with single-trial TF analysis, the present study extends our knowledge about the neural substrates of feedback processing. First of all, we found that feedback stimuli activate a large-scale network of frontoinsular brain regions indexed by widely distributed high γ (>50 Hz) power modulations. This network includes the dorsal anterior cingulate gyrus (dACC) and the pre-SMA in the frontal medial cortex, the DLPFC, the OFC, and the anterior insula. This frontoinsular network responds to

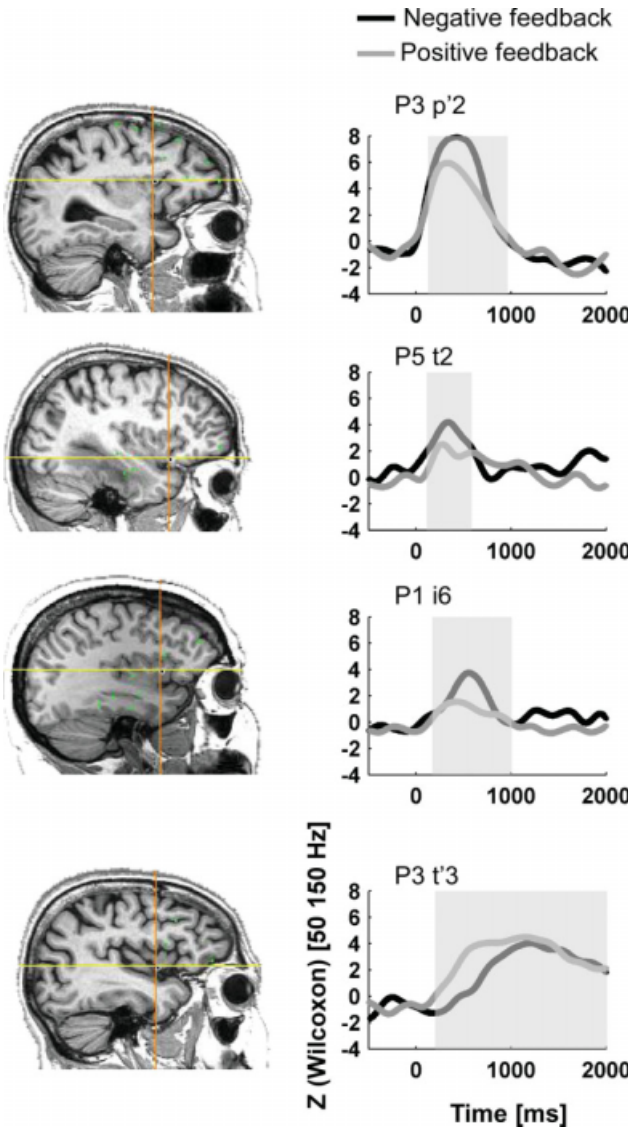

Figure 6.
GBRs in the insula in response to feedback on performance. In six sites across four patients, feedback stimuli induced GBRs. For five sites in the anterior insula (four sites) or posterior insula (one site), GBRs were stronger for negative feedback than positive feedback. For one site in the inferior insula, GBRs were stronger for positive feedback than for negative feedback. The anatomical pictures show the corresponding sites reconstructed onto individual subject MRIs for four of those sites generating typical GBRs. The time course of GBRs (50–150 Hz) for the two types of feedback is displayed, and segments with statistically significant differences between positive and negative feedback are shown as shaded regions. Four typical responses are shown for the anterior insula (three upper waveforms) and one for the inferior insula (bottom waveform). [Color figure can be viewed in the online issue, which is available at www.interscience.wiley.com.]

feedback with an increase of neural activity in the γ-band, referred to here as GBRs, while specific regions in the medial frontal cortex show a transient interruption of pre-stimulus γ-band activity. Moreover, we show that the time course of the activations in those regions is largely time-overlapping but distinct: the DLPFC, the insula, and the OFC displayed short responses lasting less 1,000 ms; on the contrary, responses in the pre-SMA and the dACC were more sustained and lasted more than 1,000 ms. Finally, we found that each component of this network is preferentially tuned to one type of feedback: the medial OFC and dACC respond stronger to positive feedback, while pre-SMA, DLPFC, lateral OFC, and anterior insula have stronger responses following negative feedback.

Before discussing this network, let us first consider possible interpretations for the high-frequency population-level activity found here. The current understanding of GBRs is that they correspond to a local synchronization mechanism that facilitates neural communication: increased γ-band activity would thus mean that neurons

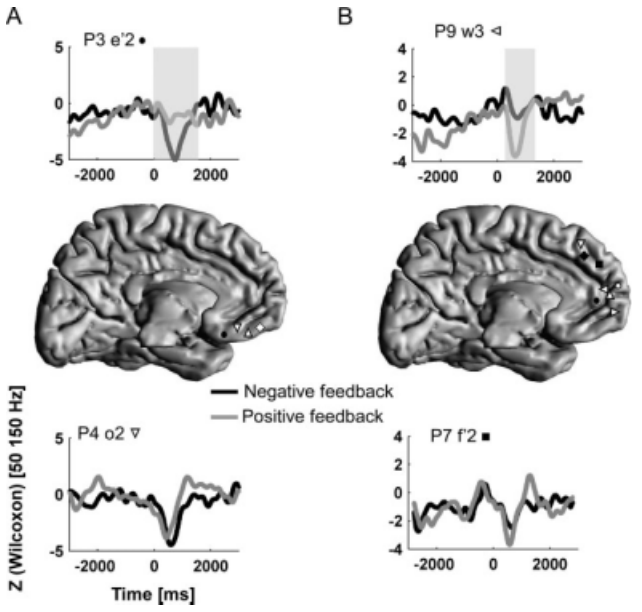

Figure 7.
γ-band suppressions in the gyrus rectus of the OFC (**A**) and in the medial prefrontal cortex (**B**) in the PM task. For four sites, feedback stimuli induced transient γ-band suppressions in the gyrus rectus (A) and for eight sites feedback stimuli induced transient γ-band suppressions in the medial prefrontal cortex (B). The anatomical locations of those sites are shown onto the standard MNI single-subject 3D MRI reconstruction for sites in the medial prefrontal cortex and gyrus rectus. Two typical time course of γ-band suppressions (50–150 Hz) in the gyrus rectus (A) and medial prefrontal cortex (B) for the two types of feedback are displayed, and segments with statistically significant differences between positive and negative feedback are shown as shaded regions.

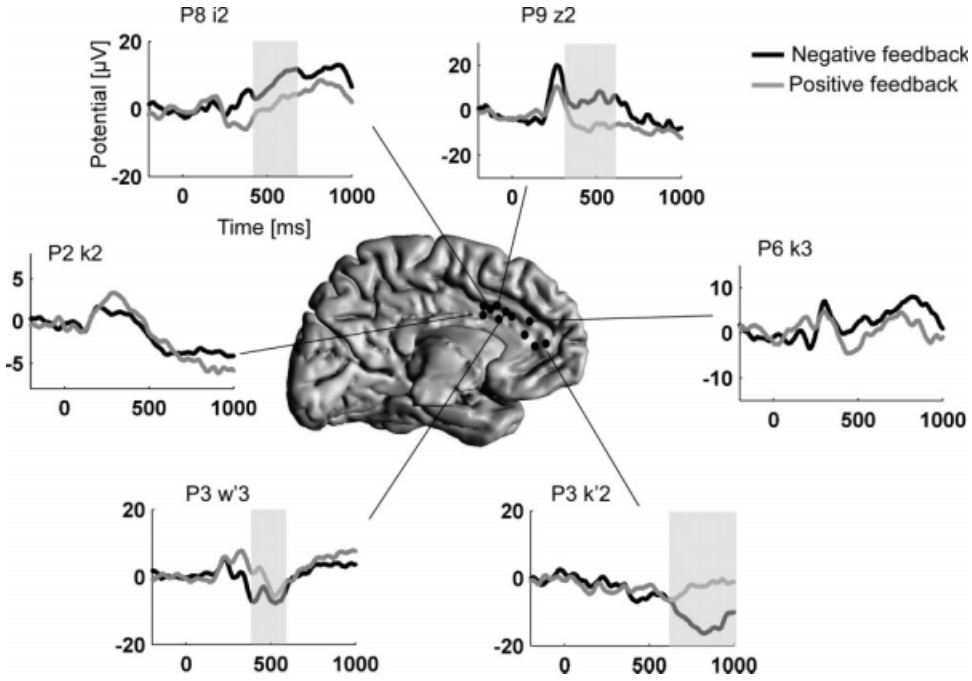

Figure 8.

ERPs in the dorsal anterior cingulate gyrus. The anatomical locations of six sites in dorsal anterior cingulate gyrus for which ERPs were found in response to feedback stimuli are shown onto the standard MNI single-subject 3D MRI reconstruction. ERPs for the two types of feedback are displayed, and segments with statistically significant differences between positive and negative feedback are shown as shaded regions. In three of the six sites, ERP amplitude was stronger for negative feedback (after 400 ms), while in one site, ERP amplitude was stronger for positive feedback (after 400 ms).

around the electrode get recruited by the task-at-hand (Jacobs et al., 2007; Nir et al., 2007). By analogy, γ-band suppressions, that is, transient decrease in γ-band energy, would correspond to an interruption of local communication and a withdrawing from the task (Lachaux et al., 2008). For this reason, GBRs have been proposed as precise markers of the cortical networks underlying cognition (Jensen et al., 2007; Jerbi et al., 2009; Lachaux et al., 2003), a suggestion that has meanwhile received further support by studies of multiple cognitive processes. Still, cognitive processes such as working memory or spatial navigation may also trigger activity modulations in other frequency bands, such as task-induced θ-band (4–7 Hz) modulations (Ekstrom et al., 2005; Raghavachari et al., 2001). The observation that both γ and θ power increases during cognitive processing may suggest that the two rhythms interact with each other. Indeed, θ–γ interactions have been reported in humans (Canolty et al., 2006).

Evaluating the Outcome of Actions Triggers Responses in Widespread Frontal Regions

Feedback induced GBRs in two distinct regions of the frontal medial wall, in the dorsal dACC (dACC) and the pre-SMA. The recruitment of dACC during feedback processing has been well-established, both in humans and monkeys; however, the exact nature of the dACC response is still under debate. EEG studies in humans have localized in the dACC the source of a FRN, between 200 and 300 ms after performance feedback (Miltner et al., 1997). The FRN has been observed in simple learning tasks and monetary gambling games and is larger in amplitude for negative feedback (Nieuwenhuis et al., 2004). Those results have been interpreted as evidence for a dACC-generated FRN specific to negative feedback [although that view has been recently challenged (Holroyd et al., 2008)]. Our high-frequency results contradict the view that the dACC would respond specifically to negative feedback, since GBRs were larger for positive feedback. This apparent discrepancy between noninvasive and invasive EEG results is most likely explained by the fact that the FRN and dACC GBRs correspond to different neural phenomena with distinct frequency ranges and possibly different functions. Indeed, ERP analysis of our data revealed consistent differences between feedback types after 300 ms in dACC sites, that is, at a slighty longer latency than the scalp FRN. This latency range is more compatible with the P300 or Pe recorded with scalp-EEG. Therefore, our results suggest that the dACC contributes possibly to the P300 or Pe

recorded with scalp-EEG, but not directly to the FRN (Herrmann and Knight, 2001; Herrmann et al., 2004; Polich, 2007).

Our observations are in line with recent studies in monkeys showing responses in the dACC to both correct and error feedback, even in single neurons (Michelet et al., 2007; Quilodran et al., 2008). These studies suggest that the stronger response we observed here to positive feedback, in two patients, might not be a general property of dACC neurons. On the whole, our findings indicate that the human dACC is not specifically and certainly not by itself involved solely in error detection. Our data fit better with the view that the dACC monitors the consequences of our own actions for online behavioral adaptation (Rushworth et al., 2004). In this view, both positive and negative feedback would activate the dACC, to reinforce or correct previous behavior.

Lastly, the dACC is also supposed to be the origin of θ-band (4–7 Hz) activity modulations in response to feedback stimuli. Our data indeed show transient (<400 ms) θ-band activity modulations in two patients. It is noteworthy that the two dACC sites generating GBRs also generated GBRs, in line with previous studies showing links between γ- and θ-band modulations (Canolty et al., 2006). Further work including more responding sites is needed to evaluate the possibility of cross-frequency coupling in those frequency bands.

Still, these short θ-band activity modulations do not provide any evidence that the underlying activity is rhythmic in the sense of repeating over multiple cycles. Power increase in the θ range could also result from the TF transformation of evoked potentials.

Not far from the dACC, feedback stimuli also activated the pre-SMA. However, pre-SMA sites had stronger responses to negative feedback, which is consistent with several fMRI findings (Ullsperger and von Cramon, 2003; Zanolie et al., 2008). The pre-SMA responses can be interpreted in multiple ways, since the pre-SMA has been associated with several cognitive systems mediating attention (Hon et al., 2006), motor planning (Akkal et al., 2002), and time estimation (Coull et al., 2004). In the present experiment, the task involved the production of a stereotyped motor pattern, defined by precise timing demands. The pre-SMA is known to be involved in planning sequences of movements, and for instance, pre-SMA neurons are recruited when monkeys update motor plans for subsequent temporally ordered movements (Shima et al., 1996). This suggests that in the present task, pre-SMA responses to feedback might participate in reshaping the precise motor pattern that has to be produced for successful task completion (Isoda and Hikosaka, 2007).

Feedback also elicited responses in the DLPFC, which were stronger for negative feedback. This effect has been seldom reported in humans [but see Zanolie et al. (2008)]. Neuroimaging studies have associated the DLPFC with related processes such as error monitoring (Debener et al., 2005) or rule switching (Monchi et al., 2001), but direct evidence of DLPFC activation during PM was lacking. In contrast, DLPFC responses to feedback have already been reported in monkeys: in animals learning arbitrary action-outcome contingencies, Matsumoto et al. (2007) have found neurons responding to feedback in the lateral PFC. However, cells did not differentiate positive and negative feedbacks. This led the authors to suggest that DLPFC neurons participate in directing attention toward the feedback stimulus. This interpretation does not conflict with our observation that negative feedback produced the strongest responses, because one might expect negative feedback to trigger a stronger attentional reaction than positive feedback for the given paradigm.

Lastly, robust responses to feedback were also observed in the OFC with a functional dissociation along a medial–lateral axis. Medial sites, between the gyrus rectus and lateral orbital sulcus, had stronger responses to positive feedback (Talairach coordinates: $25 < x < 32$). Sites more lateral than the lateral orbital sulcus had stronger responses to negative feedback ($x > 40$). Our results provide a direct confirmation that medial OFC is preferentially activated by rewarding stimuli and the lateral OFC by punishing stimuli (Kringelbach, 2005). This dissociation was exemplified in one participant (P3) with recordings from both medial and lateral parts of the OFC showing opposite responses (sites e′8 and e′12 shown in Fig. 5). More generally, our observations are in line with a large body of evidence, both in monkeys and humans, that the OFC is a key structure for estimating the reward value of external stimuli (Rolls, 2004) to guide behavior (Wallis, 2007).

Insular Responses During Feedback Processing

In complement to frontal activations, feedback stimuli produced strong responses in the anterior insula, at rather short latencies before 700 ms. The most likely interpretation is that this region participates in the emotional reaction to feedback. In this sense, our results would suggest that the reaction, in the context of the particular task used here, is stronger for negative feedback. The anterior agranular insula is part of a system underlying emotional processes. More specifically, it is involved in visceromotor, i.e. autonomic (Verberne and Owens, 1998) as well as in visceral sensory functions, underlying interoceptive awareness (Critchley, 2005), which is closely related to emotional reactions. Our interpretation is in line with a recent proposal that anterior insula might be involved in error awareness (Klein et al., 2007). As suggested by Klein et al. (2007), the response of the insula after negative feedback may be attributed to an enhanced awareness of the autonomic reaction to the error, or to the higher autonomic response itself, favoring error awareness.

Temporal Dynamics of the GBRs Within the Feedback-Processing Network

Little is known about the timing of neural responses in response to feedback in the human brain. The only information available so far has come from scalp EEG and MEG studies, which lack the sufficient spatial resolution to decipher the precise timing of individual brain regions. Our main result is that the timing of activation within the frontoinsular network is heterogeneous. This is a clear indication that feedback processing involves several distinct subprocesses that might be performed separately by the brain regions highlighted above. The main distinction is between "sustained" responses in the mesial frontal wall (dACC and pre-SMA) and more transient responses in the DLPFC, the OFC, and the insula. It is clear that the neural responses to feedback last way beyond 500 ms, that is beyond the FRN observed at the scalp level. Still, data from patients with electrodes recording from several clusters indicate possible sequence of activation within that network, more as a propagating wave than as a strict succession of responses. In this regard, data from patient P3 are particularly illustrative of a sequence starting in the DLPFC, and reaching in turn the insula, then the OFC, and finally the frontal medial wall. Although restricted to one patient, such timing observations are more in line with a succession of processes than with a global and integrated network processing feedback information as a whole through strong reciprocal interactions between simultaneous activations (Varela et al., 2001).

Transient Deactivations in the Medial Prefrontal Cortex During Feedback Processing

In sharp contrast with the activations just described, we observed in restricted parts of the medial frontal cortex a rare phenomenon referred to as negative GBRs, or γ-band suppressions (GBS). Those suppressions were characterized by a transient energy decrease in the γ-band after feedback stimuli. The phenomenon was observed in medial sites anterior to the pre-SMA and in most medial sites (gyrus rectus) of the OFC. The physiological meaning of GBS is not precisely known. The most obvious interpretation is that they correspond to local neural desynchronization and the interruption of local ongoing neural communication to attend specific demands of the cognitive task at hand. GBS have already been found during reading tasks in the ventral lateral prefrontal cortex (VLPFC) and were modulated by attention (Lachaux et al., 2008). Here, the spatial origin is different and, interestingly, it matches with a subportion of the so-called "default mode network." The default mode network is a common and reproducible network of brain areas less active during cognitive tasks than during rest, irrespective of the task (Raichle et al., 2001). This network has been identified with fMRI and PET and includes the ventromedial prefrontal cortex (V-MPFC), perhaps extending into the dACC, the posterior cingulate/precuneus/retrosplenial cortex, and the left and right lateral parietal cortices in the region of the angular gyri (Raichle and Snyder, 2007). Based on recent evidence that γ-band activity and BOLD signals appear to be stronlgy related (see above), we suggest that GBS corresponds to the deactivations found in neuroimaging studies. If this is the case, our observations would be the first direct evidence of reduced neural activity in the default network during a cognitive task. The temporal resolution of iEEG reveals that neural γ-range deactivations in the V-MPFC have a stereotyped time course, with a peak around 500 ms and a duration below 1,000 ms.

Several recent studies have implicated the anteromedial cortex in tasks requiring self-referencing and monitoring (Gusnard et al., 2001; Johnson et al., 2002). Accordingly, deactivation of this region has been interpreted as a temporary suppression of self-related activity during demanding tasks oriented toward external stimuli. In this view, deactivation of the V-MPFC indexed by GBS in our task would correspond to an attentional shift from the internal to the external world.

CONCLUSIONS

In summary, this study provides a detailed picture of the neural dynamics of the brain responses to success and failure in humans. Our results show that feedback on one's performance are processed by a large-scale network of distributed γ-range activations involving frontoinsular regions. We also demonstrate that, far from being functionally homogeneous, the dynamics of the network are differentially tuned: different regions of this network have distinct timing of activation and different sensitivity to the valence of feedback. Taken together, the results reported here provide novel insights into the intricate neural dynamics at play when our brain is faced with feedback on our performance. Finally, a better understanding of the central mechanism mediating feedback processing is bound to have direct implications on our knowledge of various cognitive processes such as adaptive behavior, skill acquisition, and ultimately of ways to improve them.

ACKNOWLEDGMENTS

We thank Pierre-Emmanuel Aguera and Patrick Bouchet for their valuable technical assistance and the Hospices Civils de Lyon.

REFERENCES

Akkal D, Bioulac B, Audin J, Burbaud P (2002): Comparison of neuronal activity in the rostral supplementary and cingulate motor areas during a task with cognitive and motor demands. Eur J Neurosci 15:887–904.

Alexander MP, Stuss DT, Picton T, Shallice T, Gillingham S (2007): Regional frontal injuries cause distinct impairments in cognitive control. Neurology 68:1515–1523.

Canolty RT, Edwards E, Dalal SS, Soltani M, Nagarajan SS, Kirsch HE, Berger MS, Barbaro NM, Knight RT (2006): High gamma power is phase-locked to theta oscillations in human neocortex. Science 313:1626–1628.

Cools R, Clark L, Owen AM, Robbins TW (2002): Defining the neural mechanisms of probabilistic reversal learning using event-related functional magnetic resonance imaging. J Neurosci 22:4563–4567.

Coull JT, Vidal F, Nazarian B, Macar F (2004): Functional anatomy of the attentional modulation of time estimation. Science 303:1506–1508.

Critchley HD (2005): Neural mechanisms of autonomic, affective, and cognitive integration. J Comp Neurol 493:154–166.

Debener S, Ullsperger M, Siegel M, Fiehler K, von Cramon DY, Engel AK (2005): Trial-by-trial coupling of concurrent electroencephalogram and functional magnetic resonance imaging identifies the dynamics of performance monitoring. J Neurosci 25:11730–11737.

Ekstrom AD, Caplan JB, Ho E, Shattuck K, Fried I, Kahana MJ (2005): Human hippocampal theta activity during virtual navigation. Hippocampus 15:881–889.

Engel AK, Fries P, Singer W (2001): Dynamic predictions: Oscillations and synchrony in top–down processing. Nat Rev Neurosci 2:704–716.

Fries P, Nikolic D, Singer W (2007): The gamma cycle. Trends Neurosci 30:309–316.

Gehring WJ, Willoughby AR (2002): The medial frontal cortex and the rapid processing of monetary gains and losses. Science 295:2279–2282.

Genovese CR, Lazar NA, Nichols T (2002): Thresholding of statistical maps in functional neuroimaging using the false discovery rate. Neuroimage 15:870–878.

Gusnard DA, Akbudak E, Shulman GL, Raichle ME (2001): Medial prefrontal cortex and self-referential mental activity: Relation to a default mode of brain function. Proc Natl Acad Sci USA 98:4259–4264.

Herrmann CS, Knight RT (2001): Mechanisms of human attention: Event-related potentials and oscillations. Neurosci Biobehav Rev 25:465–476.

Herrmann MJ, Rommler J, Ehlis AC, Heidrich A, Fallgatter AJ (2004): Source localization (LORETA) of the error-related-negativity (ERN/Ne) and positivity (Pe). Brain Res Cogn Brain Res 20:294–299.

Holroyd CB, Nieuwenhuis S, Yeung N, Nystrom L, Mars RB, Coles MG, Cohen JD (2004): Dorsal anterior cingulate cortex shows fMRI response to internal and external error signals. Nat Neurosci 7:497–498.

Holroyd CB, Pakzad-Vaezi KL, Krigolson OE (2008): The feedback correct-related positivity: Sensitivity of the event-related brain potential to unexpected positive feedback. Psychophysiology 45:688–697.

Hon N, Epstein RA, Owen AM, Duncan J (2006): Frontoparietal activity with minimal decision and control. J Neurosci 26:9805–9809.

Isnard J, Guenot M, Ostrowsky K, Sindou M, Mauguiere F (2000): The role of the insular cortex in temporal lobe epilepsy. Ann Neurol 48:614–623.

Isoda M, Hikosaka O (2007): Switching from automatic to controlled action by monkey medial frontal cortex. Nat Neurosci 10:240–248.

Ito S, Stuphorn V, Brown JW, Schall JD (2003): Performance monitoring by the anterior cingulate cortex during saccade countermanding. Science 302:120–122.

Jacobs J, Kahana MJ, Ekstrom AD, Fried I (2007): Brain oscillations control timing of single-neuron activity in humans. J Neurosci 27:3839–3844.

Jensen O, Kaiser J, Lachaux JP (2007): Human gamma-frequency oscillations associated with attention and memory. Trends Neurosci 30:317–324.

Jerbi K, Ossandon T, Hamame C, Senova S, Dalal S, Jung J, Minotti L, Bertrand O, Berthoz A, Kahane P, Lachaux JP (2009): Task-related gamma-band dynamics from an intracerebral perspective: Review and implications for surface EEG and MEG. Hum Brain Mapp 30:1758–1771.

Johnson SC, Baxter LC, Wilder LS, Pipe JG, Heiserman JE, Prigatano GP (2002): Neural correlates of self-reflection. Brain 125(Pt 8):1808–1814.

Jung J, Hudry J, Ryvlin P, Royet JP, Bertrand O, Lachaux JP (2006): Functional significance of olfactory-induced oscillations in the human amygdala. Cereb Cortex 16:1–8.

Jung J, Mainy N, Kahane P, Minotti L, Hoffmann D, Bertrand O, Lachaux JP (2008): The neural bases of attentive reading. Hum Brain Mapp 29:1193–1206.

Kahana MJ (2006): The cognitive correlates of human brain oscillations. J Neurosci 26:1669–1672.

Klein TA, Endrass T, Kathmann N, Neumann J, von Cramon DY, Ullsperger M (2007): Neural correlates of error awareness. Neuroimage 34:1774–1781.

Kringelbach ML (2005): The human orbitofrontal cortex: Linking reward to hedonic experience. Nat Rev Neurosci 6:691–702.

Lachaux JP, Rudrauf D, Kahane P (2003): Intracranial EEG and human brain mapping. J Physiol Paris 97(4–6):613–628.

Lachaux JP, Fonlupt P, Kahane P, Minotti L, Hoffmann D, Bertrand O, Baciu M (2007): Relationship between task-related gamma oscillations and BOLD signal: New insights from combined fMRI and intracranial EEG. Hum Brain Mapp 28:1368–1375.

Lachaux JP, Jung J, Mainy N, Dreher JC, Bertrand O, Baciu M, Minotti L, Hoffmann D, Kahane P (2008): Silence is golden: Transient neural deactivation in the prefrontal cortex during attentive reading. Cereb Cortex 18:443–450.

Lee D (2003): Coherent oscillations in neuronal activity of the supplementary motor area during a visuomotor task. J Neurosci 23:6798–6809.

Logothetis NK, Pauls J, Augath M, Trinath T, Oeltermann A (2001): Neurophysiological investigation of the basis of the fMRI signal. Nature 412:150–157.

Luu P, Tucker DM, Derryberry D, Reed M, Poulsen C (2003): Electrophysiological responses to errors and feedback in the process of action regulation. Psychol Sci 14:47–53.

Mainy N, Kahane P, Minotti L, Hoffmann D, Bertrand O, Lachaux JP (2007): Neural correlates of consolidation in working memory. Hum Brain Mapp 28:183–193.

Mainy N, Jung J, Baciu M, Kahane P, Schoendorff B, Minotti L, Hoffmann D, Bertrand O, Lachaux JP (2008): Cortical dynamics of word recognition. Hum Brain Mapp 29:1215–1230.

Matsumoto M, Matsumoto K, Abe H, Tanaka K (2007): Medial prefrontal cell activity signaling prediction errors of action values. Nat Neurosci 10:647–656.

Michelet T, Bioulac B, Guehl D, Escola L, Burbaud P (2007): Impact of commitment on performance evaluation in the rostral cingulate motor area. J Neurosci 27:7482–7489.

Miltner WHR, Braun CH, Coles MGH (1997): Event-related brain potentials following incorrect feedback in a time-estimation task: Evidence for a 'generic' neural system for error detection. J Cogn Neurosci 9:788–798.

Monchi O, Petrides M, Petre V, Worsley K, Dagher A (2001): Wisconsin Card Sorting revisited: Distinct neural circuits participating in different stages of the task identified by event-related functional magnetic resonance imaging. J Neurosci 21:7733–7741.

Mukamel R, Gelbard H, Arieli A, Hasson U, Fried I, Malach R (2005): Coupling between neuronal firing, field potentials, and FMRI in human auditory cortex. Science 309:951–954.

Nieuwenhuis S, Holroyd CB, Mol N, Coles MG (2004): Reinforcement-related brain potentials from medial frontal cortex: Origins and functional significance. Neurosci Biobehav Rev 28:441–448.

Nieuwenhuis S, Slagter HA, von Geusau NJ, Heslenfeld DJ, Holroyd CB (2005): Knowing good from bad: Differential activation of human cortical areas by positive and negative outcomes. Eur J Neurosci 21:3161–3168.

Nir Y, Fisch L, Mukamel R, Gelbard-Sagiv H, Arieli A, Fried I, Malach R (2007): Coupling between neuronal firing rate, gamma LFP, and BOLD fMRI is related to interneuronal correlations. Curr Biol 17:1275–1285.

Picard N, Strick PL (1996): Motor areas of the medial wall: A review of their location and functional activation. Cereb Cortex 6:342–353.

Polich J (2007): Updating P300: An integrative theory of P3a and P3b. Clin Neurophysiol 118:2128–2148.

Polli FE, Barton JJ, Thakkar KN, Greve DN, Goff DC, Rauch SL, Manoach DS (2008): Reduced error-related activation in two anterior cingulate circuits is related to impaired performance in schizophrenia. Brain 131(Pt 4):971–986.

Quilodran R, Rothe M, Procyk E (2008): Behavioral shifts and action valuation in the anterior cingulate cortex. Neuron 57:314–325.

Raghavachari S, Kahana MJ, Rizzuto DS, Caplan JB, Kirschen MP, Bourgeois B, Madsen JR, Lisman JE (2001): Gating of human theta oscillations by a working memory task. J Neurosci 21:3175–3183.

Raichle ME, Snyder AZ (2007): A default mode of brain function: A brief history of an evolving idea. Neuroimage 37:1083–1090; discussion 1097–1099.

Raichle ME, MacLeod AM, Snyder AZ, Powers WJ, Gusnard DA, Shulman GL (2001): A default mode of brain function. Proc Natl Acad Sci USA 98:676–682.

Rolls ET (2004): The functions of the orbitofrontal cortex. Brain Cogn 55:11–29.

Ruchsow M, Grothe J, Spitzer M, Kiefer M (2002): Human anterior cingulate cortex is activated by negative feedback: Evidence from event-related potentials in a guessing task. Neurosci Lett 325:203–206.

Rushworth MF, Walton ME, Kennerley SW, Bannerman DM (2004): Action sets and decisions in the medial frontal cortex. Trends Cogn Sci 8:410–417.

Shima K, Mushiake H, Saito N, Tanji J (1996): Role for cells in the presupplementary motor area in updating motor plans. Proc Natl Acad Sci USA 93:8694–8698.

Singer W (1999): Neuronal synchrony: A versatile code for the definition of relations? Neuron 24:49–65, 111–125.

Talairach J, Tournoux P (1988): Co-planar Stereotaxic Atlas of the Human Brain. 3-Dimensional Proportional System: An Approach to Cerebral Imaging. Stuttgart: Thieme.

Tallon-Baudry C, Bertrand O, Delpuech C, Pernier J (1997): Oscillatory gamma-band (30–70 Hz) activity induced by a visual search task in humans. J Neurosci 17:722–734.

Thakkar KN, Polli FE, Joseph RM, Tuch DS, Hadjikhani N, Barton JJ, Manoach DS. (2008): Response monitoring, repetitive behaviour and anterior cingulate abnormalities in autism spectrum disorders (ASD). Brain 131(Pt 9):2464–2478.

Ullsperger M, von Cramon DY (2003): Error monitoring using external feedback: Specific roles of the habenular complex, the reward system, and the cingulate motor area revealed by functional magnetic resonance imaging. J Neurosci 23:4308–4314.

van Veen V, Holroyd CB, Cohen JD, Stenger VA, Carter CS (2004): Errors without conflict: Implications for performance monitoring theories of anterior cingulate cortex. Brain Cogn 56:267–276.

Varela F, Lachaux JP, Rodriguez E, Martinerie J (2001): The brainweb: Phase synchronization and large-scale integration. Nat Rev Neurosci 2:229–239.

Verberne AJ, Owens NC (1998): Cortical modulation of the cardiovascular system. Prog Neurobiol 54:149–168.

Wallis JD (2007): Orbitofrontal cortex and its contribution to decision-making. Annu Rev Neurosci 30:31–56.

Walton ME, Devlin JT, Rushworth MF (2004): Interactions between decision making and performance monitoring within prefrontal cortex. Nat Neurosci 7:1259–1265.

Zanolie K, Van Leijenhorst L, Rombouts SA, Crone EA (2008): Separable neural mechanisms contribute to feedback processing in a rule-learning task. Neuropsychologia 46:117–126.